U.S. Department
of Commerce

Volume 114
Number 1
January 2016

Fishery Bulletin

The *Fishery Bulletin* (ISSN 0090-0656) is published quarterly by the Scientific Publications Office, National Marine Fisheries Service, NOAA, 7600 Sand Point Way NE, Seattle, WA 98115-0070.

The Secretary of Commerce has determined that the publication of this periodical is necessary according to law for the transaction of public business of this Department. Use of funds for printing of this periodical has been approved by the Director of the Office of Management and Budget.

For Sale by the Superintendent of Documents, U.S. Government Printing Office, Washington, DC 20402. Subscription price per year: $32.00 domestic and $44.80 foreign. Cost per single issue: $19.00 domestic and $26.60 foreign. **See back for order form.**

Fishery Bulletin

***Fishery Bulletin* web site: www.fisherybulletin.noaa.gov**

The *Fishery Bulletin* carries original research reports on investigations in fishery science, engineering, and economics. It began as the Bulletin of the United States Fish Commission in 1881; it became the Bulletin of the Bureau of Fisheries in 1904 and the *Fishery Bulletin* of the Fish and Wildlife Service in 1941. Separates were issued as documents through volume 46; the last document was no. 1103. Beginning with volume 47 in 1931 and continuing through volume 62 in 1963, each separate appeared as a numbered bulletin. A new system began in 1963 with volume 63 in which papers are bound together in a single issue. Beginning with volume 70, number 1, January 1972, *Fishery Bulletin* became a periodical, issued quarterly. In this form, it is available by subscription from the Superintendent of Documents, U.S. Government Printing Office, Washington, DC 20402. It is also available free in limited numbers to libraries, research institutions, state and federal agencies, and in exchange for other scientific publications.

U.S. Department of Commerce
Seattle, Washington

Volume 114
Number 1
January 2016

Fishery Bulletin

Contents

Articles

NOAA
National Marine
Fisheries Service

Fishery Bulletin
established 1881

Spencer F. Baird
First U.S. Commissioner
of Fisheries and founder
of *Fishery Bulletin*

Elasmobranch bycatch associated with the shrimp trawl fishery off the Pacific coast of Costa Rica, Central America

Tayler M. Clarke[1,2]
Mario Espinoza[2,3]
Robert Ahrens[4]
Ingo S. Wehrtmann[2,3]

Email for contact author: taylermc@gmail.com

[1] Programa Gestión Integrada de Áreas Costeras Tropicales (GIACT)
Centro de Investigación en Ciencias del Mar y Limnología (CIMAR)
Universidad de Costa Rica
11501-2060 San José, Costa Rica

[2] Unidad de Investigación Pesquera y Acuicultura (UNIP)
CIMAR
Universidad de Costa Rica
11501-2060 San José, Costa Rica

[3] Escuela de Biología
Universidad de Costa Rica
11501-2060 San José, Costa Rica

[4] Fisheries and Aquatic Sciences
School of Forest Resources and Conservation
University of Florida
P.O. Box 110410
Gainesville, Florida 32653

Abstract—Demersal sharks and rays are common yet vulnerable components of the bycatch in tropical bottom-trawl fisheries. Little is known about the elasmobranch assemblages associated with most of these fisheries, particularly within the eastern tropical Pacific. This study characterized the elasmobranch assemblage associated with the shrimp trawl fishery along the Pacific coast of Costa Rica. Between August 2008 and August 2012, 346 trawl hauls were conducted at depths of 18–350 m. These hauls resulted in a sample of 4564 elasmobranchs from 25 species and 13 families. The Panamic stingray (*Urotrygon aspidura*), rasptail skate (*Raja velezi*), brown smoothhound (*Mustelus henlei*), and witch guitarfish (*Zapteryx xyster*) accounted for more than 66% of the elasmobranch abundance within the bycatch. Depth was the main factor influencing the elasmobranch assemblage; species richness was significantly higher at depths <100 m than at other depths. Two groups of elasmobranchs were identified: the first was found in shallow waters (<50 m), and the second was observed at depths of 50–350 m. Sex and size segregation patterns are also influenced by depth. Moreover, we documented the shift of the bottom-trawl fishery toward shallow-water resources—a change that could be problematic considering that elasmobranch diversity is higher in shallow waters.

Manuscript submitted 26 August 2014.
Manuscript accepted 10 September 2015.
Fish. Bull. 114:1–17 (2016).
Online publication date: 22 October 2015.
doi: 10.7755/FB.114.1

Overfishing and habitat degradation have caused significant declines in elasmobranch abundance (Dulvy et al., 2008; Ferretti et al., 2008; Dulvy et al., 2014). Most of the global elasmobranch catch is incidental and originates from fisheries that target higher-valued teleosts or crustaceans (Stevens et al., 2000; Walker, 2005; Wehrtmann et al., 2012; Worm et al., 2013). In general, elasmobranch bycatch is not regulated or even reported, especially in developing countries (Barker and Schluessel, 2005; Cheung et al., 2005; Walker, 2005). Furthermore, sharks and rays tend to exhibit slow growth rates, late maturity, and low fecundity, and, therefore, they have a low resilience to intense fishing pressures (Cortés, 2000; Dulvy and Reynolds, 2002; Frisk et al., 2005). The severity of this issue increases in the tropics as a result of the interaction between a high diversity of elasmobranch species and data-deficient fisheries (Barker and Schluessel, 2005; Cheung et al., 2005; White and Sommerville, 2010).

Several studies conducted in the tropics have reported large declines in the abundance of demersal elasmobranchs associated with bottom-trawl fisheries (e.g., Thailand: Stevens et al., 2000; Australia: Graham et al., 2001; Gulf of Mexico: Shepherd and Myers, 2005). Nevertheless, elasmobranch bycatch has been poorly studied in many tropical regions, including the Eastern Tropical Pacific (ETP; from Mexico to Peru), where abundance trends remain unclear (Mejía-Falla and Navia[1]; López-Mar-

[1] Mejía-Falla, P. A., and A. F. Navia (eds.). 2011. Estadísticas pesqueras de tiburones y rayas en el Pacífico Colombiano. Documento técnico Fundación SQUALUS No. FS0111, 70 p. [Available at website.]

tínez et al., 2010; Clarke et al., 2014). The best information available is obtained from the Pacific coast of Colombia, where significant changes in elasmobranch species composition and abundance have been detected since the 1990s (Mejía-Falla and Navia[1]). Other countries, such as Mexico (López-Martínez et al., 2010), have basic information that is limited to species lists and short-term relative abundance. In the remaining countries of the ETP, even this basic information is not available. Scarcity of published data has hindered attempts to estimate the effect of shrimp trawl fisheries on the elasmobranch assemblage in the ETP (Espinoza et al., 2012; Espinoza et al., 2013; Clarke et al., 2014).

The commercial shrimp trawl fishery of Costa Rica operates exclusively along the Pacific coast, in shallow-water and deepwater areas (Wehrtmann and Nielsen-Muñoz, 2009). The shallow-water (<100 m) fishery began in the 1950s, but the rapid depletion of coastal resources forced the fleet to expand their oprations toward deeper waters by the 1980s (Wehrtmann and Nielsen-Muñoz, 2009). The shrimp trawl fishery in Costa Rica has elevated bycatch rates of up to 93% of the total biomass catch (Wehrtmann and Nielsen-Muñoz, 2009; Arana et al., 2013). Moreover, the results of a long-term (2004–2012) fishery-independent monitoring program indicate that a shift has occurred in the overall structure of the demersal community of Costa Rica (Wehrtmann and Nielsen–Muñoz, 2009; Hernáez et al., 2011; Wehrtmann et al., 2012; Espinoza et al., 2012, 2013). Changes in elasmobranch abundance associated with this shift remain poorly understood, given that this monitoring program was designed to study deepwater shrimp resources and the crustacean bycatch associated with the fisheries that target them.

Together, the lack of biological information and the unreliability or nonexistence of landing statistics have limited the development of sustainable management practices and conservation strategies for elasmobranchs in Costa Rica. Given the fishery's current management framework is poorly enforced, the sustainability and environmental impacts have become a serious concern. Concern regarding the effect of this fishery culminated in a constitutional judgment (Sentence No. 2013-10540), enacted by the government of Costa Rica and that prohibited the Costa Rican Institute of Fisheries and Aquaculture (INCOPESCA) from granting or renewing commercial shrimp trawl licenses. All current licenses for this fishery are set to expire in 2018, and an ongoing national decision process will eventually define the legal framework requirements for any sustainable shrimp trawling in Costa Rica.

According to the Code of Conduct for Responsible Fisheries, the effects of a fishery on an ecosystem should be accounted for in management policies (FAO, 1995). In data-deficient situations, information on bycatch may provide estimates of a fishery's effects on an ecosystem. We aimed to characterize the relative composition of elasmobranch bycatch associated with the data-poor shrimp trawl fishery of Costa Rica. More specifically, we examined 1) elasmobranch distribution patterns in relation to geographic position, depth, year, season, and diel period; 2) the relationship between depth and number of elasmobranch species; 3) sex and size segregation patterns of the most common elasmobranch species; 4) the effects of latitude, depth, season, year, and sampling type on elasmobranch species composition; and 5) and a comparison of our results of species composition with those from historical data. This baseline information on the demersal elasmobranch assemblage of Costa Rica will enable an examination of the effects of management strategies to be implemented in the near future.

Materials and methods

Study area

The Pacific coastline of Costa Rica is highly irregular and is approximately 1254 km long, borders 3 large gulfs and a continental shelf that together cover an area of 15,600 km^2 (Fig. 1; Wehrtmann and Cortés, 2009). Costa Rica has pronounced rainy (May–November) and dry (December–April) seasons (Fiedler and Talley, 2006). Although temperature remains relatively constant across seasons (27–30°C), coastal productivity along most of the central and southern Pacific coast increases during the rainy season as a consequence of nutrient input from the largest rivers in this country: the Tempisque, Tárcoles, and Térraba rivers (Fiedler and Talley, 2006; Wehrtmann and Cortés, 2009).

The northern Pacific coast is characterized by strong, seasonal upwelling between December and February and by a limited freshwater input resulting from the absence of large rivers (Jiménez, 2001; Fiedler, 2002). The coast of the central Pacific region is influenced by 2 large estuarine systems, the Golfo de Nicoya and the Térraba-Sierpe delta; both estuaries have large mangrove forests in close proximity to coral communities or rocky reefs (Quesada-Alpízar and Cortés, 2006). The southern Pacific coast has a very steep continental slope and includes the Golfo Dulce tropical fjord (Quesada-Alpízar and Cortés, 2006).

Sampling

Sampling effort was concentrated near the main fishing port, Puntarenas, located in the northern Pacific region (Fig.1). Data for this study were collected from 3 types of surveys: 1) deepwater, 2) monitoring, and 3) commercial (Fig. 1). Sampling depth range was divided into shallow (<50 m), intermediate (50–100 m).and deep (>100 m). Bottom trawls were carried out exclusively on soft sand or mud because of sampling gear limitations.

Deepwater surveys were conducted annually along the entire Pacific coastline of Costa Rica to examine the bycatch associated with the deepwater shrimp trawl fishery. A total of 4 deepwater surveys were conducted, 2 during the rainy season (August 2008 and May 2009) and 2 during the dry season (March 2010

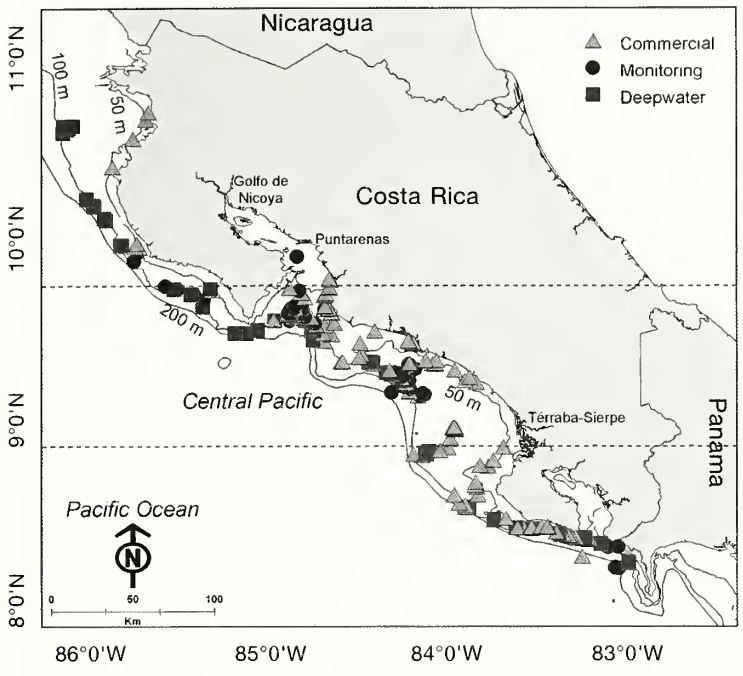

Figure 1

Map of the geographic regions and sampling locations for elasmobranch bycatch along the Pacific coast of Costa Rica, Central America, during 2010–2012. Solid lines represent the 50-m, 200-m, and 500-m depth contours. Dotted lines represent the boundaries of the central Pacific region.

and February 2011). These surveys followed a systematic sampling design, in which 15-min trawl hauls were conducted at 3 different depths: 150, 250, and 350 m. Hauls were conducted in areas where shrimp were expected to be caught. Strict grids were not used to determine sampling sites in order to respect marine protected areas but were distributed as evenly as possible along the coast.

Monitoring surveys were part of a program designed to analyze crustacean bycatch and were carried out on a monthly basis between 2010 and 2012; they consisted of one nocturnal and one diurnal set of four 20-min trawl hauls conducted at depths of approximately 100, 140, 180, and 220 m (Fig. 1). The location of each haul was determined by the vessel's captain; therefore, the majority of the sampling effort was concentrated in shrimp fishing grounds in the central Pacific region (Fig. 1). These sampling stations were chosen because of their general proximity to the main port of Puntarenas and their high probability of yielding large catches of shrimps, according to the captain's previous experience.

Commercial sampling was carried out during the same trips as those conducted by the monitoring surveys. Commercial sampling points were not selected on the basis of a systematic grid; instead, sampling occurred at locations where the captain had previously targeted shrimps. Sampling occurred on a monthly basis from April 2010 to August 2012 and included trawl hauls conducted at depths of 18–350 m.

Sampling for all 3 surveys was carried out aboard commercial shrimp trawlers (22.5 m), equipped with a 270-hp engine and 2 standard epibenthic nets (20.5 m long; mouth opening of 5.35×0.85 m; mesh size of 4.45 cm; and codend mesh size of 3.0 cm). Trawl speed varied between 2.1 and 5.7 km/h during all surveys. Information recorded for each trawl haul included geographic coordinates (latitude and longitude), depth (measured in meters with an installed sonar), and trawl duration (defined as the time, in minutes, during which the net was on the bottom).

Elasmobranchs were identified, classified according to sex, measured (total length [TL] for sharks and disc width [DW] for rays), and weighed (total weight [TW]) (Bussing and López, 1993; Compagno et al., 2005). Maturity stage was assessed by macroscopic examination of the reproductive tract (Conrath, 2005; Clarke et al., 2014).

General abundance and distribution patterns

The effects of depth, latitude, year, diel period (day: 0600–1800; night: 1800–0600), and season (rainy and dry) on elasmobranch abundance were examined by using a delta-lognormal generalized linear model (delta-GLM). This method is commonly applied to zero-inflated fishery data, which tend to violate key assumptions of many statistical techniques (Stefánsson, 1996). The delta-GLM approach comprised 2 stages: 1) elasmobranch presence and absence data were modeled by using a binomial GLM with a logit-link, and 2) the observed positive densities were modeled with a log-transformed positive subset, which was assumed to be Gaussian with an identity link function. Because of the differences in the sampling design between the 3 survey methods, separate delta-GLMs were applied to deepwater, monitoring, and commercial data. Total elasmobranch abundance was standardized to catch per unit of effort (CPUE), defined as the number of individuals per hour of trawling.

For deepwater surveys, the independent variables considered in the analyses were depth, latitude, year, and season. Diel period was excluded from the model for deepwater trips because hauls were carried out only during the day. The independent variables considered in models for monitoring and commercial surveys included depth, latitude, year, season, and diel period. In all 3 models, depth and latitude were treated as continuous variables, and year, diel period, and season were treated as factors. In order to avoid strong interactions between depth and longitude, depth and latitude were used to represent the geographic location of each trawl survey. Interactions between variables could not be considered because of the small size of the available

data sets, although we recognize that they would likely be important to consider should a larger data set become available (Venables and Dichtmont, 2004).

For each delta-GLM, forward selection was used to select separately the binomial model based on presence and absence data and the lognormal model based on log-transformed data for elasmobranch CPUE. The effects that explained more than 5% of the deviance were considered to have a high explanatory power (Tascheri et al., 2010). Chi-square tests were run for the binomial model, and *F*-tests were run for the lognormal model. The performance of the models was also compared by using Akaike information criterion (AIC). Analyses were conducted with R, vers. 3.0.2 (R Core Team, 2013).

Patterns in species richness related to depth were explored with a nonparametric test, Spearman's rank correlation coefficient (ρ), because data did not conform to a normal distribution. In this analysis, the independent variable was depth and the dependent variable was the average number of species per trawl haul (α=0.05). Data from all survey methods conducted between 2010 and 2012 were pooled for this analysis. General patterns of sex and size segregation were analyzed in relation to depth and diel period by using pooled data from all types of survey conducted between 2010 and 2012. This analysis was undertaken to determine whether a larger proportion of females and immature individuals was caught in shallow waters. Diel period was included in this analysis to detect changes in activity levels associated with sex and maturity stage. Variations in the proportion of females and immature individuals with depth range (<50 m, 50–100 m, >100 m) and diel period (day and night) were examined with a binomial GLM (logit link) (Venables and Ripley, 2002). Only species with at least 100 individuals were used in this analysis.

Elasmobranch assemblage

The importance of depth on elasmobranch assemblage was further explored with PRIMER[2], vers.6.2.1 (PRIMER-E Ltd., Plymouth, UK). We used data from all surveys conducted in the central Pacific region during 2010–2012. A matrix was constructed with the transformed species CPUE per haul in columns (log [(individuals/hour)+1]) and depth ranges in rows. To reduce the influence of extremely abundant species, CPUE was transformed (Clarke and Warwick, 2001). Rare species caught in less than 5 trawl hauls were excluded from our analyses (Clarke and Warwick, 2001). Differences in elasmobranch assemblages among depth ranges were examined by using an analysis of similarity (ANOSIM; α=0.05; Clarke and Warwick, 2001). A similarity percentage (SIMPER) analysis was used to identify species that showed the highest contribution to the dissimilarities among depth ranges (Clarke and Warwick, 2001).

Redundancy analyses (RDAs) were applied to examine the relationship between environmental variables and elasmobranch assemblages (Borcard et al., 2011). An RDA is a constrained ordination technique that combines a multivariate, multiple linear regression with a principal component analysis. We performed RDAs that were based on covariance matrixes to confer a higher weight to the common species in these analyses.

A separate RDA was conducted for each survey type to avoid biases that may have resulted from combining the 3 survey methods. For all analyses, a Hellinger transformation was applied to the species CPUE to minimize the effects of the large number of zeros in the data set (Borcard et al., 2011). Rare species (caught in less than 5 trawl hauls) were excluded from the analysis to prevent strong distorting effects. The environmental variables considered in the RDAs were standardized depth, standardized latitude, year, season, and diel period. The statistical significance of the ordination axes was examined with a Monte Carlo permutation test. Results were plotted on a correlation biplot, in which angles between species and environmental variables represent correlations between variables (Borcard et al., 2011). These analyses were conducted by using the vegan library in R, vers. 3.0.2 (R Core Team, 2013).

Results

For this study, data were examined from 346 trawl hauls conducted along the entire Pacific coast of Costa Rica from 2008 to 2012. Of these hauls, 108 were from deep water surveys, 111 were from monitoring surveys, and 127 were from commercial surveys (Fig. 1). Commercial and monitoring sampling efforts were highest in the central Pacific region, where 76% of commercial hauls and 91% of monitoring surveys were conducted (Table 1). Most commercial trawl hauls occurred at depths <100 m, and the majority of monitoring and all deepwater trawl hauls were conducted in deeper waters (Table 1). The average standardized elasmobranch abundance was 9.37 individuals/hour in deep water surveys, 6.96 individuals/hour in monitoring surveys, and 7.92 individuals/hour in commercial surveys.

Elasmobranch diversity and distribution patterns

During the entire sampling period, 4564 elasmobranchs from 25 species, 13 families, and 6 orders were captured as bycatch (Table 2). Four species represented more than 66% of the entire elasmobranch abundance: Panamic stingray (*Urotrygon aspidura*) accounted for 26%, rasptail skate (*Raja velezi*) contributed 16%, brown smoothhound (*Mustelus henlei*) composed 15%, and witch guitarfish (*Zapteryx xyster*) accounted for 9%. Of the remaining 21 species, 10 were relatively

[2] Mention of trade names or commercial companies is for identification purposes only and does not imply endorsement by the National Marine Fisheries Service, NOAA.

Table 1

Sampling effort for surveys of bycatch of elasmobranchs conducted along the Pacific coast of Costa Rica, Central America, in 2008–2012 at 3 depth ranges: shallow (<50 m), intermediate (50–100 m), and deep (>100 m). Number of trawling hours (h) and trawl hauls (Hauls) per geographic area and depth range. The highest sampling effort occurred in the central geographic region at depths <50 m with commercial surveys (underlined).

		2008		2009		2010		2011		2012		Total	
Region	Depth	h	Hauls	h	Hauls	h	Hauls	h	Hauls	h	Hauls	h	Hauls
Commercial sampling													
Northern	<50 m	–	–	–	–	–	–	3.7	2	5.9	1	9.6	3
	50–100 m	–	–	–	–	10.3	2	9.3	3	–	–	24.1	5
Central	<50 m	–	–	–	–	24.6	5	61.8	14	28.6	6	115.0	25
	50–100 m	–	–	–	–	115.2	20	45.1	10	62.9	14	223.1	44
	>100 m	–	–	–	–	29.6	14	18.9	9	6.2	4	54.7	27
Southern	50–100 m	–	–	–	–	–	–	6.1	1	–	–	6.1	1
	>100 m	–	–	–	–	12.5	6	–	–	53.2	16	65.7	22
Monitoring sampling													
Northern	50–100 m	–	–	–	–	6.0	1	–	–	–	–	6.0	1
	> 100 m	–	–	–	–	1.4	4	–	–	–	–	1.4	4
Central	<50 m	–	–	–	–	0.7	2	–	–	–	–	0.7	2
	50–100 m	–	–	–	–	2.7	8	4.0	12	2.2	6	8.9	26
	>100 m	–	–	–	–	6.5	19	11.6	35	6.6	19	24.7	73
Southern	50–100 m	–	–	–	–	0.3	1	–	–	–	–	0.3	1
	>100 m	–	–	–	–	1.5	4	–	–	–	–	1.5	4
Deepwater sampling													
Northern	>100 m	2.1	8	2.1	8	2.1	8	2.6	10	–	–	8.9	34
Central	>100 m	3.2	12	3.1	12	3.0	12	2.7	10	–	–	12.0	46
Southern	>100 m	2.3	8	2.0	8	1.7	7	1.3	5	–	–	7.0	27
Total		12.1	27	7.3	28	218.0	113	167.3	111	165.6	66	570.0	345

common (1–5% of total abundance) and 11 were rare (<1% of total abundance).

Species richness and distribution patterns of elasmobranchs were examined across depths. Overall, 2279 individuals of 24 species were recorded at shallow depths (<50 m), 1642 individuals from 14 species were found at depths between 50 and 100 m, and only 643 individuals from 7 species were observed at depths >100 m (Table 2). The number of species caught per trawl haul varied from 0 through 9. A significant, negative relationship was detected between the average number of species per haul and depth (Spearman's = −0.831, $P<0.001$; Fig. 2).

Body size ranged from 21.8 to 138.0 cm TL for sharks and from 2.6 to 107.7 cm DW for rays (Fig. 3). The large number of small species (<50 cm TL or DW) were mainly from the families of Narcinidae, Urotrygonidae, and Rajidae. The sicklefin smoothhound (*Mustelus lunulatus*), prickly shark (*Echinorhinus cookei*), Pacific angel shark (*Squatina californica*), and longtail stingray (*Dasyatis longa*) were the largest species recorded; and these species collectively represented nearly 5% of the total elasmobranch abundance. The percentage of species that were small (<50 cm TL) was larger in shallow waters (depths <50 m, Fig. 3A) than at other depths (Fig. 3, B and C). Although most species presented narrow depth ranges, trends in size were apparent for some species with wide depth distributions (Fig. 3). Large, adult-size brown smoothhound dominated all depth categories. Smaller individuals of the rasptail skate were found in the shallower limit of the depth range for this species: 50–100 m. Likewise, average sizes of the sicklefin smoothhound, Peruvian torpedo (*Torpedo peruana*), and witch guitarfish increased across depth ranges (Fig. 3).

Elasmobranch presence in deepwater surveys was low, given that elasmobranchs were absent from 63% of the trawl hauls. Of the surveys in which elasmobranchs were present, 16.6% had a CPUE of 1–10 individuals/hour and 20.4% had CPUE of 10–152 individuals/hour. The delta-GLM applied to the deepwater survey data revealed that depth had a significant effect on the density of elasmobranch CPUE, and depth and latitude had a significant effect on the proportion of positive trawl hauls (Table 3). In monitoring surveys, we found that elasmobranchs were absent from 65.8% of all trawl hauls. The lognormal submodel of the delta-GLM applied to monitoring data did not detect significant effects. In contrast, the binomial submodel revealed that depth, latitude, and year had significant effects on elasmobranch presence (Table 3). In commercial surveys, 17.8% of trawl hauls did not result in elasmobranch catch. The delta-GLM for commercial data indicated that depth was the only significant factor

Table 2

For the elasmobranch species captured as bycatch in the shrimp trawl fisheries of the Pacific coast of Costa Rica, Central America, during 2008–2012, total number of individuals (*N*); percentages of the species sample caught in commercial (C), monitoring (M), and deepwater (D) surveys; percentages of abundance per depth category (<50 m, with 2279 individuals in total; 50–100 m, with 1642 individuals in total; and >100 m, with 643 individuals in total). Data for the most abundant species are presented in bold type.

			Survey type			Depth range		
Order and family	Common name (scientific name)	*N*	C	M	D	<50 m	50–100 m	>100 m
Carcharhiniformes								
Carcharhinidae	Pacific sharpnose shark (*Rhizoprionodon longurio*)	6	100	–	–	0.26	–	–
Sphyrnidae	Scalloped hammerhead (*Sphyrna lewini*)	4	100	–	–	0.18	–	–
Triakidae	*Brown smoothhound (Mustelus henlei)*	**696**	**55.9**	**21.3**	**22.8**	**0.44**	**23.45**	**46.81**
	Sicklefin smoothhound (*Mustelus lunulatus*)	122	99.2	0.8	–	0.26	7	0.16
Squaliformes								
Echinorhinidae	Prickly shark (*Echinorhinus cookei*)	11	–	–	100	–	–	1.71
Squatiniformes								
Squatinidae	Pacific angel shark (*Squatina californica*)	57	94.7	3.5	1.8	0.04	3.23	0.47
Myliobatiformes								
Dasyatidae	Longtail stingray (*Dasyatis longa*)	35	100	–	–	1.14	0.55	–
Myliobatidae	Spotted eagle ray (*Aetobatus laticeps*)	2	100	–	–	0.09	–	–
	Golden cownose ray (*Rhinoptera steindachneri*)	39	100	–	–	0.13	2.19	–
Urotrygonidae	*Panamic stingray (Urotrygon aspidura)*	**1178**	**100**	–	–	**51.56**	**0.18**	–
	Blotched stingray (*Urotrygon chilensis*)	189	100	–	–	7.81	0.67	–
	Denticled roundray *Urotrygon cimar*	1	100	–	–	0.04	–	–
	Spiny stingray (*Urotrygon munda*)	1	100	–	–	0.04	–	–
	Dwarf stingray (*Urotrygon nana*)	16	100	–	–	0.7	–	–
	Thorny stingray (*Urotrygon rogersi*)	143	100	–	–	6.27	–	–
Gymnuridae	California butterfly ray (*Gymnura marmorata*)	1	100	–	–	0.04	–	–
Rajiformes								
Rajidae	Equatorial skate (*Raja equatorialis*)	88	100	–	–	1.97	2.62	–
	Rasptail skate (Raja velezi)	**750**	**89.6**	**3.6**	**6.8**	**0.04**	**34.65**	**27.99**
	Cortez skate (*Raja cortezensis*)	1	100	–	–	0.04	–	–
Rhinobatidae	Whitesnout guitarfish (*Rhinobatos leucorhynchus*)	90	100	–	–	3.91	0.06	–
	Witch guitarfish (Zapteryx xyster)	**393**	**96.4**	**3.6**	–	**2.63**	**19.98**	**0.78**
Torpediniformes								
Narcinidae	Bullseye electric ray (*Diplobatis ommata*)	206	100	–	–	8.86	0.24	–
	Giant electric ray (*Narcine entemedor*)	152	100	–	–	6.06	0.85	–
	Vermiculate electric ray (*Narcine vermiculatus*)	165	100	–	–	7.24	–	–
Torpedinidae	*Peruvian torpedo (Torpedo peruana)*	**218**	**59.6**	**22.9**	**17.4**	**0.22**	**4.32**	**22.08**
Total		4564				100	100	100

in both the lognormal and binomial submodels (Table 3).

Many of the elasmobranch species observed were segregated by sex and maturity stage (Table 4). Binomial GLMs indicated that neither depth nor diel period had a significant effect on sex ratios in the catch of brown smoothhound, sicklefin smoothhound, blotched stingray (*Urotrygon chilensis*), thorny stingray (*U. rogersi*), rasptail skate, witch guitarfish, bullseye electric ray (*Diplobatis ommata*), giant electric ray (*Narcine entemedor*), or vermiculate electric ray (*N. vermiculatus*) (Table 4). Conversely, depth had a significant effect on the sex ratios of the catch of Panamic stingray (Table 4): females of this species dominated at shallow depths (<50 m) but were absent from depths >50 m (Fig. 4). Diel period had a significant effect on the sex ratios of the catch of Peruvian torpedo; more females were caught during the day than during the night (Table 4). For all depths and diel periods, the proportion of males in the catch of brown smoothhound was higher than the proportion of females. Sex ratios were skewed toward females in the catch of species that were distributed mainly in shallow waters (depths <50 m): namely in the catches of Panamic stingray, thorny stingray, bullseye electric ray, giant electric ray, and vermiculate electric ray (Fig. 4A).

Binomial GLMs indicated that depth and diel period did not influence maturity ratios of the catch of sicklefin smoothhound, blotched stingray, witch guitarfish, bullseye electric ray, vermiculate electric ray, and Peru-

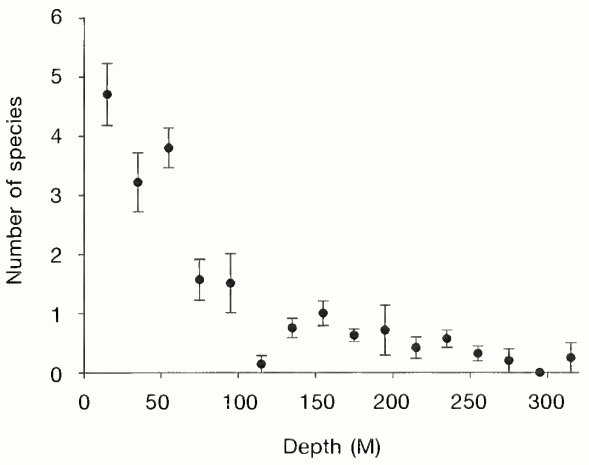

Figure 2

Spearman's rank correlation coefficient for the relationship between depth and species richness for elasmobranchs caught during surveys conducted along the Pacific coast of Costa Rica during 2010–2012. Relationship is between 20-m depth categories and average number of species per trawl haul. Error bars indicate standard errors of the means.

vian torpedo (Table 4). Conversely, depth was a factor that significantly influenced maturity ratios of brown smoothhound, rasptail skate, and giant electric ray. Although mature brown smoothhound were more abundant at all depths, the proportion of immature individuals peaked at the depths of 50–100 m (Fig. 4). For the rasptail skate and giant electric ray, proportions of immature individuals were higher in the shallow limits of these species' depth ranges (50–100 m and <50 m, respectively) (Fig. 4). Maturity ratios in the catch of Panamic stingray and thorny stingray varied significantly among diel periods; proportionally more immature individuals were caught during the day than during the night (Fig. 5). A high proportion (>50%) of immature Peruvian torpedo was recorded across all depths and diel periods. For the witch guitarfish, a high proportion (73%) of immature individuals was found at shallow depths (<50 m), and a high proportion (57%) of mature individuals was found at depths of 50–100 m. A higher abundance of mature round stingrays (*Urotrygon* spp.) was observed at shallow depths than at other depths.

Elasmobranch assemblage

The elasmobranch assemblage varied significantly among depths (ANOSIM R=0.710, P=0.001). The elasmobranch assemblage in shallow waters differed from the assemblages in intermediate-depth (R=0.792, P=0.001) and deep (R=0.934, P=0.001) waters. The shallow-water assemblage was characterized by the dominance of Panamic stingray (0.00–138.70 individuals/hour); the remaining species were less abundant (0.01–2.15 individuals/hour). The deepwater assemblage was composed of rasptail skate, brown smoothhound, witch guitarfish, Peruvian torpedo, prickly shark, and Pacific angel shark, of which the first 2 species were most abundant. The elasmobranch assemblage in intermediate-depth waters was characterized by a combination of both shallow-water and deepwater species. Differences in the elasmobranch assemblage between deep and intermediate-depth waters were the smallest (R=0.474, P=0.001). A SIMPER analysis revealed that Panamic stingray, rasptail skate, brown smoothhound, witch guitarfish, and Peruvian torpedo were also responsible for 49.8–75.8% of the differences in the elasmobranch assemblage between depths.

In the RDA applied to deepwater survey data, depth, latitude, year, and season represented 13% of the variance in species data (Fig. 6A). The biplot that resulted from this analysis displays 97.2% of this variability in its first 2 axes, and all canonical axes were significant (Fig. 6A; F=4.224, P=0.002). This RDA biplot shows the brown smoothhound, rasptail skate, and Peruvian torpedo as a group. This group was negatively correlated with depth and strongly related to the years 2008 and 2009. The species in this group were separated mainly by latitude: the brown smoothhound was slightly more associated with southern latitudes, and the Peruvian torpedo was slightly more associated with northern latitudes. The prickly shark was placed separately and presented a strong positive correlation with depth.

The RDA for monitoring survey data explained 12% of the variability between environmental variables and species data (Fig. 6B). A biplot captures 91.4% of this variability, and all canonical axes were significant (Fig. 6B; F=3.222, P=0.002). Although all species are grouped quite closely together in this biplot, the strongest associations were between the witch guitarfish and the rasptail skate. All species had negative correlations with depth and positive associations with the diel period of 0600–1800 and the rainy season. As in the deepwater RDA, the brown smoothhound was more common at the southern limit of the latitudinal range, and the Peruvian torpedo and witch guitarfish were associated with the northern limits of the latitudinal range.

In the RDA applied to commercial survey data, depth, latitude, diel period, season, and year explained 10% of the variance in species data (Fig. 6C). The biplot that resulted from this analysis represents 76.9% of this variance, and all canonical axes were significant (Fig. 6C; F=2.772, P=0.002). This RDA biplot separates 2 groups of species, mainly according to depth and latitude. The shallow-water assemblage was composed of golden cownose ray (*Rhinoptera steindachneri*), whitesnout guitarfish (*Rhinobatos leucorhynchus*), giant electric ray, bullseye electric ray, vermiculate electric ray, longtail stingray, equatorial skate (*Raja equatorialis*), blotched stingray, thorny stingray, and Panamic stingray. The deepwater assemblage was composed of witch guitarfish, sicklefin smoothhound, brown smoothhound,

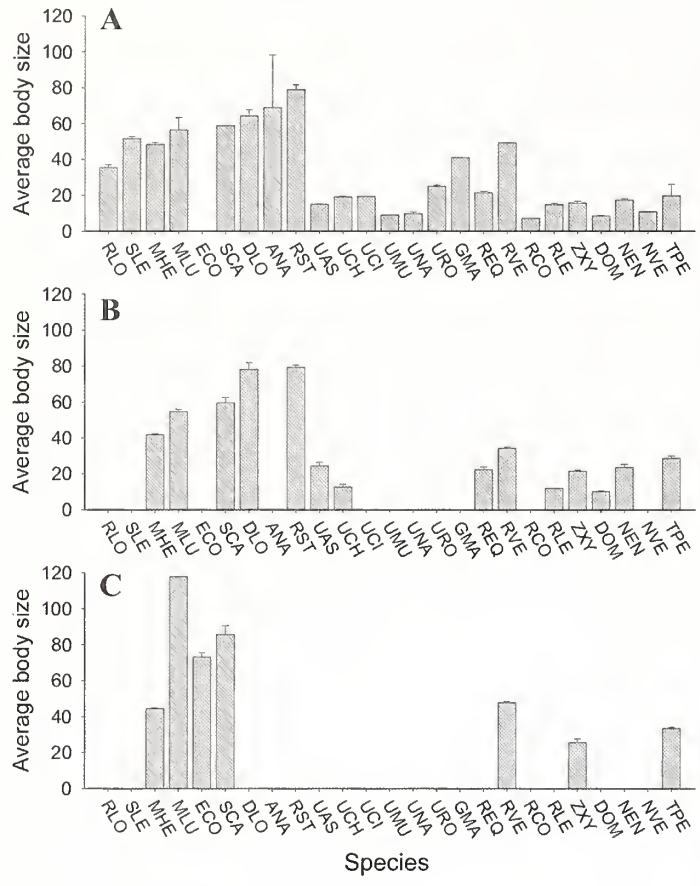

Figure 3

Average body sizes in cm, with standard errors indicated by error bars, of shark and ray species caught in 3 depth ranges, (**A**) <50 m, (**B**) 50–100 m, and (**C**) >100 m), along the Pacific coast of Costa Rica in 2010–2012. Body size is presented as total length in sharks and disc width in rays. The following species abbreviations are used: RLO (Pacific sharpnose shark [*Rhizoprionodon longurio*]), SLE (scalloped hammerhead [*Sphyrna lewini*]), MHE (brown smoothhound [*Mustelus henlei*]), MLU (sicklefin smoothhound [*Mustelus lunulatus*]), ECO (prickly shark [*Echinorhinus cookei*]), SCA (Pacific angel shark [*Squatina californica*]), DLO (longtail stingray [*Dasyatis longa*]), ANA (spotted eagle ray [*Aetobatus laticeps*]), RST (golden cownose ray [*Rhinoptera steindachneri*]), UAS (Panamic stingray [*Urotrygon aspidura*]), UCH (blotched stingray [*Urotrygon chilensis*]), UCI (denticled roundray [*Urotrygon cimar*]), UMU (Spiny stingray [*Urotrygon munda*]), UNA (dwarf stingray [*Urotrygon nana*]), URO (thorny stingray [*Urotrygon rogersi*]), GMA (California butterfly ray [*Gymnura marmorata*]), REQ (equatorial skate [*Raja equatorialis*]), RVE (rasptail skate [Raja velezi]), RCO (Cortez skate [*Raja cortezensis*]), RLE ((whitesnout guitarfish [*Rhinobatos leucorhynchus*]), ZXY (witch guitarfish [*Zapteryx xyster*]), DOM (bullseye electric ray [*Diplobatis ommata*]), NEN (giant electric ray [*Narcine entemedor*]), NVE (vermiculate electric ray [*Narcine vermiculatus*]), and TPE (Peruvian torpedo [*Torpedo peruviana*]).

Pacific angel shark, and the Peruvian torpedo. Within this group, the Peruvian torpedo had the strongest positive correlation with depth, whereas the witch guitarfish and Pacific angel shark had the strongest negative correlation with depth. The deepwater assemblage was weakly associated with the night, the rainy season, and the years 2010 or 2012.

Discussion

Elasmobranch diversity and distribution patterns

The results of our study revealed that elasmobranch bycatch of the shrimp trawl fishery in Costa Rica comprised 25 species, which account for more than 35% of the species richness reported for the Pacific coast of Costa Rica (Bussing and López, 2009). Most of these bycatch species have wide distribution ranges that include the entire ETP. Consequently, the few studies available on elasmobranch bycatch from shrimp fisheries in this region reveal similar species compositions (Gulf of California, Mexico: López-Martínez et al., 2010; Pacific coast of Colombia: Mejía-Falla and Navia[1]) (Table 5). The strong similarity between elasmobranch bycatch in Costa Rica and Colombia (14 species in common) reflects the biogeographic patterns proposed by Robertson and Cramer (2009). Costa Rica and Colombia form part of the Panamic biogeographic province that is composed solely of tropical fishes (Robertson and Cramer, 2009), and the Gulf of California belongs to the Cortez biogeographic province, which is characterized by the convergence of temperate, subtropical, and tropical marine fish fauna (Mora and Robertson, 2005; Rodríguez-Romero et al., 2008).

Our results revealed that the elasmobranch assemblage varies along the Pacific coast of Costa Rica (~1254 km of coastline). This variation is probably due to differences in oceanographic conditions along the coastline, with the north affected by upwelling and the central and South Pacific affected by freshwater inflows. Delta-GLMs indicated that latitude was an important predictor of elasmobranch presence in deepwater and monitoring surveys; however, these differences may reflect the higher sampling efforts in deep waters of the northern and southern Pacific areas. Therefore, the effect of latitude on elasmobranch diversity needs to be interpreted with caution. The uneven sampling effort along the coast was the result of an overall dependence on the presence of commercial shrimp trawl-

Table 3

Results of the 3 delta-lognormal generalized linear models (delta-GLMs) applied to abundance (CPUE) of elasmobranchs from deepwater, monitoring, and commercial surveys conducted along the Pacific coast of Costa Rica during 2008–2012: degrees of freedom (df), deviance change (Deviance), residual degrees of freedom (Residual df), residual deviance (Res. dev.), Akaike information criterion (AIC), and the probability (*P*) from the *F*-test for lognormal submodels or chi-square test for binomial models.

Model	df	Deviance	Residual df	Res. dev.	AIC	*P*
Deepwater delta-GLM						
Lognormal submodel						
Intercept			39	52.43	128.34	
Depth	1	5.92	38	46.51	125.54	0.03
Binomial submodel						
Intercept	1		107	141.45	143.45	
Depth	1	13.12	106	128.32	132.32	<0.01
Latitude	1	6.10	105	122.22	128.22	0.01
Monitoring delta-GLM						
Lognormal submodel						
Intercept	1		37	62.41	130.69	
Depth	1	4.76	36	57.65	129.68	0.09
Binomial submodel						
Intercept			110	142.65	144.65	
Depth	1	20.33	109	122.32	126.32	<0.01
Latitude	1	6.08	108	116.24	122.24	0.01
Year	2	11.00	106	105.24	115.24	<0.01
Commercial delta-GLM						
Lognormal submodel						
Intercept			103	189.15	361.35	
Depth	1	12.54	102	176.61	356.21	<0.01
Binomial submodel						
Intercept	1		126	120.16	122.16	
Depth	1	18.90	125	101.25	105.25	<0.001

ing vessels. Although sampling depths from monitoring surveys were predefined, the location of sampling stations was chosen by the captain. Consequently, both commercial and monitoring surveys were concentrated in the central Pacific region.

The nonrandom sampling design of both monitoring and commercial surveys may have introduced biases in the estimates of distribution and abundance that must be considered when interpreting the results of our study (e.g., elasmobranch abundance and composition covaries with shrimp abundance). Moreover, it is likely that interactions between environmental variables drive patterns in both species distribution and community structure; however, interactions were not explored because of the small data set. The small sample size may also have limited our ability to detect patterns in elasmobranch diversity across the examined explanatory variables (e.g., depth, latitude, geographic region, year, season, and diel period). This limited ability is the most probable cause of the low percentage of the variance in species abundance data that was explained by the RDAs.

Our findings indicate that depth is a major factor influencing elasmobranch assemblages along the Pacific coast of Costa Rica. Both species richness and abundance peaked in shallow waters and decreased with the increasing depth. This feature is common and has been reported previously for both demersal (MacPherson, 2003; Massuti and Moranta, 2003; Gouraguine et al., 2011) and pelagic (Smith and Brown, 2002) elasmobranch species. Nearshore environments are very heterogeneous and tend to concentrate a large number of species with small depth ranges, whereas a small number of species with large depth ranges inhabit homogeneous deepwater environments (Smith and Brown, 2002; Knip et al., 2010; Mejía-Falla and Navia[1]). Depth-related changes in environmental factors, such as temperature and productivity, may partially explain observed trends in species richness (Levinton, 1995).

Temperature is known to be an important factor influencing species richness, given that it may affect speciation rates (Allen et al., 2002). Productivity can also influence species richness; for example, areas with higher primary productivity tend to have species with high trophic levels, large body sizes, and high energetic requirements (Smith and Brown, 2002; Leathwick et al., 2006; Knip et al., 2010), including sharks and rays (Priede et al., 2006).

Table 4

Spatial distribution for sex and maturity ratios of the elasmobranch assemblage, by depth range (<50 m, 50–100 m, or >100 m) and diel period (day or night), along the Pacific coast of Costa Rica, Central America, in 2010–2012. The degrees of freedom (df), deviance, residual deviance (Res. dev), and probability (*P*) of the binomial generalized linear models (GLMs) applied to both maturity and sex ratios of the most abundant elasmobranch species. Significant *P*-values are in bold (α=0.05). The following species abbreviations are used: MHE (brown smoothhound [*Mustelus henlei*]), MLU (sicklefin smoothhound [*Mustelus lunulatus*]), UAS (Panamic stingray [*Urotrygon aspidura*]), UCH (blotched stingray [*Urotrygon chilensis*]), URO (thorny stingray [*Urotrygon rogersi*]), RVE (rasptail skate [*Raja velezi*]), ZXY (witch guitarfish [*Zapteryx xyster*]), DOM (bullseye electric ray [*Diplobatis ommata*]), NEN (giant electric ray [*Narcine entemedor*]), NVE (vermiculate electric ray [*Narcine vermiculatus*]), and TPE (Peruvian torpedo [*Torpedo peruviana*]).

		Sex ratios				Maturity ratios			
Species	Factors	df	Deviance	Res. dev.	*P*	df	Deviance	Res. dev.	*P*
MHE	Intercept	1	358.0			1	612.1		
	Depth	2	7.7	350.4	0.43	2	50.0	562.1	**0.04**
	Diel period	1	9.7	340.7	0.15	1	16.5	545.6	0.14
MLU	Intercept	1	24.2			1	53.5		
	Depth	2	2.0	22.3	0.41	2	6.1	47.5	0.56
	Diel period	1	0.0	22.3	0.95	1	0.0	47.5	0.98
UAS	Intercept	1	25.4			1	74.9		
	Depth	1	5.4	20.0	**0.04**	1	0.1	74.8	0.83
	Diel period	1	1.5	18.6	0.27	1	29.0	45.8	**0.00**
UCH	Intercept	1	35.0			1	43.4		
	Depth	1	3.3	31.7	0.47	1	12.3	31.1	0.20
	Diel period	1	3.2	28.4	0.47	1	1.8	29.3	0.59
URO	Intercept	1	8.7			1	21.3		
	Diel period	2	0.0	8.6	0.99	1	18.3	3.0	**0.01**
RVE	Intercept	1	196.1			1	538.0		
	Depth	2	10.4	185.7	0.16	2	70.3	467.7	**0.01**
	Diel period	1	0.2	185.6	0.80	1	2.1	465.5	0.58
ZXY	Intercept	1	118.8			1	222.6		
	Depth	2	1.8	117.1	0.69	2	19.3	203.2	0.09
	Diel period	1	0.3	116.8	0.74	1	6.9	196.3	0.19
DOM	Intercept	1	23.5			1	12.5		
	Depth	1	1.9	21.6	0.47	1	2.8	9.8	0.20
	Diel period	1	1.6	19.9	0.51	1	1.8	8.0	0.29
NEN	Intercept	1	31			1	34.2		
	Depth	1	0.0	31.0	0.92	1	7.0	27.2	**0.02**
	Diel period	1	1.2	29.8	0.34	1	2.1	1.8	0.19
NVE	Intercept	1	40.9			1	40.9		
	Diel period	1	19.4	21.5	0.10	1	1.2	21.5	0.10
TPE	Intercept	1	105.5			1	77.3		
	Depth	2	1.4	104.0	0.54	2	1.8	75.5	0.51
	Diel period	1	7.0	97.1	**0.02**	1	0.4	75.2	0.60

The elasmobranch assemblages caught by the shrimp trawl fishery were slightly influenced by diel period. Most elasmobranch species display higher activity levels during the night—a characteristic mainly related to foraging or social refuging behaviors (Wearmouth and Sims, 2008; Jacoby et al., 2012; Espinoza et al., 2011). Catch of elasmobranchs in trawl hauls, therefore, is expected to be higher during the day than at night; however, very few studies have addressed diel periodicity of bycatch (Molina and Cooke, 2012). The results of this study support the assumption that elasmobranch catch is higher during the day than at night.

Although the small sample size prevented us from detecting clear patterns for most species, a higher proportion of female Peruvian torpedo and immature round stingrays were found during the day than at night. The higher abundance of Peruvian torpedo during the day may be a result of its feeding behavior. The Pacific electric ray (*Torpedo californica*) is a bottom ambush predator during the day and actively for-

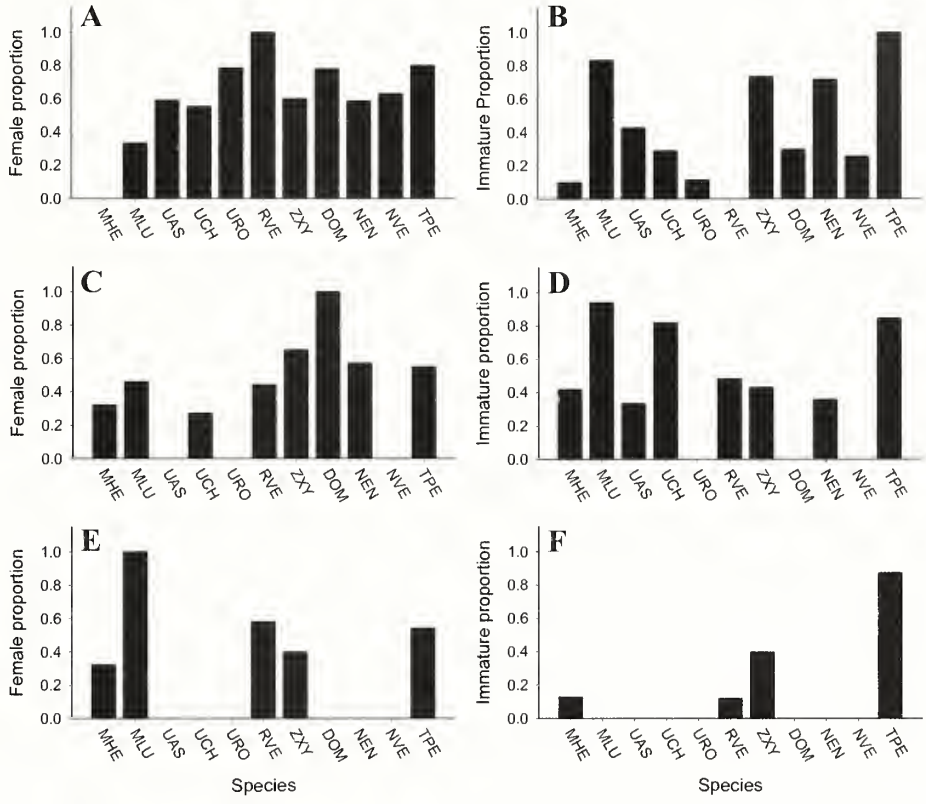

Figure 4

Proportion of females caught at 3 depth ranges, (**A**) <50 m, (**C**) 50–100 m, and (**E**) >100 m, and proportion of immature individuals caught at depth of (**B**) <50 m, (**D**) 50–100 m, and (**F**) >100 m for 11 elasmobranch species sampled along the Pacific coast of Costa Rica during 2010–2012. The following species abbreviations are used: MHE (brown smoothhound [*Mustelus henlei*]), MLU (sicklefin smoothhound [*Mustelus lunulatus*]), UAS (Panamic stingray [*Urotrygon aspidura*]), UCH (blotched stingray [*Urotrygon chilensis*]), URO (thorny stingray [*Urotrygon rogersi*]), RVE (rasptail skate [*Raja velezi*]), ZXY (witch guitarfish [*Zapteryx xyster*]), DOM (bullseye electric ray [*Diplobatis ommata*]), NEN (giant electric ray [*Narcine entemedor*]), NVE (vermiculate electric ray [*Narcine vermiculatus*]), and TPE (Peruvian torpedo [*Torpedo peruviana*]).

ages in the water column during the night (Lowe et al., 1994). If feeding habits of the Peruvian torpedo are similar to those of the Pacific electric ray, they would explain the higher catch rates for this species observed during the daytime.

Elasmobranch distribution patterns varied intraspecifically, according to sex and size. Sexual segregation has been documented widely in elasmobranchs (Wearmouth and Sims, 2008) and tends to occur more often in adult populations, although it is not restricted to them (Carlisle et al., 2007; Wearmouth and Sims, 2008). Our study showed that small ray species, such as the Panamic stingray and thorny stingray, formed large aggregations dominated by mature females in shallow waters. In the case of these small rays, sexual segregation in shallow waters may reduce intraspecific competition for food resources (Carlisle et al., 2007; Espinoza et al., 2012). In contrast, some species like the brown smoothhound had a male-biased sex ratio; male brown smoothhound occurred in deep habitats (depths >100 m) and gravid females were more abundant in warmer (>20°C), shallow, coastal habitats. Gravid females are thought to use warmer habitats that may offer thermal reproductive advantages, such as increased growth rates of embryos (Hight and Lowe, 2007; Pereyra et al., 2008; Speed et al., 2012).

Elasmobranch assemblages

The elasmobranch assemblages were characterized by the presence of 5 dominant species (i.e., rasptail skate, Panamic stingray, brown smoothhound, witch guitarfish, and Peruvian torpedo), a group that accounted for more than 75% of the total abundance of

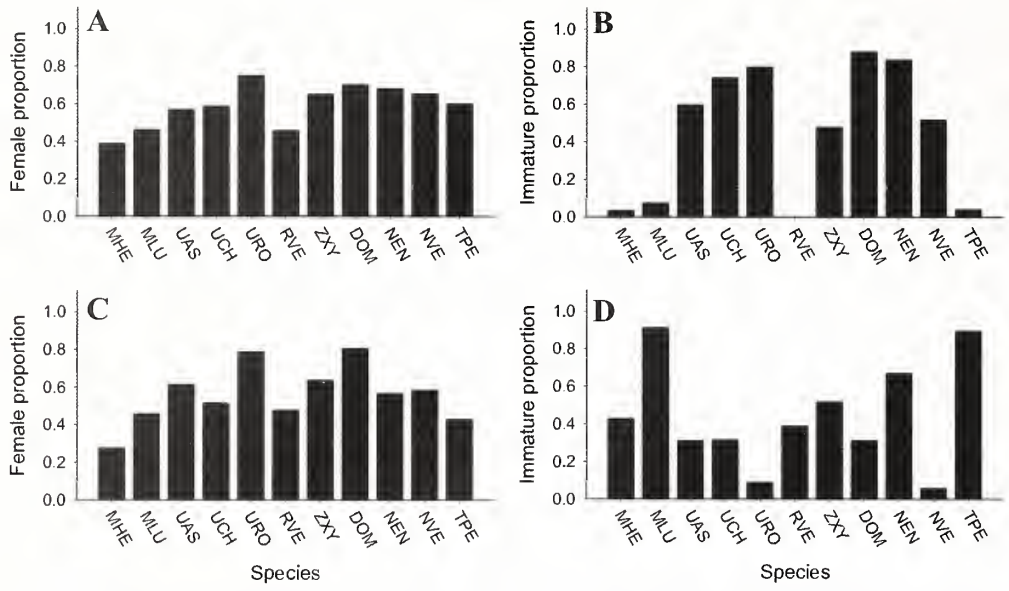

Figure 5

Proportion of females caught during (**A**) the day and (**B**) the night and proportion of immature individuals caught during (**C**) the day and (**D**) the night for 11 elasmobranch species sampled along the Pacific coast of Costa Rica during 2010–2012. The following species abbreviations are used: MHE (brown smoothhound [*Mustelus henlei*]), MLU (sicklefin smoothhound [*Mustelus lunulatus*]), UAS (Panamic stingray [*Urotrygon aspidura*]), UCH (blotched stingray [*Urotrygon chilensis*]), URO (thorny stingray [*Urotrygon rogersi*]), RVE (rasptail skate [*Raja velezi*]), ZXY (witch guitarfish [*Zapteryx xyster*]), DOM (bullseye electric ray [*Diplobatis ommata*]), NEN (giant electric ray [*Narcine entemedor*]), NVE (vermiculate electric ray [*Narcine vermiculatus*]), and TPE (Peruvian torpedo [*Torpedo peruviana*]).

Table 5

Comparison of elasmobranch species in bycatch of shrimp trawl fisheries in various countries of the eastern tropical Pacific, based on results from previous studies (noted in the reference column) and from this study

Location	Study period	Depth range (m)	Number of species			Reference
			Sharks	Rays	Species in common with this study	
Gulf of California, Mexico	2004–2005	4–137	3	16	8	López-Martínez et al.[1]
Guatemala	1996–1998	10–100	–	13	11	Ixquiac-Cabrera et al.[2]
Costa Rica	2008–2012	25–350	6	19	–	This study
Costa Rica	1983–1984	10–100	4	13	12	Campos[3]
Colombia	1993–1994, 1995–2007	10–360	11	13	14	Puentes et al.[4]

[1] López-Martínez, J., E. Herrera-Valdivia, J. Rodríguez-Romero, and S. Hernández-Vázquez. 2010. Peces de la fauna de acompañamiento en la pesca industrial de camarón en el Golfo de California, México. Rev. Biol. Trop. 58:925–942.
[2] Ixquiac-Cabrera, M., I. Franco, J. Lemus, S. Méndez, and A. López-Roulet. 2010. Identificación, abundancia, distribución espacial de batoideos (rayas) en el Pacífico Guatemalteco. Proyecto FONDECYT No. 34-2006, 79 p. [Available at website.]
[3] Campos, J. A. 1986. Fauna de acompañamiento del camarón en el Pacífico de Costa Rica. Rev. Biol. Trop. 34:185–197.
[4] Puentes, V., N. Madrid, and L. A. Zapata. 2007. Catch composition of the deep sea shrimp fishery (*Solenocera agassizi* Faxon, 1893; *Farfantepenaeus californiensis* Holmes, 1900 and *Farfantepenaeus brevirostris* Kingsley, 1878), in the Colombian Pacific Ocean. Gayana 71:84–95. Article

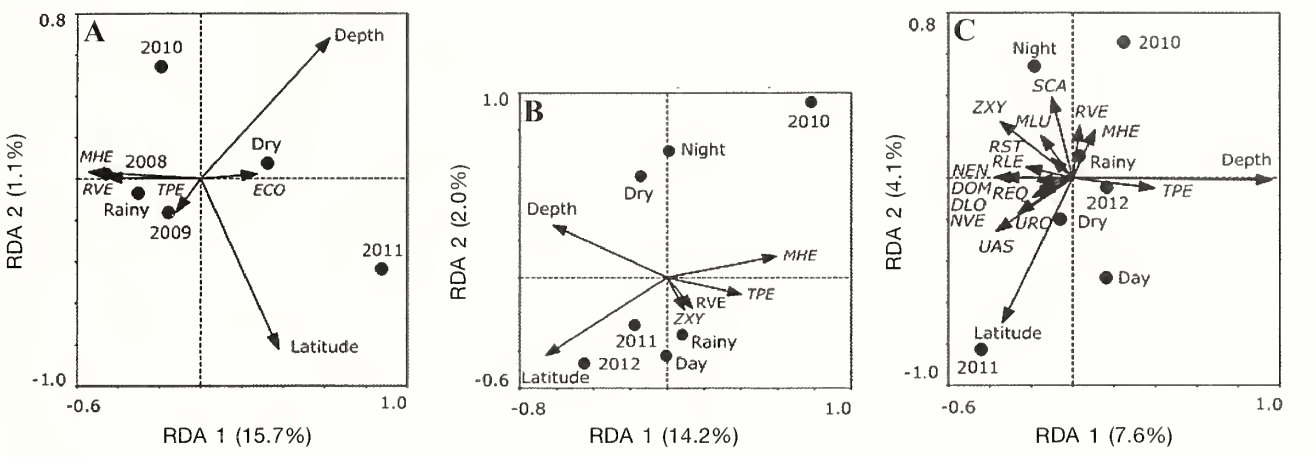

Figure 6

Redundancy analysis between environmental variables and elasmobranch abundance (measured as catch per unit of effort [CPUE]) along the Pacific coast of Costa Rica. Dependent variables were CPUE of species caught (**A**) in deepwater surveys (2008–2011); (**B**) in monitoring surveys in the central Pacific region (2010–2012); and (**C**) in commercial surveys in the central Pacific region (2010–2012). Environmental variables were depth, latitude, year, season (rainy, dry), and diel period. Circles represent categorical variables, and arrows represent continuous variables. The values given in parentheses on the axes are the percentages of variation in the total species–environmental data represented in the biplots. The length of the vector arrow indicates the strength of the correlation, and its direction indicates the relationship with a species. The following species abbreviations are used: MHE (brown smoothhound [*Mustelus henlei*]), RVE (rasptail skate [*Raja velezi*]), TPE (Peruvian torpedo [*Torpedo peruviana*]), ZXY (witch guitarfish [*Zapteryx xyster*]), SCA (Pacific angel shark [*Squatina californica*]), MLU (sicklefin smoothhound [*Mustelus lunulatus*]), RST (golden cownose ray [*Rhinoptera steindachneri*]), RLE (whitesnout guitarfish [*Rhinobatos leucorhynchus*]), NEN (giant electric ray [*Narcine entemedor*]), DOM (bullseye electric ray [*Diplobatis ommata*]), REQ (equatorial skate [*Raja equatorialis*]), DLO (longtail stingray [*Dasyatis longa*]), NVE (vermiculate electric ray [*Narcine vermiculatus*]), URO (thorny stingray [*Urotrygon rogersi*]), and UAS (Panamic stingray [*Urotrygon aspidura*]).

elasmobranchs in this study. Similar observations have been documented for other tropical shrimp fisheries in Costa Rica (Campos, 1986), Australia (Stobutzki et al., 2001), and Mexico (López-Martínez et al., 2010). Elasmobranch bycatch from bottom-trawl fisheries is assumed to reflect the composition of demersal species; however, it is important to consider that trawling gear is designed for soft and sandy bottoms. Therefore, species that use reef or hardbottom habitats are likely to be underrepresented in bottom-trawl fisheries (López-Martínez et al., 2010). Similarly, fast-swimming or pelagic elasmobranchs (e.g., spotted eagle ray [*Aetobatus laticeps*], golden cownose ray, and scalloped hammerhead [*Sphyrna lewini*]) are less likely to be caught by bottom trawls.

The assemblage of shallow-water elasmobranchs (depths <50 m) comprised 22 species, among which the Panamic stingray was the most abundant. High abundances of small rays also have been reported for shallow-water bycatch in Colombia (Mejía-Falla and Navia[1]) and the Gulf of California (Rábago-Quiroz et al., 2011). In our study, patchy distributions and large aggregations were observed for many small round stingrays (*Urotrygon* spp.) and electric rays (*Narcine* spp.), possibly as a result of high food availability (Vianna and Vooren, 2009; Knip et al., 2010) or reproductive behavior (Vianna and Vooren, 2009).

Elasmobranch bycatch associated with the shrimp fishery in Costa Rica was first described by Campos (1986). Differences in sampling methods, however, prevent direct comparisons with our study. For example, we examined the total catch of elasmobranchs, but Campos (1986) analyzed only a small subsample of that catch in 1983–1984. Moreover, Campos (1986) surveyed a smaller depth range (<100 m), and reported only 9 batoids (skates and rays), 4 sharks, and 4 unidentified batoid species. Our study revealed the occurrence of 17 batoid and 5 shark species at similar depths. The dominant species observed by Campos (1986) in 1983–1984 were rasptail skate, witch guitarfish, and giant electric ray, but only those first 2 species were abundant in our study.

Contrary to our results, the brown smoothhound and Panamic stingray were absent or present in very low abundances during the study by Campos (1986). These results support reports based on the traditional ecological knowledge of fishermen that large aggregations of the Panamic stingray are part of recently observed shifts in the demersal assemblages off the Pacific coast of Costa Rica (senior author, personal observ.). Moreover, 11 species of batoids were found in our survey

that were absent in the study conducted during 1983–1984 (Campos, 1986). Conversely, the whitenose shark (*Nasolamia velox*) and scalloped bonnethead (*Sphyrna corona*) were caught during 1983–1984 but were absent in our surveys. The overall lower abundance of elasmobranchs reported by Campos (1986) may be related to differences in the sample size or to actual changes in demersal elasmobranch diversity, changes that probably were due to the loss of top predatory fishes (Dulvy et al., 2014; Stevens et al., 2000).

The elasmobranch assemblage at depths of 100–350 m comprised only 6 species, among which the most abundant were the rasptail skate, brown smoothhound, and Peruvian torpedo. The prickly shark, which inhabits depths up to 1100 m, was the only true deepwater elasmobranch in this assemblage (Compagno et al., 2005). Only one previous study has examined deepwater elasmobranches within the ETP (Puentes et al., 2007), and that study reported 8 elasmobranch species at depths between 72 and 360 m in Colombia. Additional studies are necessary to broaden our knowledge about deepwater communities of elasmobranchs in this region and about their relation to physical and biological features.

Because of the inherently slow growth of deepwater elasmobranchs, future studies should also focus on the interaction between deepwater species and fisheries (Simpfendorfer and Kyne, 2009). These emergent deepwater fisheries are rarely subjected to management or scientific monitoring. In Costa Rica, shrimp trawl fisheries expanded into deeper waters in the 1980s. As the deepwater shrimp stocks became rapidly depleted, the fishing fleet shifted operations to shallow waters, where they now target several economically important teleosts, such as the Pacific bearded brotula (*Brotula clarkae*) (senior author, unpubl. data). This change is problematic; for example, one of the main findings in our study was the high species richness of elasmobranchs associated with shallow waters. This shift in the target species of shrimp fisheries may increase the effects of this fishery on coastal demersal ecosystems.

A few elasmobranch bycatch species, including smoothhounds (*Mustelus* spp.) and the longtail stingray, are commonly retained in Costa Rica because of their commercial value. The sicklefin smoothhound is an important source of affordable protein in local markets in Costa Rica, and there is a growing demand for longtail stingray in both Mexico and Costa Rica (Rojas et al., 2000). In addition to noting that these species are caught by shrimp trawlers, López Garro et al. (2009) reported that the sicklefin smoothhound and longtail stingray composed 16.7% and 3.5%, respectively, of the landings of elasmobranchs in the artisanal fishery of Tárcoles, in the central Pacific region of Costa Rica during 2006–2007. Although current records are insufficient for an evaluation of long-term trends in abundance of elasmobranchs in Costa Rica, catch data from Colombian commercial shrimp fisheries indicate that abundances of the sicklefin smoothhound and longtail stingray have declined considerably since the 1990s.[1] Therefore, it seems advisable to closely monitor trends in the relative abundance of these 2 species.

Our results indicate that a large number of elasmobranchs interact with the demersal trawl fishery of Costa Rica and, therefore, may be vulnerable to high levels of exploitation. Comparisons with historical data (Campos, 1986) revealed that the species composition of elasmobranchs might have changed since the 1980s. Yet, given the lack of continuous sampling throughout the period 1980–2010, it is difficult to identify the drivers behind these changes.

The creation of independent observer programs would allow monitoring and assessment of long-term trends of bycatch, as well as prediction of potential changes in fish assemblages. In addition, knowledge of the feeding ecology and trophic interactions of elasmobranchs is critical to understanding food web dynamics and trophic cascades that may occur as a result of the loss of top predatory fishes from coastal ecosystems (Ferretti et al., 2008; Heithaus et al., 2008). This information is also essential for defining the role of mesopredators in demersal ecosystems and for developing ecosystem-based management strategies (Espinoza et al., 2015). Future research on the life history traits of these species is also necessary and will allow us to identify vulnerable species and redirect conservation efforts. The interaction between the shrimp trawl fishery and the elasmobranch assemblage may be comparable within the different countries of Central America (López-Martínez et al., 2010; Clarke et al., 2014). Therefore, the results of this study may serve as biological information that can support the development of management strategies in Central America.

Acknowledgments

This research was supported financially by Conservación Internacional, MarViva, the Universidad de Costa Rica (VI project no. 808-B0-536; 111-A4-508), and the Rainbow Jewels S. A., Puntarenas, Costa Rica. We are grateful for the collaboration of *Onuva* crewmembers D. Petete, J. Nivia, J. S. Vargas, N. Sandoval, V. Sanabria, J. C. Azofeifa, M. Herrera, F. Vargas, A. Chacón, A. Lanyon, A. Alvarado, and F. Villalobos-Rojas. G. Ávalos and H. Molina provided constructive ideas at an earlier stage of the manuscript.

Literature cited

Allen, A. P., J. H. Brown, and J. F. Gillooly.
2002. Global biodiversity, biochemical kinetics, and the energetic-equivalence rule. Science 297:1545–1548.

Arana, P. M, I. S. Wehrtmann, J. C. Orellana, V. Nielsen-Muñoz, and F. Villalobos-Rojas.
2013. Bycatch associated with fisheries of *Heterocarpus vicarius* (Costa Rica) and *Heterocarpus reedi* (Chile)

(Decapoda:Pandalidae): a six-year study (2004–2009). J. Crustac. Biol. 33:198–209.

Barker, M. J., and V. Schluessel.
2005. Managing global shark fisheries: suggestions for prioritizing management strategies. Aquat. Conserv.: Mar. Freshw. Ecosyst. 15:325–347.

Borcard, D., F. Gillet, and P. Legendre.
2011. Numerical ecology with R, 306 p. Springer, New York.

Bussing, W. A., and M. I. López.
1993. Peces demersales y pelágicos costeros del Pacifico de Centro América meridional, 164 p. Editorial Universidad de Costa Rica, San José, Costa Rica.
2009. Marine fish. *In* Marine biodiversity of Costa Rica, Central America (I. S Wehrtmann, and J. Cortés, eds.), p. 453–458. Springer, Berlin.

Campos, J. A.
1986. Fauna de acompañamiento del camarón en el Pacífico de Costa Rica. Rev. Biol. Trop. 34:185–197.

Carlisle, A., A. King, G. M. Cailliet, and J. S. Brennan.
2007. Long-term trends in catch composition from elasmobranch derbies in Elkhorn Slough, California. Mar. Fish. Rev. 69(1–4):25–45.

Cheung, W. W. L., T. J. Pitcher, and D. Pauly.
2005. A fuzzy logic expert system to estimate intrinsic extinction vulnerabilities of marine fishes to fishing. Biol. Conserv. 124:97–111.

Clarke, K. R., and R. M. Warwick.
2001. Change in marine communities. an approach to statistical analysis and interpretation, 2nd ed., 172 p. PRIMER-E Ltd., Plymouth, UK.

Clarke, T. M., M. Espinoza, and I. S. Wehrtmann.
2014. Reproductive ecology of demersal elasmobranchs from a data-deficient fishery, Pacific of Costa Rica, Central America. Fish. Res. 157:96–105.

Compagno, L., M. Dando, and S. Fowler.
2005. Sharks of the world, 496 p. Princeton Univ. Press, Princeton, NJ.

Conrath, C.
2005. Reproductive biology. *In* Management techniques for elasmobranch fisheries. FAO Fish. Tech. Pap. 474 (J. A. Musick and R. Bonfil, eds.), p. 103–126. FAO, Rome.

Cortés, E.
2000. Life history patterns and correlations in sharks. Rev. Fish. Sci. 8:299–344.

Dulvy, N. K., S. L. Fowler, J. A Musick, R. D. Cavanagh, P. M. Kyne, L. R. Harrison, J. K. Carlson, L. N. K. Davidson, S. V. Fordham, M. P. Francis, C. M. Pollock, C. A. Simpfendorfer, G. H. Burgess, K. E. Carpenter, L. J. V. Compagno, D. A. Ebert, C. Gibson, M. R. Heupel, S. R. Livingstone, J. C. Sanciangco, J. D. Stevens, S. Valenti, and W. T White.
2014. Extinction risk and conservation of the world's sharks and rays. eLife 3:e00590.

Dulvy, N. K., and J. D. Reynolds.
2002. Predicting extinction vulnerability in skates. Conserv. Biol. 16:440–450. Article

Dulvy, N. K., J. K. Baum, S. Clarke, L. J. V. Compagno, E. Cortés, A. Domingo, S. Fordham, S. Flower, M. P. Francis, C. Gibson, J. Martínez, J. A. Musick, A. Soldo, J. D. Stevens, and S. Valenti.
2008. You can swim but you can't hide: the global status and conservation of oceanic pelagic sharks and rays. Aquat. Conserv.: Mar. Freshw. Ecosyst. 18:459–482.

Espinoza, M., T. J. Farrugia, and C. G. Lowe.
2011. Habitat use, movements and site fidelity of the gray smooth-hound shark (*Mustelus californicus* Gill 1863) in a newly restored Southern California estuary. J. Exp. Mar. Biol. Ecol.:401:63–74.

Espinoza, M., T. M. Clarke, F. Villalobos-Rojas, and I. S. Wehrtmann.
2012. Ontogenetic dietary shifts and feeding ecology of the rasptail skate *Raja velezi* and the brown smoothhound shark *Mustelus henlei* along the Pacific coast of Costa Rica, Central America. J. Fish Biol. 81:1578–1595.
2013. Diet composition and diel feeding behavior of the banded guitarfish *Zapteryx xyster* along the Pacific coast of Costa Rica, Central America. J. Fish Biol. 82:286–305.

Espinoza, M., S. E. M. Munroe, T. M. Clarke, A. T. Fisk, and I. S. Wehrtmann.
2015. Feeding ecology of common demersal elasmobranch species in the Pacific coast of Costa Rica inferred from stable isotope and stomach content analyses. J. Exp. Mar. Biol. Ecol. 470:12–25.

FAO (Food and Agriculture Organization).
1995. Code of conduct for responsible fisheries, 41 p. FAO, Rome.

Ferretti, F., R. A. Myers, F. Serena, and H. K. Lotze.
2008. Loss of large predatory sharks from the Mediterranean Sea. Conserv. Biol. 22:952–964.

Fiedler, P. C.
2002. The annual cycle and biological effects of the Costa Rica Dome. Deep-Sea Res. Oceanogr., A 49:321–338.

Fiedler, P. C., and L. D. Talley.
2006. Hydrography of the eastern tropical Pacific: a review. Prog. Oceanogr. 69:143–180.

Frisk, M. G., T. J. Millar, and N. K. Dulvy.
2005. Life histories and vulnerability to exploitation of elasmobranchs: inferences from elasticity, perturbation and phylogenetic analyses. J. Northwest Atl. Fish. Sci. 35:27–45.

Gouraguine, A., M. Hidalgo, J. Moranta, D. M. Bailey, F. Ordines, B. Guijarro, M. Valls, C. Barberá, and A. De Mesa.
2011. Elasmobranch spatial segregation in the western Mediterranean. Sci. Mar. 75:653–664.

Graham, K. J., N. L. Andrew, and K. E. Hodgson.
2001. Changes in relative abundance of sharks and rays on Australian South East Fishery trawl grounds after twenty years of fishing. Mar. Freshw. Res. 52:549–561.

Heithaus, M. R., A. Frid, A. J. Wirsing, and B. Worm.
2008. Predicting ecological consequences of marine top predator declines. Trends Ecol. Evol. 23:202–210.

Hernáez, P., T. M. Clarke, C. Benavides-Varela, F. Villalobos-Rojas, J. Nívia-Ruiz, and I. S. Wehrtmann.
2011. Population demography and spatial distribution of the mantis shrimp *Squilla biformis* (Stomatopoda, Squillidae) from Pacific Costa Rica. Mar. Ecol. Prog. Ser. 424:157–168.

Hight, B. V., and C. G. Lowe.
2007. Elevated body temperatures of adult female leopard sharks, *Triakis semifasciata*, while aggregating in shallow nearshore embayments: evidence for behavioral thermoregulation? J. Exp. Mar. Biol. Ecol. 352:114–128.

Jacoby, D. M.P., D. P. Croft, and D. W. Sims.
2012. Social behaviour in sharks and rays: analysis, patterns and implications for conservation. Fish Fish. 13:399–417.

Jiménez, C.
2001. Seawater temperature measured at the surface and at two depths (7 and 12 m) in one coral reef at Culebra Bay, Gulf of Papagayo, Costa Rica. Rev. Biol. Trop. 49:153–161.
Knip, D. M., M. R. Heupel, and C. A. Simpfendorfer.
2010. Sharks in nearshore environments: models, importance, and consequences. Mar. Ecol. Prog. Ser. 402:1–11.
Leathwick, J. R., J. Elith, M. P. Francis, T. Hastie, and P. Taylor.
2006. Variation in demersal fish species richness in the oceans surrounding New Zealand: an analysis using boosted regression trees. Mar. Ecol. Prog. Ser. 321:267–281.
Levinton, J. S.
1995. Marine biology: function, biodiversity, ecology, 420 p. Oxford Univ. Press, New York.
López Garro, A., R. Arauz Vargas, I. Zanella, and L. Le Foulgo.
2009. Análisis de las capturas de tiburones y rayas en las pesquerías artesanales de Tárcoles, Pacífico central de Costa Rica. Rev. Cienc. Mar. Cost. 1:145–157.
López-Martínez, J., E. Herrera-Valdivia, J. Rodríguez-Romero, and S. Hernández-Vázquez.
2010. Peces de la fauna de acompañamiento en la pesca industrial de camarón en el Golfo de California, México. Rev. Biol. Trop. 58:925–942.
Lowe, C. G., R. N. Bray, and D. R. Nelson.
1994. Feeding and associated electrical behavior of the Pacific electric ray *Torpedo californica* in the field. Mar. Biol. 120: 161–169.
MacPherson, E.
2003. Species range size distributions for some marine taxa in the Atlantic Ocean. Effect of latitude and depth. Biol. J. Linn. Soc. 80:437–455.
Massuti, E., and J. Moranta.
2003. Demersal assemblages and depth distribution of elasmobranchs from the continental shelf and slope off the Balearic Islands (western Mediterranean). ICES J. Mar. Sci. 60:753–766.
Mejía-Falla, P. A., and A. F. Navia.
2011. Relationship between body size and geographic range size of elasmobranchs from the Tropical Eastern Pacific: an initial approximation for their conservation. Cienc. Mar. 37:305–321.
Molina, J. M., and S. J. Cooke.
2012. Trends in shark bycatch research: current status and research needs. Rev. Fish Biol. Fish. 22:719–737.
Mora, C., and D. R. Robertson.
2005. Causes of latitudinal gradients in species richness: a test with fishes of the Tropical Eastern Pacific. Ecology 86:1771–1792.
Pereyra, I., L. Orlando, W. Norbis, and L. Paesch.
2008. Spatial and temporal variation of length and sex composition of the narrownose smooth-hound *Mustelus schmitti* Springer, 1939 in the trawl fishery off the oceanic coast of Uruguay during 2004. Rev. Biol. Mar. Oceanogr. 43:159–166.
Priede, I. G., R. Froese, D. M. Bailey, O. A. Bergstad, M. A. Collins, J. E. Dyb, C. Henriques, E. G. Jones, and N. King.
2006. The absence of sharks from abyssal regions of the world's oceans. Proc. R. Soc. Ser., B 273:1435–1441.
Puentes, V., N. Madrid, and L. A. Zapata.
2007. Catch composition of the deep sea shrimp fishery (*Solenocera agassizi* Faxon, 1893; *Farfantepenaeus californiensis* Holmes, 1900 and *Farfantepenaeus brevirostris* Kingsley, 1878), in the Colombian Pacific Ocean. Gayana 71:84–95.
Quesada-Alpízar, M. A., and J. Cortés.
2006. Los ecosistemas marinos del Pacífico sur de Costa Rica: estado del conocimiento y perspectivas de manejo. Rev. Biol. Trop. 54:101–145.
R Core Team.
2013. R: a language and environment for statistical computing. R Foundation for Statistical Computing, Vienna, Austria. [Available at website, accessed January 2014.]
Rábago-Quiroz, C. H., J. López-Martínez, J. E. Valdez-Holguín, and M. O. Nevárez-Martínez.
2011. Distribución latitudinal y batimétrica de las especies más abundantes y frecuentes en la fauna acompañante del camarón del Golfo de California, México. Rev. Biol. Trop. 59:255–267.
Robertson, D. R., and K. L. Cramer.
2009. Shore fishes and biogeographic subdivisions of the Tropical Eastern Pacific. Mar. Ecol. Prog. Ser. 380:1–17.
Rodríguez-Romero, J., D. S. Palacios-Salgado, J. López-Martínez, S. Hernández-Vázquez, and G. Ponce-Díaz.
2008. Composición taxonómica y relaciones zoogeográficas de los peces demersales de la costa occidental de Baja California Sur, México. Rev. Biol. Trop. 56:1765–1783.
Rojas, J. M. R., J. Campos, M. A. Segura, M. Mug, V. R. Campos, and O. Rodríguez.
2000. Shark fisheries in Central America: a review and update. Uniciencia 17:49–56.
Shepherd, T. D., and R. A. Myers.
2005. Direct and indirect fishery effects on small coastal elasmobranchs in the northern Gulf of Mexico. Ecol. Lett. 8:1095–1104.
Simpfendorfer, C. A., and P. M. Kyne.
2009. Limited potential to recover from overfishing raises concerns for deep-sea sharks, rays and chimaeras. Environ. Conserv. 36:97–103.
Smith, K. F., and J. H. Brown.
2002. Patterns of diversity, depth range and body size among pelagic fishes along a gradient of depth. Global Ecol. Biogeogr. 11:313–322.
Speed, C. W., M. G. Meekan, I. C. Field, C. R. McMahon, and C. J. A. Bradshaw.
2012. Heat-seeking sharks: support for behavioural thermoregulation in reef sharks. Mar. Ecol. Prog. Ser. 463:231–245.
Stefánsson, G.
1996. Analysis of groundfish survey abundance data: combining the GLM and delta approaches. ICES J. Mar. Sci. 53:577–588.
Stevens, J. D., R. Bonfil, N. K. Dulvy, and P. A. Walker.
2000. The effects of fishing on sharks, rays, and chimaeras (chondrichthyans), and the implications for marine ecosystems. ICES J. Mar. Sci. 57:476–494.
Stobutzki, I. C., M. J. Miller, P. Jones, and J. P. Salini.
2001. Bycatch diversity and variation in a tropical Australian penaeid fishery; the implications for monitoring. Fish. Res. 53:283–301.
Tascheri, R., J. C. Savedra-Nievas, and R. Roa-Ureta.
2010. Statistical models to standardize catch rates in the multi-species trawl fishery for Patagonian grenadier (*Macruronus magellanicus*) of Southern Chile. Fish. Res. 105:200–214.

Venables, W. N., and C. M. Dichmont.
2004. GLMs, GAMs and GLMMs: an overview of theory for applications in fisheries research. Fish. Res. 70:319–337.

Venables, W. N., and B. D. Ripley.
2002. Modern Applied Statistics with S, 4th ed, 498 p. Springer, New York, NY.

Vianna, G. M. S., and C. M. Vooren.
2009. Distribution and abundance of the lesser electric ray *Narcine brasiliensis* (Olfers, 1831) (Elasmobranchii: Narcinidae) in southern Brazil in relation to environmental factors. Braz. J. Oceanogr. 57:105–112.

Walker, T. I.
2005. Management measures. *In* Management techniques for elasmobranch fisheries. F AO Fish Tech. Pap. 474 (J. A. Musick, and R. Bonfil, eds.), p. 216–242. FAO, Rome.

Wearmouth, V. J., and D. W. Sims.
2008. Sexual segregation of marine fish, reptiles, birds and mammals: behavior patterns, mechanisms and conservation implications. Adv. Mar. Biol. 54:107–170.

Wehrtmann, I. S., P. M. Arana, E. Barriga, A. Gracia, and P. R. Pezzuto.
2012. Deep-water shrimp fisheries in Latin America: a review. Latin Am. J. Aquat. Res. 40:497–535.

Wehrtmann, I. S., and J. Cortés (eds.).
2009. Marine biodiversity of Costa Rica, Central America. Monogr. Biol. 86, 572 p. Springer, Berlin.

Wehrtmann, I. S., and V. Nielsen-Muñoz.
2009. The deepwater fishery along the Pacific coast of Costa Rica, Central America. Lat. Am. J. Aquat. Res. 37:543–554.

White, W. T., and E. Sommerville.
2010. Elasmobranchs of tropical marine ecosystems. *In* Sharks and their relatives II: biodiversity, adaptive physiology, and conservation (J. C. Carrier, J. A Musick, and M. R. Heithaus, eds.), p. 159–240. CRC Press, Boca Raton, FL.

Worm, B., B. Davis, L. Kettemer, C. A.Ward-Paige, D. Chapman, M. R. Heithaus, S. T. Kessel, and S. H. Gruber.
2013. Global catches, exploitation rates, and rebuilding options for sharks. Mar. Policy 40:194–204.

NOAA
National Marine
Fisheries Service

Fishery Bulletin
established 1881

Spencer F. Baird
First U.S. Commissioner
of Fisheries and founder
of Fishery Bulletin

Age, growth, and recruitment of larval and early juvenile Atlantic croaker (*Micropogonias undulatus*), determined from analysis of otolith microstructure

Matthew J. Kupchik (contact author)[1]
Richard F. Shaw[2]

Email address for contact author: mkupch1@lsu.edu

[1] Department of Oceanography and Coastal Sciences
School of the Coast and Environment
Louisiana State University
2143 Energy, Coast, and Environment Building
Baton Rouge, Louisiana 70803

[2] Department of Oceanography and Coastal Sciences
School of the Coast and Environment
Louisiana State University
002Q Energy, Coast, and Environment Building
Baton Rouge, Louisiana 70803

Abstract—The Atlantic croaker (*Micropogonias undulatus*) is an important commercial species in the Gulf of Mexico, but this stock has been reduced historically as bycatch in other fisheries. Sagittal otoliths (N=190) were removed from larval and early juvenile Atlantic croaker collected within a Louisiana tidal pass over a 2-year period, from October 2006 through March 2007 and from September 2007 through March 2008. Standard length (SL) at age in days after hatching (dah), over both years, was fitted with a Laird-Gompertz growth model, and similar models were fitted separately to year and season to determine whether different spawning subgroups existed. In both years, the maximum growth rate occurred 20 days earlier in spring than in fall. Otolith microstructure measurements were used to determine the age (~40 dph) at which larvae encountered differing water mass characteristics of the coastal boundary zone (the offshore to inshore recruitment corridor). Growth rates increased after fish encountered lower-salinity (<20) waters of the coastal boundary zone and estuary of Bayou Tartellan, LA. Temporal variability in spawning of Atlantic croaker, determined with age–length keys, revealed that the highest frequency of hatch dates occurred during November in 2006 and 2007.

Manuscript submitted 28 July 2014.
Manuscript accepted 13 October 2015.
Fish. Bull. 114:18–33 (2016).
Online publication date: 5 November 2015.
doi. 10.7755/FB.114.1.2

The Atlantic croaker (*Micropogonias undulatus*) in the western Atlantic range from the Gulf of Maine to the northern Gulf of Mexico (GOM). That range potentially may extend into the southern GOM, the Lesser Antilles, and southern Caribbean and from Brazil through southern Argentina (Smith, 1997). The status of the Atlantic croaker stock is unknown (NMFS, 2009), although it is expected to be below maximum sustainable yield. The amount of Atlantic croaker harvested commercially has been cyclic, ranging from 1100 metric tons (t) per year to more than 15,000 t per year; annual levels recently were estimated at approximately 9000 t, with a value of approximately $8 million (NMFS, 2012). These fluctuations reflect the high variability in recruitment patterns driven by both small and large spatial and temporal scales of environmental conditions, such as wind field patterns, storm frequency, salinity, temperature, hypoxic zones, and local hydrographic features (Norcross, 1983; Norcross and Austin, 1988; Able, 2005; Eby et al., 2005; Montane and Austin, 2005).

The commercial stock is further affected by the amount of Atlantic croaker that is caught as bycatch, principally through shrimp trawling—an amount that is calculated to be 60–80% of the catch by weight (NMFS, 2012). The amount of Atlantic croaker caught annually as bycatch can total from 100,000 to 400,000 t, and data from the 1990s indicated that Atlantic croaker may have made up almost 73% of the total bycatch of short-lived demersal species (NMFS, 2009, 2012). The results of analysis of samples collected during 1986–2006 by Southeast Area Monitoring and Assessment Program crews show that the Atlantic croaker, which was classified as a bycatch species, to be the dominant species by weight at depths less than 30 m off the Louisiana coast (Helies and Jamison[1]). At depths

[1] Helies, F. C., and J. L. Jamison. 2009. Reduction rates, species composition, and effort: assessing bycatch within the Gulf of Mexico shrimp trawl fishery. NOAA/NMFS Cooperative Agreement Number NA07NMF4330125 (#101). Final Report, 182 p. Gulf and South Atlantic Fisheries Foundation Inc., Tampa, FL. [Available at website.]

greater than 30 m, the Atlantic croaker was either the second or third bycatch taxon by weight, depending on sampling period (Helies and Jamison[1]). This high level of bycatch and directed fishing-induced mortality may increase the importance of minor variations in mortality rates of the early life history stages to overall stock success, variations that greatly affect recruitment rates (Norcross, 1983; Diamond et al., 2000).

A peak in spawning occurs from July through December and in larval estuarine recruitment during October–November (Cowan, 1988; Ditty et al., 1988; Warlen and Burke, 1990; Barbieri et al., 1994a). Atlantic croaker spawn over a wide range of inner continental shelf depths (i.e., 54 m or shallower), and a portion of the population moves inshore toward estuaries to complete spawning during the winter and early spring months (Barbieri et al., 1994a, 1994b). Hydrologic variability at large and small spatial and temporal scales can greatly affect the numbers of Atlantic croaker larvae able to successfully recruit to estuarine nursery grounds (Norcross, 1983; Shaw et al., 1988; Raynie, 1991; Raynie and Shaw, 1994). Once larvae are in the estuary, lower water temperatures in the first winter increase their mortality rate as verified in both the field (Norcross and Austin, 1988; Hare and Able, 2007) and laboratory (Lankford and Targett, 2001a, 2001b).

Previous studies on age and growth of Atlantic croaker generally have focused on the Mid-Atlantic Bight (MAB) and South Atlantic Bight (SAB), however, limited studies have occurred in the GOM. For these studies, linear growth rate models have been created from counts of daily rings within otoliths and paired readers have found growth rates between 0.16 and 0.27 mm/d (Warlen, 1982; Thorrold et al., 1997); in the GOM, the growth rate for this species has been determined to be 0.19 mm/d (Cowan, 1988). The occurrences of higher growth rates for larval Atlantic croaker during the spawning and estuarine recruitment peak in the late summer and early fall and of lower larval growth rates during the overwinter period and into the spring have led to the notion that different spawning subgroups may exist (Warlen, 1982). This hypothesis is further supported by differences in growth rates and recruitment dynamics that are based on latitude along the estuaries of the MAB and SAB (Barbieri et al., 1994b; Thorrold et al., 1997).

Daily formation of otolith increments have been confirmed in *Micropogonias* (Campana, 1984; Cowan, 1988; Albuquerque et al., 2009), making such increments a reliable proxy for age. Otolith rings for larval fish, formed daily, not only can provide information on growth rates but can also be used to estimate approximate times of larval estuarine ingress (i.e., transport time from offshore spawning grounds to estuarine nurseries) (Hoover et al., 2012). The approximate timing of larval and early juvenile ingress of Atlantic croaker to estuarine nurseries from offshore spawning grounds in the MAB and SAB has been estimated to vary between 30 and 60 d after hatching. (Warlen, 1980; Warlen and Burke, 1990; Hettler and Hare, 1998; Hoskin, 2002; Hoover et al., 2012). Daily otolith rings have been also used to examine environmental parameters that affect growth and survivorship (Campana, 1999; Campana and Thorrold, 2001) and to determine within-season cohorts for Atlantic herring (*Clupea harengus*), on the basis of variable growth between seasons in the same year (Brophy and Danilowicz, 2002). Larval otolith growth rings and microstructure were initially examined through direct observation by paired readers using light microscopy; however, video and digital methods have become prevalent with the increase in image resolution from high-mexapixel digital imaging sensors (Ralston and Williams, 1989; Campana, 1992; Morales-Nin et al., 1998).

For this study, we had 5 primary objectives. The first objective was to define and determine an iterative digital filtering mechanism that can provide a more accurate and automated determination of daily increments in otoliths of larval Atlantic croaker. The second objective was to determine the length at age of Atlantic croaker larvae collected in a tidal pass in the northern GOM from fall through spring over a 2-year recruitment period. The third objective was to compare observed larval growth rates determined from linear and nonlinear growth models with those determined from previous studies. The fourth objective was to estimate, on the basis of ring counts corrected for hatching date and time at first ring formation, times for estuarine ingress through the tidal pass from the coastal boundary zone. Finally, the fifth objective was to determine the effect of hydrodynamic patterns associated with differences between continental shelf and estuarine waters on growth of larval and early juvenile Atlantic croaker.

Materials and methods

Sampling location

Ichthyoplankton sampling was conducted in Bayou Tartellan, near Port Fourchon, Belle Pass, Louisiana (Fig. 1A). Bayou Tartellan and Bayou LaFourche are the first major inland channel bifurcations from the connection with the GOM at Belle Pass (29°5′ 53.9″N, 90°13′17.8″W). The location of sampling was within a seasonally well-mixed tidal pass (i.e., tidal pass with little stratification in temperature, salinity or dissolved oxygen) that has high turbidity and a relatively small drainage basin that contributes a very low volume of freshwater input. The site (Fig. 1B; 29°6.82′N, 90°11.07′W) where passive sampling was conducted with a plankton net was located at the end of a dock that extended 3.7 m into the tidal pass from the northern bank of Bayou Tartellan, and the site had a water depth of approximately 10 m.

Field sampling method

Ichthyoplankton sampling was conducted with a fixed davit placed at the end of the dock and from which

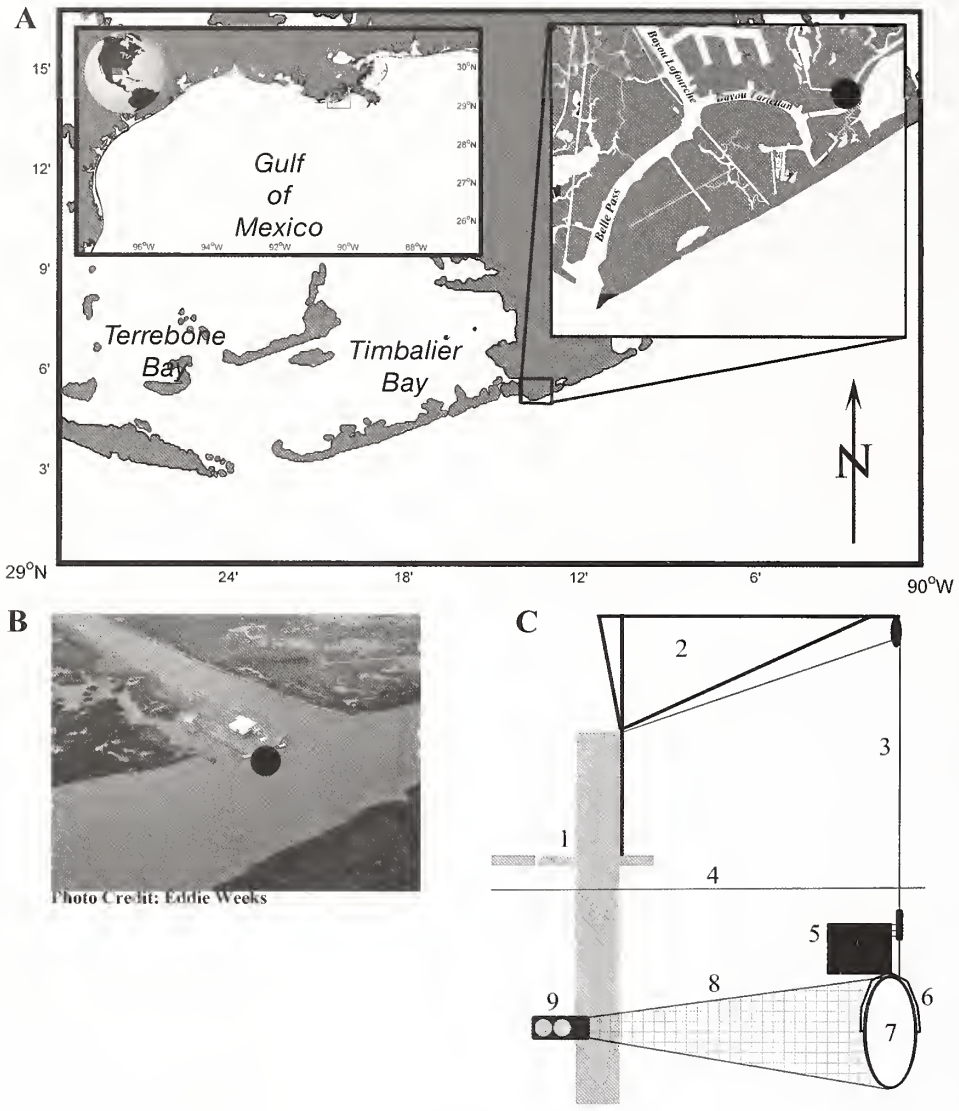

Figure 1

(**A**) Map of the sampling location for this study in relation to the Gulf of Mexico and coastal Louisiana. The upper right inset represents the area around Port Fourchon, Belle Pass, Louisiana, and the sampling site in Bayou Tartellan identified by a black circle on the map. Sampling for larval and juvenile Atlantic croaker (*Micropogonias undulatus*) was conducted from October 2006 through April 2007 and then from September 2007 through April 2008. (**B**) Aerial photograph of the sampling site on Bayou Tartellan; the black circle again identifies the sampling site. (**C**) Diagram of the sampling system: 1) fixed dock where the sampling system was attached, 2) davit that was used to extend the net farther into the channel, 3) cable system by which the net was raised and lowered, 4) water surface, 5) orientation vane for the net system, 6) 60-cm metal ring that held open the net mouth, 7) pivoting gimbal, 8) 333-µm mesh net, dyed dark green, and 9) plastic, vinyl-coated codend with 333-µm drainage ports.

a stainless steel cable was suspended from above the sampling deck to the channel bottom (Fig. 1C). Ichthyoplankton were sampled passively with a 60-cm ring net (333-µm mesh, 2-m length) that was dyed dark green to minimize visibility, and hence avoidance, and that was attached to a gimbal with a vane for orientation into the current. A plastic, vinyl-coated codend with 333-µm mesh drainage ports was attached to the end of the net to facilitate sample collection. A flowmeter (model no. 2030; General Oceanics[2], Miami, FL) with a

[2] Mention of trade names or commercial companies is for identification purposes only and does not imply endorsement by the National Marine Fisheries Service, NOAA.

slow-velocity rotor was positioned just off center of the ring to determine volume of filtered water.

Ichthyoplankton samples were collected every 4 h over a 72-h period, twice monthly from early October through April over a 2-year period (2006–2008), except December and January, when samples were taken only on a monthly basis. In addition, there were 2 sampling efforts made in September 2007. The sampling season was chosen to coincide with wind-dominant meteorological events (i.e., atmospheric cold front passages) from late fall to early spring and to increase the probability of collecting larvae and small juveniles (Hernandez et al., 2010). Individual sampling dates were chosen to match the largest astronomical tidal ranges. During passive sampling, one icthyoplankton collection was taken at the surface and another near the bottom. They were taken in random order for each sampling effort. Surface collections were 6 min long, and near-bottom collections were 10 min long to compensate for vertical differences in current speed and, ultimately, for volume of filtered water (i.e., sampling effort). For near-bottom collections, the net mouth was closed during deployment until the net was in position, was opened for sampling, and was closed for retrieval to prevent vertical contamination of the sample during transit through the water column. Surface collections had a mean filtered volume of 13.3 m^3 (standard deviation [SD] 16.8), and near bottom collections had a mean filtered volume of 16.6 m^3 (SD 22.4). Nets were washed down with a freshwater source to avoid biological contamination from marine taxa.

Ichthyoplankton samples were fixed initially for approximately 3.5 h in freshly made, buffered (sodium phosphate, dibasic $NaH_2PO_4 \cdot H_20$, and monobasic Na_2HPO_4) 10% formalin. Samples were then rinsed, thoroughly drained, and switched into a 70% ethanol solution. This procedure parallels methods described by Butler (1992). Although some studies have shown that formalin may damage otoliths of small specimens (Brothers, 1984), sagittal otoliths in other species have not shown evidence of dissolving (Ré, 1983; Landaeta et al., 2014), especially during very short exposures.

During each collection of icthyoplankton samples, estuarine hydrographic parameters were measured dockside with a portable YSI 85 instrument (YSI Inc., Yellow Springs, CO). A continuously sampling YSI 600R multiparameter water-quality sonde (YSI Inc.), moored on the bottom of the channel floor offshore of the dock, also measured the same parameters. Hydrographic data were downloaded periodically as necessary and archived. Predicted diurnal tides were obtained from NOAA's Center for Operational Oceanographic Products and Services (website) for a nearby tide gauge station at Port Fourchon (station ID: 8762075; 29°6.8 N, 90°11.9 W). Tide height data and the difference between the predicted and measured tidal prism were downloaded for that station.

A bottom-mounted, upward-looking acoustic Doppler current profiler (ADCP), a 1200-kHz broadband Workhorse H-ADCP (Teledyne RD Instruments, Poway, CA), was placed in the center of Bayou Tartellan (offshore of the dock), for the duration of the study, to measure the vertical profile of current velocity and direction. Boat surveys were also conducted along Bayou Tartellan and Bayou LaFourche out to Belle Pass through the use of downward-looking ADCPs to provide a channel-wide correction factor for the mid-channel, stationary upward-facing ADCP. A volume transport was calculated in cubic meters per second for Bayou Tartellan from these data. To remove the effects of tide and inertia, a sixth-order 40-h Butterworth low-pass filter (Roberts and Roberts, 1978) was applied to the raw volume transport to produce a net water transport (NWT). These net transport data effectively show the lower-frequency subtidal oscillations associated with atmospheric cold front events and other wind-forcing factors, and these data filter out the higher-frequency diurnal tidal oscillations (Li et al., 2009).

Laboratory methods

In the laboratory, ichthyoplankton collections with a volume of material greater than 200 mL were divided in half with a Motodo plankton splitter (Motodo Plankton Splitter, Aquatic Research Instruments, Hope, ID 83836), and those collections with a volume greater than 400 mL were split into quarters. Samples were sorted under a dissecting stereoscope, and all ichthyoplankton were removed. A subset of sorted samples was checked for completeness of ichthyoplankton removal by a second party and sorted again if necessary.

Ichthyoplankton were identified to the lowest taxonomic level possible, depending on size and physical condition of each organism. Some larval fishes that were difficult to identify were stained with Alizarin blue and Alizarin red to facilitate meristic counts. Atlantic croaker larvae and early juveniles (hereafter referred to as larvae for brevity) were separated and stored for otolith analysis. Identifications were based on literature from Fahay (1983), and Richards (2006).

Atlantic croaker larvae were subsampled for otolith analysis on the basis of a normal distribution of standard length (SL) of all specimens collected. Measurement of SL to the nearest 0.1 mm was conducted with a Leica MZ6 stereoscope (Leica Microsystems Inc., Buffalo Grove, IL) calibrated against a stage micrometer. Atlantic croaker larvae were sampled from every collection that contained this target species. For samples in which 3 or less Atlantic croaker larvae were collected, all larvae of this species were scheduled for otolith removal. For samples that contained more than 3 larvae of Atlantic croaker, 3 larvae, specifically the shortest and longest specimens, along with one that was closest to the mean SL for all Atlantic croaker in the sample, were selected and scheduled for otolith removal.

Otolith removal, preparation, and age interpretation

Removal and preparation of sagittal otoliths from Atlantic croaker larvae selected for dissection followed

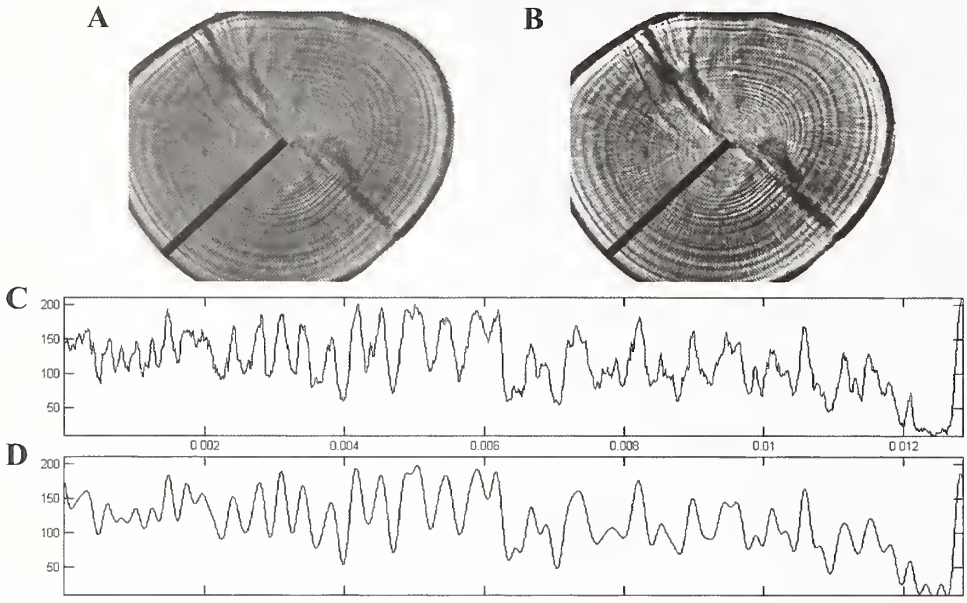

Figure 2

(**A**) Initial image taken under light microscopy of otolith from larval Atlantic croaker (*Micropogonias undulatus*) collected from Bayou Tartellan, Louisiana, from October 2006 through March 2007 and from September 2007 through March 2008. The black line from the center to the lower left represents the radius used for reading. (**B**) Otolith image after digital image enhancement. The black line from the center to the lower left is the same radius as the one on the previous image. (**C**) Initial grayscale measurement along the radius from the center of the otolith to the edge. (**D**) Grayscale measurements along the same radius after low pass filtering.

the method described by Barbieri et al. (1994a, 1994b). All dissections were conducted with an Olympus SZX12 stereoscope (Olympus Corp., Tokyo) with a 1× objective lens. Both left and right sagittal otoliths were removed and placed on a slide with Permount mounting medium (Thermo Fisher Scientific, Waltham, MA), the left otolith concave side up and the right otolith concave side down. Otoliths were polished with 0.3-µm alumina paste and a microcloth to reveal the core. Otoliths were etched with 0.1-N hydrochloric acid for between 10 and 20 s to facilitate readability under a compound stereoscope. Digital images were taken at a magnification from 500× to 1250× with an Olympus BX41 compound stereoscope equipped with a phase contrast filter to highlight light- and dark-ring discontinuity zones of otoliths with oil immersion (Fig. 2A).

Adobe Photoshop CS4, vers. 11.0 (Adobe Systems Inc., San Jose, CA) was used to convert the image from color to grayscale and to enhance differences between light and dark rings by increasing contrast and brightness (Fig. 2B). Measurements of otolith radii lengths, the distance from the otolith nucleus to the distal edge, and of grayscale values for each radius were conducted with ImageJ image analysis software, vers. 1.44p, (National Institutes of Health, Bethesda, MD). Measurement of each radius produced a calibrated length and corresponding grayscale values that ranged from 0 (black) to 255 (white) along that radius. A central radius and 2 radii to the left and right of the central radii, offset by a single pixel each, were measured. All 5 radii were averaged to produce the grayscale values later used for filter analysis, to avoid the bias that could be introduced by choice of the radius for reading (Morales-Nin et al., 1998). Radius length and grayscale data were collected for each otolith that was imaged (Fig. 2C).

Image data were imported into MATLAB, vers. 7.6.0.324 R2008a (The MathWorks Inc., Natick, MA) for filtering and nominal age determination. Low pass filter structure was determined with a fast Fourier transform (FFT) to transform the initial radii measurements into frequencies to identify and exclude high-frequency subdaily discontinuities from the otolith radius. The low-pass filter was fitted iteratively to the individual otoliths, on the basis of the understanding that the Nyquist frequency is the daily otolith increment accreted by the larvae. As noted by Morales-Nin et al. (1998), this iterative fitting is done for each otolith because of increments of varying radius length between otoliths, differences in magnification, and variable growth rates for individuals. An inverse FFT was then performed to transform the signal from the frequency domain back

into the distance measurements for location of the sinusoidal peaks and, therefore, of the position and width of the respective rings along the radius used for reading (Fig. 2D).

Ten otoliths were selected at random to be analyzed by using the traditional paired-reader method. These results were then used to compare them against 2 new, independently run FFT-generated ring counts. The same number of rings were observed for all 10 otoliths through the independently run FFT method, and only 1 otolith had a difference of 1 ring between the FFT method and the paired-reader method.

Otolith aging and larval hatching dates

Larval age, estimated as days after hatching (dah), was determined from the increment counts for each otolith radius with the methods previously described. Daily formation of increments has been validated and deposition has been confirmed to have a positive relationship to growth of larval Atlantic croaker (Searcy, 2005). Moreover, daily increment formation has been confirmed and validated for other species in the family Sciaenidae that live in similar environments, such as red drum (*Sciaenops ocellatus*; Wilson et al., 1987) and spot (*Leiostomus xanthurus*; Warlen and Chester, 1985). For the purposes of our analysis, we, therefore, assumed that increment deposition occurs daily. Following the methods used by Cowan (1988) and on the basis of laboratory work (Arnold[3]), we applied a 4-d lag for first increment formation after hatching for larvae of Atlantic croaker, (Warlen and Chester, 1985). This application resulted in a calculation of total age by adding 4 to the otolith count. Estimated ages were calculated for specimens for which otolith radii were measured. Ages were estimated for all other larvae and early juveniles not selected for dissection by using age–length keys and the FSA package for R software, vers. 2.13.0 (R Development Core Team, 2011). The hatching date was determined by subtracting the age (dah) from the date of collection.

Growth and timing of estuarine ingress

A linear model was run to allow direct comparison of our results with those of previous studies where a linear model was used. Larval growth of Atlantic croaker is slowest near the hatching date, increases thereafter, and slows again as larvae settle and begin further organ and sensory development; therefore, a derivative of the Gompertz model was selected as the nonlinear model for our study because it highlights this specific pattern of growth (Gompertz, 1825). Somatic growth of larval Atlantic croaker was modeled with only the directly analyzed otolith data by using a Laird-Gompertz growth model (Laird et al., 1965; Zweifel and Lasker, 1976; Lozano et al., 2012). This model had a set intercept of L_{null}=1.5 mm in notochord length (NL) to accurately represent the hatching length (dah=0; Warlen, 1980; Cowan, 1988; Barbieri et al., 1994a, 1994b). We used the following equation for the Laird-Gompertz growth model:

$$L_t = L_{null} e^{k(1-e^{-at})}, \quad (1)$$

where L_t = the SL, measured in millimeters, at an age (dah);
L_{null} = the SL at hatching for Atlantic croaker;
a = the rate of exponential decay; and
k = a dimensionless parameter so that ka represents the instantaneous growth rate at hatching.

Hindcasting was used to estimate growth rates with the Laird-Gompertz growth model (Lozano et al., 2012) for ages of larvae that were not sampled, because larvae were located offshore at these early ages,

Instantaneous growth rates (i.e., the rate of growth at a particular time in dah) were estimated with the maximum growth rates calculated both from the equation for the first derivative of the Laird-Gompertz model and from the mean growth rates calculated on 10-d intervals. We used the following equation to determine the first derivative of the Laird-Gompertz model:

$$G_{DI} = L_{null} e^{k(1-e^{-at})} * (kae^{-at}), \quad (2)$$

where G_{DI} = the instantaneous daily growth rate by means of the first derivative of the Laird-Gompertz model.

Mean growth rates for the 10-d interval were calculated with the following equation:

$$G_{\overline{10}} = \frac{(L_{t2} - L_{t1})}{\Delta t}, \text{ where } t2 > t1 \quad (3)$$

and where $G_{\overline{10}}$ = the average growth rate for that 10-d interval;
L_{t1} = the modeled SL at an initial time ; and
L_{t2} = the modeled SL at time .

Instantaneous growth rates then were determined from the natural log of the lengths in the mean growth equation described above.

The estuarine recruitment date for larvae was determined from the difference in the width of the daily increments and variation in distance of the ring from the otolith core. The recruitment date for the pretransformation larvae (<10 mm) was determined as the day after hatching at which there was an increase in the ring width and an increase in the distance between 2 adjacent rings. Movement by the larvae into the estuary, where there is lower salinity, increased nutrient loads, and higher primary production, has been shown to cause a rapid increase in growth for larvae and young-of-the-year juveniles (Hoss et al., 1988; Moser and Gerry, 1989).

A multivariate analysis of variance (MANOVA) was performed to test for differences in length and

[3] Arnold, C. R. 1983. Univ. of Texas Mariculture Project 1982–1983, 36 p. Marine Science Institute, Univ. Texas, Port Aransas, TX.

age between seasons, nested within years. A significant result from a MANOVA model would indicate that there were differences in the composition of length and ages in the larvae and early juveniles of Atlantic croaker that were collected. Growth rates were tested with an F-test to compare the residual sums of squares for the pooled Laird-Gompertz growth model with those of the Laird-Gompertz growth models that were fitted by season and sampling year (Chen et al., 1992).

Distributions of lengths and calculated ages that were based on readings of otoliths were tested for normality with a Shapiro-Wilk's test. A mixed model was applied by using R software (vers. 2.13.0) to look at growth rates of individual larvae with respect to salinity, temperature, and NWT within the tidal pass:

$$y_{ij} = \beta_0 + \beta_1 Salinity_{ij} + \beta_2 WaterTemp_{ij} + \beta_3 NWT_{ij} + \beta_4 Tide_{ij} + \tau_i + \varepsilon_{ij}, \quad (4)$$

where y_{ij} = the response variable of growth rate for the random group i and individual j;
β_0 = the intercept term;
β parameters = the effects for each of the variables (i.e., salinity, water temperature, and NWT), with tide being a binary dummy variable for each of the tide states (i.e., flood or ebb);
τ_i = the random effect of sampling month when the larvae were collected; and
ε_{ij} = the random error term for the model.

Results

Hydrology

There were no statistical differences in water temperature by sampling depth. This result is consistent with a seasonally, vertically well-mixed tidal pass, such as Bayou Tartellan. Generally, water temperatures followed the normal seasonal trends, in which water was warmer during the early fall (i.e., September and October) and cooler during the winter before rising again during March and April. There was a noticeable drop in temperature during November 2006, and median water temperature remained below 15°C through early February 2007. During the winter months, colder temperatures and greater temperature fluctuations were recorded than those recorded during fall or spring months. In particular, for the December 2007 sampling effort, there was a fluctuation range of 10.2°C during the 72-h sampling period. Although water temperature also decreased in November 2007, the median water temperature did not fall below 17°C during all remaining sampling efforts, resulting in higher water temperatures during year 2 of sampling.

No statistically significant differences were found between surface or near-bottom salinities, once again supporting a seasonally, vertically well-mixed estuary. In general, 95% of all measured practical salinity values fell between 21.5 and 31.4 within a total range of 14.5–33.2 and with a mean of 27.32. Median salinity values dropped by more than 5 between December 2006 and January 2007. In early February 2007, the median value was similar to that of January 2007 but ranged from as high as 32 to a low of nearly 20 over a 4-d period. Aside from median salinities of approximately 28 in late February 2007, the median salinity in Bayou Tartellan remained below 25 until early April 2007. Salinities during late 2007 and early 2008, with the exception of early March, showed less variation and were generally higher than those of the previous sampling year.

Catches of larval Atlantic croaker

There were 3118 larval and early juvenile Atlantic croaker collected from October 2006 through March 2007, and 425 larvae were collected from September 2007 through March 2008. Sampling continued through April in both 2007 and 2008; however, no Atlantic croaker were collected during that period. Catches in November 2006 accounted for 53.5% of the total number of Atlantic croaker larvae collected over both sampling periods. As in 2006, collections made in November 2007 had the greatest number of larvae caught in the second sampling period, but a second peak was observed in March 2008.

Table 1

Hatching dates for larval and early juvenile Atlantic croaker (*Micropogonias undulatus*) collected in Bayou Tartellan, Louisiana during 2006–2008. Hatching dates are based on back-calculated otolith ages and collection dates after application of age–length keys. Percentages of the total number of larvae collected in that sampling year and cumulative percentages are based on half-month intervals.

	2006–2007		2007–2008	
Interval	%	Cumulative %	%	Cumulative %
08/15–08/31	0.26	0.26	0.00	0.00
09/01–09/15	8.97	9.23	4.65	4.65
09/16–09/30	29.74	38.97	21.71	26.36
10/01–10/15	32.56	71.54	17.83	44.19
10/16–10/31	10.51	82.05	18.60	62.79
11/01–11/15	2.05	84.10	3.88	66.67
11/16–11/30	4.10	88.21	5.43	72.09
12/01–12/15	6.15	94.36	1.55	73.64
12/16–12/31	0.26	94.62	3.10	76.74
01/01–01/15	1.28	95.90	6.98	83.72
01/16–01/31	3.08	98.97	10.85	94.57
02/01–02/15	1.03	100.00	5.43	100.00
02/16–02/28	0.00	100.00	0.00	100.00

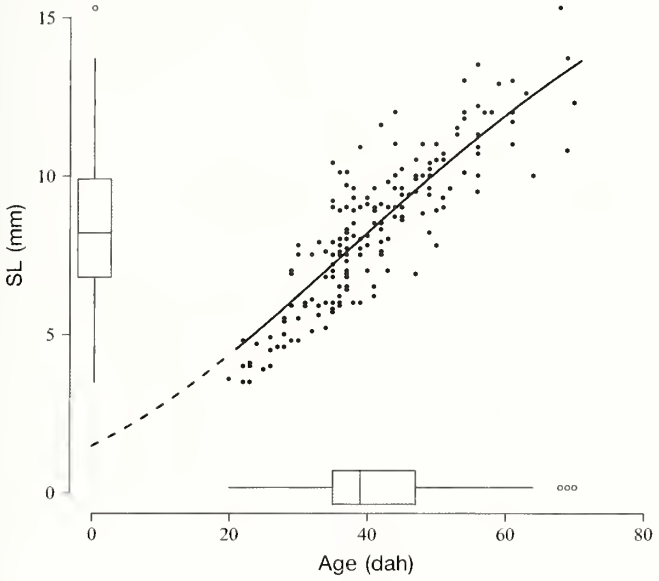

Figure 3

Relationships of estimates of standard length (SL) versus age in days after hatching (dah) determined with a Laird-Gompertz growth model, for larval Atlantic croaker (*Micropogonias undulatus*) collected from Bayou Tartellan, Louisiana, from October 2006 through March 2007 and from September 2007 through March 2008. This model was forced through the intercept at the estimated 1.5-mm notochord length at hatching to accurately reflect length at hatching. Boxplots show the median, 25% and 75% quantiles, and 95% confidence intervals, and outliers are provided for each axis. The Laird-Gompertz model was parameterized with the following equation: $SL = 1.5 \cdot e^{2.613272(1-e^{-0.026186 \cdot Age})}$.

Length, age, and hatching dates determined from counts of otolith increments

Sagittal otoliths were removed from 203 larvae and early juveniles of Atlantic croaker. Of those removed, 13 otoliths were not readable and were excluded from analysis. The length frequency plot of all larval Atlantic croaker that were aged (N=190) followed a normal distribution (Shapiro-Wilk: P=0.43), with a mean of 8.3 mm SL (SD 5.4) and range from 3.5 to 15.3 mm SL). However, the distribution of lengths was flatter in year 1 (SD=2.5 mm SL) than in year 2 (SD=2.0 mm SL). All ages of larval Atlantic croaker, from both direct measurement and estimation, also followed a normal distribution (Shapiro-Wilk: P=0.11) with a mean age of 41 dph (SD 10.1), a median of 39 dah, and a range of 20–70 dah.

In general, SL increased as the spawning and recruitment season progressed. Smaller larvae (<7 mm SL) were most prevalent in October for sampling year 1 and in September and October for sampling year 2. For both sampling periods, the median SL of larvae sampled began to stabilize in late November and early December and remained relatively constant through the spring. In both sampling years, the highest numbers of hatching dates occurred between 16 September and 31 October (Table 1). In year 1, cumulatively, more than 95% of all calculated hatching dates had occurred before 15 January 2007, but, during year 2, the 95% cumulative distribution was not reached until early February 2008, after a small, secondary peak in late January.

Modeled growth rates and dates of estuarine ingress

There was a significant linear relationship between measured lengths and estimated ages for larval Atlantic croaker (P<0.001; coefficient of determination [r^2]=0.76). The linear model indicated that the average growth rate was 0.20 mm/d, and it underestimated the hatching length (at 0.97 mm NL). The Laird-Gompertz growth model for the entirety of the data set, forced through the 1.5-mm-NL hatching length, provided a model fit that accounted for changes in growth rate due to sensory and organ development better than the fit of the linear model, which had nonstatistically independent and nonhomoscedastic errors that indicated a nonlinear relationship of growth rates that were variable through time. However, it only partially accounted for a slower initial growth rate at ages less than 20 dah (Fig. 3).

The sum of squared residuals was significantly reduced when models were fitted by season and sampling year than when a model was fitted with data pooled from both sampling years (P=0.007). Length, age, and growth were significantly different for seasons within years (P<0.001). Larvae collected during the peak spawning and recruitment season from September through December of 2006 and 2007 were shorter and younger than those collected from January through March of 2007 and 2008 (Fig. 4A; Chambers et al., 1983). Initial growth rates in the fall (September–December) of 2006 and 2007 were lower than those in the spring (January–March) of 2007 and 2008, but they steadily increased and did not level off at older ages. In contrast, larvae collected in the spring of 2007 and 2008 had higher initial growth than those collected in the previous fall seasons, but rates in both spring seasons leveled off quickly and resulted in shorter fish at ages greater than 50 dah and 60 dah, respectively (Fig. 4B). Compared with patterns observed in year 1, the difference in patterns of larval growth rates in fall compared with those in spring was more pronounced in year 2, when there were generally warmer water temperatures and higher salinities.

The ages and magnitudes of maximum growth rates for larval Atlantic croaker differed significantly within sampling year by season in the Laird-Gompertz models (P<0.001). Overall, the Laird-Gompertz models fitted by year and season showed that the maximum growth

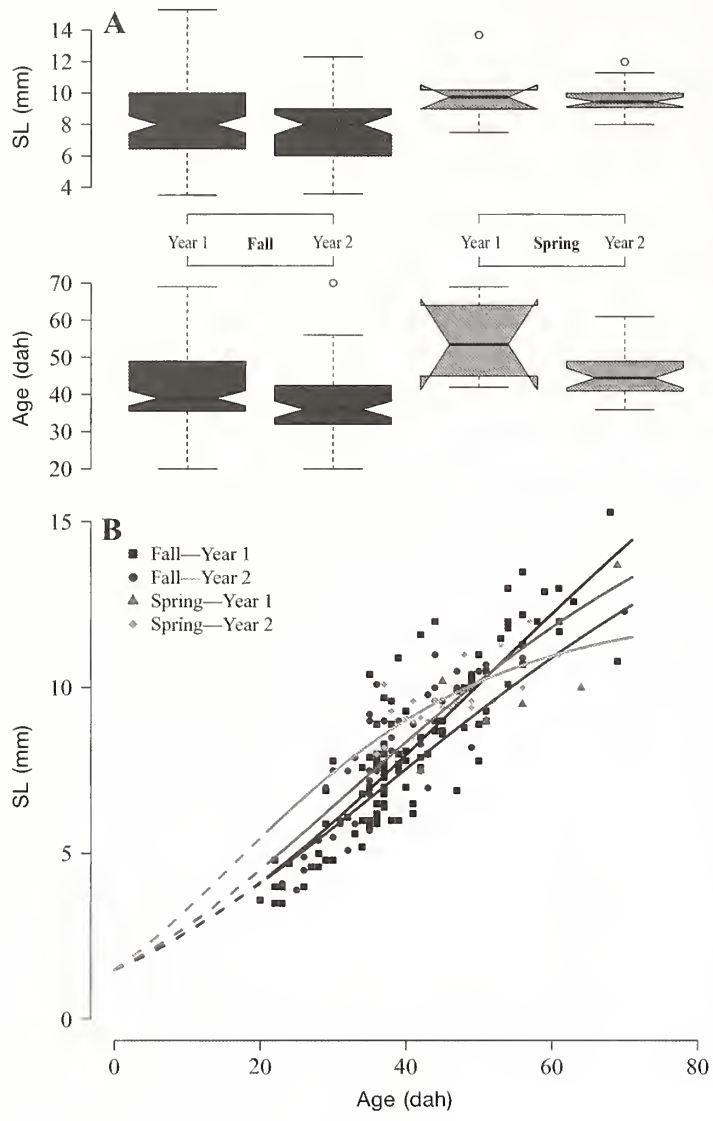

Figure 4

(**A**) Boxplots from a comparison of estimates of standard lengths (SL) and ages in days after hatching (dah), by season, for otoliths of larval Atlantic croaker (*Micropogonias undulatus*) collected from October 2006 through March 2007 (year 1) and from September 2007 through March 2008 (year 2). Fall sampling was conducted during September–December and spring sampling occurred during January–March. Nonoverlapping notches between any 2 boxplots represent "strong evidence" of statistically different median values, as described by Chambers et al. 1983. (**B**) Relationships of SL versus age determined with the Laird-Gompertz growth models for otoliths of larval Atlantic croaker, by season and sampling year. All models are forced through the intercept at the estimated 1.5-mm notochord length at hatching to accurately reflect growth rates at ages in dah less than the minimum otolith determined age. Model parameterizations were calculated as follows:

Fall of year 1: $SL = 1.5 \cdot e^{2.89159(1-e^{-0.02155 \cdot Age})}$;

Fall of year 2: $SL = 1.5 \cdot e^{2.50594(1-e^{-0.02893 \cdot Age})}$;

Spring of year 1: $SL = 1.5 \cdot e^{2.54838(1-e^{-0.02152 \cdot Age})}$;

Spring of year 2: $SL = 1.5 \cdot e^{2.11260(1-e^{-0.04726 \cdot Age})}$;

rates in the fall occurred when larvae were approximately 20 dah younger than larvae whose maximum growth rates occurred in spring. The maximum instantaneous growth rate was higher in fall 2006 (0.214 mm/d; 49 dah) than in fall 2007 (0.177 mm/d; 37 dah), but larvae in the fall of each year had the same minimum growth rate of 0.093 mm/d (Fig. 5). A greater initial instantaneous growth rate was observed in spring 2008 (0.150 mm/d) than in spring 2007 (0.113 mm/d). Although, the maximum instantaneous growth rate in spring 2008 (0.216 mm/d) was greater than the maximum rate in spring 2007 (0.196 mm/d), it occurred at an earlier age (16 dah versus 32 dah) and decreased rapidly thereafter. The 10-d averages for the 2 sampling years were slightly different. The highest average growth rate in year 1 was 0.203 mm/d at ages between 40 and 50 dah (Table 2), correlating with a peak at 49 dah in the fall of sampling year 1 (Fig. 5). In year 2, the highest average growth rate of 0.193 mm/d occurred at ages between 20 and 30 dah (Table 2)—a rate that was consistent with the peak in instantaneous growth rates that occurred at 16 dah during the spring of year 2 (Fig. 5).

The estimated average date of estuarine ingress after hatching was similar for both fall and spring seasons in both sampling years, but there were differences between seasons in the mean distance of the ring from the otolith core. Regardless of season or year, rapid changes in distance of the ring from the core and ring width happened around 40 dah, before the ontogenetic shift from late larvae to early juvenile has been reported to occur at approximately 10 mm SL (Barbieri et al., 1994a, 1994b). Mean distance of the otolith ring from the core, as a proxy for growth, was fairly stable before 40 dah and increased more rapidly and became more variable after that point (Fig. 6A). In particular, in spring 2007 and 2008, distances from the core were greater than the distances for the same age in the fall of 2006 and 2007. Mean otolith ring width was somewhat constant at approximately 0.5 µm for the fall of both sampling years and 1.1 µm for the spring of both years until 40 dah, when mean ring width became much more variable and generally increased with ring count thereafter (Fig. 6B).

Statistical analysis

The mixed model fitted for water temperature, salinity, and NWT, by tide, to the estimated growth rate of all individuals col-

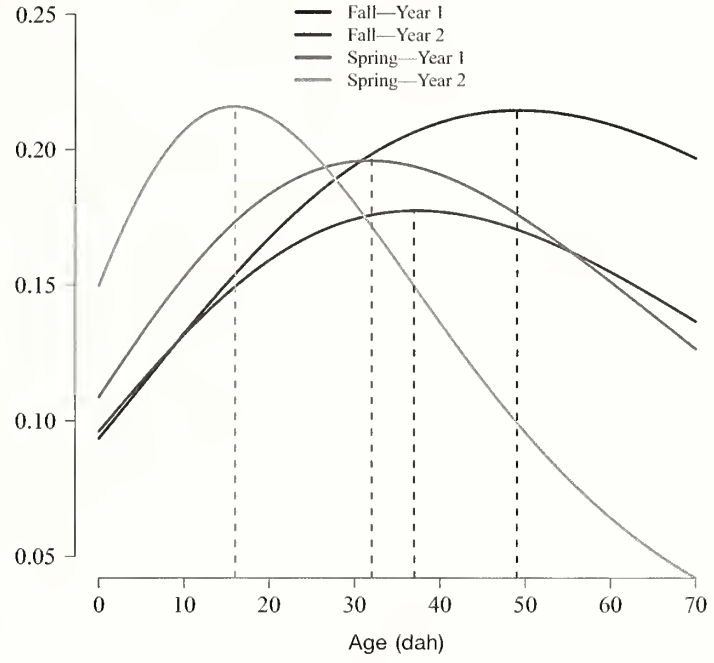

Figure 5

Maximum growth rates for Atlantic croaker (*Micropogonias undulatus*) larvae and early juveniles collected in Bayou Tartellan, Louisiana, from October 2006 through March 2007 and from September 2007 through March 2008, based on the first derivative of the Laird-Gompertz growth model for otoliths of larval Atlantic croaker. Solid lines indicate daily growth rates (mm/d) as the slopes of the estimates from the Laird-Gompertz models at any age in days after hatching (dah). Dashed lines indicate the maximum growth rates for fall of year 1 (2006), fall of year 2 (2007), spring of year 1 (2007), and spring of year 2 (2008).

lected during both sampling years, having significant model terms for all continuous variables. The only model terms that were not significant at the a priori alpha level of 0.05 were tidal stage and salinity as a function of tidal stage. The nonsignificance of the tidal stage term is likely a function of masking due to higher order interaction terms.

The individual model terms generally showed a trend of increased growth rate with ingress through the tidal pass, supporting the notion that otolith ring width and growth rate both increase at ingress, regardless of sampling year or season. The interaction of ebb tides with water temperature showed higher growth associated with colder temperatures that are indicative of shallow estuarine waters during late fall and winter (October–March) (P=0.040; Fig. 7A). The flood tide interaction with water temperature showed a similar trend, although more muted, likely a result of higher temperatures of waters from the inner continental shelf to the coast. Increased growth was also associated with decreasing salinity, regardless of tidal stage, resulting in a nonsignificant interaction (P=0.901), although the 95% confidence interval was much larger at lower salinities during flood tides (Fig. 7B). As with interactions with water temperature, modeled growth rates associated with salinities that were more consistent with estuarine conditions were significantly greater (P=0.046) than growth rates associated with higher salinities. Higher growth rates also were associated with large negative NWT on ebb tides, indicative of lower-salinity waters further up the estuary (P=0.001; Fig. 7C). However, during flood tides, no relationship was apparent statistically.

Discussion

Successful estuarine recruitment of Atlantic croaker larvae through tidal passes along the northern GOM depends on a highly variable spawning regime, on advantageous environmental conditions such as hydrographic, tidal, and wind-forcing factors, and ultimately on larval growth (Norcross and Austin, 1988; Eby et al., 2005; Montane and Austin, 2005). Hindcasting of the Laird-Gompertz growth model to 0 dah allowed us to infer growth rates of larvae along the recruitment corridor across the continental shelf and coastal zone. The bottleneck nature and the highly variable hydrodynamic environment of a seasonally well-mixed tidal pass at Bayou Tartellan, as well as the associated increase of larval growth with ingress into the estuarine nursery ground (Searcy et al., 2007), presented the challenges and rewards of successful estuarine recruitment for larval Atlantic croaker that were spawned offshore.

The highest frequency of hatching dates occurred between late September and early October for both sampling years, but hatching continued through the late winter and early spring (Fig. 5), indicating an overwinter spawning and recruitment period. The peak hatching dates corresponded well with the previously described period of July through December for peak spawning and recruitment (Warlen and Burke, 1990; Barbieri et al., 1994b) and with an overall spawning and recruitment period from August through May (Hettler and Chester, 1990). Differences in the distribution of hatching dates between year 1 and year 2 of the study highlight the variability in yearly spawning of Atlantic croaker that was due to factors on various spatial (Miller and Able, 2002) and temporal (Norcross, 1983) scales. For example, year 2 distribution of hatching dates peaked less than that of year 1. In addition, a higher percentage of larvae were recruited in the months after December 2007 than in other periods,

Table 2

Average growth rates (mm/d) and instantaneous growth rates (G) for larval and early juvenile Atlantic croaker (*Micropogonias undulatus*) collected in Bayou Tartellan, Louisiana, based on otolith data grouped by age blocks of 10 days after hatching (dah). Rates are provided for 2 sampling years—October 2006 through March 2007 and September 2007 through March 2008—and for the overall combined data.

	2006–2007		2007–2008		Overall	
Blocks (dah)	(mm/d)	G	(mm/d)	G	(mm/d)	G
0–10	0.115	0.057	0.138	0.065	0.124	0.060
10–20	0.152	0.045	0.175	0.048	0.161	0.046
20–30	0.181	0.036	0.193	0.035	0.187	0.036
30–40	0.198	0.029	0.190	0.025	0.196	0.027
40–50	0.203	0.023	0.173	0.019	0.192	0.021
50–60	0.198	0.018	0.149	0.014	0.178	0.016
60–70	0.185	0.014	0.122	0.010	0.158	0.013

indicating a more protracted spawning season (Barbieri et al., 1994a). The second peak in hatching dates in late January and early February for both sampling years indicates a possible second spawning subgroup (Fig. 6; Warlen, 1980; Thorrold et al., 1997). Warmer water temperatures during winter sampling efforts in year 2 were very similar to temperatures during the fall months in sampling year 1, potentially explaining the protracted spawning season in 2007–2008 (Lankford and Targett, 2001a, 2001b; Hare and Able, 2007).

Growth rates of larval and early juvenile Atlantic croaker collected in Bayou Tartellan increased and became variable after larvae encountered lower-salinity (<20) coastal boundary and estuarine waters, as did growth rates for Atlantic croaker when entering estuarine waters along the MAB (Nixon and Jones, 1997). The growth rate of 0.20 mm/d from the linear model in our study compares favorably with the growth rate of 0.19 mm/d documented from larvae collected from inner continental shelf waters offshore of Sabine Pass, Texas, and the Mermentau River, Louisiana (Cowan, 1988). The instantaneous maximum growth rates from the Laird-Gompertz model for the fall and spring of both sampling years fell within the range of growth rates reported for coastal waters off North Carolina: 0.16–0.27 mm/d (Warlen, 1980). The differences in seasonal growth rates within the Laird-Gompertz models provide evidence of spawning and recruitment subgroups with maximum growth rates occurring 20 dah later in the fall than in the spring—a finding indicating that the larvae spend a longer time period in a more productive and potentially more suitable essential fish habitat during the spring (Searcy et al., 2007; Sponaugle, 2010). Similar subgroups also have been observed in North Carolina waters (Warlen, 1980) and the MAB (Thorrold et al., 1997), where seasonal differences in growth rates were a result of food availability and variation in salinity.

The differences in seasonal growth rates observed in our study, however, may also be partially explained by the movement of spawning fish farther inshore as the season progressed (Barbieri et al., 1994a, 1994b), thereby shortening their time within the recruitment corridor when transiting to estuarine nursery grounds and more favorable growth conditions. Lower salinities (<15) indicative of estuarine waters have been shown to increase somatic growth rates of larval Atlantic croaker (Peterson et al., 1999). Although all analyses of growth in our study revealed similar growth rates, the use of the Laird-Gompertz model allowed more accurate hindcasting of the low growth rates of larvae in the recruitment corridor on the continental shelf because we used model true estimates of hatching length, and the linear models failed to accurately reflect or account for length at hatching.

The mean age of larval Atlantic croaker that transgressed the lower-salinity (<20) waters of the coastal boundary layer and entered the estuary was estimated to be approximately 40 dah, on the basis of changes in otolith ring width and distance of the ring from the core (Fig. 6, A and B). Ontogenetic change in otolith shape did not affect ring width or distance from the core because all otoliths in our study were roughly circular. Studies of ingress into Chesapeake Bay, Delaware Bay, and Pamlico Sound have shown ages at time of ingress to be between 30 and 60 dah (Warlen, 1980; Miller et al., 2003; Schaffler et al., 2009a, 2009b), a range that compares favorably with the results from direct aging of larvae collected for our study in the Bayou Tartellan tidal pass: between 22 and 70 dah.

The role of periodic atmospheric winter frontal passages on densities of larval Atlantic croaker has been shown to be significant in this system (Kupchik, 2014), indicating that patterns such as inlet geomorphology and wind-forcing factors can play a large role in the timing of ingress for Atlantic croaker (Raynie

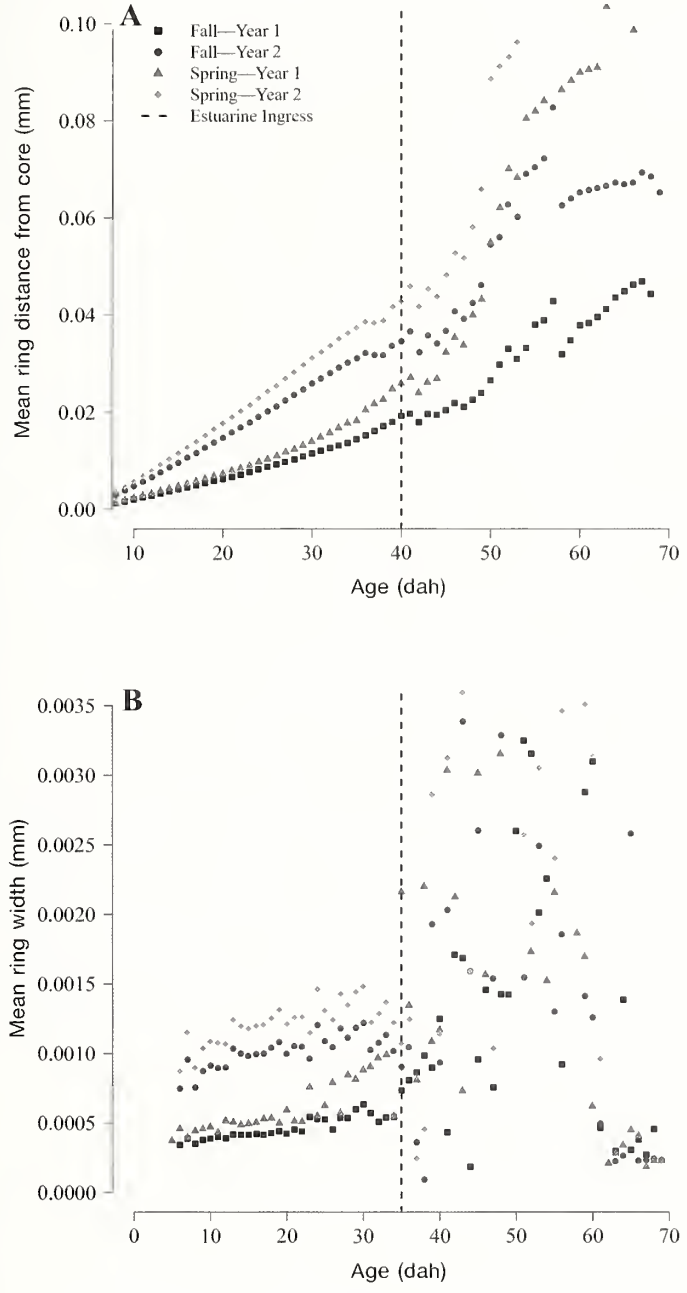

Figure 6

(**A**) Mean distance of the ring from the core, which serves as a proxy for growth, by season for otoliths of larval and early juvenile Atlantic croaker (*Micropogonias undulatus*) sampled in Bayou Tartellan, Louisiana, during 2006–2008. Data for fall of year 1 (2006), fall of year 2 (2007), spring of year 1 (2007), and spring of year 2 (2008) are provided to show differences between year and season, and the dashed line demarcates the estimated average ingress date. (**B**) Mean ring width for individual daily rings from imaged otoliths.

and Shaw, 1994; Joyeaux, 1998; Wood, 2000). Larval ingress can be driven by active mechanisms like selective tidal stream transport, but the vertically well-mixed nature of tidal passes in the northern GOM and particularly in our sampling site of Bayou Tartellan indicates that the driving forces are passive mechanisms of recruitment and retention, such as residual bottom flow (Joyeux, 1999; Schultz et al., 2003), wind-driven transport (Shaw et al., 1985; Joyeaux, 1999; Hare et al., 1999; Hare and Govoni, 2005), or flow differentials across channels due to boundary conditions and marsh edge effects (Lyczkowski-Shultz et al., 1990; Raynie, 1991; Raynie and Shaw, 1994; Kupchik, 2014).

Growth rates for Atlantic croaker larvae collected in water masses with salinities and temperatures consistent with continental shelf waters were lower than growth rates for larvae collected in water masses with characteristics associated with estuarine or coastal boundary waters. The effect of salinity on growth rate is further exemplified by the steep increase in growth rate during ebb tides, which bring low salinities indicative of waters from the upper estuarine nursery ground. Increased growth associated with lower salinities has been documented previously for larval Atlantic croaker in other estuaries (Peterson et al., 1999). Growth rate as a function of water temperature showed no difference associated with tide. Higher growth rates were associated with lower water temperatures, and those rates probably reflected the increased productivity of estuaries, which, during late fall and winter, have cooler temperatures and lower salinities than the warmer, more saline waters of the GOM. The notable exception to this pattern was the increase in growth rate that occurred during positive NWTs associated with flood tides, and this increase in growth rate may be a function of interim or prefrontal conditions associated with southerly winds and higher coastal sea level in relation to the reestablishment of the tidal prism after flushing from northerly winds of the postfrontal phase. Results from the mixed model confirmed the importance of salinity for growth of larval and juvenile Atlantic croaker that has been noted in previous studies (Sogard, 1992; Rooker and Holt, 1997; Lankford and Targett, 2001a) and the temporal and spatial variability that has been associated with differences between estuarine and continental shelf waters (Searcy et al., 2007).

Analysis of digital images of daily rings in saccular otoliths of larval Atlantic croaker, collected in Bayou Tartellan from October 2006 through March 2007 and from September 2007 through March 2008, provided a fast, reliable method for analyzing otolith rings, growth rate,

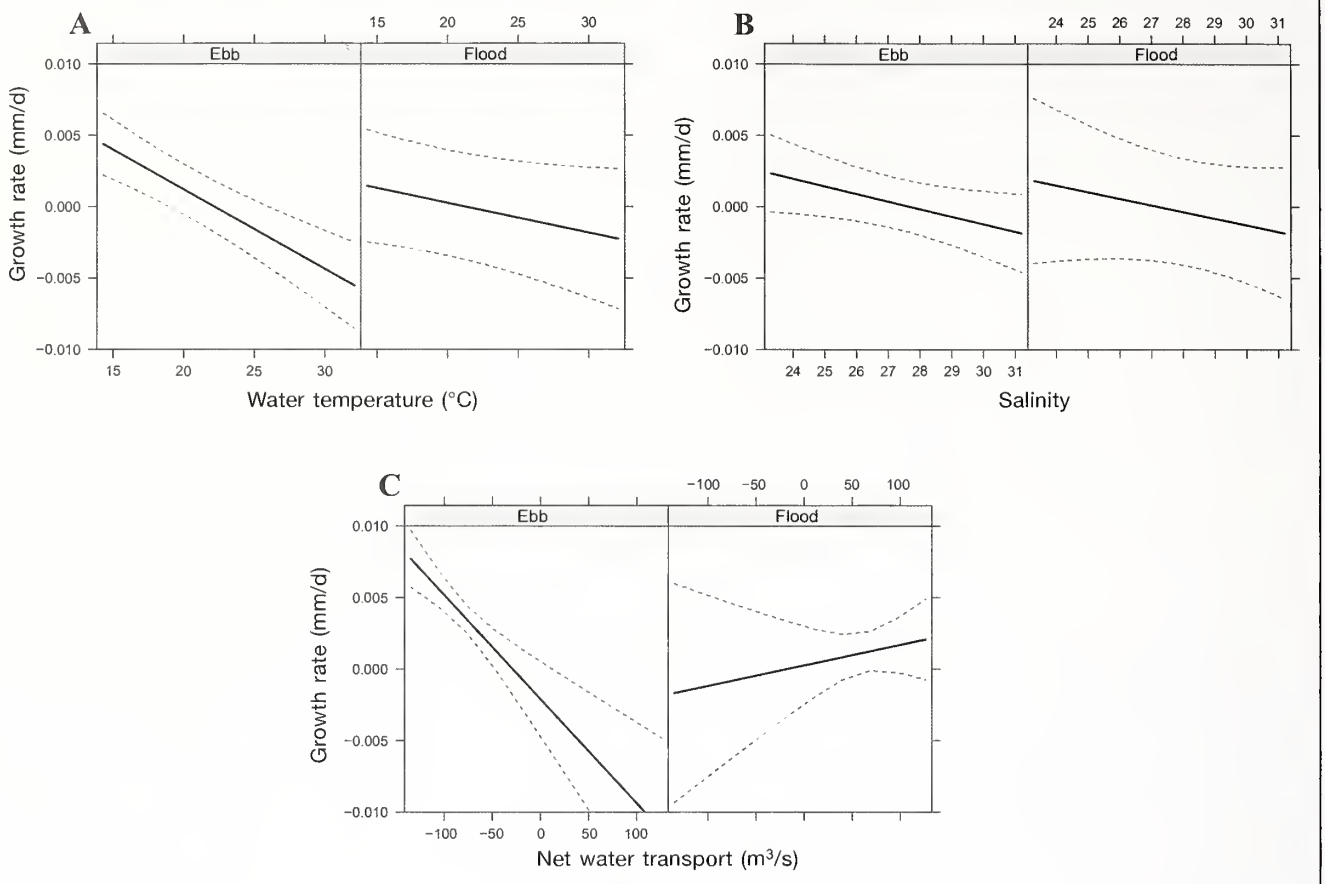

Figure 7

Partial plots of the mixed model showing growth rate data as a function of hydrodynamic parameters for larval and early juvenile Atlantic croaker (*Micropogonias undulatus*) collected from October 2006 through March 2007 and from September 2007 through March 2008 in Bayou Tartellan, Louisiana. Growth rate data were obtained from directly measured otoliths and those ages provided from age–length keys. A static value for the other model terms was assumed for all partial plots in the graphical evaluation. (**A**) Growth rate as a function of water temperature, delineated by tide. (**B**) Growth rate as a function of salinity, delineated by tide. (**C**) Growth rate as a function of net water transport, delineated by tide.

and estuarine ingress. The digital image filters reduced the need for human interpretation and allowed direct measurement and averaging of multiple readings to avoid aliasing from subdaily increments or other small scale microfeatures that could confound accurate age determination. Furthermore, the digital analysis allowed us to obtain exact measurement of otolith ring widths and distances from the core to confirm the estimated estuarine ingress date determined from changes in growth rates. Analyses of digital images of otoliths from Atlantic croaker allowed a more confident estimation of the age at which larval Atlantic croaker transition from the continental shelf to the more hydrodynamically variable and potentially more productive coastal boundary zone and lower-salinity estuarine waters.

The linear growth model was useful for comparison with results from previous studies but less effective than the Laird-Gompertz growth curves in detailing accurate growth rates of Atlantic croaker larvae. The Laird-Gompertz growth models allowed hindcasting to accurately include the NL at hatching and rate of growth more effectively in the dah before sampling. They provided more detail about the timing of ingress of Atlantic croaker into estuaries, where growth rates were expected to increase. The models revealed the limited somatic growth of larvae before recruitment into the lower-salinity estuarine system of Bayou Tartellan. Moreover, they allowed us to calculate instantaneous growth rates that reflect small-scale, daily changes affected by spatial location within the recruitment corridor without the bias introduced from overall averages expressed in a linear relationship with a singular rate of 0.20 mm/d or without the bias introduced from groupings of larvae in dah.

With the Laird-Gompertz models we estimated maximum growth rates, showing the difference of maximum growth rates that occurred later (with respect to dah)

in the fall than in the spring. The observed differences in growth rates between the fall spawning and recruitment season and the spring recruitment season provide evidence of spawning subgroups for the first time in the northern GOM—a finding that is similar to growth rates of the subgroups that have been found in North Carolina waters and in the MAB. This result was confirmed by the differences in otolith microstructure between the fall and spring for both sampling years, and the microstructure analysis was able to show within-year variability in batch spawning—a variability that would produce different cohorts with variable distances from offshore spawning grounds to inshore recruitment corridors. The highly significant salinity component in the mixed model that revealed a relationship between growth rate and the hydrodynamics in Bayou Tartellan gave evidence of the importance of the low salinity and high productivity of estuarine waters for maximizing growth for larval and, ultimately, juvenile Atlantic croaker.

Acknowledgments

We are grateful for funding under award NA06OAR4320264 06111039 to the Northern Gulf Institute by NOAA's Office of Ocean and Atmospheric Research, NGI Project File No. 07-NOAA-07. We also thank R. Nero, C. Li, and B. Marx for their help with and suggestions for our research. Finally, we thank support from T. Farooqi, A. Armas, and W. Delaune.

Literature cited

Albuquerque, C. Q., J. H. Muelbert, and L. A. N. Sampaio.
2009. Early developmental aspects and validation of daily growth increments in otoliths of *Micropogonias furnieri* (Pisces, Sciaenidae) larvae reared in laboratory. Pan.-Am. J. Aquat. Sci. 4:259–266.

Able, K. W.
2005. A re-examination of fish estuarine dependence: evidence for connectivity between estuarine and ocean habitats. Estuar. Coast. Shelf Sci. 64:5–17.

Barbieri, L. R., M. E. Chittenden Jr., and S. K. Lowerre-Barbieri.
1994a. Maturity, spawning, and ovarian cycle of Atlantic croaker, *Micropogonias undulatus*, in the Chesapeake Bay and adjacent coastal waters. Fish. Bull. 92:671–685.

Barbieri, L. R., M. E. Chittenden Jr., and C. M. Jones.
1994b. Age, growth, and mortality of Altantic croaker, *Micropogonias undulatus*, in the Chesapeake Bay region, with a discussion of apparent geographic changes in population dynamics. Fish. Bull. 92:1–12.

Brophy, D., and B. S. Danilowicz.
2002. Tracing populations of Atlantic herring (*Clupea harengus* L.) in the Irish and Celtic Seas using otolith microstructure. ICES J. Mar. Sci. 59:1305–1313.

Brothers, E. B.
1984. Otolith studies. *In* Ontogeny and systematics of fishes. Based on an International Symposium dedicated to the memory of Elbert Halvor Ahlstrom Spec. Publ. 1; La Jolla, CA, 15–18 August 1983 (H. G. Moser, W. J. Richards, D. M. Cohen, M. P. Fahay, A.W. Kendall Jr., and S. L. Richardson, eds.), p. 50–57. Am. Soc. Ichthyol. Herpetol., Lawrence, KS.

Butler, J. L.
1992. Collection and preservation of material for otolith analysis. *In* Otolith microstructure examination and analysis (D. K. Stevenson and S. E. Campana, eds.), p. 13–17. Can. Spec. Publ. Fish. Aquat. Sci. 117.

Campana, S. E.
1984. Interactive effects of age and environmental modifiers on the production of daily growth increments in otoliths of plainfin midshipman, *Porichthys notatus*. Fish. Bull. 82:165–177.
1992. Measurement and interpretation of the microstructure of fish otoliths. *In* Otolith microstructure examination and analysis (D. K. Stevenson and S. E. Campana, eds.), p.59–71. Can. Spec. Publ. Fish. Aquat. Sci. 117.
1999. Chemistry and composition of fish otoliths: pathways, mechanisms and applications. Mar. Ecol. Prog. Ser. 199:263–297.

Campana, S. E., and S. R. Thorrold.
2001. Otoliths, increments, and elements: keys to a comprehensive understanding of fish populations? Can. J. Fish. Aquat. Sci. 58:30–38.

Chambers, J. M., W. S., Cleveland, B. Kleiner, and P. A. Tukey.
1983. Graphical methods for data analysis, 395 p. Wadsworth, Belmont, CA.

Chen, Y., D. A. Jackson, and H. H. Harvey.
1992. A comparison of von Bertalanffy and polynomial functions in modelling fish growth data. Can. J. Fish. Aquat. Sci. 49:1228–1235.

Cowan, J. H., Jr.
1988. Age and growth of Atlantic croaker, *Micropogonias undulatus*, larvae collected in the coastal waters of the northern Gulf of Mexico as determined by increments in saccular otoliths. Bull. Mar. Sci. 42:349–357.

Diamond, S. L., L. G. Cowell, and L. B. Crowder.
2000. Population effects of shrimp trawl bycatch on Atlantic croaker. Can. J. Fish. Aquat. Sci. 57:2010–2021.

Ditty, J. G., G. G. Zieske, and R. F. Shaw.
1988. Seasonality and depth distribution of larval fishes in the northern Gulf of Mexico above latitude 26°00 N. Fish. Bull. 86:811–823.

Eby, L. A., L. B. Crowder, C. M. McClellan, C. H. Peterson, and M. J. Powers.
2005. Habitat degradation from intermittent hypoxia: impacts on demersal fishes. Mar. Ecol. Prog. Ser. 291:249–261.

Fahay, M. P.
1983. Guide to the early stages of marine fishes occurring in the western North Atlantic Ocean, Cape Hatteras to the southern Scotian Shelf. J. Northwest Atl. Fish. Sci. 4:3–423.

Gompertz, B.
1825. On the nature of the function expressive of the law of human mortality, and on a new mode of determining the value of life contingencies. Philos. Trans. R. Soc. Lond. 115:513–585.

Hare, J. A., and K. W. Able.
2007. Mechanistic links between climate and fisheries along the east coast of the United States: explaining population outbursts of Atlantic croaker (*Micropogonias undulatus*). Fish. Oceanogr. 16:31–45.

Hare, J. A., and J. J. Govoni.
2005. Comparison of average larval fish vertical distri-

butions among species exhibiting different transport pathways on the southeast United States continental shelf. Fish. Bull. 103:728–736.

Hare, J. A., J. A. Quinlan, F. E. Werner, B. O. Blanton, J. J. Govoni, R. B. Forward, L. R. Settle, and D. E. Hoss.
1999. Larval transport during winter in the SABRE study area: results of a coupled vertical larval behavior–three-dimensional circulation model. Fish. Oceanogr. 8 (suppl. 2):57–76.

Hernandez, F. J., Jr., S. P. Powers, and W. M. Graham.
2010. Detailed examination of ichthyoplankton seasonality from a high-resolution time series in the northern Gulf of Mexico during 2004–2006. Trans. Am. Fish. Soc. 139:1511–1525.

Hettler, W. F., Jr., and A. J. Chester.
1990. Temporal distribution of ichthyoplankton near Beaufort Inlet, North Carolina. Mar. Ecol. Prog. Ser. 68:157–168.

Hettler, W. F., Jr., and J. A. Hare.
1998. Abundance and size of larval fishes outside the entrance to Beaufort Inlet, North Carolina. Estuaries 21:476–499.

Hoover, R. R., C. M. Jones, and C. E. Grosch.
2012. Estuarine ingress timing as revealed by spectral analysis of otolith life history scans. Can. J. Fish. Aquat. Sci. 69:1266–1277.

Hoskin, S.
2002. Recruitment variability of Atlantic croaker, *Micropogonias undulatus*, with observations on environmental factors. M.S. thesis, 146 p. Old Dominion Univ., Norfolk, VA.

Hoss, D. E., L. Coston-Clements, D. S. Peters, and P. A. Tester.
1988. Metabolic responses of spot, *Leiostomus xanthurus*, and Atlantic croaker, *Micropogonias undulatus*, larvae to cold temperatures encountered following recruitment to estuaries. Fish. Bull. 86:483–488.

Joyeux, J. C.
1998. Spatial and temporal entry patterns of fish larvae into North Carolina estuaries: comparisons among one pelagic and two demersal species. Estuar. Coast. Shelf Sci. 47:731–752.
1999. The abundance of fish larvae in estuaries: within-tide variability at inlet and immigration. Estuaries 22:889–904.

Kupchik, M. J.
2014. Larval transport and recruitment dynamics in a Louisiana tidal pass. Ph.D. diss., 374 p. Louisiana State Univ., Baton Rouge, LA.

Laird, A. K., S. A. Tyler, and A. D. Barton.
1965. Dynamics of normal growth. Growth 29:233–248.

Landaeta, M. F., J. E. Contreras, C. A. Bustos, and G. Muñoz.
2014. Larval growth of two species of lanternfish at near-shore waters from an upwelling zone based on otolith microstructure analyses. J. Appl. Ichthyol. 31:106–113.

Lankford, T. E., Jr., and T .E. Targett.
2001a. Low-temperature tolerance of age-0 Atlantic croakers: recruitment implications for U.S. Mid-Atlantic estuaries. Trans. Am. Fish. Soc. 130:236–249.
2001b. Physiological performance of young-of-the-year Atlantic croakers from different Atlantic coast estuaries: implications for stock structure. Trans. Am. Fish. Soc. 130:367–375.

Li, C., E. Weeks, and J. L. Rego.
2009. In situ measurements of saltwater flux through tidal passes of Lake Pontchartrain estuary by Hurricanes Gustav and Ike in September 2008. Geophys. Res. Lett. 36:L19609. Article

Lozano, C., E. D. Houde, R. L. Wingate, and D. H. Secor.
2012. Age, growth and hatch dates of ingressing larvae and surviving juveniles of Atlantic menhaden *Brevoortia tyrannus*. J. Fish Biol. 81:1665–1685.

Lyczkowski-Shultz, J., D. L. Ruple, S. L. Richardson, J. Cowan Jr., and H. James.
1990. Distribution of fish larvae relative to time and tide in a Gulf of Mexico barrier island pass. Bull. Mar. Sci. 46:563–577.

Miller, M. J., and K. W. Able.
2002. Movements and growth of tagged young-of-the-year Atlantic croaker (*Micropogonias undulatus* L.) in restored and reference marsh creeks in Delaware Bay, USA. J. Exp. Mar. Biol. Ecol. 267:15–33.

Miller, M. J., D. M. Nemerson, and K. W. Able.
2003. Seasonal distribution, abundance, and growth of young-of-the-year Atlantic croaker (*Micropogonias undulatus*) in Delaware Bay and adjacent marshes. Fish. Bull. 101:100–115.

Montane, M. M., and H. M. Austin.
2005. Effects of hurricanes on Atlantic croaker (*Micropogonias undulatus*) recruitment to Chesapeake Bay (K. G. Sellner, ed.), p. 185–192. Hurricane Isabel in perspective, Chesapeake Research Consortium, CRC Publication, 05–160. CRC, Edgewater, MD.

Morales-Nin, B., A. Lombarte, and B. Japón.
1998. Approaches to otolith age determination: image signal treatment and age attribution. Sci. Mar. 62:247–256.

Moser, M. L., and L. R. Gerry.
1989. Differential effects of salinity changes on two estuarine fishes, *Leiostomus xanthurus* and *Micropogonias undulatus*. Estuaries 12:35–41.

Nixon, S. W., and C. M. Jones.
1997. Age and growth of larval and juvenile Atlantic croaker, *Micropogonias undulatus*, from the Middle Atlantic Bight and estuarine waters of Virginia. Fish. Bull. 95:773–784.

NMFS (National Marine Fisheries Service).
2009. Our living oceans. Report on the status of U.S. living marine resources, 6th ed. NOAA Tech. Memo. NMFS-F/SPO-80, 369 p.
2012. Fisheries of the United States 2011. Current Fishery Statistics No. 2011, 124 p. [Available at website.]

Norcross, B. L.
1983. Climate scale environmental factors affecting year-class fluctuations of Atlantic croaker (*Micropogonias undulatus*) in the Chesapeake Bay. Ph.D. diss., 388 p. College of William & Mary, Williamsburg, VA.

Norcross, B. L., and H. M. Austin.
1988. Middle Atlantic Bight meridional wind component effect on bottom water temperatures and spawning distribution of Atlantic croaker. Cont. Shelf Res. 8: 69–88.

Peterson, M. S., B. H. Comyns, C. F. Rakocinski, and G. L. Fulling.
1999. Does salinity affect somatic growth in early juvenile Atlantic croaker, *Micropogonias undulatus* (L.)? J. Exp. Mar. Biol. Ecol. 238:199–207.

R Development Core Team.
2011. R: a language and environment for statistical computing. R Foundation for Statistical Computing, Vienna, Austria. [Available at website, accessed April 2011.]

Ralston, S. and H. A. Williams.
1989. Numerical integration of daily growth increments: an efficient means of aging tropical fishes for stock assessment. Fish. Bull. 87:1–16.
Raynie, R. C.
1991. Study of the spatial and temporal ichthyoplankton abundance along a recruitment corridor from offshore to estuarine nursery. M.S. thesis, 189 p. Louisiana State Univ., Baton Rouge, LA.
Raynie, R. C., and R. F. Shaw.
1994. Ichthyoplankton abundance along a recruitment corridor from offshore spawning to estuarine nursery ground. Estuar. Coast. Shelf Sci. 39:421–450.
Ré, P.
1983. Daily growth increments in the sagitta of pilchard larvae *Sardina pilchardus* (Walbaum, 1792), (Pisces: Clupeidae). Cybium 7(3):9–15.
Richards, W. J. (ed.)
2006. Early stages of Atlantic fishes: an identification guide for the western central North Atlantic. vols I and II, 2636 p. CRC Press, Boca Raton, FL.
Roberts, J., and T. D. Roberts.
1978. Use of the Butterworth low-pass filter for oceanographic data. J. Geophys. Res., C. 83:5510–5514.
Rooker, J. R., and S. A. Holt.
1997. Utilization of subtropical seagrass meadows by newly settled red drum *Sciaenops ocellatus*: patterns of distribution and growth. Mar. Ecol. Prog. Ser. 158:139–149.
Schaffler, J. J., C. S. Reiss, and C. M. Jones.
2009a. Spatial variation in otolith chemistry of Atlantic croaker larvae in the Mid-Atlantic Bight. Mar. Ecol. Prog. Ser. 382:185–195.
2009b. Patterns of larval Atlantic croaker ingress into Chesapeake Bay, USA. Mar. Ecol. Prog. Ser. 378:187–197.
Schultz, E. T., K. M. M. Lwiza, M. C. Fencil, and J. M. Martin.
2003. Mechanisms promoting upriver transport of larvae of two species in the Hudson River estuary. Mar. Ecol. Prog. Ser. 251:263–277.
Searcy, S. P.
2005. Is growth a reliable indicator of essential fish habitat. Ph.D. diss., 316 p. North Carolina State Univ., Raleigh, NC.
Searcy, S. P., D. B. Eggleston, and J. A. Hare.
2007. Is growth a reliable indicator of habitat quality and essential fish habitat for a juvenile estuarine fish? Can. J. Fish. Aquat. Sci. 64:681–691.
Shaw, R. F., J. H. Cowan Jr., and T. L. Tillman.
1985. Distribution and density of *Brevoortia patronus* (Gulf menhaden) eggs and larvae in the continental shelf waters of western Louisiana. Bull. Mar. Sci. 36:96–103.
Shaw, R. F., B. D. Rogers, J. H. Cowan Jr., and W. H. Herke.
1988. Ocean-estuary coupling of ichthyoplankton and nekton in the northern Gulf of Mexico. Am. Fish. Soc. Symp. 3:77–89.
Smith, C. L.
1997. National Audubon Society field guide to tropical Marine Fishes: Caribbean, Gulf of Mexico, Florida, Bahamas, and Bermuda, 720 p. Alfred A. Knopf Inc., New York.
Sogard, S. M.
1992. Variability in growth rates of juvenile fishes in different estuarine habitats. Mar. Ecol. Prog. Ser. 85:35–53.
Sponaugle, S.
2010. Otolith microstructure reveals ecological and oceanographic processes important to ecosystem-based management. Environ. Biol. Fish. 89:221–238.
Thorrold, S. R., C. M. Jones, and S. E. Campana.
1997. Response of otolith microchemistry to environmental variations experienced by larval and juvenile Atlantic croaker (*Micropogonias undulatus*). Limnol. Oceanogr. 42:102–111.
Warlen, S. M.
1980. Age and growth of larvae and spawning time of Atlantic croaker larvae in North Carolina. Proc. Annu. Conf. SEAFWA34:204–214.
Warlen, S. M., and J. S. Burke.
1990. Immigration of larvae of fall/winter spawning marine fishes into a North Carolina estuary. Estuaries 13:453–461.
Warlen, S. M., and A. J. Chester.
1985. Age, growth, and distribution of larval spot, *Leiostomus xanthurus*, off North Carolina. Fish. Bull. 83: 587–599.
Wilson, C. A., D. W. Beckman, and J. M. Dean.
1987. Calcein as a fluorescent marker of otoliths of larval and juvenile fish. Trans. Am. Fish. Soc. 116:668–670.
Wood, R. J.
2000. Synoptic scale climatic forcing of multispecies fish recruitment patterns in Chesapeake Bay. Ph.D. diss., 277 p. College of William & Mary, Williamsburg, VA.
Zweifel, J. R., and R. Lasker.
1976. Prehatch and posthatch growth of fishes—a general model. Fish. Bull. 74:609–621.

NOAA
National Marine
Fisheries Service

Fishery Bulletin
established 1881

Spencer F. Baird
First U.S. Commissioner
of Fisheries and founder
of *Fishery Bulletin*

Age, growth, and population structure of the red flying squid (*Ommastrephes bartramii*) in the North Pacific Ocean, determined from beak microstructure

Zhou Fang[1,5,4]
Jianhua Li[1,2,3,5]
Katherine Thompson[4]
Feifei Hu[1]
Xinjun Chen (contact author)[1,2,3,5]
Bilin Liu[1,2,3,5]
Yong Chen[4,5]

Email address for contact author: xjchen@shou.edu.cn

[1] College of Marine Sciences
Shanghai Ocean University
999 Hucheng Ring Road
Shanghai 201306, China

[2] National Engineering Research Center for Oceanic Fisheries
Shanghai Ocean University
999 Hucheng Ring Road
Shanghai 201306, China

[3] Key Laboratory of Sustainable Exploitation of Oceanic Fisheries Resources
Ministry of Education
Shanghai Ocean University
999 Hucheng Ring Road
Shanghai 201306, China

[4] School of Marine Sciences
218 Libby Hall
University of Maine
Orono, Maine 04469

[5] Collaborative Innovation Center for Distant-water Fisheries
999 Hucheng Ring Road
Shanghai 201306, China

Abstract—To explore the feasibility of using beak microstructure to estimate the age of oceanic squid, sagittal sections in the upper beak were used to validate the age of the red flying squid (*Ommastrephes bartramii*) in the North Pacific Ocean. The growth rates of mantle length (ML) and body weight (BW) were estimated on the basis of beak increments. We compared growth curves derived from previous statolith-based studies and those from this study. Results indicate that the mean age of females and males was 203 d (standard deviation [SD] 55) and 180 d (SD 45). The hatching period occurred during October–June of the following year, and hatching peaked during January–April on the basis of back-calculation. All sampled squid belonged to the winter–spring cohort. Females and males had a similar growth pattern in ML and BW with increased ages, except for male ML after age 301–350 d. An exponential model best described the relationships between age and ML as well as BW for both sexes. The difference in growth curves and lower growth rates reported here, compared with those of previous studies, may result from different stock structures and extreme weather. This study confirmed that beak length works well for estimating the age of oceanic squid.

Manuscript submitted 18 February 2015.
Manuscript accepted 19 October 2015.
Fish. Bull. 114:34–44 (2016).
Online publication date: 5 November 2015.
doi. 10.7755/FB.114.1.3

The red flying squid (*Ommastrephes bartramii*) is distributed in subtropical and temperate waters worldwide but is commercially exploited only in the North Pacific Ocean, where it plays an important role in the marine ecosystem (Jereb and Roper, 2010; Navarro et al., 2013). It has become a primary target species in East Asian countries since the oceanic squid fishery began in the 1970s. This squid is not only important as a fishery resource but also serves as an indicator of large-scale oceanographic changes (Chen et al., 2007; Nishikawa et al., 2014). The population of red flying squid in the North Pacific Ocean consists of 2 main cohorts, the autumn cohort that yields large squid (>350 mm mantle length [ML]) and the winter–spring cohort that is represented by relatively small squid (<350 mm ML) (Chen and Chiu, 2003). Abundance of both cohorts fluctuates greatly with large-scale oceanographic and climatic changes (e.g., El Ninõ or La Ninã), as well as with regional-scale environmental changes (Yatsu et al., 2000; Chen et al., 2007).

Age estimation and growth analyses provide critical information for fisheries stock assessments and management. Hard structures often are used for aging squid and most studies measure statoliths (Spratt, 1978; Lipinski, 1986; Jackson et al., 1993; Durholtz et al., 2002). Although statolith-based age determination methods have advanced greatly over the past 30 years (Arkhipkin and Shcherbich, 2012), the process of preparing statoliths for aging is rather complicated and often has a

relatively low success rate. Potential use of alternative methods has been the topic of recent discussions (Moltschaniwskyj and Cappo, 2009). For example, the beak, which is the main feeding organ for squids, has a stable morphological structure because of its chitinous structure (Clarke, 1986) and could potentially be used for determination of a squid's age. Removing a whole beak from the buccal mass is much easier than extracting a statolith from the statocyst. The beak, therefore, has been identified as an appropriate structure for studies of squid biology and ecology (Jackson et al., 1997; Gröger et al., 2000; Martínez et al., 2002; Cherel and Hobson, 2005; Guerra et al., 2010).

Clarke (1965) first identified the incremental structure in the beak of *Moroteuthis ingens* and demonstrated its potential for estimating age. Raya and Hernández-González (1998) suggested the sagittal plane of a rostrum sagittal section (RSS) as the optimal plane for aging common octopus (*Octopus vulgaris*), and longitudinal increments deposited in RSS were also observed to have periodic light and dark bands. The lateral wall surface (LWS) of the beak also can be used for reading growth increments, and a study over a specific period indicated that one ring represents 1 d of life in post-larvae (Hernández-López et al., 2001). Perales-Raya et al. (2010) improved beak aging methods and compared the precision of readable growth increments between RSS and LWS methods. They found that the RSS yielded more precise age estimates but that the LWS was quicker and simpler to prepare (Perales-Raya et al., 2010). Canali et al. (2011) and Castanhari and Tomás (2012) also analyzed the upper beak microstructure and the relationship between increments and ML or body weight (BW). Examination of the upper beak has been recommended as a simple and effective approach for estimating cephalopod age (Canali et al., 2011; Castanhari and Tomás, 2012).

Previous studies on squid growth have focused primarily on seasonal and population variability in body size (Chen and Chiu, 2003; Ichii et al., 2004). Variation of oceanographic conditions and feeding habits can greatly impact the growth of red flying squid (Watanabe et al., 2004; Ichii et al., 2009). Oceanic squid tend to migrate over long-distances between their spawning or nursery grounds and their feeding grounds (Semmens et al., 2007). Individuals are exposed to varied environmental conditions during ontogenesis. Therefore, age estimation is an important part of analyzing growth rates for the different life stages of squids. The age-based calculation of growth rates that is based on measurements of statoliths is a popular method and has been used in making growth estimations for oceanic squid. The growth rates of ML and BW for some ommasterphid species have also been derived from statoliths (Markaida et al., 2004; Keyl, 2009; Chen et al., 2011, 2013).

In this study, we used beak microstructure of red flying squid to identify its spawning season and to examine age composition. The relationships between ML, BW, main beak morphometric variables, and age were defined in order to examine squid growth patterns. The relative differences between females and males were also investigated. This study is one of the first in which oceanic ommasterphid squid has been aged by using beak measurements. These methods can be applied to age and growth analyses of other oceanic cephalopods.

Materials and methods

Squid samples were randomly collected from Chinese commercial jigging vessels FV *Jinhai 827* and FV *Ningtai 21* in fishing grounds (between 154°E–174°W and 39°N–45°N) of the North Pacific Ocean from July through November in 2011 (Fig. 1). Samples were immediately frozen at −18°C for subsequent laboratory work.

After samples were thawed in the laboratory, dorsal ML and BW were measured to the nearest 1 mm and 1 g, respectively. The upper and lower beaks were then dissected from the buccal mass, washed with fresh water, and stored in a solution of 75% ethyl alcohol. The following 12 morphological variables were measured to the nearest 0.1 mm: upper hood length, upper crest length, upper rostrum length (URL), upper rostrum width, upper lateral wall length, upper wing length, lower hood length, lower crest length, lower rostrum length, lower rostrum width, lower lateral wall length, and lower wing length (Fig. 2A; Chen et al., 2012).

For age estimation, the use of RSS has been reported to be more precise than the use of LWS (Perales-Raya et al., 2010). The lower beak is more likely to be subject to erosion because it always covers the upper beak during biting and chewing. Moreover, the rostrum tip of the lower beak also has the function of paralyzing prey organisms (Nixon, 1973). The upper beak has a relatively complete rostrum tip, although erosion may still occur. Therefore, we measured the RSS of the upper beak in this study. The upper beak was cut in half with scissors, producing 2 RSS pieces. To count increments as accurately as possible, we cut the RSS into 2 different sizes and used the larger one, which tended to have a preserved focal plane representing all growth rings in the central section. The larger half of the RSS was cleaned with water to remove mucus and was embedded in a small mold with epoxy resin. We ground the focal plane with 120-, 600-, and 1200-grit waterproof sandpaper until the growth increments became clearly visible. Finally, we polished the RSS slice with 0.05-μm aluminium oxide powder to remove scratches on the surface. This preparation process is similar to that for statoliths (Dawe and Natsukari, 1991).

The number of increments in each RSS were counted with a microscope (Olympus Corp.,[1] Tokyo) at magnifications of 10×, 40×, and 400×. Images of different sections were taken with a charge coupled device (CCD)

[1] Mention of trade names or commercial companies is for identification purposes only and does not imply endorsement by the authors or the National Marine Fisheries Service, NOAA.

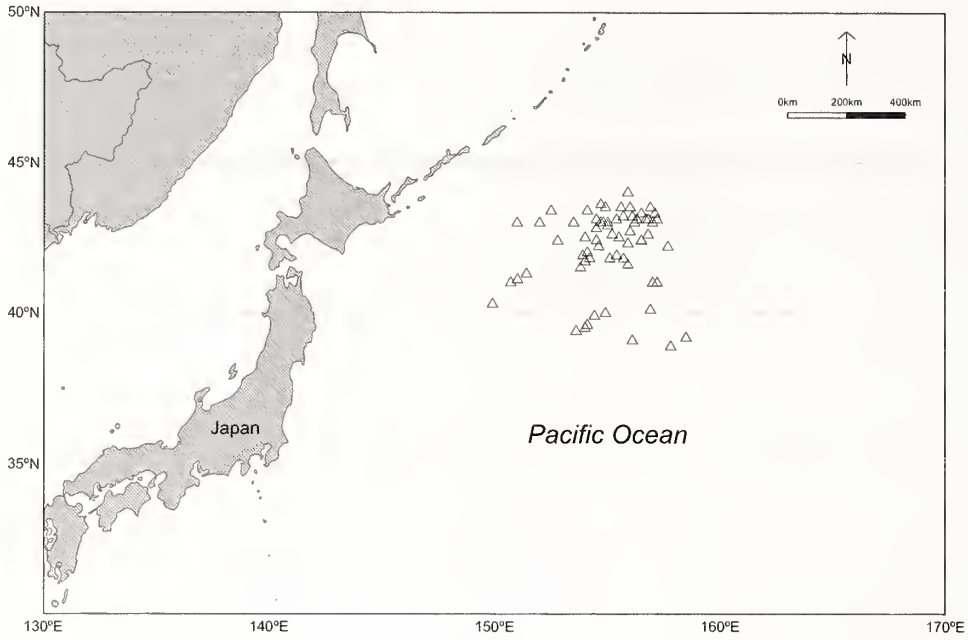

Figure 1

Locations where samples of red flying squid (*Ommastrephes bartramii*) were collected for this study in the North Pacific Ocean from July through November in 2011.

then processed with Adobe Photoshop CS 5.0 (Adobe Systems Inc., San Jose, CA). Two readers counted the number of increments, and readings were accepted only when the difference in mean counts between the 2 independent readers was less than 10% (Chen et al., 2013). Beak growth increments in previous studies were assumed to be deposited daily for several octopuses species (Raya and Hernández-González, 1998; Hernández-López et al., 2001; Perales-Raya et al., 2010, 2014; Canali et al., 2011; Castanhari and Tomás, 2012; Rodríguez-Domínguez et al., 2013; Bárcenas et al., 2014). A strict age validation for ommasterphid squids with the use of statolith and beak measurements has been performed and the results of those experiments indicate that the beak is a reliable material for age estimation (Hu et al., 2015; Liu et al., 2015). If the beak is a reliable structure for age estimates, we can back-calculate hatching dates from the capture dates documented in our study.

The relationships between age and ML, BW, and URL were established with 4 types of curves: linear, power, exponential, and logarithmic. Akaike's information criterion was used to compare the fits of models, by following the calculations of Haddon (2001). Differences in growth curves between sexes also were evaluated by using analysis of covariance (ANCOVA).

Instantaneous growth rate (G) and absolute daily growth rate (DGR) of ML or BW were measured in millimeters per day or grams per day and estimated for each 50-d interval by sex. The G and DGR were calculated with the following models proposed by Forsythe and Van Heukelem (1987):

$$G = \frac{ln(S_2) - ln(S_2)}{t_2 - t_1} \times 100\% \quad (1)$$

and

$$DGR = \frac{S_2 - S_1}{t_2 - t_1}, \quad (2)$$

where S_1 and S_2 = mean ML or BW at the beginning (t_1) and end (t_2) of the time interval.

Statistical analyses were conducted with SPSS, vers 19.0 (IBM Corp, Armonk, NY).

Results

Microstructure of growth increments in red flying squid

The microstructure of a beak RSS of a red flying squid in this study is shown in Figure 2. The longitudinal increments in the transverse surface were easily visible from the tip of rostrum to the joint of the hood and crest (Fig. 2B), and the hood was darker than the crest because of pigmentation (Fig. 2B). The tip of the rostrum was missing in some samples because of erosion from feeding behavior. Increments were more obvious in the center of the focal line and were visible as bands that were alternately dark and light (Fig. 2C). The increments in the middle of each internal rostral axis were much thicker than those in the anterior and posterior areas. The middle parts of the RSS had the widest incremental width in relation to other RSS parts (Fig. 2C). The interval widths tended to vary in different parts of the RSS at increased magnification

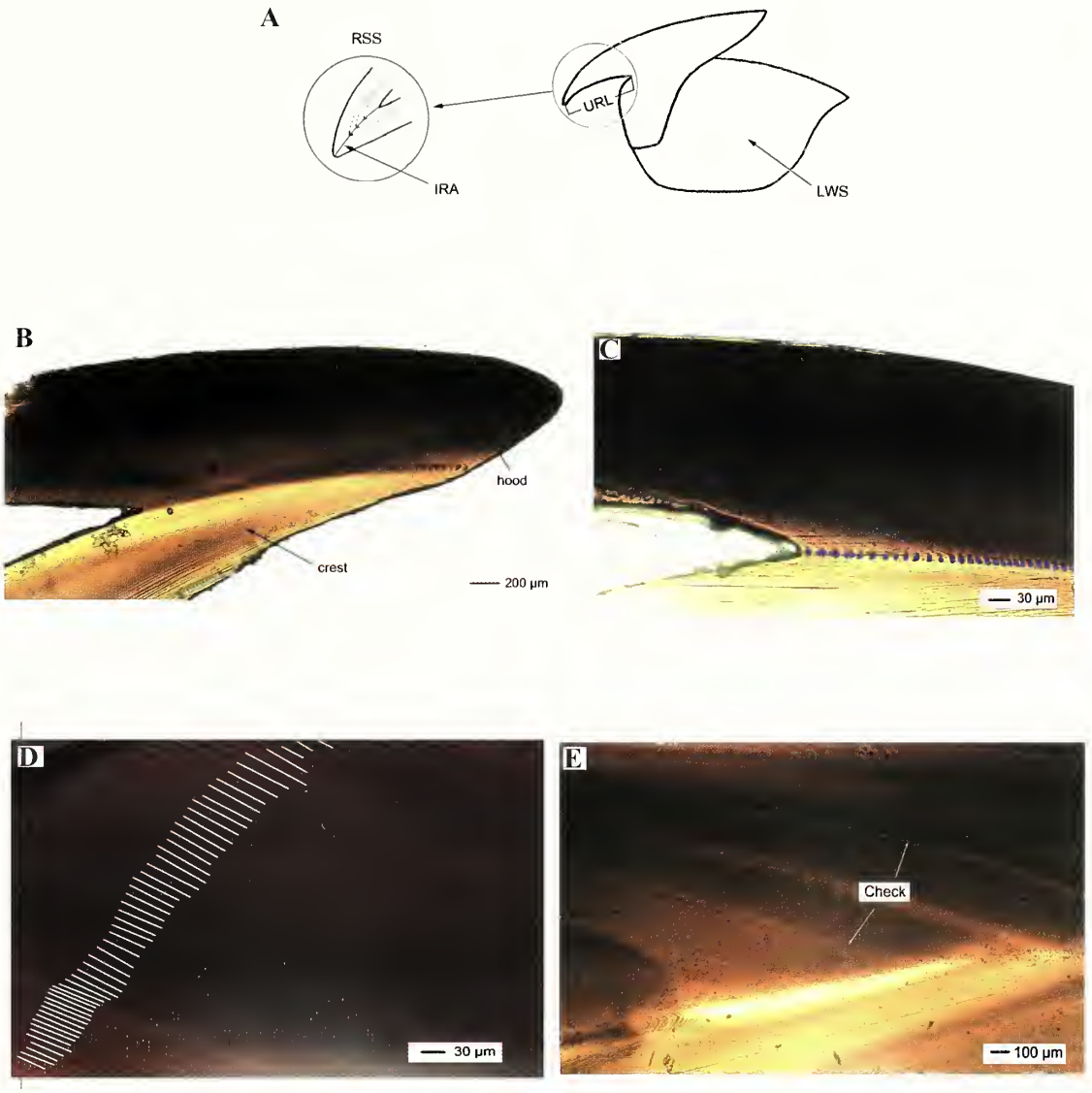

Figure 2

(**A**) Schematic diagram of the rostrum sagittal sections (RSS), the internal rostral axis (IRA), and upper rostral length (URL) in the beak of red flying squid (*Ommastrephes bartramii*). Photographic images of (**B**) a whole RSS and (**C**) IRA of a male individual with mantle length of 245 mm and age of 174 d, every blue dot represents one ring, and images with (D) longitudinal increments in the hood of the RSS of a female individual with mantle length of 390 mm and age of 268 d, every white line represents one ring, and (E) a check ring at 40× magnification.

(400×) (Fig. 2D). The mean width of increments in the RSS was 12.6 µm (standard deviation [SD] 0.03).

In some atypical beak samples, we found "check" rings, which were similar to the rings in the microstructure of the statolith (Fig. 2E). A check ring was an extremely light band that appeared in multiple increments. These types of increments were easy to discern in comparison with the surrounding regular increments. This structure occurred much more frequently in females than in males.

Age composition and hatching time

The total sample size was 211 Squid, of which 109 were females and 102 were males. The ML of females ranged from 199 to 417 mm (average=268 mm [SD 44]). The majority (85.4%) of females ranged from 240 to 320 mm in ML. Male ML ranged from 201 to 354 mm (average=248 mm [SD 33]); 85.4% males ranged from 240 to 280 mm ML (Fig. 3A). Female BW ranged from 140 to 2230 g (average=603 g [SD 353]); 72.7% of females

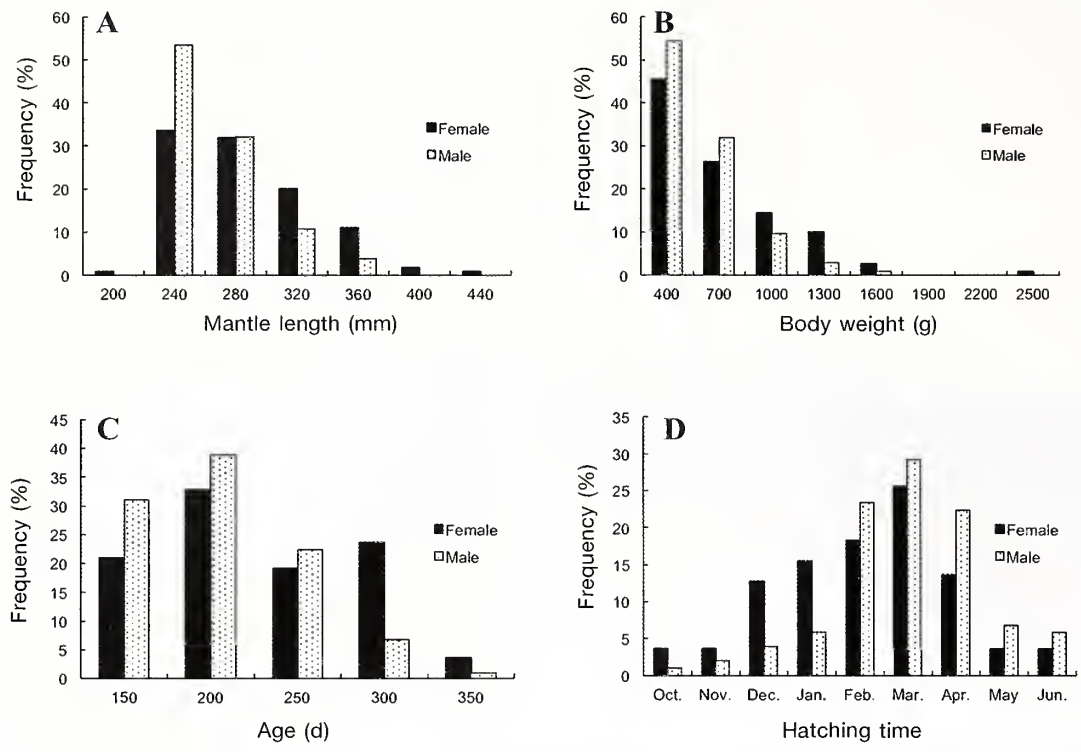

Figure 3

Composition of (**A**) mantle length, (**B**), body weight (**C**) age, and (**D**) hatching time, by sex, for red flying squid (*Ommastrephes bartramii*) collected for this study in the North Pacific Ocean from July through November in 2011.

Table 1

Absolute daily growth rates (DGR) as defined by Forsythe and Van Heukelem (1987) and instantaneous growth rate (G) for mantle length (ML) and body weight (BW) of red flying squid (*Ommastrephes bartramii*) by sex and age class. Squid were collected in the North Pacific Ocean from July through November 2011.

			Mantle length			Body weight		
Sex	Age class (d)	Sample size	Mean ML (mm)	DGR (mm/d)	G	Mean BW (g)	DGR (g/d)	G
Female	>150	23	219.13	–	–	302.42	–	–
	151–200	34	241.74	0.45	0.20	374.67	1.44	0.43
	201–250	20	277.67	0.72	0.28	619.55	4.90	1.01
	251–300	26	321.27	0.87	0.29	1005.18	7.71	0.97
	301–350	4	374.75	1.07	0.31	1571.85	11.33	0.89
Male	>150	32	216.88	–	–	287.76	–	–
	151–200	38	241.16	0.49	0.21	399.54	2.24	0.66
	201–250	23	277.22	0.72	0.27	613.65	4.28	0.86
	251–300	7	318.71	0.83	0.28	959.06	6.91	0.89
	301–350	1	354.00	0.71	0.21	1440.30	9.62	0.81

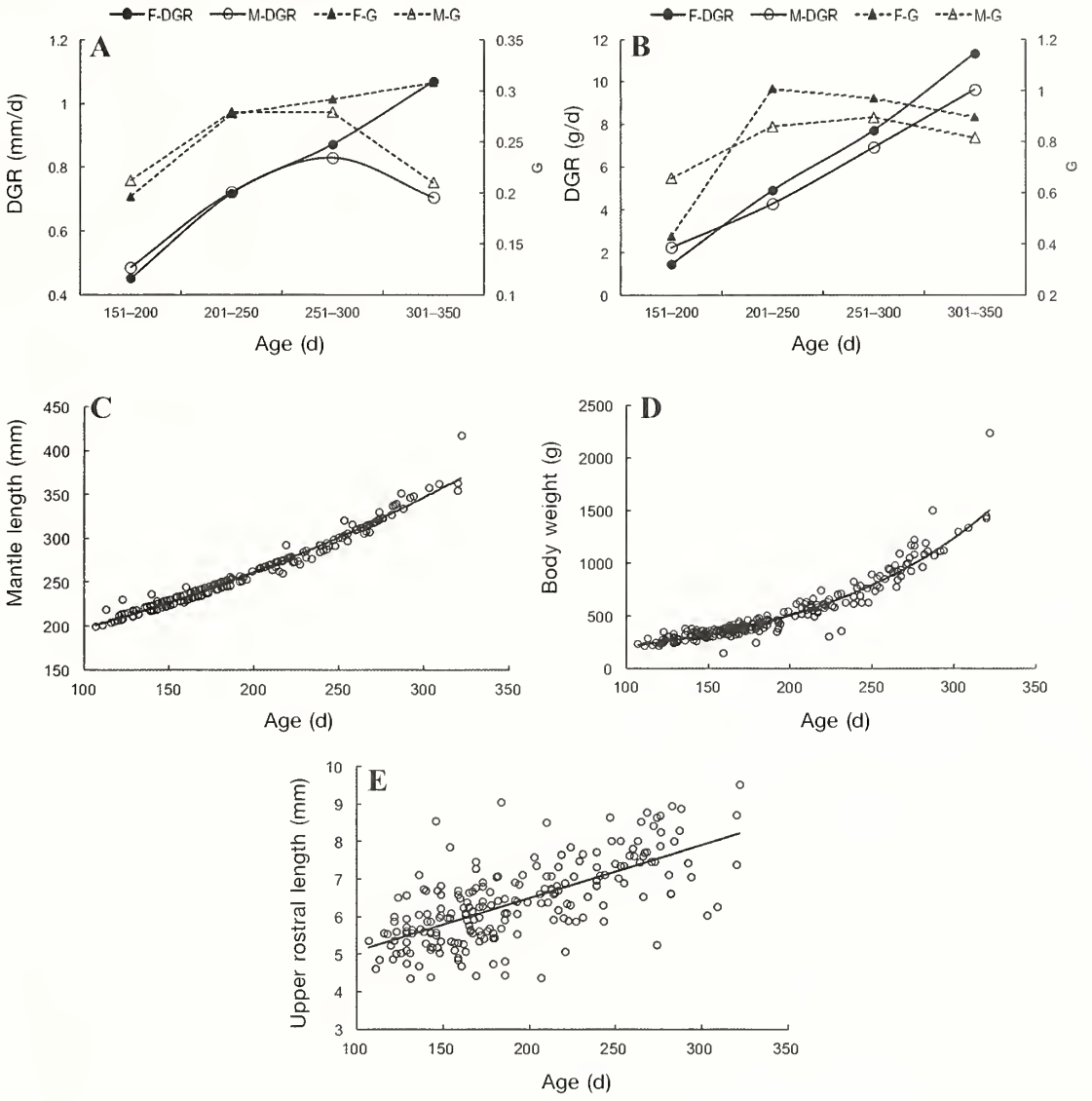

Figure 4

Variation of instantaneous growth rate (G) and absolute daily growth rate (DGR) measured in (**A**) mantle length (ML) and (**B**) body weight (BW) for male (M) and female (F) red flying squid (*Ommastrephes bartramii*), and growth curves in relation to (**C**) ML and age, (**D**) BW and age, and (**E**) upper rostral length and age of red flying squid in this study.

ranged from 150 to 250 g. The BW of males ranged from 210 to 1440 g (average=462 g [SD 225]); 92.7% of males ranged from 150 to 250 g (Fig. 3B).

The estimated age, which was based on the microstructure of upper beak RSS, ranged from 107 to 322 d (mean age=203 d [SD 55]) for females. The dominant age for females ranged from 150 to 300 d—a range that accounted for 75.4% of the female samples. Estimated age ranged from 110 to 320 d (mean age=180 d [SD 45]) for males, and the dominant age, from 110 to 250 d, which accounted for 92.2% of male samples (Fig. 3C). The back-calculated hatching time in this study ranged from October 2010 through June 2011. The peak hatching time occurred from January through April for females, accounting for 72.7% of female samples, and from February through April for males, accounting for 74.7% of male samples (Fig. 3D). Most of the squid in this study hatched in late winter and early spring.

Growth rate patterns

Growth rate patterns were similar between ML and BW despite squid age (Table 1; Fig. 4, A and B). For female squids, the maximum DGR was 1.07 mm/d for

Table 2

Results from an analysis of covariance between sexes of red flying squid (*Ommastrephes bartramii*) in the relationships between age and the following variables: mantle length (ML), body weight (BW), and upper rostral length (URL). No differences between sexes were significant.

Measurements	df	*F*	*P*
ML	107	0.125	0.725
BW	199	0.065	0.806
URL	151	1.974	0.166

ML and 11.33 g/d for BW within 301–350 d (Table 1; Fig. 4, A and B), and the maximum G was 0.31 for ML within 301–350 d and 0.97 for BW within 251–300 d. In males, maximum DGR occurred within 251–300 d for ML (0.83 mm/d) and then decreased, and maximum G also occurred during within 251–300 d for both ML (0.28) and BW (0.89) (Table 1, Fig. 4, A and B).

On the basis of results of the ANCOVA test, there was no significant difference in ML, BW, and URL between females and males ($P>0.05$) (Table 2). Therefore, we used the pooled data to analyze the relationship between ML, BW, URL, and age. Growth curves of ML–age and BW–age relationships were fitted with an exponential model, and the URL–age relationship provided the best fit with a linear model (Fig. 4, C–E) because it represented the best fit to the data (Table 3). These relationships were calculated with the following equations:

ML–age relationship: $ML = 148.47e^{0.0028age}$ (coefficient of determination [r^2]=0.980, n=211, $P<0.01$)

BW–age relationship: $BW = 83.80e^{0.009age}$ (r^2=0.914, n=211, $P<0.01$)

URL–age relationship: $URL = 0.0141age + 3.6816$ (r^2=0.460, n=211, $P<0.01$)

Table 3

Estimated model parameters and Akaike's information criterion (AIC) values of the relationship between age and the following variables: mantle length [ML], body weight (BW), and upper rostrum length (URL) for red flying squid (*Ommastrephes bartramii*). Underlined values are the lowest AIC values chosen with the best model. Linear=linear function: $y=a+bx$; power=power function: $y=ax^b$; exponential=exponential function: $y=ae^{bx}$; logarithmic=logarithmic function: $y=a\ln(x)+b$; AIC=Akaike's information criterion.

		Age (d)		
Body variables	Model	*a*	*b*	AIC
ML	Linear	0.763	111.766	846.971
	Power	12.773	0.573	924.242
	Exponential	147.200	0.003	<u>755.171</u>
	Logarithm	−500.730	145.350	1020.454
BW	Linear	5.389	−500.970	2008.414
	Power	0.008	2.102	1918.870
	Exponential	74.541	0.010	<u>1850.317</u>
	Logarithm	−4704.3	1003.1	2091.505
URL	Linear	0.014	3.682	<u>−93.550</u>
	Power	0.682	0.427	−91.991
	Exponential	4.211	0.002	−93.228
	Logarithm	−7.775	2.711	−89.493

Discussion

The beak has been used to estimate age for a few neritic molluscan species (e.g., the common octopus, Perales-Raya et al., 2014; *Octopus maya*, Bárcenas et al., 2014). On the basis of the results of our study, we can see that the microstructure of the beak in red flying squid is similar to that in different cephalopods, as was reported in a previous study (Perales-Raya et al., 2010). Although the rostrum in squids seems to account for a much larger proportion of the crest than it does in octopuses, RSS increments are smaller in squid than in octopuses, nearly 12 µm in this study compared with roughly 20 µm for common octopus (Raya and Hernández-González, 1998) and with 15–30 µm after 50 increments reported by Perales-Raya et al. (2010). In this study, we used only reflected light to observe the increments clearly, as opposed to the use of violet or ultraviolet light by Perales-Raya et al. (2010). It is easy to distinguish RSS increments at low magnification with reflected light, but this method should be used with caution because it is easy to confuse "first-order" and "second-order" increments, as it is with statoliths (Arkhipkin and Shcherbich, 2012). Check rings were also found in this study, and those rings may have resulted from stressful conditions, such as spawning (Perales-Raya et al., 2014). The microstructure of statoliths also displays check rings (Chen et al., 2013).

This study is one of the first that has provided estimated ages for oceanic species of ommasterphid squid on the basis of beak microstructure. Cephalopods are typically short-lived invertebrates, and the lifespan of red flying squid was estimated to average about 1 year in previous reports (Bigelow and Landgraph, 1993; Yatsu et al., 1997; Chen and Chiu, 2003; Chen et al., 2011). All the squid analyzed in this study were less than 1 year in age, and the results of this study are consistent with the results of previous studies where ages were

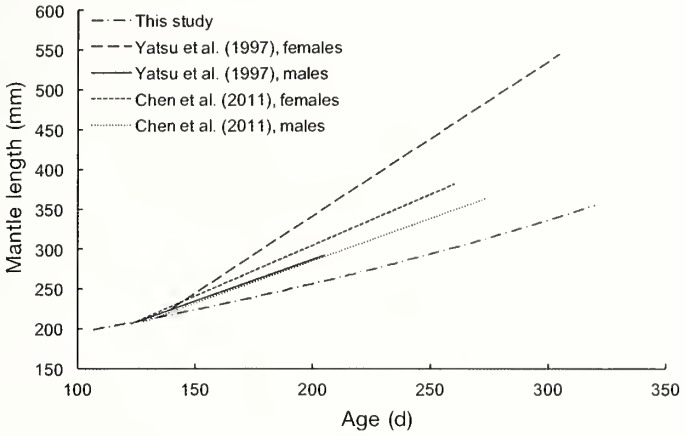

Figure 5

Comparison of growth curves in relation to mantle length (ML) and age for red flying squid (*Ommastrephes bartramii*) from different studies of the age and growth of this species.

estimated from statolith growth increments (Yatsu et al., 1997; Yatsu, 2000).

In a previous study, hatching time was estimated to be from January through April, indicating that samples belonged to the winter–spring cohort (Chen and Chiu, 2003). The winter–spring cohort inhabits traditional fishing grounds (150° to 170°E) in the Northwest Pacific (Bower and Ichii, 2005). We obtained results for hatching time, using a back-calculation based on upper beak increments, and our results were similar to estimates from statoliths for squid caught in a similar area and time during a previous study (Chen et al., 2011). Meanwhile, age were validated for the same species by using statoliths and beaks (Liu et al., 2015). The results from that previous study showed that beak increments had a high correlation with statolith increments for red flying squid: beak increments=1.0177×statolith increments – 6.6795 (r^2=0.969, n=21, P<0.001) (Liu et al., 2015). Therefore, we conclude that the beak is a hard structure that can be used reliably for age determination of ommasterphid species.

Females and males presented a similar growth pattern during ontogenesis (Table 1, Fig. 4). This finding differs from the observation of Chen et al. (2011), who suggested that females grow faster than males in every age class and that the peak growth rates occur in a relatively younger age class (140–220 d) (Chen et al., 2011). Sexual asynchrony of growth for red flying squid at different life stages also was found by Yatsu et al. (1997) and Brunetti et al. (2006). Chen and Chiu (2003) analyzed the growth of 2 geographically distinct stocks of red flying squid in the North Pacific Ocean and divided the females into 2 groups: large-size (>350 mm ML) and small-size (<350 mm ML) females. They found that small-size females in the northwestern stock had a growth mode that was similar to that of males that can be described best with a Gompertz function, but large-size females in the northwestern stock grew much faster than males in either stock. Therefore, the female samples in our study may belong to the small-size group of females in the northwestern stock—a possibility that could explain the nearly synchronous growth between sexes. It is also notable that the ML DGR for males was much lower than that for females after ages 301–350 d (Fig. 4). The reason for this difference may be the greater energy need of females to support their metabolism during gametogenesis (Rocha et al., 2001).

There was no significant difference in growth curves between the 2 sexes, according to the results of ANCOVA (P>0.05). Exponential curves seem to be appropriate for ML–age and BW–age relationships, whereas a linear curve was suitable for the URL–age relationship, although it showed a low correlation between the two variables. Different relationships between age and ML and BW have been found with various techniques in previous studies (e.g., exponential model for paralarve, Bigelow and Landgraph, 1993; Yatsu, 2000; linear model, Yatsu et al., 1997, Chen et al., 2011; Gompertz model, Chen and Chiu, 2003). The exponential curve is a logical choice for describing the very fast growth rate of squid, especially for paralarve (Bigelow and Landgraph, 1993; Sakai et al., 1999, 2006; Yatsu, 2000).

We also compared the growth curves for adult red flying squid with those derived from 2 other studies, and we found that our reported growth rate was relatively lower than those rates in the other 2 studies (Fig. 5). There are 2 potential reasons for this difference: 1) the female squids in this study belonged to the group of small-size females in the northwestern stock (Chen and Chiu, 2003), a group that tends to have a low growth rate than that of the squid used in the other 2 studies, especially in the study by Yatsu et al. (1997), whose samples may have belonged to large-size females of that stock, and 2) the size and life span of squid can be influenced by ambient temperature, an influence that is more obvious in extreme weather (e.g., El Ninõ or La Ninã), as has been documented for the jumbo squid (*Dosidicus gigas*) (Arkhipkin et al., 2015).

Compared with squid in our 2011 study, squid in previous studies tended to attain larger sizes but have a shorter life span (in years) with warm temperatures (i.e., squid hatched during 1991–1993 for Yatsu's [2000] study and in 1997 for Chen and Chiu's [2003] study) and to attain smaller sizes but a long life span with cold temperatures (i.e., squid hatched in 2007 for the Chen et al. [2011] study). However, model selection can be influenced by sample size and sampling range. Additional sampling and a greater size range of individuals will be needed to evaluate growth functions more thoroughly.

Acknowledgments

The support of those scientists on scientific surveys conducted with 2 commercial jigging vessels, FV *Jinhai 827* and FV *Ningtai 21* is gratefully acknowledged. This work was funded by the National Science Foundation of China (NSFC41306127 and NSFC41276156), National Science Foundation of Shanghai (13ZR1419700), the Innovation Program of Shanghai Municipal Education Commission (13YZ091), State 863 projects (2012AA092303), the Funding Program for Outstanding Dissertations in Shanghai Ocean University, the Funding Scheme for Training Young Teachers in Shanghai Colleges and Shanghai Leading Academic Discipline Project (Fisheries Discipline). The involvement of Y. Chen was supported by SHOU International Center for Marine Studies and Shanghai 1000 Talent Program.

Literature cited

Arkhipkin, A. I., and Z. N. Shcherbich.
2012. Thirty years' progress in age determination of squid using statoliths. J. Mar. Biol. Assoc. U.K. 92: 1389–1398.

Arkhipkin, A., J. Argüelles, Z. Shcherbich, and C. Yamashiro.
2015. Ambient temperature influences adult size and life span in jumbo squid (*Dosidicus gigas*). Can. J. Fish. Aquat. Sci. 72:400–409.

Bárcenas, G. V., C. Perales-Raya, A. Bartolomé, E. Almansa, and C. Rosas.
2014. Age validation in *Octopus maya* (Voss and Solís, 1966) by counting increments in the beak rostrum sagittal sections of known age individuals. Fish. Res. 152:93–97.

Bigelow, K. A., and K. C. Landgraph.
1993. Hatch dates and growth of *Ommastrephes bartramii* paralarvae from Hawaiian waters as determined from statolith analysis. *In* Recent advances in cephalopod fisheries biology (T. Okutani, R. K. O'Dor, and T. Kubodera, eds.), p. 15–24. Tokai Univ. Press, Tokyo.

Bower, J. R., and T. Ichii.
2005. The red flying squid (*Ommastrephes bartramii*): a review of recent research and the fishery in Japan. Fish. Res. 76:39–55.

Brunetti, N. E., M. L. Ivanovic, A. Aubone, and L. N. Pascual.
2006. Reproductive biology of red squid (*Ommastrephes bartramii*) in the Southwest Atlantic. Rev. Invest. Desarr. Pesq. 18:5–19.

Canali, E., G. Ponte, P. Belcari, F. Rocha, and G. Fiorito.
2011. Evaluating age in *Octopus vulgaris*: estimation, validation and seasonal differences. Mar. Ecol. Prog. Ser. 441:141–149.

Castanhari, G., and A. R. G. Tomás.
2012. Beak increment counts as a tool for growth studies of the common octopus *Octopus vulgaris* in southern Brazil. Bol. Inst. Pesca, São Paulo. 38:323–331.

Chen, C.-S.
2010. Abundance trends of two neon flying squid (*Ommastrephes bartramii*) stocks in the North Pacific. ICES J. Mar. Sci. 67:1336–1345.

Chen, C.-S., and T.-S. Chiu.
2003. Variations of life history parameters in two geographical groups of the neon flying squid, *Ommastrephes bartramii*, from the North Pacific. Fish. Res. 63:349–366.

Chen, X. J., X. H. Zhao, and Y. Chen.
2007. Influence of El Niño/La Niña on the western winter–spring cohort of neon flying squid (*Ommastrephes bartramii*) in the northwestern Pacific Ocean. ICES J. Mar. Sci. 64:1152–1160.

Chen, X.-J., J. Ma, B.-L. Liu, H.-J. Lu, and J. Cao.
2011. Population structure, age and growth of neon flying squid (*Ommastrephes bartramii*) in the northwest Pacific Ocean based on statolith microstructure. J. Fish. China 35:1191–1198. [In Chinese with English abstract.]

Chen, X., H. Lu, B. Liu, Y. Chen, S. Li, and M. Jin.
2012. Species identification of *Ommastrephes bartramii*, *Dosidicus gigas*, *Sthenoteuthis oualaniensis* and *Illex rgentines* (Ommastrephidae) using beak morphological variables. Sci. Mar. 76:473–481.

Chen, X., J. Li, B. Liu, Y. Chen, G. Li, Z. Fang, and S. Tian.
2013. Age, growth and population structure of jumbo flying squid, *Dosidicus gigas*, off the Costa Rica Dome. J. Mar. Biol. Assoc. U.K. 93:567–573.

Cherel, Y., and K. A. Hobson.
2005. Stable isotopes, beaks and predators: a new tool to study the trophic ecology of cephalopods, including giant and colossal squids. Proc. R. Soc., B. 272:1601–1607.

Clarke, M. R.
1965. "Growth rings" in the beaks of the squid *Moroteuthis ingens* (Oegopsida: Onychoteuthidae). Malacologia 3:287–307.

Clarke, M. R. (ed.)
1986. A handbook for the identification of cephalopod beaks, 273 p. Clarendon Press, Oxford, UK.

Dawe, E. G., and Y. Natsukari.
1991. Light microscopy. *In* Squid age determination using statoliths. Proceedings of the International Workshop held in the Istituto di Tecnologia della Pesca e del Pescato (ITPP-CNR), Spec. Publ. 1; Mazara del Vallo, Italy, 9–14 October 1989 (P. Jereb, S. Ragonese, and S. Von Boletzky, eds.), p. 83–95. ITPP, Mazara del Vallo, Italy.

Durholtz, M. D., M. R. Lipinski, and J. G. Field.
2002. Laboratory validation of periodicity of incrementation in statoliths of the South African chokka squid *Loligo vulgaris reynaudii* (d'Orbigny, 1845): a reevaluation. J. Exp. Mar. Biol. Ecol. 279:41–59.

Forsythe J. W., and W. F. Van Heukelem.
1987. Growth. *In* Cephalopod life cycles. Volume II: comparative reviews (P. R. Boyle, ed.), p. 135–156. Academic Press, London.

Guerra, Á., A. B. Rodríguez-Navarro, Á. F. González, C. S. Romanek, P. Álvarez-Lloret, and G. J. Pierce.
2010. Life-history traits of the giant squid *Architeuthis dux* revealed from stable isotope signatures recorded in beaks. ICES J. Mar. Sci. 67:1425–1431.

Gröger, J., U. Piatkowski, and H. Heinemann.
2000. Beak length analysis of the Southern Ocean squid *Psychroteuthis glacialis* (Cephalopoda: Psychroteuthidae) and its use for size and biomass estimation. Polar Biol. 23:70–74.

Haddon, M.
2001. Modelling and quantitative methods in fisheries, 406 p. Chapman and Hall, London.

Hernández-López, J. L., J. J. Castro-Hernández, and V. Hernández-García.
2001. Age determined from the daily deposition of concentric rings on common octopus (*Octopus vulgaris*) beaks. Fish. Bull. 99:679–684.

Hu, G., X. Chen, B. Liu, and Z. Fang.
2015. Microstructure of statolith and beak for *Dosidicus gigas* and its determination of growth increments. J. Fish. China 39:361–370. [In Chinese with English abstract.]

Ichii, T., K. Mahapatra, M. Sakai, D. Inagake, and Y. Okada.
2004. Differing body size between the autumn and the winter–spring cohorts of neon flying squid (*Ommastrephes bartramii*) related to the oceanographic regime in the North Pacific: a hypothesis. Fish. Ocean.13:295–309.

Ichii, T., K. Mahapatra, M. Sakai, and Y. Okada.
2009. Life history of the neon flying squid: effect of the oceanographic regime in the North Pacific Ocean. Mar. Ecol. Prog. Ser. 378:1–11.

Jackson, G. D., A. I. Arkhipkin, V. A. Bizikov, and R. T. Hanlon.
1993. Laboratory and field corroboration of age and growth from statoliths and gladii of the loliginid squid *Sepioteuthis lessoniana* (Mollusca: Cephalopoda). *In* Recent advances in cephalopod fisheries biology (T. Okutani, R. K. O'Dor, and T. Kubodera, eds.), p. 189–199. Tokai Univ. Press, Tokyo.

Jackson, G. D., N. G. Buxton, and M. J. A. George.
1997. Beak length analysis of *Moroteuthis ingens* (Cephalopoda: Onychoteuthidae) from the Falkland Islands region of the Patagonian Shelf. J. Mar. Biol. Assoc. U.K. 77:1235–1238.

Jereb, P., and C. F. E. Roper (eds.).
2010. Cephalopods of the world. An annotated and illustrated catalogue of cephalopod species known to date. Vol. 2. Myopsid and oegopsid squids. FAO Species Catalogue for Fishery Purposes 4, 605 p. FAO, Rome.

Keyl, F.
2009. The cephalopod *Dosidicus gigas* of the Humboldt Current system under the impact of fishery and environmental variability. Ph.D. thesis, 214 p. Univ. Bremen, Bremen, Germany.

Lipinski, M.
1986. Methods for the validation of squid age from statoliths. J. Mar. Biol. Assoc. U.K. 66:505–526.

Liu, B. L., X. J. Chen, Y. Chen, and G. Y. Hu.
2015. Determination of squid age using upper beak rostrum sections: technique improvement and comparison with the statolith. Mar. Biol. 162:1685–1693.

Markaida, U., C. Quiñónez-Velázquez, and O. Sosa-Nishizaki.
2004. Age, growth and maturation of jumbo squid *Dosidicus gigas* (Cephalopoda: Ommastrephidae) from the Gulf of California, Mexico. Fish. Res. 66:31–47.

Martínez, P., A. Sanjuan, and A. Guerra.
2002. Identification of *Illex coindetii*, *I. illecebrosus* and *I. rgentines* (Cephalopoda: Ommastrephidae) throughout the Atlantic Ocean; by body and beak characters. Mar. Biol. 141:131–143.

Moltschaniwskyj, N., and M. Cappo.
2009. Alternatives to sectioned otoliths: the use of other structures and chemical techniques to estimate age and growth for marine vertebrates and invertebrates. *In* Tropical fish otoliths: information for assessment, management and ecology (B. S. Green, B. D. Mapstone, G. Carlos, and G. A. Begg, eds.) p. 133–173. Springer Netherlands, Heidelberg, Germany.

Navarro, J., M. Coll, C. J. Somes, and R. J. Olson.
2013. Trophic niche of squids: insights from isotopic data in marine systems worldwide. Deep Sea Res. (II. Top. Stud. Oceanogr.) 95:93–102.

Nishikawa, H., H. Igarashi, Y. Ishikawa, M. Sakai, Y. Kato, M. Ebina, N. Usui, M. Kamachi, and T. Awaji.
2014. Impact of paralarvae and juveniles feeding environment on the neon flying squid (*Ommastrephes bartramii*) winter–spring cohort stock. Fish. Ocean. 23:289–303.

Nixon, M.
1973. Beak and radula growth in *Octopus vulgaris*. J. Zool. 170:451–462.

Perales-Raya, C., A. Bartolomé, M. T. García-Santamaría, P. Pascual-Alayón, and E. Almansa.
2010. Age estimation obtained from analysis of octopus (*Octopus vulgaris* Cuvier, 1797) beaks: improvements and comparisons. Fish. Res. 106:171–176.

Perales-Raya, C., A. Jurado-Ruzafa, A. Bartolomé, V. Duque, M. N. Carrasco, and E. Fraile-Nuez.
2014. Age of spent *Octopus vulgaris* and stress mark analysis using beaks of wild individuals. Hydrobiologia 725:105–114.

Raya, C. P., and C. L. Hernández-González.
1998. Growth lines within the beak microstructure of the octopus *Octopus vulgaris* Cuvier, 1797. S. Afr. J. Mar. Sci. 20:135–142.

Rocha, F., A. Guerra, and A. F. González.
2001. A review of reproductive strategies in cephalopods. Biol. Rev. Camb. Philos. Soc., 76:291–304.

Rodríguez-Domínguez, A., C. Rosas, I. Méndez-Loeza, and U. Markaida.
2013. Validation of growth increments in stylets, beaks and lenses as ageing tools in *Octopus maya*. J. Exp. Mar. Biol. Ecol. 449:194–199.

Sakai, M., N. E. Brunetti, M. Ivanovic, and B. Elena.
1999. Validation of daily increments of *Illex argentines* statolith. *In* Advances in methods and technology applied to fisheries research. Final seminar of INIDEP-JICA Project on assessment and monitoring of fisheries resources 1994–1999, p. 95–97. Instituto Nacional de Investigación y Desarrollo Pesquero (INIDEP), Mar del Plata, Argentina.

Sakai, M., N. Brunetti, J. Bower, B. Elena, T. Goto, T. Ichii, M. Ivanovic, Y. Sakurai, T. Wakabayashi and A. Yatsu.
2006. Upper-beak growth increments in ommastrephid paralarvae. *In* Cephalopod life cycles: Cephalopod International Advisory Council Symposium 2006 (CIAC '06); Hobart, Tasmania, Australia, 6–10 February, p. 54. Univ. Tasmania, Hobart, Australia. [Abstract]

Semmens, J. M., G. T. Pecl, B. M. Gillanders, C. M. Waluda, E. K. Shea, D. Jouffre, T. Ichii, K. Zumholz, O. N. Katugin, S. C. Leporati, and P. W. Shaw.
2007. Approaches to resolving cephalopod movement and migration patterns. Rev. Fish Biol. Fish. 17:401–423.

Spratt, J. D.
1978. Age and growth of the market squid, *Loligo opalescens* Berry, in Monterey Bay. Calif. Dep. Fish Game, Fish Bull. 169:35–44.

Watanabe, H., T. Kubodera, T. Ichii, and S. Kawahara.
2004. Feeding habits of neon flying squid *Ommastrephes bartramii* in the transitional region of the central North Pacific. Mar. Ecol. Prog. Ser. 266:173–184.

Yatsu, A., S. Midorikawa, T. Shimada, and Y. Uozumi.
1997. Age and growth of the neon flying squid, *Ommastrephes bartrami*, in the North Pacific Ocean. Fish. Res. 29:257–270.

Yatsu, A.
2000. Age estimation of four oceanic squids, *Ommastrephes bartramii*, *Dosidicus gigas*, *Sthenoteuthis oualaniensis*, and *Illex rgentines* (Cephalopoda, Ommastrephidae) based on statolith microstructure. Japan Agric. Res. Q. 34:75–80.

Yatsu, A., T. Watanabe, J. Mori, K. Nagasawa, Y. Ishida, T. Meguro, Y. Kamei, and Y. Sakurai.
2000. Interannual variability in stock abundance of the neon flying squid, *Ommastrephes bartramii*, in the North Pacific Ocean during 1979–1998: impact of driftnet fishing and oceanographic conditions. Fish. Ocean. 9:163–170.

NOAA
National Marine
Fisheries Service

Fishery Bulletin
established 1881

Spencer F. Baird
First U.S. Commissioner
of Fisheries and founder
of *Fishery Bulletin*

Fish species associated with shipwreck and natural hard-bottom habitats from the middle to outer continental shelf of the Middle Atlantic Bight near Norfolk Canyon

Steve W. Ross[1]
Mike Rhode[1]
Stephen T. Viada[2]
Rod Mather[3]

Email address for contact author: rosss@uncw.edu

[1] Center for Marine Science
University of North Carolina at Wilmington
5600 Marvin Moss Lane
Wilmington, North Carolina 28409

[2] CSA Ocean Sciences Inc.
8502 SW Kansas Avenue
Stuart, Florida 34997

[3] Applied History Lab
Department of History
University of Rhode Island
80 Upper College Road
Kingston, Rhode Island 02881

Abstract—Fish species of the Middle Atlantic Bight (MAB) continental shelf are well known; however, species occupying hard-bottom habitats, particularly on the outer shelf, are poorly documented. Reef-like habitats are relatively uncommon on the MAB shelf; therefore, shipwrecks may represent a significant habitat resource. During fall 2012 and spring 2013, 9 sites (depths: 42–126 m) near Norfolk Canyon were surveyed by using remotely operated vehicles. One site consisted of sand bottom, one consisted of predominantly natural hard bottom, and 7 sites included 8 large shipwrecks. Of 38 fish taxa identified, 33 occurred on hard bottom and 25 occurred on soft substrata. Fourteen fish taxa occurred almost exclusively on hard bottom, and 6 species were observed only on soft bottom. The most abundant taxa, especially on reef habitat, were the chain dogfish (*Scyliorhinus retifer*), a scorpionfish (*Scorpaena* sp.), the yellowfin bass (*Anthias nicholsi*), the red barbier (*Baldwinella vivanus*), the black sea bass (*Centropristis striata*), unidentified anthiine serranids, and the deepbody boarfish (*Antigonia capros*). Depth, location, and season did not significantly influence fish assemblages. Fish assemblages on natural and artificial hard-bottom habitat were similar but significantly different from soft-bottom assemblages. Deep-reef fishes of the southern MAB may be constrained by zoogeography, depth, and inadequate habitat—limitations that could increase their vulnerability.

Manuscript submitted 13 February 2015.
Manuscript accepted 21 October 2015.
Fish. Bull. 114:45–57 (2016).
Online publication date: 10 November 2015.
doi. 10.7755/FB.114.1.4

The fish fauna of the shelf and upper slope of the U.S. Middle Atlantic Bight (MAB) (from Cape Hatteras to Cape Cod) is considered cool temperate, although fish enter from colder and warmer regions to the north and south, respectively. The estuarine and shelf fishes are particularly well studied in this region (e.g., Grosslein and Azarovitz, 1982; Colvocoresses and Musick, 1984; Gabriel, 1992; Murdy et al., 1997; Able and Fahay, 1998), in large part, because of decades of standardized, fishery-independent trawl surveys. Although fish communities have been documented on the open shelf and upper slope, their presence on untrawlable habitats (i.e., canyon walls, rocky bottom, and shipwrecks) has not been well documented.

The shelf of the Middle Atlantic Bight has a lower percentage of exposed natural hard substrata than that of other areas in U.S. Atlantic waters (Steimle and Zetlin, 2000; SEAMAP-SA, 2001). Therefore, habitat may be limiting for fauna in the MAB that require hard substrata, and therefore introduced shipwrecks or other reef-like habitats probably represent significant habitat resources. Even so, there has been little assessment of the fishes associated with either natural or artificial hard-bottom habitats in the MAB (Eklund, 1988; Adams, 1993; Steimle and Zetlin, 2000). Although direct observation techniques are preferred for assessment of the fauna of rugged hard substrata (e.g., Caillet et al., 1999; Quattrini and Ross, 2006; Ross and Quattrini, 2007), these methods have not been widely applied on the MAB shelf. Three studies that involved nearshore surveys in the MAB used direct observation to document fishes on various bottom types, including hard bottom, at depths ≤55 m (Auster et al., 1991;

Table 1

Details from dives of remotely operated vehicles (ROVs) on the continental shelf of the Middle Atlantic Bight during 2012 (ROV *Kraken II*) and 2013 (ROV *Jason II*), which were conducted from the NOAA ship *Nancy Foster* and the NOAA ship *Ronald H. Brown*. For site names, W=shipwreck sites; SS=shallow, soft-substrata site; NHB=natural hard-bottom site. Total time and depth range are for times when the ROV was on the bottom. Daytime (D)=0800–2000 h EDT; nighttime (N)=2000–0800 h EDT. n/a=not available.

Dive no.	Site name	Date	Time	Total time (min)	Start latitude (N)	Start longitude (W)	End latitude (N)	End longitude (W)	Depth range (m)
ROV-2012-NF-21	SS	20-Sep-12	D	304	37°10.90′	74°56.24′	37°10.85′	74°56.26′	42–43
ROV-2012-NF-22	W-1	22-Sep-12	D	622	37°09.40′	74°45.30′	n/a	n/a	81
ROV-2012-NF-23	W-2	23-Sep-12	D	612	37°09.40′	74°34.60′	37°09.20′	74°34.40′	113
ROV-2012-NF-24	W-3	24-Sep-12	D	519	37°13.90′	74°33.00′	37°14.00′	74°33.00′	124–126
ROV-2012-NF-26	W-4	26-Sep-12	D	223	37°11.50′	74°34.40′	37°11.50′	74°34.40′	100–106
ROV-2012-NF-27	W-5	26-Sep-12	D	363	37°16.90′	74°32.10′	37°17.20′	74°32.00′	118–119
ROV-2012-NF-28	NHB	27-Sep-12	D	291	37°01.06′	74°39.26′	37°00.92′	74°39.64′	98–117
ROV-2012-NF-29	W-6	27-Sep-12	D	251	36°54.80′	74°42.40′	36°54.80′	74°42.40′	84–85
ROV-2012-NF-30	W-7	28-Sep-12	D	174	37°11.90′	74°45.40′	37°11.90′	74°45.40′	68–69
ROV-2013-RB-692	W-4	19-May-13	N	295	37°11.50′	74°34.50′	37°11.50′	74°34.40′	91–105
ROV-2013-RB-693	W-2	20-May-13	D	894	37°09.40′	74°34.40′	37°09.40′	74°34.70′	90–116
ROV-2013-RB-694	W-3	21-May-13	D	861	37°13.90′	74°33.10′	37°14.00′	74°33.10′	101–126
ROV-2013-RB-695	W-5	22-May-13	D	504	37°16.80′	74°32.10′	37°17.00′	74°32.20′	106–121
ROV-2013-RB-696	W-2	23-May-13	D	197	37°09.40′	74°34.50′	37°09.40′	74°34.60′	90–114

Adams, 1993; Diaz et al., 2003). Similar assessments in deeper waters of the middle to outer shelf are lacking, aside from those obtained from submersible surveys directed toward tilefish (*Lopholatilus chamaeleonticeps*) at depths of 117–268 m (Grimes et al., 1986). In these studies, the physical structure of habitat was observed to be correlated with fish distribution patterns. Higher profile, more complex habitats generally supported greater fish species richness and higher abundance for some species. Bioengineering by tilefish and associated species in and near canyon heads also created complex habitats for other outer shelf fauna (Grimes et al., 1986).

Non-natural hard substrata (e.g., shipwrecks) aggregate fish and invertebrates. The effects of artificial reefs composed of shipwrecks and other structures (e.g., drilling platforms and fish attracting devices) are well known but their use as fish habitat is still being debated (Stephan and Lindquist, 1989; Grossman et al., 1997; Perkol-Finkel et al., 2006). It is unclear whether artificial reef structures actually increase populations of fish as opposed to simply concentrating them, and understanding the role of artificial reefs is increasingly important considering the decline of natural reefs worldwide (Perkil-Finkel et al., 2006). However, Arena et al. (2007) reported that vessel-reefs off southeastern Florida supported significantly higher fish species richness and abundance than at natural reefs and that different community structures and trophic patterns were observed for the 2 habitat types, and they suggested that vessel-reefs enhanced local fish populations. The extent to which artificial reefs mimic natural reef functions requires further study, and artificial reefs may only approach the functions of natural reefs if their physical structures are similar (Perkol-Finkel et al., 2006).

As part of a larger survey of submarine canyons and nearby features in the MAB, historically important shipwrecks, naturally occurring hard bottom, and sandy bottom areas on the outer continental shelf near Norfolk Canyon were surveyed with remote operated vehicles (ROVs) in 2012 and 2013. In this article, we document 1) species of overall fish communities on shelf-depth artificial (shipwrecks) substrata and natural hard substrata and nearby soft-bottom habitats, 2) relative abundance of fish species in those communities, and 3) behaviors and distributions of fishes on shipwreck and nonshipwreck open bottom for 2 seasons (fall in 2012 and spring in 2013). The degree to which fishes were associated with hard bottom and the degree to which such habitats supported unique communities were investigated.

Materials and methods

Study area

On the middle to outer continental shelf (depths of 42–126 m) of the southern MAB, 9 locations in the vicinity of Norfolk Canyon were surveyed with ROVs (Table 1, Fig. 1). These study sites had been mapped with multibeam sonar in 2011. The shallowest location (site SS) was the only one entirely composed of flat, soft sediment

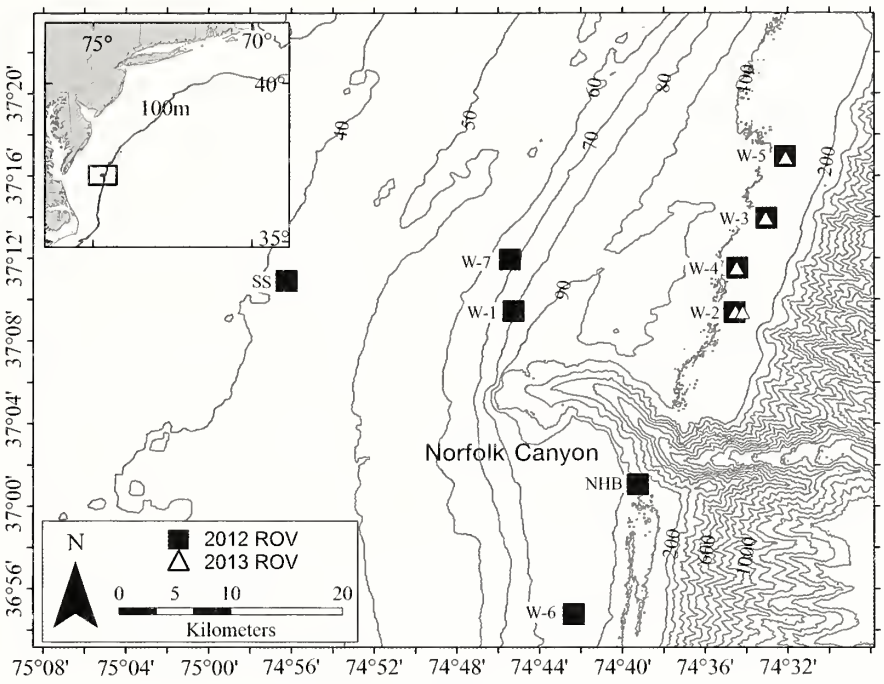

Figure 1

Locations of the 9 sites, 7 shipwreck sites (W-1 through W-7), 1 mostly natural hard-bottom (NHB) site, and 1 soft-bottom (SS) site, where remotely operated vehicles (ROVs) were used to collect data concerning fish assemblages on 20–28 September 2012 and 19–23 May 2013. Depth contours are given in meters. The inset illustrates the Middle Atlantic Bight; the rectangle indicates the study area.

bottom. All other sites comprised predominately hard, complex substrata, but they were also surrounded by soft substrata (see "Habitat definitions" section). The natural hard-bottom (NHB) location was dominated by hard, rough bottom, including boulders, rubble fields, and walls of consolidated mud. The dominant habitat in 7 of the study sites (e.g., W-1) was composed of 8 historically important shipwrecks, all sunk during the early 1920s (i.e., 6 of the ships were part of the "Billy Mitchell fleet" [Lee, 1949]). These shipwrecks had the following lengths and maximum heights off bottom: W-1 (45×6 m), W-2 (167×18 m), W-3 (141×7 m), W-4 (301×3 m), W-5 (2 shipwrecks about 685 m apart; 64×3 m and 53×2 m), W-6 (171×14 m), W-7 (72×3 m). The shipwrecks were surrounded by soft substrata (sand or gravel). All shipwrecks were covered to varying degrees with lost fishing gear (trawls, Fig. 2, A and C).

Remotely operated vehicle

Dives of the ROV were conducted with the University of Connecticut ROV *Kraken II* deployed from the NOAA Ship *Nancy Foster* on 20–28 September 2012 and, during a second research cruise, with the Woods Hole Oceanographic Institution ROV *Jason II* deployed from the NOAA Ship *Ronald H. Brown* on 19–23 May 2013. The site SS, the site NHB, and sites W-1, W-6, and W-7 each were sampled with 1 ROV dive, and each of the other shipwreck sites were sampled either 2 (W-3, W-4, and W-5) or 3 (W-2) times for a total of 14 ROV dives (Table 1). The position of the ROV was recorded continuously by using an ultrashort baseline tracking system, and navigation data were time synchronized with all imagery and samples. An SBE 911plus[1] conductivity, temperature, and depth (CTD) instrument (Sea-Bird Electronics Inc., Bellevue, WA) was attached to the ROVs to record conductivity (in microSiemens per centimeter), temperature (degrees Celsius), salinity, density ($\sigma\theta$, in kilograms per cubic meter), dissolved oxygen (DO, in milliliters per liter), depth, and pH at a frequency of once per second during each dive. Only temperature, salinity, and DO data recorded during dives while the ROVs were on or near bottom are presented.

Digital video was collected as the ROVs moved along transects at slow speeds, <~25 cm/s (<0.5 kt), across all habitat types and with the vehicles as near to bottom as possible. At each shipwreck, video and still image photo-mosaics were recorded over a series of parallel transects that covered the entire shipwreck. This digital imagery was used for vessel identification, examination of present ambient conditions and documentation

[1] Mention of trade names or commercial companies is for identification purposes only and does not imply endorsement by the National Marine Fisheries Service, NOAA.

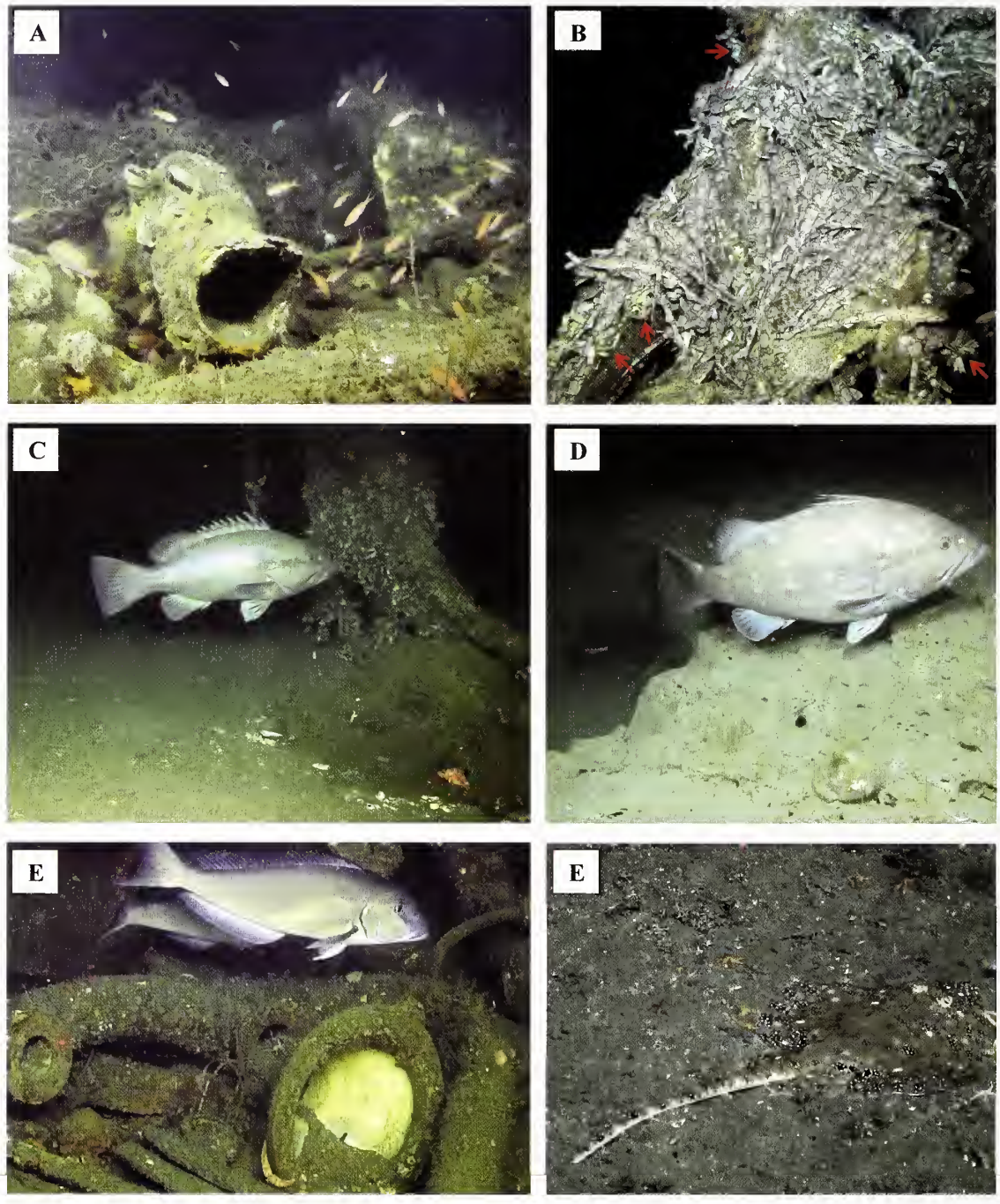

Figure 2

Photographs of fishes and habitats surveyed with remotely operated vehicles in 2012 and 2013 near Norfolk Canyon in the Middle Atlantic Bight: (**A**) school of unidentified anthiine serranids and at least one yellowtail bass (*Anthias nicholsi*, mid-left) on shipwreck site W-1, 81 m, 22 September 2012; (**B**) dense aggregations of chain dogfish (*Scyliorhinus retifer*) lying on shipwreck structure (site W-5, ~115 m, 26 September 2012), 4 yellowfin bass (2 upper right, 2 lower right), and red arrows indicate clusters of egg cases of chain dogfish; (**C**) warsaw grouper (*Hyporthodus nigritus*), and a scorpionfish (*Scorpaena* sp., lower right lying on trawl net) on shipwreck site W-5, 118 m, 26 September 2012; (**D**) snowy grouper (*Hyporthodus niveatus*) on the natural hard-bottom (NHB) site, ~110 m, 27 September 2013; the scaling laser dots near the anal fin indicate that this fish is at least 150 cm long in total length; (**E**) 2 blueline tilefish (*Caulolatilus microps*) on shipwreck site W-2, ~100 m, 20 May 2013; and (**F**) rosette skate (*Leucoraja garmaini*) on sandy habitat near shipwreck site W-2, ~100 m, 23 May 2013.

of biota and habitats. The color video cameras attached to the ROVs had scaling lasers (10-cm spacing) used to estimate total length (TL) of fish. During transect surveys, the cameras were positioned to record directly in front of the ROV and were set on wide angle (or near wide angle). The video cameras recorded continuously throughout the ROV dives (whether the ROV was moving over transects or was stationary on bottom), and digital still images were taken frequently to augment video collection.

Habitat definitions

A main objective was to determine to what degree fishes were associated with general habitats on a large scale; therefore, habitat definition was reduced to 2 broad, relatively simple types: 1) soft substrata (SS) of sand or mud—relatively flat substrata and with few structuring features aside from gravel, burrows, depressions, and animal tracks; and 2) artificial (shipwreck) substrata and natural hard bottom (AS/NHB), which included World War I-era shipwrecks with substantial vertical profile and one site with natural hard bottom (consolidated mud, ledges, and boulders). Additional habitat metrics included bottom depth and environmental data recorded by the CTD instruments mounted on the ROVs.

Video analysis: community and habitat association

A preferred method for documenting fauna in complex habitats, visual observations (here based on ROV-collected video) were used to describe the fish communities and associated habitats at the 9 study sites. Tracks of ROV dives were processed initially to conservatively remove erroneous tracking data (location points) as described by Quattrini et al. (2012). To determine community structure and habitat associations of fishes at sites, much as described in Ross and Quattrini (2007), videos from each dive were viewed multiple times for habitat classifications (see "Habitat definitions" section) and for identification (to the lowest possible taxa) and enumeration of fishes by time of observation. Video segments were designated when the ROV stopped or started movement, when the video quality changed, or when the habitat changed. Depth was recorded by the ROV-mounted SBE 911plus for every time segment. Unusable video (out of focus, too far off bottom, because of malfunction, sediment clouds) was removed from the data set.

Species composition and relative abundances (fish counts) were determined from the wide-angle video and were compared within each of and between the 2 habitat types. To compare abundances of all species within a habitat type, relative abundances were calculated in percentages as the number of individuals per taxa per habitat type divided by the total number of individuals observed per habitat type and then multiplied by 100. For comparisons between habitat type, analysis was restricted to benthic fishes identified to at least family level and with overall abundances ≥2. Occurrence of at least 2 individuals allowed for the possibility of a taxa occurring in both habitat types. Relative abundances by habitat type were calculated for each taxon by dividing the number of individuals in a particular habitat type by the total number of individuals of the same species from both habitat types and multiplying the result by 100.

Multivariate analyses were conducted in PRIMER 6 and PERMANOVA+ (PRIMER-E Ltd., Ivybridge, U.K.) (Clarke and Warwick, 2001; Clarke and Gorley, 2006; Anderson et al., 2008) to determine differences in benthic fish assemblages between habitat types. Sample units were the numbers of each species per habitat type (SS or AS/NHB) per ROV dive; samples with no species present were removed from the data set. Because transect times were variable, abundances of species were standardized per sample by dividing the number of individuals per species by the total number of fishes per sample. Standardized abundances were fourth-root transformed to down-weight the abundant species in relation to rare species. The Bray-Curtis similarity coefficient was used to calculate similarities between samples, and on the basis of the resulting similarity matrix a nonmetric multidimensional scaling ordination (MDS) plot and a dendrogram with group average linking were created. One-way analysis of similarities (ANOSIM) and post-hoc multiple comparison tests were used to determine whether there were significant differences between fish assemblages in the 2 different habitat types. Similarity percentage (SIMPER) analysis was used to determine which species contributed to the dissimilarities among habitat types.

Results

On the 9 study sites (depths of 42–126 m), 14 ROV dives were completed, 9 dives in September 2012 and 5 dives in May 2013 (Table 1, Fig. 1), resulting in 84.4 h of usable video data on hard-bottom (AS/NHB) habitat and 16.5 h of video data on soft-bottom (SS) habitat. Soft-bottom habitat was observed exclusively with video collected during the dive at the shallowest site (Table 1, Fig. 1); however, because only 3 specimens of unidentified skates were observed during this dive, it made little contribution to our study. Although shipwrecks and natural hard bottom were the focus of the remaining dives, soft-bottom habitat surrounding those hard-bottom habitats was also surveyed during these dives.

In September 2012, mean bottom temperatures varied about 2.5°C across the study sites; the coldest temperatures (means: 11.9–13.0°C), lowest salinities (means: 33.1–34.8), and highest DO (means: 4.0–4.5 mL/L) occurred at the shallower sites (depths of 42–81 m) (Table 2). At each of the 5 deeper sites (depths of 84–126 m), bottom temperatures (means: 14.2–14.5°C), salinities (35.6–35.8), and DO (3.7–4.0 mL/L) were similar to each other. In May 2013, little variation was

Table 2

Environmental data (means, ranges, and standard errors of the means in parentheses) recorded at bottom by the SBE 911plus system (one exception indicated at the footnote) attached to the remotely operated vehicles *Kraken II* (2012) and *Jason II* (2013) during surveys of shipwrecks and sandy bottoms on the continental shelf near Norfolk Canyon in the Middle Atlantic Bight. Site locations are appended to the dive year in each dive no. (see Table 1). NA=not available. DO=dissolved oxygen.

Dive no.	Temperature (°C)	Salinity	DO (mL/L)
2012-NF-21-SS	12.16, 11.95–12.29 (0.0007)	33.14, 33.16–33.17 (0.0001)	4.51, 4.45–4.55 (0.0002)
2012-NF-22-W1	11.94, 10.73–14.61 (0.0029)	34.16, 32.92–34.94 (0.0015)	4.22, 4.08–5.54 (0.0005)
2012-NF-23-W2	NA	NA	NA
2012-NF-24-W3	14.31, 14.10–14.47 (0.0003)	35.65, 35.32–35.80 (0.0005)	3.88, 3.67–4.14 (0.0003
2012-NF-26-W4	14.47, 14.40–14.52 (0.0001)	35.78, 35.69–35.80 (0.0001)	3.98, 3.95–4.11 (0.0001)
2012-NF-27-W5	14.15, 14.00–14.46 (0.0008)	35.75, 35.74–35.80 (0.0000)	3.69, 3.51–4.84 (0.0006)
2012-NF-28-NHB	14.33, 14.22–14.39 (0.0002)	35.71, 35.50–35.77 (0.0004)	3.93, 3.83–4.06 (0.0004)
2012-NF-29-W6	14.21, 13.86–14.30 (0.0009)	35.63, 35.12–35.72 (0.0013)	3.84, 3.67–4.85 (0.0004)
2012-NF-30-W7	13.00, 12.53–13.41 (0.0013)	34.76, 34.45–35.09 (0.0008)	3.99, 3.87–4.78 (0.0004)
2013-RB-692-W4	13.16, 13.09–13.32 (0.0005)	34.83, 32.20–35.72 (0.0085)	2.99, 1.81–4.22 (0.0042)
2013-RB-693-W2	13.27, 13.18–13.50 (0.0003)	32.81, 29.66–33.14 (0.0033)	2.44, 1.38–4.31 (0.0018)
2013-RB-694-W3	13.42, 12.90–13.49 (0.0004)	35.48, 32.64–35.94 (0.0027)	3.08, 2.09–4.46 (0.0021)
2013-RB-695-W5	13.19, 13.10–13.45 (0.0004)	29.42, 26.38–35.18 (0.0010)	NA[1]
2013-RB-696-W2	13.32, 13.00–13.60 (0.0012)	35.69, 35.63–35.77 (0.0002)	4.71, 4.57–4.76 (0.0003)

[1]Data were taken from the *Jason II* conductivity, temperature, and depth (CTD) system, SBE 911plus, which was not operating.

again observed among the 5 deeper sites, but temperatures (means: 13.2–13.4°C) were on average a degree colder than they were in 2012. At these sites, more variations in salinity (means: 29.4–35.7) and DO (means: 2.4–4.7 mL/L) were recorded that those recorded in 2012. It seems unlikely that the small environmental variations were biologically significant to these temperate, wide-ranging fishes, particularly at the deeper sites, but monitoring over longer periods is required to determine the scale of environmental variation.

From analysis of the video from ROV dives, 38 unique fish taxa, representing at least 25 families, were identified (*Urophycis* sp., *Hyporthodus* sp., Anthiinae (unidentified), *Caulolatilus* sp., Labridae (unidentified), and unidentified fish not included in total counts; Table 3). Of those 38 taxa, 33 occurred on the AS/NHB habitat type (14 species were observed only on hard bottom), and 25 taxa occurred on the SS habitat type (6 occurred only on soft bottom) (Table 3). The lower number of species observed in the SS habitat type was at least partly due to lower dive effort there (Table 3). Three taxa, a requiem shark (*Carcharhinus* sp.), the greater amberjack (*Seriola dumerili*), and the ocean sunfish (*Mola mola*), that occurred over or near either habitat type are considered pelagic fish that are less constrained to benthic habitats.

Fish assemblages on each habitat type were numerically dominated by relatively few species. On the AS/NHB substrata, 96.5% of the community was composed of 7 taxa (in decreasing order of abundance): unidentified anthiine serranids, the chain dogfish (*Scyliorhinus retifer*), the yellowfin bass (*Anthias nicholsi*), the deepbody boarfish (*Antigonia capros*), the red barbier (*Baldwinella vivanus*), a scorpionfish (*Scorpaena* sp.), and the black sea bass (*Centropristis striata*). Anthiine serranids (all combined, including yellowfin bass, red barbier, and unidentified members of this subfamily) and the chain dogfish (Fig. 2, A and B) were each an order of magnitude (2 orders of magnitude compared with most species) more abundant than any other taxa in either habitat type. Most of the Anthiinae fishes that were observed were probably red barbier, but small, rapidly moving anthiines can be difficult to identify in situ; some of these fishes could have been the streamer bass (*B. aureorubens*), longtail bass (*Hemanthias leptus*), or threadnose bass (*Choranthias tenuis*). The smaller (~60–180 mm TL) fishes of the subfamily Anthiinae occurred as dense aggregations whose members swam rapidly around hard-bottom structures (Fig. 2 A), occasionally straying over nearby sandy bottom. Larger (usually ~130–200 mm TL) yellowtail bass were more solitary and often associated with the anthiine schools (Fig. 2, A and B).

Six taxa (in decreasing order of abundance: the chain dogfish, the deepbody boarfish, the black sea bass, *Scorpaena* sp., the yellowfin bass, and anthiine serranids), accounted for 93.6% of the fauna on the SS habitat type but usually exhibited a lower percent contribution to the SS habitat type than to the AS/NHB habitat type (Table 3). Species that were unique to either habitat type occurred in low abundance (<1% of total abundance within habitat).

Table 3

Relative abundance (%) of fishes observed during dives of remotely operated vehicles in 2012 and 2013 on 2 habitats types: 1) artificial (shipwreck) substrata and natural hard bottom (AS/NHB) and 2) soft substrata (SS) near Norfolk Canyon, Middle Atlantic Bight. Number of hours of observation (usable video) and depth ranges are provided under each habitat type.

Taxa	AS/NHB 84.42 h, 63–126 m	SS 16.48 h, 40–126 m
Scyliorhinidae		
Scyliorhinus retifer, chain dogfish	30.158	56.489
Carcharhinidae		
Carcharhinus sp., requiem shark	0.002	
Rajidae		
Leucoraja garmani, rosette skate		0.339
Rajidae (unidentified)	0.002	0.594
Ophichthidae		
Ophichthus cruentifer, margined snake eel		0.170
Congridae		
Conger oceanicus, conger eel	0.596	0.170
Gadiformes (unidentified), cods	0.002	0.085
Moridae		
Physiculus fulvus, metallic codling	0.094	
Phycidae		
Phycis chesteri, longfin hake	0.002	
Urophycis chuss, red hake	0.002	
Urophycis regia, spotted hake	0.006	
Urophycis sp.	0.083	0.085
Lophiidae		
Lophius americanus, goosefish		0.085
Trachichthyidae		
Gephyroberyx darwinii, big roughy	0.600	
Macroramphosidae		
Macroramphosus scolopax, longspined snipefish	0.557	0.254
Scorpaenidae		
Scorpaena sp., scorpionfish	1.249	6.107
Triglidae		
Prionotus sp., searobin	0.004	0.085
Polyprionidae		
Polyprion americanus, wreckfish	0.004	
Serranidae		
Anthias nicholsi, yellowfin bass	10.667	1.442
Anthias sp.	0.002	
Baldwinella vivanus, red barbier	3.904	0.085
Centropristis striata, black sea bass	1.180	6.531
Hyporthodus nigritus, warsaw grouper	0.015	
Hyporthodus niveatus, snowy grouper	0.058	0.085
Hyporthodus sp.	0.004	
Pronotogrammus martinicensis, roughtongue bass	0.006	
Anthiinae (unidentified)	44.606	1.442
Malacanthidae		
Caulolatilus microps, blueline tilefish	0.369	0.594
Caulolatilus sp.		0.339
Pomatomidae		
Pomatomus saltatrix, bluefish	0.137	1.781
Carangidae		
Seriola dumerili, greater amberjack	0.062	0.085
Sparidae		
Stenotomus chrysops, scup	0.009	0.509

Table continued

Table 3 (*continued*)

Taxa	AS/NHB 84.42 h, 63–126 m	SS 16.48 h, 40–126 m
Labridae		
Tautoga onitis, tautog	0.008	
Tautogolabrus adspersus, cunner	0.729	0.254
Labridae (unidentified)	0.002	
Caproidae		
Antigonia capros, deepbody boarfish	4.776	21.628
Paralichthyidae		
Paralichthys dentatus, summer flounder	0.002	0.085
Paralichthys oblongus, fourspot flounder	0.004	0.085
Bothidae (unidentified), lefteye flounders		0.254
Pleuronectidae		
Glyptocephalus cynoglossus, witch flounder	0.002	
Hippoglossoides platessoides, American plaice	0.002	
Cynoglossidae		
Symphurus stigmosus, blotchfin tonguefish		0.085
Molidae		
Mola mola, ocean sunfish	0.002	
Unidentified fishes	0.096	0.339

Chain dogfish were less abundant on the natural hard bottom (site NHB) than on the shipwreck (AS) or SS habitats. They occurred in massive numbers at the shipwreck sites, where they were often so densely packed that they lay on top of each other in layers that were several individuals thick (Fig. 2B). Individuals and aggregations of individuals were observed on all areas of the shipwreck sites, including on and within the trawl nets that covered sections of the shipwrecks. Although many chain dogfish were observed lying on soft bottom, they did so generally within tens of meters of the shipwrecks. The aggregations of chain dogfish probably reflect activity related to spawning because thousands of their egg cases were attached to the shipwreck structures and the nets that covered them (Fig. 2B).

Because shelf communities are subjected to seasonal environmental variability and may exhibit seasonal distribution patterns, multivariate analysis was used to examine seasonal differences (fall 2012 versus spring 2013) in fish distributions at the 4 study sites that were sampled during both seasons; 17 video samples (8 for fall, 9 for spring) and 29 species were examined in this analysis. Season did not have a significant impact on fish assemblages (ANOSIM, coefficient of multiple correlation [R]= −0.024, P=0.55). Likewise, there were no differences in assemblage structure over the limited depth range examined (8 sites, depths of 68–126 m, dive NF-21 at site SS excluded, R=0.026, P=0.400). The greatest distances between sites were no more than 50 km, and fish assemblages (excluding observations from dive NF-21) at the 8 sites were not significantly different (R=0.130, P=0.090) in regard to distance from one another or distance from Norfolk Canyon. Therefore, all data were combined for analysis of habitat influence on fish assemblages.

Multivariate analysis of 26 video samples (excluding those from the shallow dive NF-21) and 41 taxa, indicated a significant difference (R=0.499, P=0.001) in fish assemblage structure between the soft bottom (SS) and hard bottom (AS/NHB) habitat types (Fig. 3). The video samples from the AS/NHB habitat type were 60% dissimilar from the 2 sample groups affiliated with the SS habitat type; the video sample associated with natural hard-bottom habitat (at site NHB) grouped with the shipwreck hard-bottom (AS) samples (dive number 28, Fig. 3). The fishes most influencing the group of samples from the AS/NHB habitat type (on the basis of SIMPER analysis) were the chain dogfish, members of Anthiinae, the yellowfin bass, the deepbody boarfish, the conger eel (*Conger oceanicus*), *Scorpaena* sp., the red barbier, the cunner (*Tautogolabrus adspersus*), and the blueline tilefish (*Caulolatilus microps*). Fishes most influencing the groups of samples from the SS habitat type were the chain dogfish, *Scorpaena* sp., the deepbody boarfish, and the black sea bass.

Data indicates at least some difference in fish communities along isobaths. Within the hard bottom group, video samples (n=9) from the 4 deeper shipwreck habitats (AS) north of Norfolk Canyon (depths of 91–126 m; Fig. 1) grouped closely together (Fig. 3), although data were collected in 2 different years and seasons. The 3 shipwreck hard-bottom (AS) video samples from the shallower middle shelf (depths of 68–85 m; Fig. 1) were offset together in the overall group of samples from the AS/NHB habitat type (dive numbers 22, 29, 30; Fig. 3). The 3 samples from sandy bottom on the middle shelf (SS habitat type, dive numbers 22, 29, 30; Fig. 3) also

were set apart from most other SS samples (Fig. 3). Fishes that occurred in deeper waters (>90 m) that were missing from those 3 middle shelf sites, regardless of habitat type, were the metallic codling (*Physiculus fulvus*), the big roughy (*Gephyroberyx darwinii*), the longspine snipefish (*Macroramphosus scolopax*), groupers (*Hyporthodus* spp.), and the deepbody boarfish. Two species common on the middle shelf sites, the scup (*Stenotomus chrysops*) and the tautog (*Tautoga onitis*), were not observed on the deeper sites.

Habitat preference also was indicated by relative abundance patterns of most benthic fishes. The hard bottom (AS/NHB) habitat type contained ≥89% of the abundance of each of 22 fish taxa (i.e., the first 22 species in Fig. 4), and far more individuals were observed overall in that habitat type than in the SS habitat type. Several species, including a searobin (*Prionotus* sp.), the fourspot flounder (*Paralichthys oblongus*), the summer flounder (*P. dentatus*), and the scup, used both soft- and hard-bottom habitats frequently. A few taxa, including lefteye flounders (Bothidae), the margined snake eel (*Ophichthus cruentifer*), and the rosette skate (*Leucoraja garmani*), were observed only on soft bottom (Figs. 2F and 4).

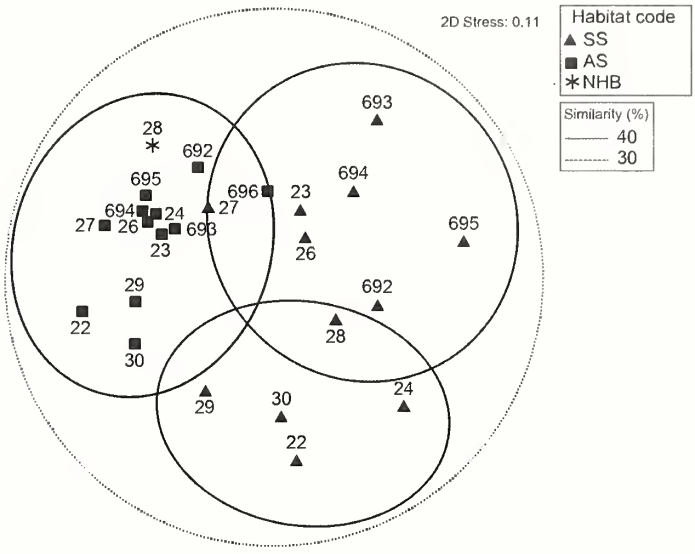

Figure 3

Multidimensional scaling ordination of 26 video samples from habitats of artificial (shipwreck) substrata (AS), natural hard bottom (NHB), and soft substrata (SS), based on the Bray-Curtis similarity matrix calculated from standardized, fourth-root transformed fish abundances (41 taxa). Numbers by symbols are the dive numbers given to each dive of the remotely operated vehicles (see Table 1).

Discussion

Fishes that occupied natural and artificial hard-bottom habitats on the middle to outer shelf of the MAB exhibited an assemblage structure in our study that was different from that of the well-documented (e.g., Murawski et al., 1983; Mahon et al., 1998) ichthyofauna of MAB soft-bottom habitats. Although the most abundant reef (i.e., hard-bottom) species also were observed and counted on soft-bottom habitat, in most cases they were never far from reef structures. The hard-bottom habitats surveyed in our study were dominated by cool-temperate and warm-temperate species that are generally considered to be reef associates, although some (e.g., the chain dogfish, black sea bass, and conger eel) have broad depth and latitudinal distributions and large-scale habitat use. Other species common to the hard-bottom habitats (e.g., most Serranidae, the tautog, the blueline tilefish, and the deepbody boarfish) exhibited more restricted distributions and tighter association with reefs. Species of Serranidae (excluding the black sea bass) in particular seemed constrained to a relatively narrow depth range (from ~70 m to at least 150 m) in the MAB, most likely because of the generally warmer (>10°C) and less variable bottom water temperatures along the outer shelf of the southern MAB (Colvocoresses and Musick, 1984).

In contrast to most of the fishes associated with soft-bottom habitats, several of the abundant hard-bottom species (Fig. 2, A–E; e.g., the yellowfin bass, the red barbier, groupers, and the blueline tilefish) were further constrained by being at or near the northern limits of their adult ranges (Moore et al., 2003; Anderson and Heemstra, 2012). Because many of the common hard-bottom species (e.g., most of the Serranidae and the chain dogfish and deepbody boarfish) likely have an obligate association with reef-like habitats (Able and Flescher, 1991; Craig et al., 2011; Anderson and Heemstra, 2012), the relatively limited extent of hard bottom in the MAB (Steimle and Zetlin, 2000) would also affect their distribution. Therefore, an abundant component of the hard-bottom fish community in the southern MAB is restricted by habitat availability, depth, and zoogeography, of which the latter 2 constraints probably are related to bottom temperature. Although this reef community of the outer shelf appears to flourish, these limitations likely make it vulnerable to overfishing, habitat damage, and large-scale environmental variations.

Results presented here differ substantially from those of other surveys of the MAB. Our ROV study sites overlapped with some of the areas of fish groupings that were based on decades of bottom trawl surveys (Colvocoresses and Musick, 1984; Mahon et al., 1998); however, the majority of species common to this study and these 2 trawl-based studies were species that are reported to be most common on sandy bottoms

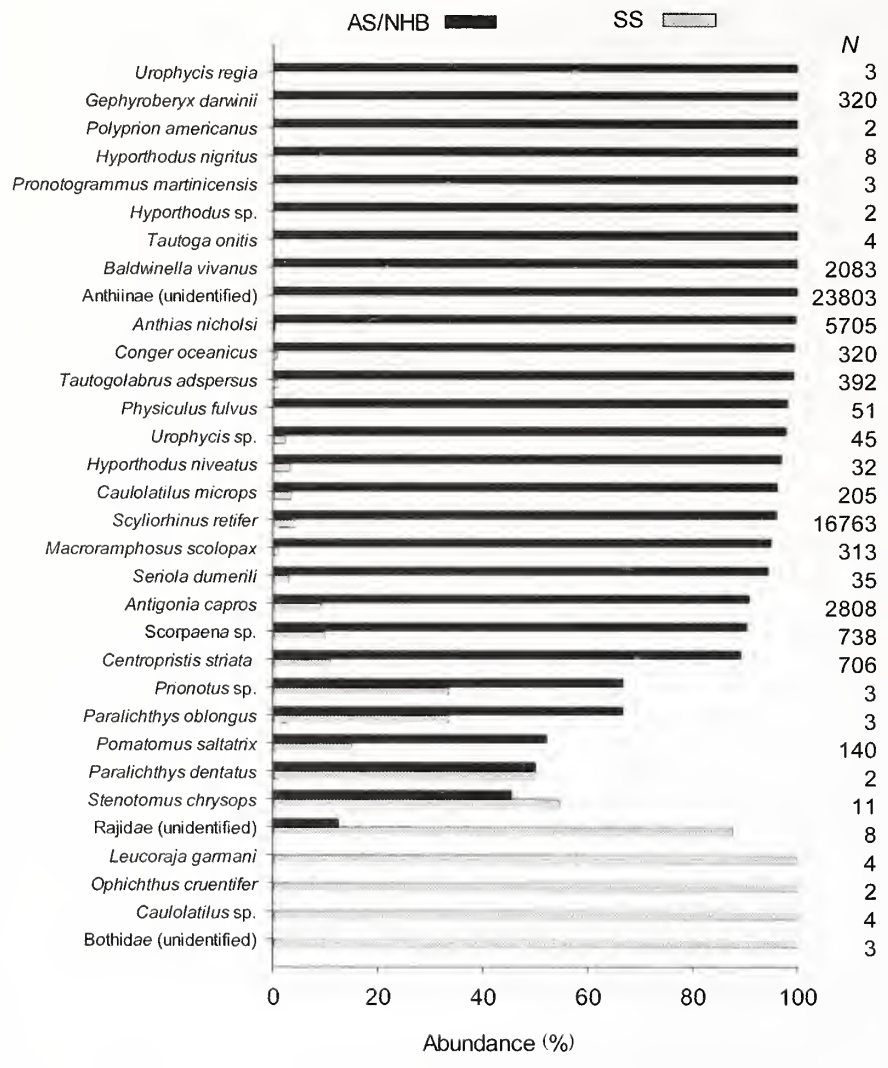

Figure 4

Relative abundance within species across 2 habitat types: 1) artificial (shipwreck) substrata and natural hard bottom (AS/NHB) and 2) soft substrata (SS), for benthic species that had 2 or more individuals identified in the analysis of video. *N*=total number of individuals counted during analysis of video collected along transects.

(e.g., goosefish [*Lophius americanus*], spotted hake [*Urophycis regia*], fourspot flounder, summer flounder). The most abundant taxa observed in our study (i.e., the chain dogfish, Anthiinae, and the deepbody boarfish), as well as others known to be reef associates (e.g., groupers, the blueline tilefish, and wrasses [Labridae]), were not abundant or were not reported in those earlier trawl-based studies (see also Grosslein and Azarovitz, 1982). The differences in species composition, largely resulting from sampling constraints imposed by trawls, emphasize the high degree of separation between fish communities on soft-bottom and those on reef-like habitats in the MAB.

Although Grimes et al. (1986) and Ross et al. (2015) conducted visual surveys that covered extensive complex habitats in the region, they reported only 2 (25% overlap) and 10 (12% overlap) fish species, respectively, in common with those observed in our study. In those 2 studies, the faunal differences can be attributed to deeper waters or a sampling areas much farther north than those surveyed in our study. Although also completed farther north (~ 41°N), visual surveys (Auster et al., 1995) conducted over flat, primarily sand and shell bottom (sites at depths of 55, 240, 712 m) yielded 37.5% fish species in common with our study, and most of those species exhibited broad habitat affinity or affinity for soft bottom. In contrast, the MAB hard-bottom habitats surveyed in our study shared 43% of the fish

fauna with a deep (depths of 237–253 m) shipwreck off Cape Fear, North Carolina, that was assessed during one earlier ROV dive (Quattrini and Ross, 2006). Many (~30%) of the reef-associated fishes reported here are common on outer shelf hard grounds throughout the southeastern United States (Grimes et al., 1982; Quattrini and Ross, 2006), also indicating a warm-temperate affinity for reef fishes of the southern MAB.

As with the reefs of the middle to outer shelf, hard-bottom habitats of the shallower inner shelf of the MAB were dominated by relatively few, but different, fish species (i.e., the black sea bass, tautog, cunner, and scup). On the deeper hard-bottom habitats surveyed in this study, the black sea bass, tautog, and scup ranked below the top 6 species in abundance. Previous shelf studies were conducted in much shallower water (depths <35 m) (Briggs, 1975; Feigenbaum et al., 1985; Eklund and Targett, 1991; Adams, 1993), and not many small species were caught in 2 studies that relied heavily on data from fish traps. However, taxa like the Anthiinae, most common on deeper reefs (Anderson and Heemstra, 2012), are unlikely to occur on inshore reefs. Although regionally limited in general, hard-bottom habitats and associated data that can be recorded there are even more rare along the outer shelf (i.e., ~100-m depth zone; Steimle and Zetlin, 2000). Despite the restricted scope of these deep shelf reefs, they support economically important fishes (e.g., groupers, tilefishes, and black sea bass) and exhibit a high species richness of fishes, as do reefs at similar depths south of Cape Hatteras (Parker and Ross, 1986; Quattrini and Ross, 2006).

A degree of faunal stability along the outer shelf of the southern MAB is indicated by similarities between years or seasons for the 4 study sites sampled in both seasons and both years. Although many fish species shift distributions by season in the MAB (Murawski et al., 1983), such movements may be less pronounced in deeper waters. A relatively small (~2°C) variation in bottom temperatures along the outer shelf (depth ~100 m) was correlated with consistent groupings of soft-bottom species across seasons and years (Colvocoresses and Musick, 1984). Grimes et al. (1986) noted that the region from southern New England to the MAB was often occupied by a warmer (9–14°C) bottom water mass from depths of about 100–300 m. In contrast, there were distinct seasonal differences in fish communities correlated with temperature, which varied over a range of 16.7°C, on an artificial reef in much shallower water, at a depth of 21 m, off Virginia (Adams, 1993). For the deeper shipwreck sites that we sampled during 2 seasons, only a mean bottom temperature difference <1.5°C was observed between the 2 survey periods. Although more continuous and long-term environmental data are needed to capture more accurate means and especially variability, our results agree with the larger data set from Colvocoresses and Musick (1984).

Colton (1972) noted a series of warming and cooling trends on the shelf in the Gulf of Maine, but there was also little apparent change in the distributions of 4 groundfish species correlated with these temperature shifts. Because obligate reef fishes usually exhibit strong site or area fidelity, as long as bottom temperatures remain within tolerances, much of the reef fish community (e.g., Anthiinae and *Hyporthodus* spp.) on the outer shelf of the MAB should continue to occupy these hard-bottom sites. However, episodic intrusions of cold water from the north or from the deep sea can jeopardize some species of the reef fish community of the MAB outer shelf and could cause mass mortalities as documented for tilefish (Marsh et al., 1999).

As previously suggested (Murawski et al., 1983; Nye et al., 2009; Møller et al., 2010), it is tempting to propose that hard-bottom habitats of the southern MAB are increasingly invaded by more warm-temperate species, possibly in response to rising ocean temperatures. North Carolina is the closest southern source where many of the species noted here are abundant on extensive outer shelf hard-bottom habitats (Grimes et al., 1982; Parker and Mays, 1998; Quattrini and Ross, 2006). Although Cape Henry, Virginia, was listed with question as the northern limit of blueline tilefish (Dooley, 1978), our observations confirm its presence in the MAB (Fig. 2E) and extend its range north of Norfolk Canyon. That species, and the yellowfin bass, had been reported from this region from the early 20th century (Firth, 1933, 1937). Snowy grouper (*Hyporthodus niveatus*) and warsaw grouper (*H. nigritus*) (Fig. 2, C and D) were reported in New England waters as early as the late 19th century, but in most of these cases the fish were juveniles collected inshore and assumed to be strays (Smith, 1971). Large adults (documented in world tackle records) of snowy grouper recently occurred in the MAB recreational hook-and-line fishery (as did blueline tilefish), but data presented here are the first descriptions of their relative abundance and adult habitat along the outer shelf of the MAB. Recent collections of red barbier near Wilmington Canyon represent the first records of that species for the MAB (Moore et al., 2003), but this small, deep-reef-specific fish could have easily escaped detection. Similarly, our observations of 3 individuals of roughtongue bass (*Pronotogrammus martinicensis*) at depths of 92 m on the natural hard bottom represent a new northern range limit (from North Carolina, Anderson and Heemstra, 2012) for this species, but this observation does not necessarily mean that this species is newly arrived to the MAB. Although historical data have been inadequate (because of a lack of appropriate sampling on deep reefs) to allow an evaluation of long-term changes in the patterns of hard-bottom species composition on the MAB outer shelf, this study, the first to examine outer shelf reef fishes of this region, should provide a baseline for future assessments.

Acknowledgments

Funding for this project was supplied by the Bureau of Ocean Energy Management (BOEM) (contracted to CSA

Ocean Sciences Inc.). We thank G. Boland (BOEM) for support during the development of the overall project. The NOAA Ships *Nancy Foster* and *Ronald H. Brown* and the *Kraken II* and *Jason II* ROVs were provided by the NOAA Office of Ocean Exploration and Research. S. Brooke (Florida State University) assisted with all aspects of organizing and managing the project and cruises. T. Munroe assisted with identifications of flatfishes. A. Quattrini assisted with some statistical analysis. We thank the ship and shore-based personnel who operated the ships and ROVs, and all the science and outreach personnel for their hard work during the cruises.

Literature cited

Able, K. W., and D. Flescher.
1991. Distribution and habitat of chain dogfish, *Scyliorhinus retifer*, in the Mid-Atlantic Bight. Copeia 1991:231–234.

Able, K. W., and M. P. Fahay.
1998. First year in the life of estuarine fishes in the Middle Atlantic Bight, 342 p. Rutgers Univ. Press, New Brunswick, NJ.

Adams, A. J.
1993. Dynamics of fish assemblages associated with an offshore artificial reef in the southern Mid-Atlantic Bight. M.A. thesis, 97 p. College of William and Mary, Williamsburg, VA.

Anderson, M. J., R. N. Gorley, and K. R. Clarke.
2008. PERMANOVA+ for PRIMER: guide to software and statistical methods, 214 p. PRIMER-E, Plymouth, U.K.

Anderson, W. D., Jr., and P. C. Heemstra.
2012. Review of Atlantic and eastern Pacific anthiine fishes (Teleostei: Perciformes: Serranidae), with descriptions of two new genera. Transactions, vol. 102, pt. 2, 192 p. Am. Philos. Soc., Philadelphia, PA.

Arena, P. T., L. K. B. Jordan, and R. E. Spieler.
2007. Fish assemblages on sunken vessels and natural reefs in southeast Florida, USA. Hydrobiologia 580:157–171.

Auster, P. J., R. J. Malatesta, and S. C. LaRosa, R. A. Cooper, and L. L. Stewart.
1991. Micro habitat utilization by the megafaunal assemblage at a low relief outer continental shelf site—Middle Atlantic Bight, USA. J. Northwest Atl. Fish. Sci. 11:59–69.

Auster, P. J., R. J. Malatesta, and S. C. LaRosa.
1995. Patterns of microhabitat utilization by mobile megafauna on the southern New England (USA) continental shelf and slope. Mar. Ecol. Prog. Ser. 127:77–85.

Briggs, P. T.
1975. An evaluation of artificial reefs in New York's marine waters. N.Y. Fish Game J. 22:51–56.

Cailliet, G. M., A. H. Andrews, W. W. Wakefield, G. Moreno, and K. L. Rhodes.
1999. Fish faunal and habitat analyses using trawls, camera sleds and submersibles in benthic deep-sea habitats off central California. Oceanologica Acta 22:579–592.

Clarke, K. R., and R. M. Warwick.
2001. Change in marine communities: an approach to statistical analysis and interpretation, 2nd ed, 172 p. PRIMER-E, Plymouth, U.K.

Clarke, K. R., and R.N., Gorley.
2006. PRIMER v6: user manual/tutorial, 192 p. PRIMER-E, Plymouth, U.K.

Colton, J. B., Jr.
1972. Temperature trends and the distribution of groundfish in continental shelf waters, Nova Scotia to Long Island. Fish. Bull. 70:637–657.

Colvocoresses, J. A., and J. A. Musick.
1984. Species associations and community composition of Middle Atlantic Bight continental shelf demersal fishes. Fish. Bull. 82:295–313.

Craig, M. T., Y. J. Sadovy de Mitcheson, and P. C. Heemstra.
2011. Groupers of the world: a field and market guide, 356 p. NISC Ltd., Grahamstown, South Africa.

Diaz, R. J., G. R. Cutter Jr., and K. W. Able.
2003. The importance of physical and biogenic structure to juvenile fishes on the shallow inner continental shelf. Estuaries 26:12–20.

Dooley, J. K.
1978. Systematics and biology of the tilefishes (Perciformes: Branchiostegidae and Malacanthidae), with descriptions of two new species. NOAA Tech. Rep. NMFS Circ. 411, 78 p.

Eklund, A-M.
1988. Fishes inhabiting hard bottom reef areas in the Middle Atlantic Bight: seasonality of species composition, catch rates and reproduction. M.S. thesis, 98 p. Univ. Delaware, Newark, DE.

Eklund, A-M., and T. E. Targett.
1991. Seasonality of fish catch rates and species composition from the hard bottom trap fishery in the Middle Atlantic Bight (US east coast). Fish. Res. 12:1–22.

Feigenbaum, D., C. H. Blair, M. Bell, J. R. Martin, and M. G. Kelly.
1985. Virginia's artificial reef study: description and results of year 1. Bull. Mar. Sci. 37:179–188.

Firth, F. E.
1933. *Anthias nicholsi*, a new fish taken off Virginia in the deep-water trawl fishery. Copeia 1933:158–160.
1937. Recent records extending the range of *Caulolatilus microps* north of Florida. Copeia 1937:189.

Gabriel, W. L.
1992. Persistence of demersal fish assemblages between Cape Hatteras and Nova Scotia, northwest Atlantic. J. Northwest Atl. Fish. Sci. 14:29–46.

Grimes, C. B., C. S. Manooch, and G. R. Huntsman.
1982. Reef and rock outcropping fishes of the outer continental shelf of North Carolina and South Carolina, and ecological notes on the red porgy and vermilion snapper. Bull. Mar. Sci. 32:277–289.

Grimes, C. B., K. W. Able, and R. S. Jones.
1986. Tilefish, *Lopholatilus chamaeleonticeps*, habitat, behavior and community structure in Mid-Atlantic and southern New England waters. Environ. Biol. Fishes 15:273–292.

Grosslein, M. D., and T. R. Azarovitz.
1982. Fish Distribution. MESA New York Bight Atlas Monograph 15, 182 p. NY Sea Grant Inst. Albany, NY.

Grossman, G. D., G. P. Jones, and W. J. Seaman Jr.
1997. Do artificial reefs increase regional fish production? A review of existing data. Fisheries 22:17–23.

Lee, J.
1949. The bombs heard round the world. Flying 45:24–25, 68.

Mahon, R., S. K. Brown, K. C. T. Zwanenburg, D. B. Atkinson, K. R. Buja, L. Claflin, G. D. Howell, M. E. Monaco, R. N. O'Boyle, and M. Sinclair.
1998. Assemblages and biogeography of demersal fishes of the east coast of North America. Can. J. Fish. Aquat. Sci. 55:1704–1738.

Marsh, R., B. Petrie, C. R. Weidman, R. R. Dickson, J. W. Loder, C. G. Hannah, K. Frank, and K. Drinkwater.
1999. The 1882 tilefish kill—a cold event in shelf waters off the north-eastern United States? Fish. Oceanogr. 8:39–49.

Møller, P. R., J. G. Nielsen, S. W. Knudsen, J. Y. Poulsen, K. Sünksen, and O. A. Jørgensen.
2010. A checklist of the fish fauna of Greenland waters. Zootaxa 2378:1–84.

Moore, J. A., K. E. Hartel, J. E. Craddock, and J. K. Galbraith,
2003. An annotated list of deepwater fishes from off the New England region, with new area records. Northeast. Nat. 10:159–248.

Murdy, E. O., R. S. Birdsong, and J. A. Musick.
1997. Fishes of Chesapeake Bay, 324 p. Smithsonian Inst. Press, Washington, DC.

Murawski, S. A., A. M. Lange, M. P. Sissenwine, and R. K. Mayo.
1983. Definition and analysis of multispecies otter-trawl fisheries off the northeast coast of the United States. J. Cons. Int. Explor. Mer 41:13–27.

Nye, J. A., J. S. Link, J. A. Hare, and W. J. Overholtz,
2009. Changing spatial distribution of fish stocks in relation to climate and population size on the Northeast United States continental shelf. Mar. Ecol. Prog. Ser. 393:111–129.

Parker, R. O., Jr., and S. W. Ross.
1986. Observing reef fishes from submersibles off North Carolina. Northeast Gulf Sci. 8:31–49.

Parker, R. O., Jr., and R. W. Mays.
1998. Southeastern U.S. deepwater reef fish assemblages, habitat characteristics, catches, and life history summaries. NOAA Tech. Rep. NMFS 138, 41 p.

Perkol-Finkel, S., N. Shashar, and Y. Benayahu.
2006. Can artificial reefs mimic natural reef communities? The roles of structural features and age. Mar. Environ. Res. 61:121–135.

Quattrini, A. M., and S. W. Ross.
2006. Fishes associated with North Carolina shelf-edge hardbottoms and initial assessment of a proposed marine protected area. Bull. Mar. Sci. 79:137–163.

Quattrini, A. M, S. W. Ross, M. C. T. Carlson, and M.S. Nizinski.
2012. Megafaunal-habitat associations at a deep-sea coral mound off North Carolina, USA. Mar. Biol. 159:1079–1094.

Ross, S. W., and A. M., Quattrini.
2007. The fish fauna associated with deep coral banks off the southeastern United States. Deep-Sea Res. (I Oceanogr. Res. Pap.) 54:975–1007.

Ross, S. W., M. Rhode, and A. M. Quattrini.
2015. Demersal fish distribution and habitat use within and near Baltimore and Norfolk canyons, U.S. middle Atlantic slope. Deep-Sea Res. (I. Oceanogr. Res. Pap.) 103:137–154.

SEAMAP-SA (Southeast Area Monitoring and Assessment Program—South Atlantic).
2001. Distribution of bottom habitats on the continental shelf from North Carolina through the Florida Keys, 166 p. SEAMAP-SA Bottom Mapping Workgroup, Atlantic States Marine Fisheries Commission, Washington, D.C.

Smith, C. L.
1971. A revision of the American groupers: *Epinephelus* and allied genera. Bull. Am. Mus. Nat. Hist. 146:67–242.

Steimle, F. W., and C. Zetlin.
2000. Reef habitats in the Middle Atlantic Bight: abundance, distribution, associated biological communities, and fishery resource use. Mar. Fish. Rev. 62(2):24–42.

Stephan, D. C., and D. G. Lindquist.
1989. A comparative analysis of the fish assemblages associated with old and new shipwrecks and fish aggregating devices in Onslow Bay, North Carolina. Bull. Mar. Sci. 44:698–717.

NOAA
National Marine
Fisheries Service

Fishery Bulletin
established 1881

Spencer F. Baird
First U.S. Commissioner
of Fisheries and founder
of *Fishery Bulletin*

A new quantitative model of multiple transitions between discrete stages, applied to the development of crustacean larvae

W. Christopher Long

Email address for author: chris.long@noaa.gov

Resource Assessment and Conservation Engineering Division
Kodiak Laboratory
Alaska Fisheries Science Center
National Marine Fisheries Service, NOAA
301 Research Court
Kodiak, Alaska 99615

Abstract—Many biological processes are described in terms of transitions between discrete stages. For example, crustacean larvae generally pass through a number of stages that are punctuated by transitional molting events. On the other hand, some continuous processes, such as embryo development, are frequently described in terms of discrete stages. Despite the widespread use of such conceptual models, a mathematical model that quantitatively describes the transitions between multiple stages has not been developed for crustacean larvae. I describe a model of multiple transitions between stages that can be fitted to such data and that holistically describes the processes and allows explicit, quantitative comparisons among treatments or studies. The base of the model is the logistic equation that is frequently used to model a transition between 2 stages. By summing together multiple logistic equations, one for each transition between stages, the model can accommodate multiple stages. Variance is modeled by treating each transition as a binomial distribution and summing the variance from each transition. To demonstrate, I fitted the model to data on larval development of red and blue king crabs (*Paralithodes camtschaticus* and *P. platypus*). The model provides an excellent fit for these data and quantitatively describes the process of larval development for these crab species.

Manuscript submitted 3 February 2015.
Manuscript accepted 4 November 2015.
Fish. Bull. 114:58–66 (2016).
Online publication date: 25 November 2015.
doi: 10.7755/FB.114.1.5

Biologists often describe biological processes as discrete stages, either on the basis of a natural underlying stepwise process or to simplify a complex continuous process. For example, crustacean larval development generally encompasses discrete stages that are punctuated by molting events (e.g., Costlow and Bookhout, 1959; Haynes, 1982). For simplicity's sake, embryo development of various species is frequently divided into stages defined by particular characteristics, although development in some stages is considered continuous rather than discrete (e.g., Kimmel et al., 1995; Bas and Spivak, 2000; Stevens, 2006). More broadly, diseases and communities are also described as transitioning between stages. Although such developmental processes are commonly described in the biological literature, no model has been developed that quantitatively describes processes which involve sequential transitions between multiple discrete stages and allows explicit comparisons among treatments or species.

Frequently, each stage is considered independently (e.g., Paul and Paul, 1999; Andrés et al., 2010; Walther et al., 2010) and each measured or estimate variable, such as stage duration, is analyzed separately by using univariate statistics (e.g., analysis of variance [ANOVA] or *t*-tests). This approach is unsatisfactory because any comparisons among treatments require a large number of statistical tests, increasing the frequency of type-I errors—problems that are similarly caused by the use of a series of univariate statistics to analyze a multivariate data set (Quinn and Keough, 2002). In addition, in studies on larval development, the method used for determining average interstage duration is often not defined (Paul and Paul, 1999; Andrés et al., 2010; Walther et al., 2010). The method is not defined because of the inherent difficulties in determining when a replicate container with many larvae has reached the next stage. Does the next stage occur the first larva transitions or when the last one does? Or does it occur on the first day when at least half have transitioned?

Red king crab and blue king crab (*Paralithodes camtschaticus* and *P. platypus*) are commercially fished species in Alaska and have a wide and overlapping distribution (Somerton, 1985). In both species, mature females molt, mate, and extrude a batch of eggs in the spring and brood the eggs for about a year (Jensen and Armstrong, 1989; Stevens and

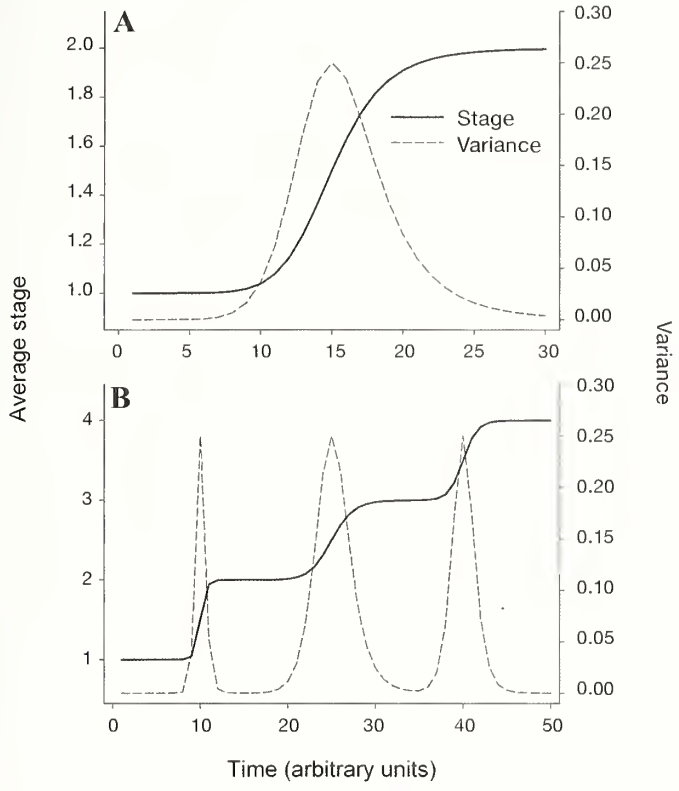

Figure 1

Relationships of stage transitions and predicted variance to time, measured in arbitrary units, from the (**A**) single-stage transition model (time at which 50% of the individuals have made the transition $[t_{50,1}]$=15, slope parameter at the transition that describes the abruptness of the transition $[s_1]$= −8) and the (**B**) Model of multiple transitions between stages with 4 stages and 3 transitions ($t_{50,1}$=10, $t_{50,2}$=25, $t_{50,3}$=40, s_1=−30, s_2=−20, s_3=−50).

Swiney, 2007). The species have a similar size–fecundity relationship (Herter et al., 2011; Swiney et al., 2012; Swiney and Long, 2015), but blue king crab reproduce only once every 2 years whereas red king crab produce a clutch annually (Jensen and Armstrong, 1989).

The larvae of both species are planktonic for 2–3 months before the glaucothoe settle into benthic habitats (Shirley and Shirley, 1989; Stevens et al., 2008). Because newly settled king crabs are highly vulnerable to predators (Stevens and Swiney, 2005), the glaucothoe typically remain planktonic until they find a complex habitat suitable for settlement (Stevens and Kittaka, 1998; Stevens, 2003; Tapella et al., 2009). Red king (Pirtle and Stoner, 2010) and blue king (Daly and Long, 2014a) crabs are vulnerable to predation from both conspecifics (Stoner et al., 2010; Daly and Long, 2014b) and other predators (Daly et al., 2013), but predation is reduced in complex habitats such as cobble, shell hash, and macroalgae (Stoner, 2009; Long et al., 2012; Long and Whitefleet-Smith, 2013). In red king crab, individuals transition into podding behavior as they grow too large to be cryptic (Powell and Nickerson, 1965; Dew, 1990), but nothing is known about blue king crab at this age. Both species mature at a carapace length of about 90 mm (Somerton and MacIntosh, 1983; Blau, 1989), although size at maturity varies among populations (Pengilly et al., 2002).

In this study, I present a simple model that describes such stepwise processes. It is flexible enough to be expanded to multiple stages and allows for explicit comparisons among species or treatments in a holistic way. Throughout this article I refer to this model of multiple transitions between stages as the MT (multiple transitions) model. To illustrate this model, I fitted larval development data from laboratory-reared red and blue king crabs. Larvae of both species pass through 4 zoeal stages (ZI–ZIV) and 1 glaucothoe stage (G) before they metamorphose to the first benthic crab stage (C1) (Sato and Tanaka, 1949; Hoffman, 1968); therefore, these larval stages provide an opportunity to explore the utility of this model.

Materials and methods

Description of the multiple transitions model

The basis of the MT model is the logistic family of equations, which are frequently used to describe a transition from one stage to another, for example, from life to death as a function of time (e.g., Long et al., 2008) or from immature to mature as a function of size (e.g., Somerton, 1980). For the power-function version used to describe the transition between 2 stages of development, the equation would be parameterized as follows:

$$Stage = 1 + \frac{1}{1 + \left(\frac{t}{t_{50,1}}\right)^{s_1}}, \quad (1)$$

where t = the independent variable (time);
$t_{50,1}$ = the time at which 50% of the individuals have made the transition; and
s_1 = the slope parameter at the transition that describes the abruptness of the transition.

This equation could be simplified as $Stage=1+p_1$, where p_1 is the probability of an individual having undergone the transition. Larger absolute values of s indicate a more rapid transition between states. The lower and upper limits for this function are 1 and 2, respectively.

This equation has the desired properties of the function being 1 at values of t far below $t_{50,1}$, rising sigmoidally to 1.5 at $t_{50,1}$, and rising toward an asymptote of 2 as t increases above $t_{50,1}$, with the amount of time both stages are present being a function of s_1 (Fig. 1A).

This function is easily expanded to n stages with $n-1$ transitions:

$$Stage = 1 + \sum_{i=1}^{n-1} \frac{1}{1 + \left(\frac{t}{t_{50,i}}\right)^{s_i}}. \quad (2)$$

This function ranges from 1 to n and increases in a stepwise fashion (Fig. 1B). Although I have used the power function in this study because the parameterization is convenient for interpretation, other sigmoidal functions could be substituted in the equation without otherwise altering the model.

Modeling the expected variance employs a similar logic. Because the variance is expected to vary continuously in this model, it is imperative to model the variance as well as the mean in a statistically valid manner (Bolker, 2008). When the logistic function (Eq. 1) is used to describe the transition between 2 states, a binomial distribution is often assumed (e.g., Long et al., 2013a) and variance is given with the following equation:

$$var = p(1 - p), \quad (3)$$

where var = the variance; and
p = the probability of the event occurring.

This variance structure is appropriate because the variance is 0 at a probability of 0 (i.e., none of the population have made the transition), maximum at a probability of 0.5 (i.e., at $t=t_{50}$, the point at which there is transition between the states), and 0 again at a probability of 1 (i.e., all of the population has made the transition; Fig. 1A).

In the MT model, a pure binomial distribution cannot be assumed because the total number of states is greater than 2; however, a similar variance structure can be achieved by treating each of the transitions as a separate binomial distribution and summing the variances together. Therefore, variance for the expanded MT model (Eq. 3) can be given with the following equation:

$$var = Cov(X_j, X_k) + \sum_{i=1}^{n-1}(1 - p_i), \quad (4)$$

where $Cov(X_j,X_k)$ = the covariance between each combination of stage transitions (where $i \neq k$) and p_i is the probability of an individual undergoing the i^{th} transition.

Because the covariance between any 2 stage transitions will be 0 if the stage transitions happen at different times (i.e., if only one of the transitions is occurring at the same time), this term is 0 under most circumstances. If, however, there is substantial overlap between 2-stage transitions (i.e., if there are times when 3 different stages are present at the same time), the covariance between those 2 stage transitions should be included in the model. This circumstance should be rare for the majority of uses for which this model is intended.

Equation 4 has properties similar to those of Equation 3 in that the variance is highest at values of t that are near one of the transitions but approaches 0 at values between transitions when all the individuals are expected to be in a single stage (Fig. 1B). At a given variance, the binomial distribution can be approximated by the normal distribution (Bolker, 2008). Although such an approximation is not as good at values of p close to 0 or 1, this approximation affects only the estimates of the tails of the error distribution and not the mean and, therefore, should not affect the fit of the model. By assuming normal distributions of error with variances that change according to Equation 4, the model allows more than 2 stages and therefore overcomes the 2-state limit of the binomial distribution. This approach allows the variance to change as if it were a binomial distribution, providing a good mechanistic match to the data structure.

Model applied to larval development

In the winter of 2010, 9 and 11 ovigerous female red king crab and blue king crabs, respectively, were collected in baited commercial pots in the Bering Sea. Crabs were identified according to the methods of Donaldson and Byersdorfer (2005). Red king crab were transported to the Kodiak Fishery Research Center in the "live well" of a commercial fishing vessel, and blue king crab were transported in coolers by air cargo. In the laboratory, the crabs were held in flow-through seawater supplied from Trident Basin, Kodiak, at ambient temperature and salinity and fed to excess on a diet of chopped frozen fish and squid.

Larval rearing procedures were similar to those of Swingle et al. (2013). In brief, larvae were collected at hatching and larvae of red and blue king crabs were pooled and each stocked in a separate 2000-L tank. Larval red king crab were stocked at 50 larvae/L, the amount collected in a single day from 8 females that were hatching at the time. Because only 6 female blue king crab produced larvae simultaneously, larvae of blue king crab were collected over 3 days and were stocked at 30 larvae/L. Because of differences in thermal tolerances (Stoner et al., 2013), the red king crab were reared at 8.8°C (standard deviation [SD] 1.0), and the blue king crab were reared at 6.5°C (SD 0.6). While the larvae were in the zoeal stages, they were fed a diet of DC DHA Selco[1] (INVE Aquaculture, Salt Lake City) enriched *Artemia* nauplii. The glaucothoe stage is a stage when larvae are not feeding (Abrunhosa and Kittaka, 1997a, 1997b); therefore, no food was provided. Each day, from stocking to the point when all of the larvae had molted to the first crab stage, 10 larvae from each species were removed, the developmental stage of each was determined, and the mean developmental stage of the 10 larvae was calculated.

[1] Mention of trade names or commercial firms does not imply endorsement by the National Marine Fisheries Service, NOAA.

Table 1

Ranking of models of larval development in red and blue king crabs (*Paralithodes camtschaticus* and *P. platypus*) with the use of Akaike information criteria, corrected for small sample sizes (AIC_c). Common parameters (species the same) or different parameters (species different) were used in the models. K=number of parameters. Likelihood=likelihood of each model relative to all the models considered.

Model	K	AIC_c	ΔAIC_c	Likelihood	AIC_c weights
Species different	20	−5974	0.00	1.00	1.00
Species the same	10	−2249	3725	0.00	0.00

The mean stage on each day was fitted to the MT model (Eq. 2) in R vers. 2.14.0 (R Development Core Team, 2011), by using maximum likelihood (mle function, stats4 package, vers. 3.1.0) and by assuming a normal distribution of errors with a variance structure defined by Equation 4. Time was expressed in degree-days (a measure that accounts for both time and temperature) to control for the difference in rearing temperatures (e.g., Stevens, 1990; Long et al., 2013b; Swiney et al., 2013) and calculated as

$$DD_m = \sum_{t=0}^{m-1} Temp_t \times 1\,day, \quad (5)$$

where DD_m = the degree-days on day m;
t = the time in days; and
$Temp_t$ = the temperature (in Celsius) on day t.

Two models were fitted, one in which the parameters were common between red and blue king crabs and one in which parameters differed between the species. Models were compared with the Akaike information criteria, corrected for small sample sizes (AIC_c):

$$AIC_C = -\log(L) + 2K\left(\frac{n}{1-K-1}\right), \quad (6)$$

where L = the likelihood of the model;
K = the number of parameters in the model; and
n = the sample size; and

where the AIC_c was used to select the best model (Burnham and Anderson, 2002). Normality of the errors was checked through examination of the standardized residuals of the best model.

Results

The model of larval development with independent parameters for red and blue king crabs was the one in which red and blue king crabs provided the best fit (Table 1) with a coefficient of determination (r^2, calculated with the raw data) for red and blue king crabs of 0.98 and 0.97, respectively (Fig. 2). The model in which they did not differ had a ΔAIC_c of 3700, indicating that there was no support for this model (Burnham and Anderson, 2002).

In terms of degree-days, larvae of red king crab molted to the ZII, ZIII, and ZIV stages earlier than larvae of blue king crab, both species molted to the G stage at about the same time, and blue king crab molted to the C1 stage earlier than red king crab (Fig. 2, Table 2). The stage transitions of red king crab were more rapid than those of blue king crab (Fig. 2, Table 2), although the precision in the estimates for s

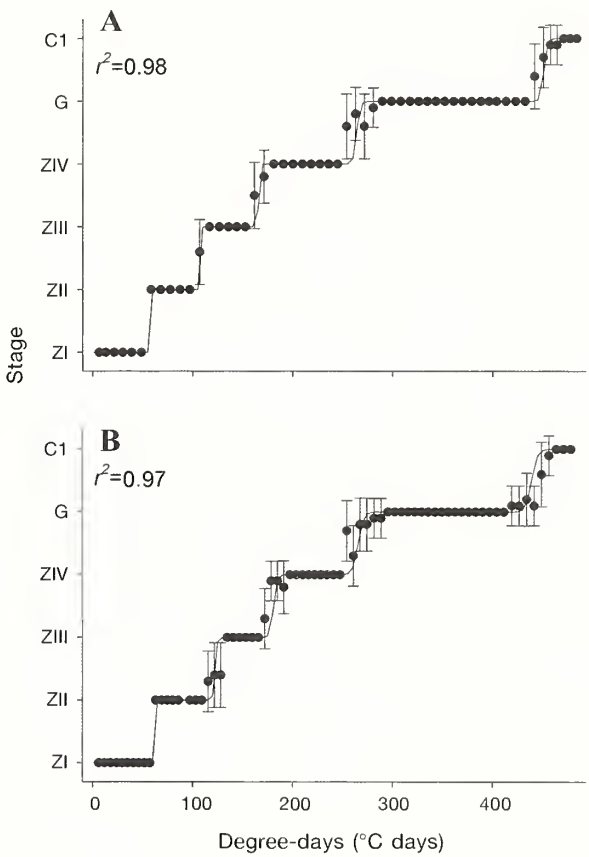

Figure 2

Larval development of (**A**) red king crab (*Paralithodes camtschaticus*) and (**B**) blue king crab (*P. platypus*) from the first zoeal stage through the first crab stage. Points represent the mean stage as determined each day throughout development. Error bars are one standard deviation; note that on days when all the larvae were at one stage the standard deviation was 0. Lines represent the best-fit stage-transition model for each species. The larval stages shown are the 4 zoeal stages (ZI–ZIV), the glaucothoe stage (G), and the first benthic crab stage (C1). r^2=coefficient of determination.

Table 2

Mean estimates, with standard errors in parentheses, of the t_{50} parameter (the time at which 50% of individuals have made the transition) and the s parameter (the slope at the transition) for the transitions between each stage in the larval development of red and blue king crabs (*Paralithodes camtschaticus* and *P. platypus*). The stages are the 4 zoeal stages (Z1–IV) and the glaucothoe stage (G). The stage given in the first column indicates that the transition is from that stage to the next one (e.g., "G" indicates the transition from the glaucothoe stage to the first crab stage). The estimates for t_{50} are given in degree-days.

	Red king crab			Blue king crab		
Stage	t_{50}	s	$-s/t_{50}$	t_{50}	s	$-s/t_{50}$
ZI	57.0 (SE 0.0002)	−1743 (SE 2929)	30.57	61.5 (SE 0.0004)	−1434 (SE 58)	23.31
ZII	107.2 (SE 0.6)	−642 (SE 1208)	5.99	122.5 (SE 0.1)	−129 (SE 1.2)	1.05
ZIII	165.7 (SE 0.1)	−225 (SE 4)	1.36	180.9 (SE 0.3)	−113 (SE 1.3)	0.62
ZIV	263.9 (SE 0.1)	−158 (SE 0.1)	0.60	265.6 (SE 0.1)	−101 (SE 0.1)	0.38
G	450.6 (SE 0.2)	−286 (SE 6)	0.64	438.9 (SE 0.8)	−158 (SE 6.8)	0.36

were low for several stages because of the rapidity of the transition.

Discussion

In this article, I describe a new method for modeling biological processes that involve multiple transitions between discrete stages. The summing of simple logistic equations, which are frequently used for stage-transition models, is analogous to commonly used time-series analyses that model periodic phenomena as a sum of multiple cosine waves (e.g., Linhart and Zucchini, 1986). The method provides a concise, mathematical description of such transitional processes, is mechanistically sound, and provides easily interpreted parameters. The t_{50} for each transition is used easily to determine the length of time between stages, is objective and quantitative, allows for explicit comparisons among studies, and avoids problems with qualitative determinations, such as the time when molts are observed (e.g., Swingle et al., 2013). The s parameter, which is proportional to the rate of change between stages, may also be of interest to investigators.

The MT model provided an excellent fit to the data for larval development of red and blue king crabs and provided estimates of the standard error (SE) in the estimates of parameters that allow comparisons among studies. It is worth noting that I used these data as example data (the original purpose for rearing the larvae was to produce crabs for use in other experiments), and no conclusions can be drawn about reasons for the differences between the red and blue king crabs in this experiment because there was no replication and multiple factors (e.g., species, stocking density, and temperature) differed between the tanks. However, the estimates for development time can be compared with those of other studies, and they agree well with them.

Kurata (1960) compiled results from a number of experiments on larval rearing of red king crab and reported a range of 260.4–397.8 degree-days (mean: 325.0) from hatching to the G stage and a range of 392.4–514.8 degree-days (mean: 462.8) from hatching to the C1 stage. My estimates of 263.9 degree-days (from hatching to G) and 450.6 degree-days (from hatching to C1) fall within both ranges from that earlier study. Similarly, larvae of red king crab from the Barents Sea had stage durations of 66.0, 68.7, 69.3, and 79.1 (284 total) degree-days for the Z1–Z4 stages (Kovatcheva et al., 2006) compared with my estimates of 57.0, 50.2, 58.5, and 98.2 (263.9 total). Blue king crab have been studied less than red king crab, but our estimate of 265.6 degree-days for hatching through the G stage and 438.9 degree-days for hatching through the C1 stage are very similar to the 254.4 degree-days (from hatching to G) and 439.4 degree-days (from hatching through C1) averages found by Stevens et al. (2008).

In general, the estimates for the s parameters were good, but on a couple of the transitions, particularly the first 2 transitions for the red king crab, the estimates had poor precision (Table 2). In these cases, there were 0–1 observations of the actual transition, and, therefore, the MT model could not precisely estimate the rapidity of the transitions. Values of s that approach infinity are possible given the data; therefore, the SE in the parameter estimate is high. If the estimate of s is of particular interest, then the precision of the estimate can be increased by increasing the frequency of observations.

Theoretically, there is no limit to the number of stages that can be modeled with this approach. I originally developed this technique to model embryo development in golden king crab (*Lithodes aequispinus*) and was able to obtain a good fit for a 13-stage model (Long and Van Sant, 2016). However, as the number of stages and the number of parameters increase, it becomes more difficult for the algorithms to find the global minimum in the log-likelihood surface (Bolker, 2008), and the model fitting becomes more sensitive to the starting values for the parameters (Appendix).

The starting values for the t_{50} parameters are fairly easily estimated by simply examining the data for the times when the transitions are occurring; however, the s parameters are more difficult to estimate. Therefore, the use of an iterative process to determine reasonable starting values for these parameters may be helpful. When fitting the MT model or any model with a large number of parameters, it is highly recommended to fit the data under multiple sets of starting parameter values, and it is imperative to graph the model and data together to ensure that the fit is optimal and realistic.

In most cases, t_{50} will be a parameter of interest; however, there are times when the rapidity of the transition between stages may be relevant to the question posed by an investigator. For example, many crab species are cannibalistic, especially immediately after molting, when soft crabs are particularly vulnerable (e.g., Borisov et al., 2007). Therefore, to minimize cannibalism, a hatchery may find it valuable to determine under what conditions molting is highly synchronous among individuals within a tank (because all the individuals transition within a short space of time). The s parameter, as stated previously, indicates how quickly the transition between one stage and another occurs. However, s values cannot be compared directly with each other without first normalizing them to the t_{50} values. The derivative of Equation 1 evaluated at t_{50} is

$$\frac{dp}{dt}(t_{50}) = \frac{-s}{4t_{50}}. \quad (6)$$

This derivative demonstrates that the slope at t_{50} is dependent on both s and t_{50}.

In cases where comparisons in the rate of the stage transitions are important, it is necessary to calculate the ratio of s to t_{50} to make the comparison. For example, in Figure 1B, the first transition, which has an s of −30, occurs more rapidly than the third transition, which has an s of −50. Interpreting the s values alone would indicate that the third transition should be the most rapid, and it is not. However, the ratios of s to t_{50} for the first and third transitions are −3.0 and −0.8, respectively, and comparing the absolute values of these ratios allows an investigator to make a correct interpretation of the relative rapidity of transitions (Fig. 1B).

The data on larval development provide an example of how this ratio can be used to compare the rapidity of stage transitions. For both red and blue king crabs, the rapidity of the transition between stages decreases with each additional stage transition (Fig. 2, Table 2). The individual variance in developmental time leads to this decrease, which has been previously observed in both species (Stevens et al., 2008; Persselin and Daly, 2010), and it is reasonable to conclude that individual differences in feeding and growth rates would result in a larger spread in molting times later in development. In addition, the larvae of red king crab consistently had faster transitions between stages than did the larvae of blue king crab (Fig. 2, Table 2). This difference is most likely a result of the red king crab having been stocked in a single day, compared with the blue king crab, which were stocked over 3 days.

The MT model presented in this article provides a flexible and holistic approach for a quantitative description of complicated biological processes. This model is particularly well suited to crustaceans and indeed to arthropods in general, given that they develop though a series of transitional molts; however, any biological process that is divided into discrete stages (e.g., Kimmel et al., 1995) can be modeled with this technique. Treating the process with a single model affords investigators the ability to compare treatments by using model selection techniques (Burnham and Anderson, 2002), while avoiding the increase in the type-I error rate inherent in analyzing a large number of response variables with univariate statistics (Quinn and Keough, 2002).

Metadata for the data produced in the study described in this article are available at InPort (website).

Acknowledgments

I thank the staff, particularly K. Swiney, A. Emley, S. Van Sant, R. Fields, and S. Dresdow, of the seawater laboratory complex of the Kodiak Laboratory, NOAA Alaska Fisheries Science Center, for assistance in rearing the larvae in this paper. Previous versions of this paper were improved by comments from D. Urban, J. Long, and R. Foy, and 5 anonymous reviewers.

Literature cited

Abrunhosa, F., and J. Kittaka.
1997a. Functional morphology of mouthparts and foregut of the last zoea, glaucothoe and first juvenile of the king crabs *Paralithodes camtschaticus*, *P. brevipes* and *P. platypus*. Fish. Sci. 63:923–930.
1997b. Morphological changes in the midgut, midgut gland and hindgut during the larval and postlarval development of the red king crab *Paralithodes camtschaticus*. Fish. Sci. 63:746–754.

Andrés, M., G. Rotllant, and C. Zeng.
2010. Survival, development and growth of larvae of the blue swimmer crab, *Portunus pelagicus*, cultured under different photoperiod conditions. Aquaculture 300: 218–222.

Bas, C. C., and E. D. Spivak.
2000. Effect of salinity on embryos of two southwestern Atlantic estuarine grapsid crab species cultured *in vitro*. J. Crust. Biol. 20:647–656.

Blau, F. S.
1990. Size at maturity of female red king crabs (*Paralithodes camtschatica)* in the Adak Management Area, Alaska. *In* Proceedings of the international symposium on king and Tanner crabs; Anchorage, AK, 28–30 November 1989 (B. Metleff, ed.), p. 105–116. Univ. Alaska Fairbanks, Alaska Sea Grant College Program Rep. AK-SG-90-04.

Bolker, B. M.
2008. Ecological models and data in R, 408 p. Princeton Univ. Press, Princeton, NJ.

Borisov, R. R., A. B. Epelbaum, N. V. Kryakhova, A. G. Tertitskaya, and N. P. Kovatcheva.
2007. Cannibalistic behavior in red king crabs reared under artificial conditions. Russ. J. Mar. Biol. 33: 227–231.

Burnham, K. P., and D. R. Anderson.
2002. Model selection and multimodel inference: a practical information-theoretic approach, 488 p. Springer-Verlag, New York.

Costlow, J. D., Jr., and C. G. Bookhout.
1959. The larval development of *Callinectes sapidus* Rathbun reared in the laboratory. Biol. Bull. 116:373–396.

Daly, B., G. L. Eckert, and T. D. White.
2013. Predation of hatchery-cultured juvenile red king crabs (*Paralithodes camtschaticus*) in the wild. Can. J. Fish. Aquat. Sci. 70:358–366.

Daly, B., and W. C. Long.
2014a. Intra-guild predation among early benthic phase red and blue king crabs: evidence for a habitat-mediated competitive advantage. J. Exp. Mar. Biol. Ecol. 451:98–104.
2014b. Inter-cohort cannibalism of early benthic phase blue king crabs (*Paralithodes platypus*): Alternate foraging strategies in different habitats lead to different functional responses. PLoS ONE 9:e88694.

Dew, C. B.
1990. Behavioral ecology of podding red king crab, *Paralithodes camtschatica*. Can. J. Fish. Aquat. Sci. 47:1944–1958.

Donaldson, W. E., and S. C. Byersdorfer.
2005. Biological field techniques for lithodid crabs, 76 p. Univ. Alaska Fairbanks, Alaska Sea Grant College Program Rep. AK-SG-05-03.

Haynes, E.
1982. Description of larvae of the golden king crab, *Lithodes aequispina*, reared in the laboratory. Fish. Bull. 80:305–313.

Herter, H., B. Daly, J. S. Swingle, and C. Lean.
2011. Morphometrics, fecundity, and hatch timing of blue king crabs (*Paralithodes platypus*) from the Bering Strait, Alaska, USA. J. Crust. Biol. 31:304–312.

Hoffman, E. G.
1968. Description of laboratory-reared larvae of *Paralithodes platypus* (Decapoda, Anomura, Lithodidae). J. Fish. Res. Board Can. 25:439–455.

Jensen, G. C., and D. A. Armstrong.
1989. Biennial reproductive cycle of blue king crab, *Paralithodes platypus*, at the Pribilof Island, Alaska and comparison to a congener, *P. camtschatica*. Can. J. Fish. Aquat. Sci. 46:932–940.

Kimmel, C. B., W. W. Ballard, S. R. Kimmel, B. Ullmann, and T. F. Schilling.
1995. Stages of embryonic development of the zebrafish. Dev. Dyn. 203:253–310.

Kovatcheva, N., A. Epelbaum, A. Kalinin, R. Borisov, and R. Lebedev.
2006. Early life history stages of the red king crab *Paralithodes camtschaticus* (Tilesius, 1815): biology and culture, 116 p. VNIRO Publishing, Moscow.

Kurata, H.
1960. Studies on the larvae and postlarvae of *Paralithodes camtschatica* III. The influence of temperature and salinity on the survival and growth of the larvae. Bull. Hokkaido Reg. Fish. Res. Lab. 21:9–14.

Linhart, H., and W. Zucchini.
1986. Model selection, 301 p. John Wiley & Sons, New York.

Long, W. C., B. J. Brylawski, and R. D. Seitz.
2008. Behavioral effects of low dissolved oxygen on the bivalve *Macoma balthica*. J. Exp. Mar. Biol. Ecol. 359:34–39.

Long, W. C., J. Popp, K. M. Swiney, and S. B. Van Sant.
2012. Cannibalism in red king crab, *Paralithodes camtschaticus* (Tilesius, 1815): effects of habitat type and predator density on predator functional response. J. Exp. Mar. Biol. Ecol. 422–423:101–106.

Long, W. C., K. M. Swiney, and R. J. Foy.
2013a. Effects of ocean acidification on the embryos and larvae of red king crab, *Paralithodes camtschaticus*. Mar. Pollut. Bull. 69:38–47.

Long, W. C., K. M. Swiney, C. Harris, H. N. Page, and R. J. Foy.
2013b. Effects of ocean acidification on juvenile red king crab (*Paralithodes camtschaticus*) and Tanner crab (*Chionoecetes bairdi*) growth, condition, calcification, and survival. PLoS ONE 8:e60959.

Long, W. C., and S. B. Van Sant.
2016. Embryo development in golden king crab, *Lithodes aequispinus*. Fish. Bull. 114:67–76.

Long, W. C., and L. Whitefleet-Smith.
2013. Cannibalism in red king crab: habitat, ontogeny, and the predator functional response. J. Exp. Mar. Biol. Ecol. 449:142–148.

Paul, A. J., and J. M. Paul.
1999. Development of larvae of the golden king crab *Lithodes aequispinus* (Anomura: Lithodidae) reared at different temperatures. J. Crust. Biol. 19:42–45.

Pengilly, D., S. F. Blau, and J. E. Blackburn.
2002. Size at maturity of Kodiak area female red king crab. *In* Crabs in cold water regions: biology, management, and economics (A. J. Paul, E. G. Dawe, R. Elner, G. S. Jamieson, G. H. Kruse, R. S. Otto, B. Sainte-Marie, T. C. Shirley, and D. Woodby, eds.), p. 213–224. Univ. Alaska Fairbanks, Alaska Sea Grant College Program Rep. AK-SG-02-01.

Persselin, S., and B. Daly.
2010. Diet and water source effects on larval red king crab cultivation. *In* Biology and management of exploited crab populations under climate change (G. H. Kruse, G. L. Eckert, R. J. Foy, R. N. Lipcius, B. Sainte-Marie, D. L. Stram, and D. Woodby, eds.), p. 479–494. Univ. Alaska Fairbanks, Alaska Sea Grant College Program Rep. AK-SG-10-01.

Pirtle, J. L., and A. W. Stoner.
2010. Red king crab (*Paralithodes camtschaticus*) early post-settlement habitat choice: structure, food, and ontogeny. J. Exp. Mar. Biol. Ecol. 393:130–137.

Powell, G. C., and R. B. Nickerson.
1965. Aggregations among juvenile king crabs (*Paralithodes camtschatica*, Tilesius) Kodiak, Alaska. Anim. Behav. 13:374–380.

Quinn, G. P., and M. J. Keough.
2002. Experimental design and data analysis for biologists, 553 p. Cambridge Univ. Press, Cambridge, U.K.

R Development Core Team.
2011. R: a language and environment for statistical computing. R Foundation for Statistical Computing, Vienna, Austria. [Available at website, accessed Nov. 2011.]

Sato, S., and S. Tanaka.
1949. Study on the larval stage of *Paralithodes camtschatica* (Tilesius) I. About morphological research. Bull. Hokkaido Reg. Fish. Res. Lab. 1:7–24.
Shirley, S. M., and T. C. Shirley.
1989. Interannual variability in density, timing and survival of Alaskan red king crab *Paralithodes camtschatica* larvae. Mar. Ecol. Prog. Ser. 54:51–59.
Somerton, D. A.
1980. A computer technique for estimating the size of sexual maturity in crabs. Can. J. Fish. Aquat. Sci. 37:1488–1494.
1985. The disjunct distribution of blue king crab, *Paralithodes platypus*, in Alaska: some hypotheses. *In* Proceedings of the international king crab symposium, Anchorage, AK (B. R. Melteff, ed.), p. 13–21. Univ. Alaska Fairbanks, Alaska Sea Grant Program Rep. AK-SG-85-12.
Somerton, D., and R. MacIntosh.
1983. The size at sexual maturity of blue king crab, *Paralithodes platypus*, in Alaska. Fish. Bull. 81:621–628.
Stevens, B. G.
1990. Temperature-dependent growth of juvenile red king crab (*Paralithodes camtschatica*) and its effects on size-at-age and subsequent recruitment in the eastern Bering Sea. Can. J. Fish. Aquat. Sci. 47:1307–1317.
2003. Settlement, substratum preference, and survival of red king crab *Paralithodes camtschaticus* (Tilesius, 1815) glaucothoe on natural substrata in the laboratory. J. Exp. Mar. Biol. Ecol. 283:63–78.
2006. Embryo development and morphometry in the blue king crab *Paralithodes platypus* studied by using image and cluster analysis. J. Shellfish Res. 25:569–576.
Stevens, B. G., and J. Kittaka.
1998. Postlarval settling behavior, substrate preference, and time to metamorphosis for red king crab *Paralithodes camtschaticus*. Mar. Ecol. Prog. Ser. 167:197–206.
Stevens, B. G., S. Persselin, and J. Matweyou.
2008. Survival of blue king crab *Paralithodes platypus* Brandt, 1850, larvae in cultivation: effects of diet, temperature and rearing density. Aquac. Res. 39:390–397.
Stevens, B. G., and K. M. Swiney.
2005. Post-settlement effects of habitat type and predator size on cannibalism of glaucothoe and juveniles of red king crab *Paralithodes camtschaticus*. J. Exp. Mar. Biol. Ecol. 321:1–11.
2007. Hatch timing, incubation period, and reproductive cycle for captive primiparous and multiparous red king crab, *Paralithodes camtschaticus*. J. Crust. Biol. 27:37–48.
Stoner, A. W.
2009. Habitat-mediated survival of newly settled red king crab in the presence of a predatory fish: role of habitat complexity and heterogeneity. J. Exp. Mar. Biol. Ecol. 382:54–60.
Stoner, A. W., L. A. Copeman, and M. L. Ottmar.
2013. Molting, growth, and energetics of newly-settled blue king crab: effects of temperature and comparisons with red king crab. J. Exp. Mar. Biol. Ecol. 442: 10–21.
Stoner, A. W., M. L. Ottmar, and S. A. Haines.
2010. Temperature and habitat complexity mediate cannibalism in red king crab: observations on activity, feeding, and prey defense mechanisms. J. Shellfish Res. 29:1005–1012.
Swiney, K. M., and W. C. Long.
2015. Primiparous red king crab *Paralithodes camtschaticus* are less fecund than multiparous crab. J. Shellfish Res. 34:493–498.
Swiney, K. M., W. C. Long, G. L. Eckert, and G. H. Kruse.
2012. Red king crab, *Paralithodes camtschaticus,* size-fecundity relationship, and interannual and seasonal variability in fecundity. J. Shellfish Res. 31:925–933.
Swiney, K. M., W. C. Long, and S. L. Persselin.
2013. The effects of holding space on juvenile red king crab, *Paralithodes camtschaticus* (Tilesius, 1815), growth and survival. Aquac. Res. 44:1007–1016.
Swingle, J. S., B. Daly, and J. Hetrick.
2013. Temperature effects on larval survival, larval period, and health of hatchery-reared red king crab, *Paralithodes camtschaticus*. Aquaculture 384–387:13–18.
Tapella, F., M. C. Romero, B. G. Stevens, and C. L. Buck.
2009. Substrate preferences and redistribution of blue king crab *Paralithodes platypus* glaucothoe and first crab on natural substrates in the laboratory. J. Exp. Mar. Biol. Ecol. 372:31–35.
Walther, K., K. Anger, and H. O. Portner.
2010. Effects of ocean acidification and warming on the larval development of the spider crab *Hyas araneus* from different latitudes (54° vs. 79° N). Mar. Ecol. Prog. Ser. 417:159–170.

Appendix

This appendix provides R code with annotations for fitting data (by using maximum likelihood) to a multiple-stage transition model with 3 stages. The code can be expanded by adding more stages. The procedure requires that data to be in a data frame called "Stg" that consists of at least 2 vectors, one called "stage," which contains the stage for each sample, and one called "time," containing the time at which each sample was measured. Annotations are in italics.

```
library(stats4)  #The stats4 library contains the required mle function

Stage=function(T50_1,T50_2,s1,s2){      #this function calculates the negative log likelihood
                                        #given the data and a set of parameters. Additional stages
                                        #would require further parameters to be included here.
    ave=1+(1/(1+(Stg$Time/T50_1)^s1))+   #"ave" is the average stage at each time
```

```
        (1/(1+(Stg$ Time /T50_2)^s2))          #additional stages would be added by
                                               # summing additional logistic equations here. A
                                               #fourth stage would require 2 more parameters:
                                               #T50_3 and s_3
        var=(1/(1+(Stg$ Time /T50_1)^s1))*(1-(1/(1+(Stg$ Time /T50_1)^s1)))+   #calculates
        (1/(1+(Stg$ Time /T50_2)^s2))*(1-(1/(1+(Stg$ Time /T50_2)^s2)))        #the variance
                                               #additional stages require the variance for each
                                               #transition to be added here.
        -sum(dnorm(Stg$Stage,ave,var^.5,log=TRUE))  #calculates the negative log likelihood
        }
param=list(T50_1=10, T50_2=25,s1=-10,s2=-20)   #initial parameter estimates. If the model is
                                               #expanded to more stages, then the
                                               #necessary parameters and estimates need
                                               #to be added to this list.
mStage=mle(Stage,start=param)                  #fits the data to the model through the
                                               #use of maximum likelihood
summary(mStage)                #gives a summary of the fit, including estimates of the
                               #parameter, their standard errors, and the -2 log
                               #likelihood of the fit.
```

NOAA
National Marine
Fisheries Service

Fishery Bulletin
established 1881

Spencer F. Baird
First U.S. Commissioner
of Fisheries and founder
of *Fishery Bulletin*

Embryo development in golden king crab (*Lithodes aequispinus*)

W. Christopher Long (contact author)
Scott B. Van Sant

Email address for contact author: chris.long@noaa.gov

Resource Assessment and Conservation Engineering Division
Kodiak Laboratory
Alaska Fisheries Science Center
National Marine Fisheries Service, NOAA
301 Research Court
Kodiak, Alaska 99615

Abstract—The golden king crab (*Lithodes aequispinus*) is a commercially important species in Alaska waters with an asynchronous reproductive cycle and lecithotrophic larvae. In this study, we qualitatively and quantitatively describe embryo development for this species. Six female multiparous golden king crab were captured from the Aleutian Islands, Alaska, and mated in the laboratory. Their embryos were photographed on average once every 9 days throughout embryogenesis. We describe 13 stages of embryo development on the basis of both visual observations and embryo morphometrics from 1241 measured embryos. Embryo development was similar to that of other cold-water crab species, with the exceptions that 1) golden king crab did not have a diapause and 2) that the average percentage of the area occupied by the yolk at hatching, at about 40%, was much higher than that of other species. Both of these differences likely are attributable to the fact that the larvae are lecithotrophic and, therefore, do not need to synchronize hatch time with planktonic food availability but do need energy reserves to develop to the first crab stage. This study increases our understanding of the reproductive biology of the golden king crab and provides a baseline for future studies of embryo development.

Manuscript submitted 3 February 2015.
Manuscript accepted 5 November 2015.
Fish. Bull. 114:67–76 (2016).
Online publication date: 25 November 2015.
doi: 10.7755/FB.114.1.6

The golden king crab (*Lithodes aequispinus*) is an important fishery species in Alaska waters; the annual harvest of the Aleutian Islands stock has averaged around 5–6 million lb since 1996 (NPFMC, 2015). In North American waters, golden king crab are distributed primarily along the upper portion of the continental slope, on seamounts, and in fjords in the Gulf of Alaska and to southern British Columbia, along the Aleutian Islands, and in the Bering Sea (Butler and Hart, 1962; Sloan, 1985; Donaldson and Byersdorfer, 2005). They have been harvested in the Bering Sea since the early 1980s, and the harvest levels there have been among the most stable for any crab species or stock (Orensanz et al., 1998; NPFMC, 2015).

Female golden king crab reach maturity, on average, at a carapace length (CL) of about 98–111 mm, depending on the stock and latitude (Jewett et al., 1985; Somerton and Otto, 1986). The reproductive cycle of golden king crab is not an annual event and is probably asynchronous in many areas (Hiramoto, 1985; Otto and Cummiskey, 1985; Somerton and Otto, 1986; Paul and Paul, 2000, 2001). Like all lithodids, female golden king crab must molt before mating (Paul and Paul, 2001), after which they extrude a clutch of up to 27,000 eggs (Jewett et al., 1985). Golden king crab have lower fecundities than similar-size red (*Paralithodes camtschaticus*) and blue (*Paralithodes platypus*) king crabs (Haynes, 1968; Somerton and MacIntosh, 1985; Swiney et al., 2012). They have much larger embryos because their larvae are lecithotrophic and therefore are supplied with greater energy reserves than are the larvae of red and king crab (Shirley and Zhou, 1997; Paul and Paul, 1999). For golden king crab, the brooding duration is about 362 days, and the time between the completion of larval hatching and extrusion of a new clutch is about 194 days; however, these parameters have been estimated only in the laboratory at temperatures that were higher than the temperatures experienced by crab in the field and are likely underestimates (Paul and Paul, 2001). After hatching, larvae pass through 3 zoeal stages and 1 glaucothoe stage before they molt to the first benthic crab stage (Shirley and Zhou, 1997; Paul and Paul, 1999).

One of the current gaps in our understanding of the biology of the golden king crab is the process of embryo development. The embryos of both the red king crab (Nakani-

shi, 1987) and the blue king crab (Stevens, 2006) have been described in detail, but little attention has been given to the golden king crab up to this point. It is likely that, given the asynchronous reproductive cycle and the lecithotrophic development of larvae, golden king crab embryos are substantially different from those of the other 2 species. The asynchronous cycle could lead to greater differences among females, and lecithotrophic larval development could result in differences in embryo morphology, particularly in yolk size, at hatching. In this study, we examined and measured the embryos of golden king crab from time of extrusion though hatching and describe their development.

Materials and methods

Golden king crab were caught in commercial pots along the Aleutian Islands, Alaska, in the fall of 2005 and 2006 and transported to the Kodiak Laboratory of the NOAA Alaska Fisheries Science Center in air cargo. Crab were identified according to the methods of Donaldson and Byersdorfer (2005). Crab were held in 2000-L tanks with flow-through seawater chilled to 3–4°C, a range that reflects the temperatures experienced by female golden king crab in the Aleutian Islands (Blau et al., 1996; Stabeno et al., 2005) and were fed chopped frozen fish and squid to excess. Tanks were covered with opaque sheets of foam both to provide insulation and to keep the females in mostly dark conditions.

Six females, 4 captured in 2005 and 2 caught in 2006, were used in this study. Females were either late-stage ovigerous, as evinced by eyed embryos, or they were hatched out, as evinced by empty egg cases found when collected. They were between 120 and 141 mm CL. Six mature males, 128–132 mm CL, were kept with pre-mating females in a holding tank because females may molt and mate anywhere from 5 to 464 days after they finish hatching larvae (Paul and Paul, 2001).

When pre-mating grasping occurred, a crab pair was moved to a separate tank to ensure that the female would not be eaten after molting. After the females molted, they mated and extruded a new clutch of eggs. At this point, they were placed in another tank where all the postmating females were held together with no males. The day of extrusion was considered day 1 of brooding and embryo development.

Embryos were collected regularly throughout development from a random location within the clutch. Throughout development for each female, time between samples varied with the stage of development but averaged once every 9 days or a mean of 48 times (range: 42–54 times). At sampling, embryos were examined and photographed under a stereomicroscope. Uneyed embryos were stained for 5 min in Bouin's solution to enable staging (Stevens, 2006). In addition, for image analysis, photographs were taken of up to 10 unstained embryos at 90° to the sagittal plane under a stereomicroscope. These images were calibrated each day with a micrometer because the scope had an adjustable zoom and this calibration ensured that measurements were accurate. A total of 1241 embryos were measured. On a number of occasions, the calibration procedure was not followed, and we did not perform image analysis on the photographs, although stage data were still collected and used. Measurements were made with Image-Pro Plus[1], vers. 7.0 (Media Cybernetics Inc., Rockville, MD).

In this study, the term egg refers to the entire embryo (i.e., the entire contents of the fertilized egg), the term *embryo* refers to the differentiated part of the egg as distinct from the yolk, and the term *yolk* refers to the undifferentiated deutoplasm. For each egg, the area and the mean, minimum, and maximum diameter were measured. The mean, minimum, and maximum diameters were determined from 180 measurements of the diameter at 2°-intervals around the entire egg. When the embryo became visible, the yolk area also was measured by tracing the yolk in Image-Pro Plus, and the percentage of egg area that was yolk (hereafter *percent area of yolk*, calculated as yolk area×100/egg area; before the embryo becomes visible, the yolk area equals the egg area) and the embryo area (calculated as egg area – yolk area) were determined. Finally, when the eyes became visible, the eye area and the mean, minimum, and maximum diameter were measured with same techniques as above. All measurements were made at 90° to the sagittal plane.

Stages were described by visual examination of the eggs as well as on the basis of the changes observed in the measured parameters, and these descriptions were based, in part, on staging systems previously developed for embryos of the blue king crab (Stevens, 2006) and snow crab (*Chionoecetes opilio*) (Moriyasu and Lanteigne, 1998). The median stage of development (see the Results section for descriptions) was determined for each female on each sampling day. The data for developmental stages were fitted to a model of multiple-transitions between stages (MT model, Long, 2016). In brief, each stage transition was modeled as a logistic regression:

$$stage = \frac{1}{1+\left(\frac{t}{t_{50}}\right)^{s}}, \quad (1)$$

where t = the time in days;
t_{50} = the time at which half of the embryos have transitioned to the next stage; and
s = a parameter that is proportional to the slope at the transition.

The data were fitted by using maximum like-lihood in R, vers. 2.14.0 (R Development Core Team., 2011).

Morphometric analysis was used to visualize differences among the developmental stages and to examine whether embryo measurements can be used to distin-

[1] Mention of trade names or commercial companies is for identification purposes only and does not imply endorsement by the National Marine Fisheries Service, NOAA.

guish the different stages. To visualize stage differences, the morphometric data were normalized and then analyzed with principal component analysis (PCA). To determine whether morphometric measurements would allow us to distinguish the stages, the data were fourth-root transformed and an analysis of similarity (ANOSIM) was performed on a Bray-Curtis similarity matrix with female and stage as factors. All morphometric analyses were performed in Primer, vers. 6.1.15 (PRIMER-E Ltd., Ivybridge, U.K.; Clarke and Warwick, 2001).

When females approached time of hatching, they were isolated in individual containers with flow-through water. Larvae released from each female were collected in nets that were checked daily. The first and last day of hatching were noted.

Results

Females extruded their eggs between 25 September 2006, and 6 May 2007, and they began hatching between 3 December 2007, and 23 July 2008. The mean duration of brooding (from extrusion to the first day of hatching) was 437.6 days (standard deviation [SD] 6.7). We identified 13 stages of embryo development (12 of them are shown in Fig. 1) by visual examination of the embryos and their morphometric features. The MT model was an excellent fit to the data for stage transitions (Fig. 2) and provided estimates for the average day of transition (t_{50}) for each stage (Table 1). The mean duration of stages was between 10 and 95 days. There were some differences among the females (Fig. 2), as demonstrated by the increased SD in the average embryo stage among females, particularly during some of the shorter stages (i.e., stages 3, 4, and 5) and during stages 9, 10, and 11. The following sections describe the 13 stages identified.

Stage 0 (precleavage)

At this stage, the eggs were newly extruded and firmly attached to the pleopods; however, no division had yet occurred. There was no visible separation between the yolk, which was a creamy yellow, and the egg membrane.

Stage 1 (cleavage and blastula)

This stage began with the first cleavage to the 2-cell stage; this cleavage occurred between days 10 and 11, and development progressed rapidly (Fig. 1A). By day 13, most yolks were at the 8-to 16-cell stage and by day 15 they were at the 32-to 64-cell stage. During these stages of early division, the yolk often took on a lumpy shape and was frequently separated from the egg membrane, and a nucleus was visible in each cell as a light-colored circle when stained with Bouin's solution. By about day 50, the blastula formed, and individual cells were no longer discernible.

Stage 2 (gastrula)

The beginning of this stage was marked by the blastopore (Fig. 1B) becoming visible in embryos stained with Bouin's solution. This stage began on average on day 60 and lasted for about 32 days (Table 1).

Stage 3 (v-shaped embryo)

This stage began with the appearance of the embryo as a yellow v-shape when it was stained in Bouin's solution (Fig. 1C). This stage was short, beginning on about day 91 and lasting for about 24 days (Table 1).

Stage 4 (prenauplius)

During this stage, the embryos began to rapidly form differentiated parts. This stage began when the optical lobe, antennules, antennas, mandibles, and abdomen were visible as separate entities as opposed to the undifferentiated v-shape of the previous stage in embryos stained with Bouin's solution (Fig. 1D). The individual parts were still somewhat indistinct and widely separated from each other; in particular, the abdomen was well-separated from the optical lobe, mandibles, and antennas. This stage lasted for approximately 27 days, starting on day 115 (Table 1).

Stage 5 (nauplius)

This stage was brief, starting at around day 142 and lasting only about 18 days (Table 1). During this stage, the optical lobes, antennules, antennas, mandibles, and abdomen were more distinct, and they lengthened and coalesced so that the abdomen was situated between the antennas and mandibles and immediately below the optical lobes (Fig. 1E).

Stage 6 (maxilliped formation)

This stage was another brief one, starting at around day 160 and lasting only about 15 days (Table 1). It began when the maxillipeds became distinct from the mandibles. During this stage, the abdomen became more elongate (Fig. 1F). Before this stage, there were almost no changes in the morphological features of the eggs; the egg size and dimensions remained constant, and the embryo was not visible in unstained embryos (Fig. 3). But, during this stage, the embryo became visible in unstained embryos, and size and percent area of yolk began to decrease (Fig. 4).

Stage 7 (metanauplius)

The metanauplius stage began when the abdomen was fully bifurcated and the carapace became visible. This stage was characterized by the lengthening of the antennules, antennas, mandibles, and maxillipeds (Fig. 1G). Late in this stage, the telson became visible. Growth of the embryo and reduction in the yolk hap-

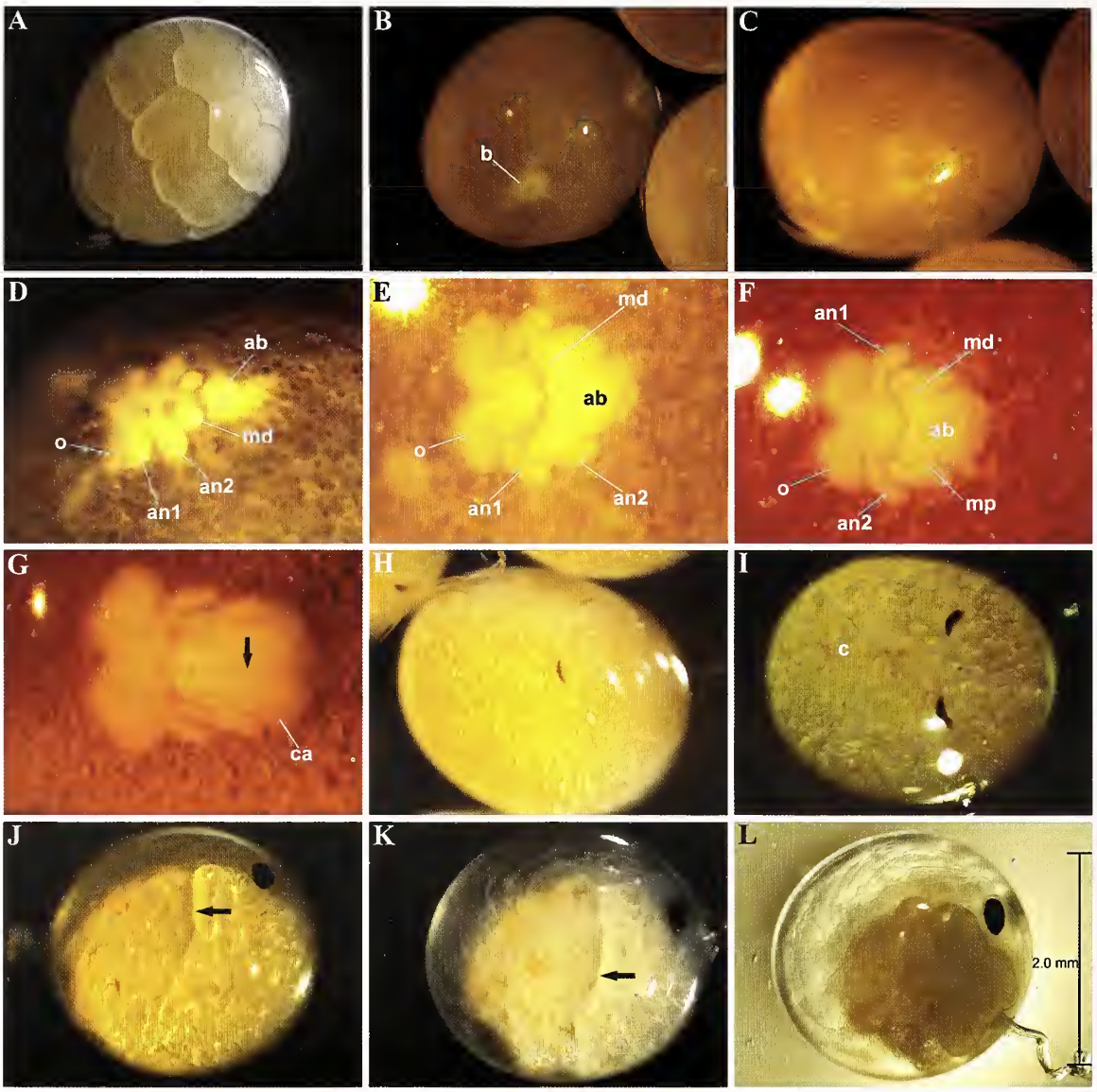

Figure 1

Photographs of golden king crab (*Lithodes aequispinus*) embryos taken throughout development. Sections **A–L** show embryo stages 1–12, respectively; stage 0 is not provided. In sections B–G, photographs are of stained embryos. Light levels and colors in photographs have been adjusted to make the pertinent details clear. Key morphological features used to identify stages are labeled: blastopore (b), optical lobe (o), antennule (an1), antenna (an2), abdomen (ab), mandible (md), maxilliped (mp), carapace (ca), and chromatophores (c). In section G, the arrow indicates bifurcated abdomen. In panel J, the arrow indicates partially bifurcated yolk. In section K, the arrow indicates a fully bifurcated yolk.

pened at a very slow rate (Figs. 3 and 4). This stage started at around day 175 and lasted 38 days.

Stage 8 (eye formation)

The beginning of this stage, which began on day 213, was marked by the eyes of the embryo becoming visible as thin, pigmented crescents in unstained embryos (Fig. 1H). During this stage, the size of the eyes rapidly increased—the width (minimum diameter) increasing faster than the length (maximum diameter)—so that the shape gradually became a fuller crescent shape (Fig. 5). Although embryo growth was faster in this stage than in stage 7, it was still relatively slow (Fig. 3). The telson became distinct and developed setae in embryos as evident in embryos stained with Bouin's solution. This stage

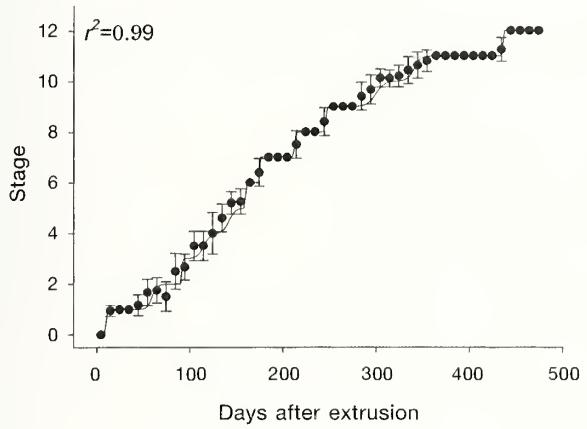

Figure 2

Average (among females) developmental stage of golden king crab (*Lithodes aequispinus*) embryos plotted against days from extrusion, for each 10-day increment of embryo development. The line represents the best fitting multiple-stage transition model. Error bars indicate ±1 standard deviation of the mean. See Table 1 for parameter estimates. r^2=coeficcient of determination.

marked the midpoint in embryo development, beginning on day 213 and lasting for about 33 days (Table 1).

Stage 9 (chromatophore formation)

The beginning of this stage was marked by chromatophores becoming visible in unstained embryos (Fig. 1I). Chromatophores increased in size and number throughout this stage. Growth of the embryo and shrinking of the yolk accelerated from the previous stage (Figs. 3 and 4). The eyes grew rapidly, both in length and width. Because width increased much faster than length, the eyes progressed from a crescent shape to a nearly spherical one (Fig. 5B). From this stage onward in development, egg area began to increase as well (Fig. 3), although during this stage the increase was slight. The yolk became separated into 2 halves when the egg was viewed dorsally. This stage began on day 246 and lasted for 54 days.

Stage 10 (rapid growth)

This stage, which lasted about 41 days and began on day 300 (Table 1), was marked by a rapid increase in the size of the egg, embryo, and eyes, and a slight decrease in the yolk area and percent area of yolk (Figs. 3, 4, and 5). The shape of the eye did not change during this period and remained nearly spherical (Fig. 5B). When viewed on the sagittal plane, the yolk developed a partial anterior–posterior bifurcation (Fig. 1J). We marked the beginning of this stage with the beginning of this bifurcation and marked the completion of this stage with the completion of this bifurcation.

Stage 11 (prehatching)

At the beginning of this stage, the yolk was completely bifurcated (Fig. 1K). Growth of the eye and embryo were at their maximum rates during this stage (Figs. 3 and 5). Yolk area and percent area of yolk dropped rapidly, with the percent area of yolk dropping from 70% to less than 50% (Fig. 4). The eyes continued to lengthen and increase in area, but the width did not

Table 1

Timing and duration of each stage of embryo development of golden king crab (*Lithodes aequispinus*). Mean values, with standard errors in parentheses, are provided for t_{50} (the time in days at which 50% of the embryos transitioned to a given stage), and for s, a slope parameter for the transition to the next stage. Length is the average length (in days) of each stage, and $-s/t_{50}$ is a measure of the rapidity of the transition to the next stage.

Stage	Description	t_{50} (d)	Length (d)	s	$-s/t_{50}$
0	Precleavage	–	10.00	−509.76 (SE 1660.70)	50.98
1	Cleavage and blastula	10.00 (SE 0.03)	49.47	−22.76 (SE 0.37)	0.38
2	Gastrula	59.47 (SE 0.20)	32.02	−278.22 (SE 71.06)	3.04
3	V-shaped embryo	91.49 (SE 0.16)	23.53	−31.24 (SE 3.74)	0.27
4	Prenauplius	115.02 (SE 1.35)	27.18	−42.08 (SE 2.39)	0.30
5	Nauplius	142.20 (SE 0.73)	17.75	−577.71 (SE 233.35)	3.61
6	Maxilliped formation	159.95 (SE 0.80)	14.58	−2006.63 (SE 8853.47)	11.50
7	Metanauplius	174.53 (SE 6.47)	38.18	−314.76 (SE 27.35)	1.48
8	Eye formation	212.71 (SE 0.19)	33.32	−420.90 (SE 67.60)	1.71
9	Chromatophore formation	246.03 (SE 0.25)	53.79	−65.52 (SE 0.37)	0.22
10	Rapid growth	299.82 (SE 0.39)	40.96	−99.09 (SE 0.05)	0.29
11	Prehatching	340.78 (SE 0.29)	95.25	−1266.33 (SE 36.33)	2.90
12	Hatching	436.03 (SE 0.08)	25.67	–	–

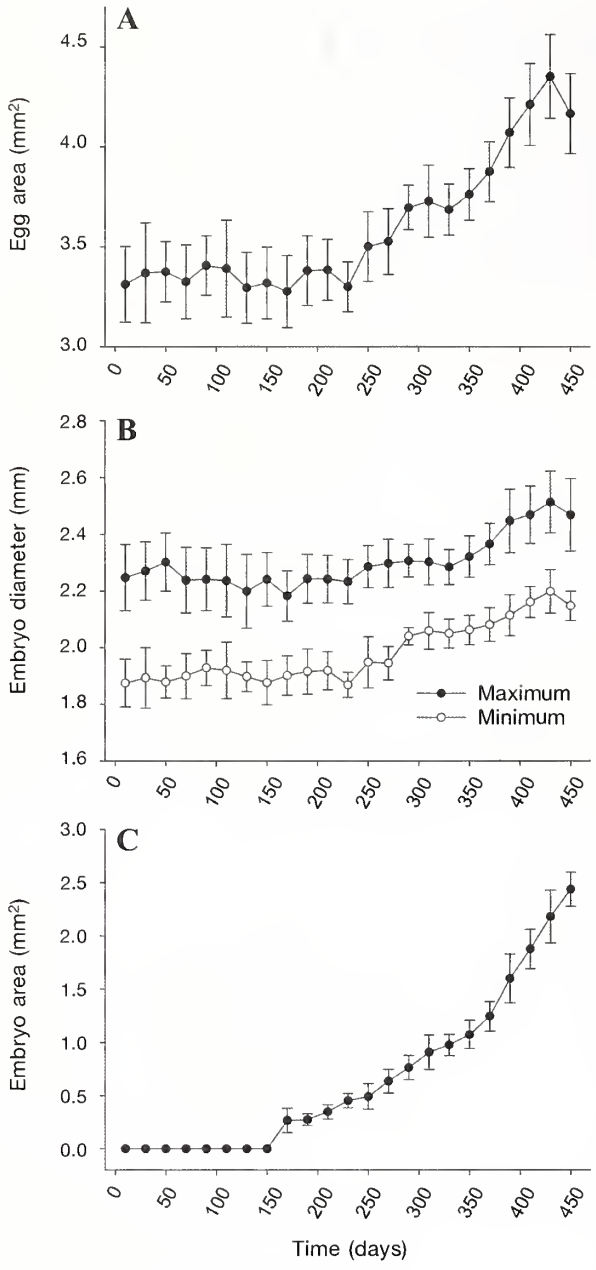

Figure 3

Average (**A**) egg area, (**B**) egg diameter, and (**C**) embryo area for all embryos measured during each 20-day increment throughout larval development of golden king crab (*Lithodes aequispinus*). Error bars indicate ±1 standard deviation of the mean.

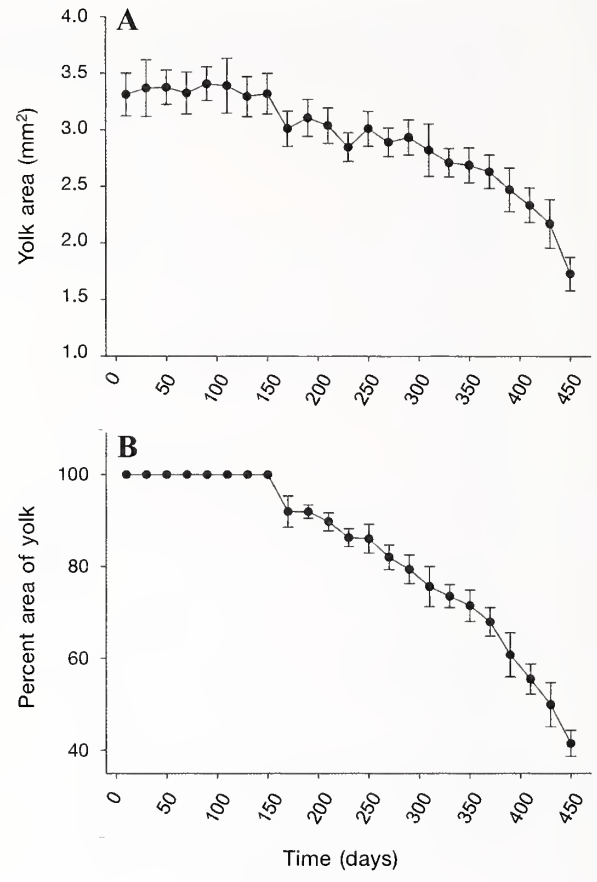

Figure 4

Average (**A**) yolk area and (**B**) percent area of yolk for all embryos measured during each 20-day increment throughout embryo development of golden king crab (*Lithodes aequispinus*). Error bars indicate ±1 standard deviation of the mean.

change, and, as a result, the eye became more oblong in shape (Figs. 1K and 5B). Additionally, development of the ommatidia gave the eye a visibly granular texture and caused a halo effect around the eye. This stage, beginning on day 340, was the longest one, lasting 95 days on average (Table 1). The end of this stage was marked by the beginning of hatching.

Stage 12 (hatching)

During hatching, embryos reached their maximum size, and the yolks reached their minimum, at about 40% of the total area of the egg (Figs. 1L, 3, and 4). The anterior and posterior sections of the yolk became differentiated from each other, with the posterior becoming more globular and less distinct (Fig. 1L). Hatching began on about day 436, and the last day of hatching occurred on average at 464 days (SD 8.6), and the average duration of hatching was 25.7 days (SD 6.1) (Table 1).

Morphometric analysis

The first 2 principal components (PCs) of the PCA explained 83.3% and 9.5% of the variance in embryo morphometrics of golden king crab and were retained (Table 2). The first PC was positively correlated with yolk size, negatively correlated with embryo, eye, and egg size, and was interpreted as embryo maturity, and

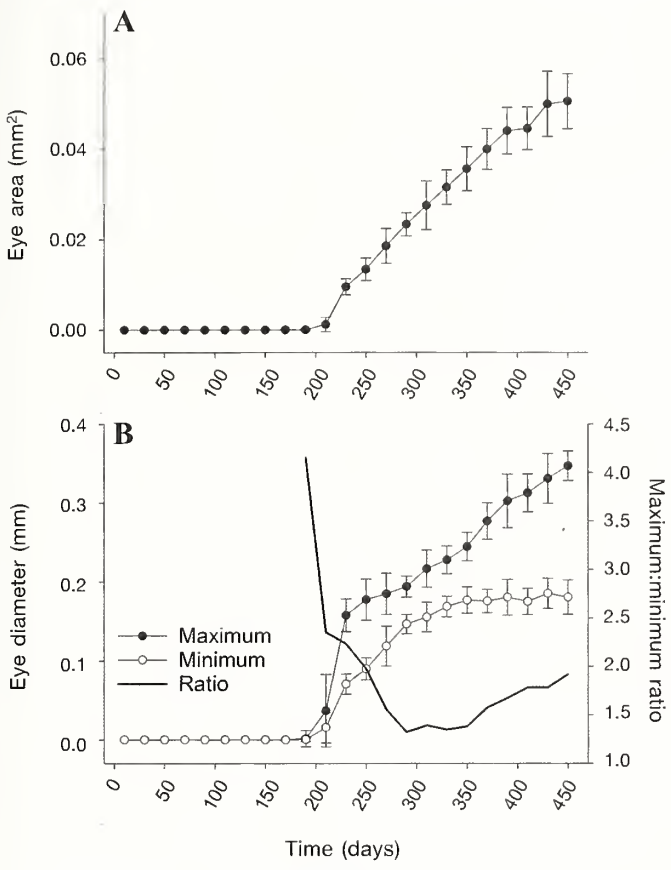

Figure 5

Average (**A**) eye area and (**B**) maximum and minimum eye diameters for all embryos measured during each 20-day increment during embryo development of golden king crab (*Lithodes aequispinus*). In section B, the line without points represents the ratio between the maximum and minimum eye diameters as an indicator of eye shape. Error bars indicate ±1 standard deviation of the mean.

smaller numbers corresponded to more mature embryos (Table 2, Fig. 6). The second PC was negatively correlated with egg size and yolk area and explained variation in egg sizes within a given stage (Table 2, Fig. 6). There were significant differences in embryo morphometrics among females (ANOSIM: global R=0.229, P<0.001) and stages (ANOSIM: global R=0.730, P<0.001). Although it is significant, the low value for the global R statistic indicates that, although there were statistical differences among the females the differences were probably negligible (Clarke and Warwick, 2001). Ordination by both PCA and nonmetric multidimensional scaling confirmed this conclusion. Pairwise comparisons of the stages showed that, in general, stages 0–5 could not be distinguished from each other (i.e., P> 0.050 or global R<0.200 and usually both) and that stages 6–12 each differed significantly from all other stages (in all cases P<0.001 and global R>0.300). These results confirmed the results from PCA (see the PCA plot, Fig. 6).

Discussion

Embryo development in golden king crab examined in this study was similar to that reported in other studies for the red king crab (Nakanishi, 1987), blue king crab (Stevens, 2006), and snow crab (Moriyasu and Lanteigne, 1998). Most of the stages described in our study match closely stages identified in those other studies. This similarity is not surprising, especially for the similarities noted among the 3 closely related species of king crabs. Despite the general similarity, there were some aspects of embryogenesis in golden king crab that were distinct, such as the lack of a diapause and the rate of decrease in yolk area.

Blue king crab undergo a diapause stage that lasts for approximately 2 months (Stevens, 2006) between the stages of chromatophore formation and eye enlargement (approximately equivalent to our stages 9 and 10). Snow crab undergo a 6-month diapause once they reach the gastrula stage and a second diapause of 3–4 months after the eye pigment formation stage (approximately equivalent to our stage 8) in the field (Moriyasu and Lanteigne, 1998). Tanner crab (*Chionoecetes bairdi*) also undergo a diapause of 3–6 months after the gastrula stage (Swiney, 2008). In snow crab, the diapauses seem to be the mechanism for switching between a 1-year and 2-year brooding period (Moriyasu and Lanteigne, 1998; Webb et al., 2007), and, in both snow crab and Tanner crab, the purpose of varying the duration of embryonic development is likely to ensure that larval release coincides with the spring planktonic bloom (Swiney, 2008). It is probable that the golden king crab lacks a diapause stage because its larval development is lecithotrophic. Lecithotrophic larvae do not need to feed, and golden king crab larvae do not appear to feed at all (Shirley and Zhou, 1997); therefore, there is no need to synchronize the release of larvae with food availability and, thus, there is no advantage to having a diapause stage. This interpretation matches with the observation of an asynchronous reproductive cycle for this species (Somerton and Otto, 1986).

Another major, and expected, difference in golden king crab embryogenesis, compared with that of other crab species, is the rate at which the yolk area decreases, and the amount of yolk remaining at hatching. The percent area of yolk decreases at a much faster rate in blue king crab than it does in golden king crab, and at the beginning of hatching blue king crab have only about 13% area of yolk (Stevens, 2006). Snow crab embryos have, at most, a trace of yolk left at hatching (Moriyasu and Lanteigne, 1998), as do Tanner crab (Swiney et al., in press). In this study, golden king crab had more than 40% area of yolk remaining at hatching. Again, however, this difference is driven by the requirements of lecithotrophic larval development; the larvae

Table 2

Results of a principal component analysis of embryo morphometrics of golden king crab (*Lithodes aequispinus*). Percent variation and cumulative variation represent the percentage of variance in the data explained by each principal component (PC) and the cumulative variance explained. Max=maximum; min=minimum.

PC	Eigenvalues	Variation (%)	Cumulative variation (%)
1	9.160	83.3	83.3
2	1.040	9.5	92.8
3	0.521	4.7	97.5
4	0.216	2.0	99.5
5	0.024	0.2	99.7
6	0.018	0.2	99.8
7	0.015	0.1	100
8	0.003	0	100
9	0.000	0	100
10	0.000	0	100
11	0.000	0	100

	Eigenvectors	
Measurement	PC1	PC2
Egg area	−0.301	−0.385
Egg max diameter	−0.217	−0.614
Egg min diameter	−0.278	−0.098
Egg mean diameter	−0.301	−0.377
Embryo area	−0.324	0.072
Yolk area	0.277	−0.449
Percent area of yolk	0.324	−0.122
Eye area	−0.324	0.124
Eye max diameter	−0.321	0.154
Eye min diameter	−0.314	0.182
Eye mean diameter	−0.319	0.172

need a greater energy reserve at hatching than the energy reserve of feeding larvae to ensure that they can develop to the first crab stage.

The developmental time between extrusion and hatching (brooding time) and the duration of hatching in this study both differ from previous reported values. Paul and Paul (2001) reported an average brooding time of 362 days (2269 degree-days [number of days multiplied by the average temperature in degrees Celsius]) and an average hatching duration of 34 days (202 degree-days), whereas we observed an average brooding time of 436 days (~1526 degree-days) and an average hatch duration of 26 days (~91 degree-days).

This dissimilarity between studies may have resulted from the crabs in each study having come from different locations: Prince William Sound (Paul and Paul, 2001) and the Aleutian Islands (in this study). However, it is more likely due to the differences in holding temperatures. Paul and Paul (2001) held crab at the ambient temperatures found at a depth of 75 m in Prince William Sound, 3.5–9.5°C, a range 1–4°C higher than the range of temperatures of the deeper waters in Prince William Sound where the golden king crab occur. We held the crab at a constant temperature between 3°C and 4°C—a range that is probably more reflective of their natural environment. Along the Aleutian Islands, most mature females are distributed at depths between about 300 and 500 m (Blau et al., 1996) where temperatures vary from about 3.5 to 4.5 throughout the year (Stabeno et al., 2005). The increase in the number of degree-days necessary for development with increasing temperature also occurs in the blue king crab (Stevens et al., 2008) and snow crab (Webb et al., 2007).

Morphometric analysis of golden king crab embryos failed to provide a quantitative method for staging larvae. Stevens (2006) successfully used multivariate statistical techniques to identify stages in blue king crab and indicated that analyses could be used to better compare embryogenesis over a diverse range of crustacean species. Using similar techniques, we were not able to distinguish among the first 5 stages, which represent about 160 days or a third of the developmental time for embryos. These stages are difficult to distinguish morphometrically because the embryo and eyes are not yet measurable. This technique worked for the blue king crab because eggs decreased steadily in size during these stages (Stevens, 2006), but it cannot work for the golden king crab because the egg size in this species remained constant for about the first 250 days of development in our study. On the other hand, the MT model (Long, 2016) provided an excellent fit to the data for stage transitions, explaining 99% of the variation in the data. These data provide quantitative estimates of the average duration of each embryonic stage and will serve as a baseline for studies of embryo development in the golden king crab.

Climate change, that is, changes in temperature (Webb et al., 2007; Stevens et al., 2008), and ocean acidification (Long et al., 2013a; Long et al., 2013b) can have substantial effects on the early life histories of cold-water crabs. This study provides a baseline for future studies that examine either variability in embryo development times among different populations of the golden king crab or the effect of environmental variables on embryo development. Future studies on the reproductive biology of the golden king crab should determine whether primiparous and multiparous crabs differ in their reproductive cycles (e.g., Moriyasu and Lanteigne, 1998; Swiney, 2008; Swiney and Long, 2015) and what drives the high variability in the time between the end of hatching and the time of mating in the golden king crab (Paul and Paul, 2001).

Acknowledgments

We thank the observers in fishery observer program of Alaska Department of Fish and Game and the captains and crews of fishing vessels from which the golden king

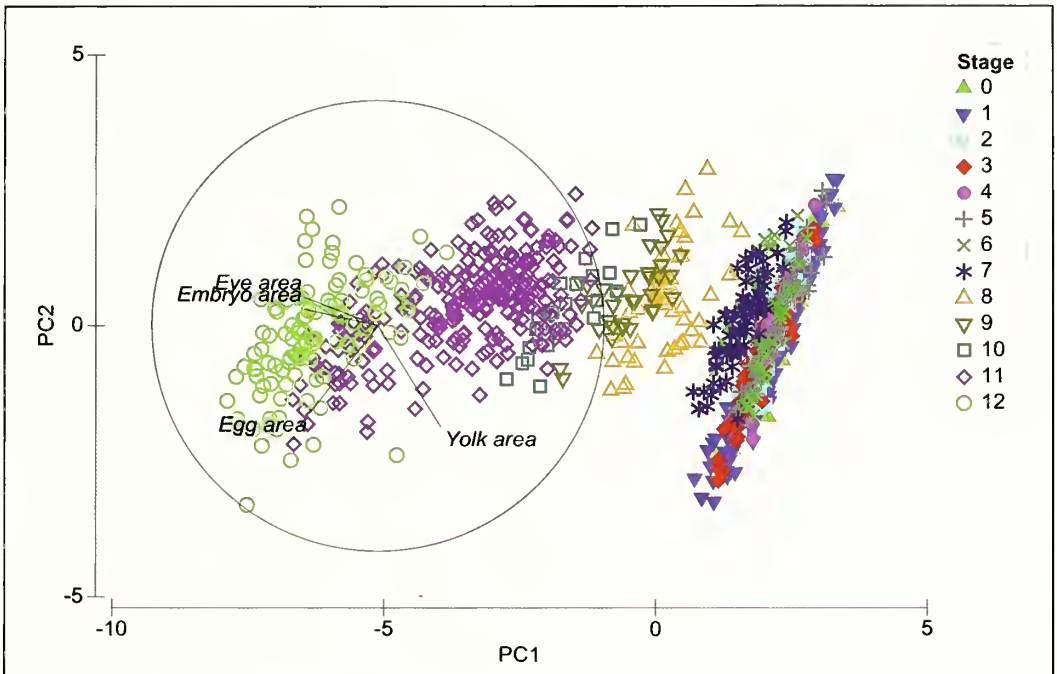

Figure 6

Plot of principal component analysis (PCA) of morphometrics of golden king crab (*Lithodes aequispinus*) embryos during 13 stages of development. Each point represents a single embryo. The first 2 PCs (plotted here) accounted for 93% of the variance in the data. Vectors are shown for egg, embryo, yolk, and eye areas.

crab were collected for this experiment. We thank B. Stevens for training, sharing techniques, and helpful suggestions, K. Reppond for assistance; and R. Foy for discussions. We also thank the staff, interns, and volunteers of the seawater laboratory complex of the Kodiak Laboratory, NOAA Alaska Fisheries Science Center, for assistance in performing experiments. Previous versions of this article were improved by comments from R. Foy, J. Long, K. Swiney, and 3 anonymous reviewers.

The metadata associated with this project are available at InPort (website) under the catalog item ID 26894 and the title "AFSC/RACE/SAP/Long: Data from: Embryo development in golden king crab, *Lithodes aequispinus*." The data are available at the following website.

Literature cited

Blau, S. F., D. Pengilly, and D. A. Tracy.
1996. Distribution of golden king crabs by sex, size, and depth zones in the Eastern Aleutian Islands, Alaska. *In* High latitude crabs: biology, management, and economics. Alaska Sea Grant College Program Rep. AK-SG-96-02, p. 167–185. Univ. Alaska Fairbanks, Fairbanks, AK.

Butler, T., and J. F. Hart.
1962. The occurrence of the king crab, *Paralithodes camtschatica* (Tilesius), and of *Lithodes aequispina* Benedict in British Columbia. J. Fish. Res. Board Can. 19:401–408.

Clarke, K. R., and R. M. Warwick.
2001. Change in marine communities: an approach to statistical analysis and interpretation, 2nd ed, 172 p. PRIMER-E, Plymouth, U.K.

Donaldson, W. E., and S. C. Byersdorfer.
2005. Biological field techniques for lithodid crabs, 76 p. Univ. Alaska Fairbanks, Alaska Sea Grant College Program Rep. AK-SG-05-03.

Haynes, E.
1968. Relation of fecundity and egg length to carapace length in the king crab, *Paralithodes camtschatica*. Proc. Natl. Shellfisheries Assoc. 58:60–62.

Hiramoto, K.
1985. Overview of the golden king crab, *Lithodes aequispina*, fishery and its fisheries biology in the Pacific waters of Central Japan. *In* Proceedings of the International King Crab Symposium, Alaska Sea Grant College Program AK-SG-85-12; Anchorage, AK, 22–24 January, p. 297–317. Univ. Alaska Fairbanks, Fairbanks, AK.

Jewett, S. C., N. A. Sloan, and D. A. Somerton.
1985. Size at sexual maturity and fecundity of the fjord-dwelling golden king crab *Lithodes aequispina* Benedict from northern British Columbia. J. Crust. Biol. 5:377–385.

Long, W. C.
2016. A new quantitative model of multiple transitions between discrete stages, applied to the development of crustacean larvae. Fish. Bull. 114:58–66.

Long, W. C., K. M. Swiney, and R. J. Foy.
2013a. Effects of ocean acidification on the embryos and larvae of red king crab, *Paralithodes camtschaticus*. Mar. Pollut. Bull. 69:38–47.
Long, W. C., K. M. Swiney, C. Harris, H. N. Page, and R. J. Foy.
2013b. Effects of ocean acidification on juvenile red king crab (*Paralithodes camtschaticus*) and Tanner crab (*Chionoecetes bairdi*) growth, condition, calcification, and survival. PLoS ONE 8:e60959.
Moriyasu, M., and C. Lanteigne.
1998. Embryo development and reproductive cycle in the snow crab, *Chionoecetes opilio* (Crustacea: Majidae), in the southern Gulf of St. Lawrence, Canada. Can. J. Zool. 76:2040–2048.
Nakanishi, T.
1987. Rearing condition of eggs, larvae and post-larvae of king crab. Bull. Japan Sea Reg. Fish. Res. Lab. 37: 57–161.
NPFMC (North Pacific Fishery Management Council).
2015. Stock assessment and fishery evaluation report for the king and Tanner crab fisheries of the Bering Sea and Aleutian Islands regions: 2015 final crab SAFE, 950 p. [Available at website.]
Orensanz, J. M., J. Armstrong, D. Armstrong, and R. Hilborn.
1998. Crustacean resources are vulnerable to serial depletion—the multifaceted decline of crab and shrimp fisheries in the Greater Gulf of Alaska. Rev. Fish Biol. Fish. 8:117–176.
Otto, R. S., and P. A. Cummiskey.
1985. Observations on the reproductive biology of golden king crab (*Lithodes aequispina*) in the Bering Sea and Aleutian Islands. *In* Proceedings of the International King Crab Symposium; Anchorage, AK, 22–24 January, p. 131–144. Univ. Alaska Fairbanks, Alaska Sea Grant College Program Rep. AK-SG-85-12.
Paul, A. J., and J. M. Paul.
1999. Development of larvae of the golden king crab *Lithodes aequispinus* (Anomura: Lithodidae) reared at different temperatures. J. Crust. Biol. 19:42–45.
2000. Changes in chela heights and carapace lengths in male and female golden king crabs *Lithodes aequispinus* after molting in the laboratory. Alaska Fish. Res. Bull. 6:70–77.
2001. The reproductive cycle of golden king crab *Lithodes aequispinus* (Anomura: Lithodidae). J. Shellfish Res. 20:369–372.
R Development Core Team.
2011. R: a language and environment for statistical computing. R Foundation for Statistical Computing, Vienna, Austria. [Available at website, accessed November 2011.]
Shirley, T. C., and S. Zhou.
1997. Lecithotrophic development of the golden king crab *Lithodes aequispinus* (Anomura: Lithodidae). J. Crust. Biol. 17:207–216.
Sloan, N.
1985. Life history characteristics of fjord-dwelling golden king crabs *Lithodes aequispina*. Mar. Ecol. Prog. Ser. 22:219–228.
Somerton, D. A., and R. A. MacIntosh.
1985. Reproductive biology of the female blue king crab *Paralithodes platypus* near the Pribilof Islands, Alaska. J. Crust. Biol. 5:365–376.
Somerton, D. A., and R. S. Otto.
1986. Distribution and reproductive biology of the golden king crab, *Lithodes aequispina*, in the eastern Bering Sea. Fish. Bull. 84:571–584.
Stabeno, P. J., D. G. Kachel, N. B. Kachel, and M. E. Sullivan.
2005. Observations from moorings in the Aleutian Passes: temperature, salinity and transport. Fish. Oceanogr. 14:39–54.
Stevens, B. G.
2006. Embryo development and morphometry in the blue king crab *Paralithodes platypus* studied by using image and cluster analysis. J. Shellfish Res. 25:569–576.
Stevens, B. G., K. M. Swiney, and L. Buck.
2008. Thermal effects on embryonic development and hatching for blue king crab *Paralithodes platypus* (Brandt, 1850) held in the laboratory, and a method for predicting dates of hatching. J. Shellfish Res. 27:1255–1263.
Swiney, K. M.
2008. Egg extrusion, embryo development, timing and duration of eclosion, and incubation period of primiparous and multiparous Tanner crabs (*Chionoecetes bairdi*). J. Crust. Biol. 28:334–341.
Swiney, K. M., and W. C. Long.
2015. Primiparous red king crab *Paralithodes camtschaticus* are less fecund than multiparous crab. J. Shellfish Res. 34:493–498.
Swiney, K. M., W. C. Long, G. L. Eckert, and G. H. Kruse.
2012. Red king crab, *Paralithodes camtschaticus,* size-fecundity relationship, and inter-annual and seasonal variability in fecundity. J. Shellfish Res. 31:925–933.
Swiney, K. M., W. C. Long, and R. J. Foy.
In press. Effects of ocean acidification on Tanner crab reproduction and early life history, Part I: long-term exposure reduces hatching success and female calcification, and alters embryonic development. ICES J. Mar. Sci.
Webb, J. B., G. L. Eckert, T. C. Shirley, and S. L. Tamone.
2007. Changes in embryonic development and hatching in *Chionoecetes opilio* (snow crab) with variation in incubation temperature. Biol. Bull. 213:67–75.

NOAA
National Marine
Fisheries Service

Fishery Bulletin
established 1881

Spencer F. Baird
First U.S. Commissioner
of Fisheries and founder
of *Fishery Bulletin*

Age validation of the North Atlantic stock of wreckfish (*Polyprion americanus*), based on bomb radiocarbon (^{14}C), and new estimates of life history parameters

Adam R. Lytton (contact author)
Joseph C. Ballenger
Marcel J. M. Reichert
Tracey I. Smart

Email address for contact author: lyttona@dnr.sc.gov

South Carolina Department of Natural Resources
217 Fort Johnson Road
Charleston, South Carolina 29412-9110

Abstract—The wreckfish (*Polyprion americanus*), a commercially important, long-lived, demersal fish, is found in the eastern Atlantic from Norway to South Africa and in the western Atlantic from the Grand Banks, Newfoundland, to Argentina. Using bomb radiocarbon analysis, we validated the annual increment formation observed in otoliths and determined that increment counts are a good proxy for age. The maximum observed age was 80 years, more than double the previously reported maximum age of 39 years in the North Atlantic population. The updated fit of the length-at-age information to the von Bertalanffy growth model resulted in L_∞, k, and t_0 estimates of 1026 mm in fork length, 0.124/year, and −4.96 years, respectively. We used these updated values for maximum age and growth parameters to estimate rates of instantaneous and age-varying natural mortality, and found that instantaneous natural mortality ranged from 0.088 to 0.091 and age-varying natural mortality reached an asymptote of 0.07–0.12 by 15 years of age. This study highlights the need for age validation in long-lived fish species to prevent inaccurate estimates of age that ultimately can lead to mismanagement of a species

Manuscript submitted 11 February 2015.
Manuscript accepted 16 November 2015.
Fish. Bull. 114:77–88 (2016).
Online publication date: 3 December 2015.
doi: 10.7755FB.114.1.7

Deepwater fishes (depths >400 m) are becoming increasingly important to commercial fisheries (Clarke et al., 2003). Unfortunately, the general longevity—some species such as orange roughy (*Hoplostethus atlanticus*) live up to 150 years—and slow maturation rates of many deepwater fishes make them highly susceptible to overfishing and slow to recover from an overfished state (Clark, 2001; Roberts, 2002; Clarke et al., 2003). An additional issue is that deepwater fish species are difficult to age (Fenton et al., 1991, Friess and Sedberry, 2011;). Accurate aging is critical for the estimation of several life history parameters, such as growth, mortality, and stock productivity, and is essential for any age-structured model of population dynamics.

One deepwater species whose age estimates are subject to aging error is the wreckfish (*Polyprion americanus*). This grouper-like, commercially important, long-lived, demersal fish is found in the eastern Atlantic from Norway to South Africa and in the western Atlantic from the Grand Banks, Newfoundland, to Argentina, although it is noticeably absent from tropical latitudes—an absence that indicates an antitropical distribution for this species (Sedberry et al., 1999). Using microsatellite genetic markers, Ball et al. (2000) determined that North Atlantic and South Atlantic populations are genetically distinct. Our study focused on the North Atlantic, and unless otherwise specified, *wreckfish* hereafter refers to the stock in the North Atlantic. Adult wreckfish are found concentrated around steep, rocky bottoms and deep coral reefs, occurring in lower concentrations along flat hard bottom, from depths of 40 to 800 m; however, most wreckfish occur in waters deeper than 300 m, and at a maximum reported depth of 1000 m (Sedberry et al., 1999). They grow to a size of 2 m and can approach 50 kg in weight (Sedberry et al., 1999).

Until the mid-1980s, when crews aboard pelagic longliners accidentally "discovered" the resource along the Charleston Bump, an area off the coast of South Carolina (Sedberry et al., 1999), wreckfish were unexploited commercially in the western North Atlantic. The fishery for this species developed rapidly, and the majority of effort was focused on or around the Charleston Bump, where landings peaked at 4.2 million lb whole weight (ww) in 1989 (Vaughan et al.,

2001). The rapid expansion of the fishery for wreckfish, along with growing concern among fishermen and managers about the sustainability of this fishery, resulted in the establishment of an "individual transferable quota system" for wreckfish in 1990 by the South Atlantic Fishery Management Council (SAFMC), and several subsequent management changes have been implemented since then. Currently the total allowable catch is set at 235,000 lb ww, and the fishery for wreckfish was estimated to be worth $700,000 in 2012.

Despite the widespread distribution and commercial importance of wreckfish, there have been only 2 publications in which the age of this species has been documented and its associated life history traits have been described: one on the North Atlantic population (Vaughan et al., 2001) and another on the South Atlantic population (Peres and Haimovici, 2004). These 2 studies differed widely in their estimate of maximum age for wreckfish; Vaughan et al. (2001) suggested a maximum age of 39 years and Peres and Haimovici (2004) suggested maximum ages for males and females of 62 and 76 years, respectively. Unfortunately, neither study included attempts to validate age estimates despite the suggestion in other literature that maximum age differences of this magnitude between populations of the same species are unlikely (Collins et al., 1987; Begg and Sellin, 1998). A related species, hapuku (*Polyprion oxygeneios*), reaches ages in excess of 60 years in the South Pacific (Francis et al., 1999). Another observation that indicates potential underaging of wreckfish is the lack of decoupling of size at age in the von Bertalanffy growth model (VBGM) presented by Vaughan et al. (2001); this decoupling is often characteristic of long-lived fish species (Coulson et al., 2009; Friess and Sedberry, 2011).

Using bomb radiocarbon analysis, we validated age estimates for wreckfish caught in the North Atlantic, in particular for fish captured in the area of the Charleston Bump. We presumed that wreckfish attain a much higher maximum age than has been reported previously for the North Atlantic population. We then recalculated various life history parameters, including length at age, growth, and natural mortality on the basis of the validated age estimates.

Materials and methods

Collection of samples

Personnel from the National Marine Fisheries Service and South Carolina Department of Natural Resources collected otoliths from commercially landed wreckfish from 1991 through 2011 at ports in South Carolina, Florida, and North Carolina. Data recorded for most fish included fork length (FL, in millimeters), although, on some fish, measures of standard length (SL, in millimeters) and total length (TL, in millimeters) also were taken. We developed a FL-TL meristic conversion to facilitate the conversion to and from different length measurements. Fishermen generally gutted all fish at sea and kept them on ice until landed, a process that prevented sex-specific analyses. For aging purposes, port samplers removed at least the left sagittal otolith, although removal of both sagittal otoliths occurred in some cases.

Age validation

The otoliths that were used for bomb radiocarbon analysis were collected in 1991 (n=323) from wreckfish that had at least a measurement of TL and both sagittal otoliths were removed. Vaughan et al. (2001) did not provide detailed information about the technique they used for processing otoliths, and we based our otolith processing on a slightly modified protocol detailed in Peres and Haimovici (2004). After an otolith was embedded in a marine grade epoxy, we cut a series of transverse sections (~0.25–0.35 mm thick) from the left sagittal otolith, ensuring that at least one section included the otolith core. Sectioning was done with an IsoMet Low Speed Saw[1] (Buehler, Lake Bluff, IL) with a diamond-coated waffering blade. We mounted (and cleared) resulting sections, typically 2 sections per otolith, on glass slides, using Cytoseal XYL medium (Thermo Fisher Scientific Inc., Waltham, MA).

Two readers independently examined otoliths for age determination, without knowledge of fish size, capture date, or the results of the other reader, with an Eclipse 55i compound microscope (Nikon, Tokyo) under transmitted light at magnifications of 40–100×. Readers prioritized reading the section that contained the core, unless there was an obvious reason, such as damage to the otolith, not to use that section. Counts of increments were determined by counting all opaque growth increments along the medial surface of the transverse otolith section ventral to the sulcus. Identification of the first growth increment was based on the protocol of Peres and Haimovici (2004), in which the first increment follows 1–3 "false" rings and exhibits a discontinuity, which is a thin crack-like structure running between a translucent and opaque increment.

After determining initial increment counts, we selected 20 specimens for analysis of bomb radiocarbon levels for age validation. We selected for analysis those specimens with a birth year between 1950 and 1980, as determined from increment count and year of capture (1991), and agreement between readers. If reader disagreement was greater than 1 year, we excluded the specimen from consideration. We embedded the right sagittal otolith of the specimen in resin and obtained a single, 1-mm-thick transverse section through the core. The resultant section was washed with deionized water and dried overnight. Extraneous otolith material surrounding the core was removed with a Dremel, model 732, rotary tool (Robert Bosch Tool Corp., Mt. Prospect, IL) with a carbide-cutting wheel.

[1] Mention of trade names or commercial companies is for identification purposes only and does not imply endorsement by the authors or the National Marine Fisheries Service, NOAA.

To prevent cross-contamination between samples we used a new carbide cutting wheel for each otolith and removed the core under a ventilation system. We removed additional surface contaminants by rinsing the extracted otolith cores for two 30-s intervals in deionized water, followed by an acid bath in 10% HNO_3 for 30 s, and a final rinse with deionized water.

After the otoliths had dried overnight, we measured each otolith core to the nearest 0.01 mg to ensure that enough material (>8 mg) had been obtained for bomb radiocarbon analysis. We did not obtain enough material from a single section for several specimens; for such specimens, we removed and processed a second section from the same otolith using the same technique, adding the additional material to the original sample.

We shipped the resultant core samples in plastic 5-mL vials to the National Ocean Sciences Accelerator Mass Spectrometry Facility (NOSAMS) at the Woods Hole Oceanographic Institution. Preparation of the samples for bomb radiocarbon analysis followed the protocol outlined by NOSAMS for inorganic carbonate materials. First, samples underwent acid hydrolysis, with an H_3PO_4 solution, to form CO_2. The evolving CO_2 was then removed by using an automated system that included acidification and sparging with nitrogen, and the CO_2 was reduced with a catalyst (Fe or Co) in the presence of excess hydrogen to form graphite. The graphite was then loaded into the accelerator mass spectrometer for reading ^{14}C levels. Staff of the NOSAMS subsequently compared the observed ^{14}C concentrations for each specimen to ^{14}C levels found in 19th century wood formed before nuclear testing, using ^{13}C concentrations to correct for any natural or machine-generated fractionation effects. The resultant statistic ($\Delta^{14}C$, in parts per million) provides a measure of the increase in ^{14}C due to uptake of ^{14}C from nuclear bomb testing in the 1950s through early 1970s compared with ^{14}C levels found in early 19th century wood.

To facilitate comparisons with other studies, we transformed the raw $\Delta^{14}C$ chronologies to proportion of total bomb radiocarbon ($\%C_i^{14}$),

$$\%C_i^{14} = \frac{C_{min}^{14} + C_i^{14}}{C_{min}^{14} + C_{max}^{14}}, \quad (1)$$

where C_{min}^{14} = the inverse of the lowest radiocarbon level found;
C_{max}^{14} = the highest radiocarbon value found;
C_i^{14} = the ^{14}C level of the i^{th} sample; and
$\%C_i^{14}$ = the percentage of total bomb radiocarbon of the i^{th} sample.

We then fitted $\%C^{14}$ values to a logistic curve,

$$\%C^{14} = \frac{\alpha}{1 + e^{(\beta - \text{Birth Year}/\lambda)}}, \quad (2)$$

where α (asymptote), β (inflection point), and λ (scaling parameter determining curve shape) are the 3 parameters of the logistic curve to be estimated by nonlinear regression.

We analyzed the accuracy of our initial increment counts as a proxy for age by comparing the wreckfish $\%C_i^{14}$ chronology to a reference $\%C_i^{14}$ chronology of validated ages for haddock (*Melanogrammus aeglefinus*) collected from Newfoundland (Campana, 1997). We used a variance ratio test to determine if there was any significant difference between the 2 chronologies. We conducted all analyses using R, vers. 3.0.2 (R Core Team, 2012).

Age and growth analysis

Because of our desire to use more recently caught fish, which presumably would better represent recent growth patterns in the population, we excluded all specimens used in previous bomb radiocarbon analysis, instead randomly selecting 500 specimens collected from 2000 through 2011. Almost all randomly selected fish measured between 800 and 1000 mm FL because of the high availability of these size classes in the sample archive—an availability that is likely due to commercial fishing practices. To improve growth curve fit, we included all available specimens from 2000 through 2011 that were smaller than 700 mm FL (n=44) or larger than 1100 mm FL (n=24) and that were not already randomly selected in the age and growth analysis. Our intent with this selection strategy was to reduce the sensitivity of the growth curve to small sample sizes of younger and older age classes. Furthermore, inclusion of the oldest fish, under the assumption that larger fish are generally older, improves our probability of identifying the oldest fish in the fishery-dependent sample database. Because many mathematical estimators of natural mortality (M) make use of maximum age, proper identification of the oldest fish in the sample is vital.

For specimens used in the age and growth analysis, we processed otoliths to the same approximate thickness (0.25–0.35 mm) and mounted them as we did for the bomb radiocarbon study. We used only the left otolith for age estimates, and the 2 readers, once again, performed the readings blindly and independently. If readers disagreed on an age, the otolith was aged concurrently to reach a consensus on age. If disagreement persisted, the otolith was excluded from this study.

We fitted the length-at-age data to the VBGM,

$$L_t = L_\infty(1 - e^{-k(t - t_0)}), \quad (3)$$

where L_t (in millimeters) = length at age t (in years);
L_∞ (in millimeters) = the asymptotic length;
k (1/year) = the Brody growth coefficient; and
t_0 = the theoretical age (in years) at which length is 0 (von Bertalanffy, 1938).

We fitted the VBGM and obtained estimates of growth model parameters, using a nonlinear regression in R, vers. 3.0.2.

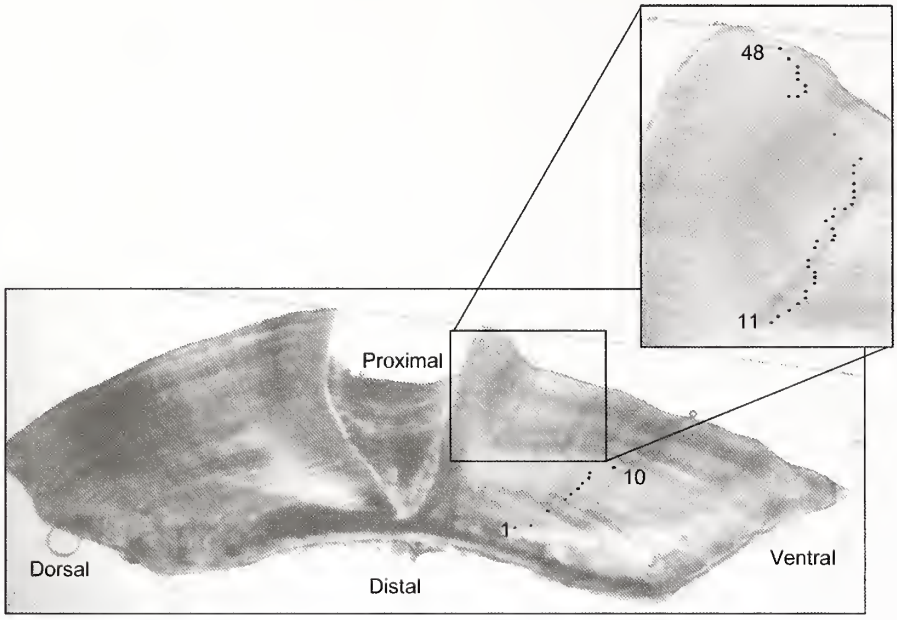

Figure 1

Transverse section of a sagittal otolith, taken from a wreckfish (*Polyprion americanus*) caught in the North Atlantic in 2005, that shows the typical pattern of increment formation. Each black dot (opaque growth increment) represents 1 year of growth. The fish from which this otolith was removed was estimated to be 48 years old.

Natural mortality

We investigated 4 distinct M estimators, 2 age-constant estimators from Then et al. (2015, eqs. 4 and 5),

$$M = 4.899(t_{\max}{}^{-0.916}) \text{ and} \quad (4)$$

$$M = (4.118k^{0.73})(L_{\infty}{}^{-0.33}), \quad (5)$$

and 2 age-varying M estimators from Gislason et al. (2010, eq. 6) and Charnov et al. (2013, eq. 7),

$$M = e^{(0.55-1.61\times \mathrm{Ln}(L_t)+1.44\times \mathrm{Ln}(L_\infty)+\mathrm{Ln}(k))} \text{ and} \quad (6)$$

$$M = \left(\frac{L_t}{L_\infty}\right)^{-1.5} \times k. \quad (7)$$

Each of these estimators used either estimates for VBGM parameters (k and L_∞) or maximum age ($t_{\max}$) to predict M.

Results

Examination of otoliths and growth increments

External examination of 3 of the whole otoliths from wreckfish that were selected for use in the age and growth analysis revealed a misshaped translucent otolith with white crystalline lumps along the external surface. We sectioned one otolith with these characteristics to examine growth increment formation, only to discover that the otolith contained no distinguishable growth increments. We excluded these 3 specimens from further analysis.

Otolith sections exhibited a distinct opaque core, trapezoid in shape, between 5 and 6 mm in length and from 2 to 3 mm in height. Growth increments in transverse otolith sections were most visible along the medial surface ventral to the sulcus, although the first few increments were highly variable in width and spacing in any plane (Fig. 1). The first 4–6 opaque bands were broad and tended to widen or begin to bifurcate as they extended to the ventral surface of the section. Often, the first 4–6 opaque increments were followed by a distinct, crack-like structure. Thereafter, the growth bands continued to be broad and diffuse until an increment count of 10–15, after which the growth increments became noticeably more compact and regularly spaced but harder to discern.

Earlier, broader increments (<15) were read more easily at a lower magnification (40×) by bringing the increments in and out of focus and allowing the reader to focus on the more distinct increment patterns. The later and more compact opaque increments (>15) were more easily read at higher magnification (100×), which

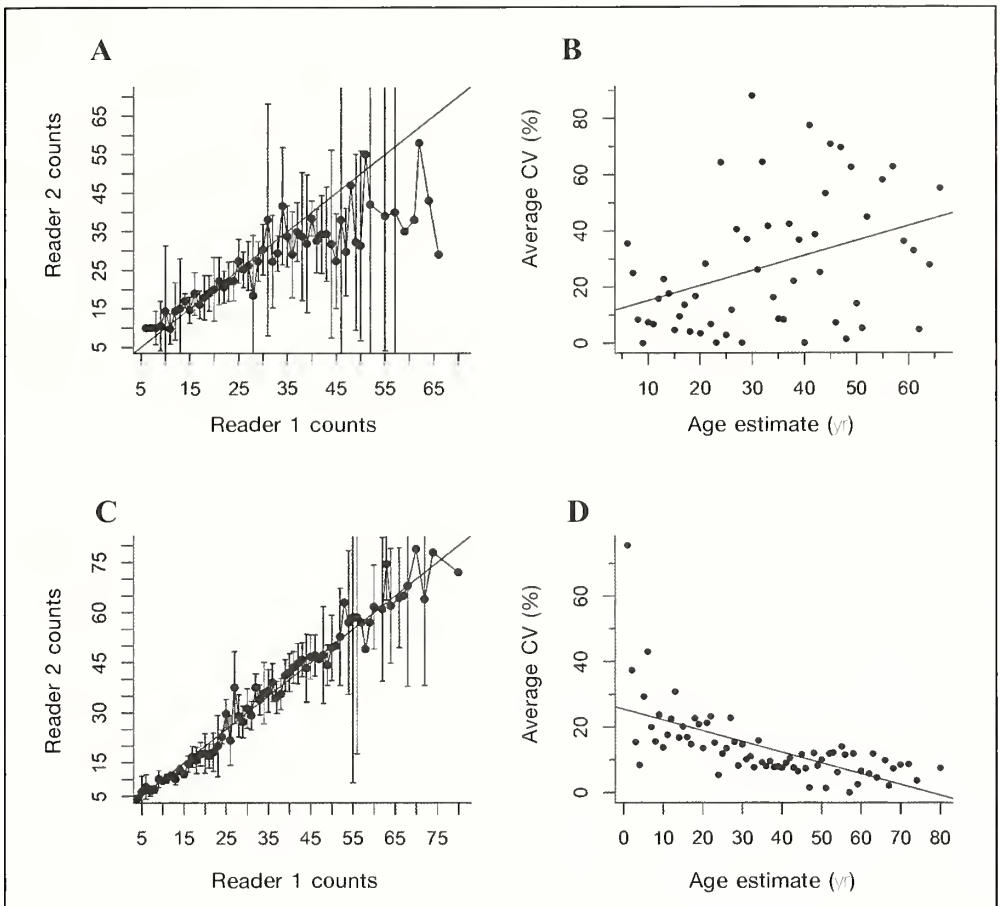

Figure 2

Bias plots of increment counts made by readers 1 and 2: (**A**) for identification of appropriate specimens for bomb radiocarbon analysis before identification of strict increment identification protocols, and (**C**) for growth analyses. Coefficients of variation (CV) in age estimates made by (**B**) reader 1 and (**D**) reader 2. Error bars in panels A and C represent 95% confidence intervals. Increment count-specific CVs increased (y=0.53x+9.86; coefficient of determination [r^2]=0.12, P=0.005) with increment number before identification of strict aging protocols. For specimens analyzed for growth analysis, CVs decreased with increment count (y=−0.33x+25.47; r^2=0.39, P<0.001).

allowed for better resolution between tightly compacted increments that may have otherwise been grouped together. In many of the otoliths, readability decreased at various points along the chosen reading axis, forcing readers to shift to a new reading axis by following a growth increment along a lateral plane.

Age validation

Although increment counts for otoliths of wreckfish were relatively difficult to determine because increments could be difficult to discern, no samples were identified as unreadable and all specimens (n=323) were included for possible selection for bomb radiocarbon analysis. Lengths of the specimens ranged from 880 to 1070 mm TL. Initial estimated increment counts ranged from 6 to 66 increments for reader 1 and from 6 to 60 increments for reader 2. Count disagreements between readers ranged from 0 to 35 increments (average disagreement of 9 increments). Readers produced identical counts only 4.3% of the time, were within 1 increment 13.3% of the time, and were within 5 increments 45.7% of the time. Bias plots revealed that reader 2 counted fewer increments than reader 1 when reader 1 counted greater than 35 increments, indicating a bias between readers in fish of older ages (Fig. 2A). At increment counts of less than 35 for reader 1, there was no bias pattern between readers. Coefficients of variation (CV) increased significantly with age (P=0.005; Fig. 2B). The average CV between readers was 27.5%—a result that is likely due to the lack of validation-based aging criteria at this stage.

The wreckfish used in bomb radiocarbon analysis (n=20) had increment counts ranging from 11 to 43,

Table 1

Summary of results of the bomb radiocarbon analysis of otoliths from wreckfish (*Polyprion americanus*) that were collected in the North Atlantic in 1991. The last column provides the standard errors (SE) associated with the $\Delta^{14}C$ (‰) values. An asterisk (*) indicates that 2 sections were used to meet the weight requirement for processing otoliths with accelerator mass spectrometry.

Collection number	Number of growth increments	Birth year	Weight (mg) of otolith core	$\Delta^{14}C$ (‰)	SE
910086-18	43	1948	11.5	−63.36	2.5
910076-15	40	1951	13.2	−14.98	4.5
910084-5	40	1951	10.7	−67.43	2.2
910085-14	40	1951	8.5	−60.97	2.5
910084-11	36	1955	11.2	−60.35	2.5
910078-11	34	1957	9.6	−57.15	3.5
910082-32	29	1962	11.3*	−64.32	2.5
910086-2	27	1964	8.9	−63.87	2.7
910083-46	26	1965	12.8	−18.90	2.5
910076-5	25	1966	15.2	−18.47	4.8
910078-17	23	1968	9.6	20.67	2.5
910076-2	22	1969	15.1*	47.48	4.4
910078-28	22	1969	9.4	98.90	2.7
910083-13	22	1969	11.0	57.52	2.5
910079-10	20	1971	12.4	35.80	2.5
910079-16	18	1973	16.7*	65.90	3.4
910079-14	17	1974	12.8*	72.14	2.9
910086-1	16	1975	8.6	87.13	2.7
910085-6	15	1976	9.5	80.04	4.4
910080-19	11	1980	10.1	90.88	2.7

and birth years (based on one increment formed per year) ranging from 1948 to 1980 (Table 1). The otolith core weights ranged from 8.5 to 16.5 mg; however, 4 samples required the use of a second section to meet the requirement for the minimum material needed for analysis with accelerated mass spectrometery. Otolith core values of $\Delta^{14}C$ ranged from −7.43‰ in birth year 1951 to 98.90‰ in birth year 1969, well within the range of previously published $\Delta^{14}C$ levels from haddock (Campana, 1997). Levels of $\Delta^{14}C$ in otolith cores from wreckfish showed a prominent increase beginning in the early 1960s, peaking around 1975 and leveling off thereafter (Fig. 3A). There was no evidence of the expected decline in $\Delta^{14}C$ levels after 1975, possibly as a result of the lack of sufficient samples past that date. Wreckfish with birth years before 1963 exhibited relatively constant low levels $\Delta^{14}C$, with the exception of one outlier fish that had an estimated birth year of 1951 ($\Delta^{14}C$= −14.98‰). Another possible outlier was a fish with a birth year of 1969 ($\Delta^{14}C$=98.90‰). Because most samples exhibited a good fit to the logistic regression curve, we believe the outliers resulted from a contamination issue during core removal rather than from aging error.

The $\%^{14}C$ uptake chronology for wreckfish (α=0.87, β=1967, λ=1.31) exhibits an uptake pattern similar in shape to the published $\%^{14}C$ chronology for haddock (α=0.93, β=1962, λ=2.35) (Campana, 1997; Fig. 3B). However, the fitted logistic curve for $\%^{14}C$ of wreckfish fell below the fitted logistic curve for $\%^{14}C$ of haddock for the entire time period (Fig. 3B), and there was a noticeable phase shift of 5–6 years between the models (wreckfish β=1967 and haddock β=1962). The variance ratio test confirmed that the curves were significantly different (P<0.001). Despite the small difference in curves, which indicates potential underaging, the similarity in uptake patterns between the 2 curves indicates annual growth increments.

Age and growth

After completion of all otolith readings (n=568) for age and growth analysis, we omitted 14 otoliths because of disagreements between readers. Specimens ranged in size from 452 to 1340 mm FL (Fig. 4.). Ignoring the potential phase shift identified in the bomb radiocarbon validation study, ages of wreckfish ranged from 1 to 80 years for reader 1 and from 2 to 79 years for reader 2, with an average disagreement of 4 years. Readers produced identical counts 10.8% of the time, had agreement within 1 year 30.4% of the time, and had agreement within 5 years 72.7% of the time, a considerable improvement over the bomb radiocarbon readings. This improvement resulted from the development and use

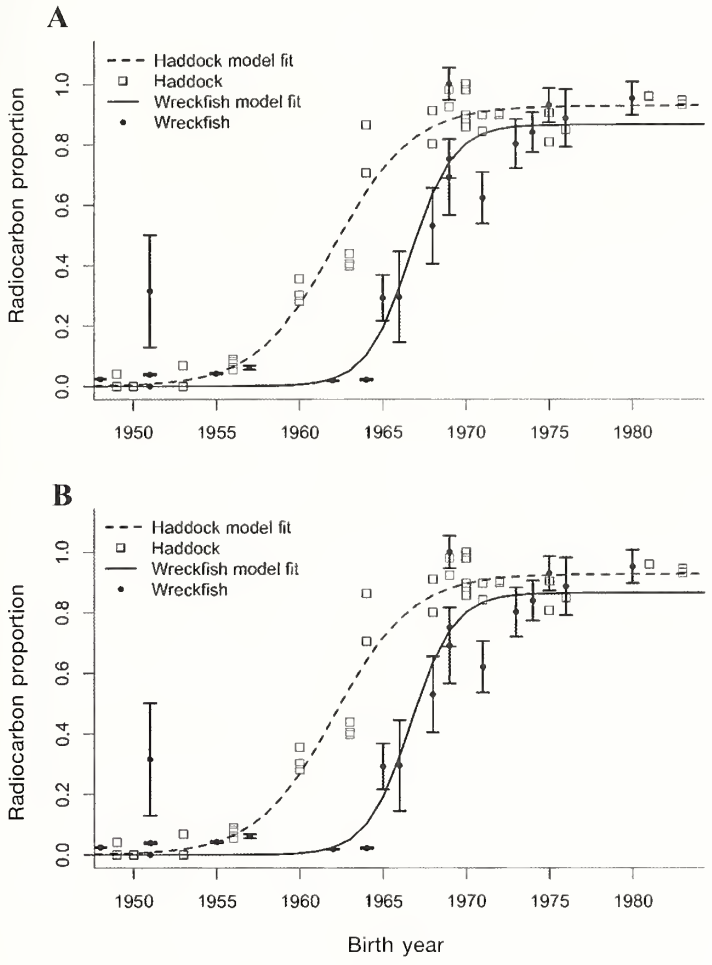

Figure 3

(**A**) Mean proportion of total bomb radiocarbon (%^{14}C) of total $\Delta^{14}C$ by birth year for otolith cores from wreckfish (*Polyprion americanus*) collected in the North Atlantic in 1991. We fitted a logistical regression model (solid line) to the data. (**B**) Mean %^{14}C values for wreckfish from this study and for haddock (*Melanogrammus aeglefinus*) from Campana (1997). Symbols represent observed values, and lines represent fits of the logistic model for wreckfish (dotted) and haddock (solid), respectively. In both panels, error bars represent the standard errors around the means.

of a strict aging protocol for these readings, a protocol that had not been put in place before the bomb radiocarbon readings.

After completion of the consensus readings, age estimates ranged from 1 to 80 years. There was no clear pattern of bias between readers in age estimates (Fig. 2C). The CV decreased with increasing age, and the average CV for age estimates was 17.4% ($P<0.001$; Fig. 2D). The highest CV value of 75.4% occurred for fish aged as 1 year old by reader 1. When we exclude the CV for age-1 fish, because the CV is susceptible to inflation as the mean approaches 0 and only reader 1 estimated specimens to be 1 year old, the CV estimate dropped to 12.2%. The reduced CV estimates, after development of aging protocols, are in the range of CV reported by other researchers for long-lived, deepwater, difficult-to-age species (Friess and Sedberry, 2011; Harris et al., 2004).

The VBGM fit to the remaining sample of 554 wreckfish used for age and growth analysis resulted in

$$L_t = 1026(1 - e^{-0.12(t-4.96)}).$$

This result indicates that wreckfish experience rapid growth during the early years of life, attaining approximately 95% of asymptotic length, on average, by 20 years of age. After age 20, growth in length slows dramatically, and fish older than approximately 20 years in the population exhibit similar size distributions (Fig. 5).

To allow for comparison of VBGM parameters from previous age and growth studies on wreckfish, all FL measurements were converted to TL measurements and the VBGM was rerun, resulting in

$$L_t = 1071(1 - e^{-0.12(t-4.96)}). \quad (8)$$

In comparison with the 2 previous studies of wreckfish (Fig. 6, Table 2), our data indicate a more rapid growth rate at younger ages and a smaller asymptotic length.

Natural mortality

For calculation of our M estimates, we used the maximum age (t_{ma}=80 years) observed in the fish aged for growth curve analysis and the estimates of von Bertalanffy growth curve parameters k (0.124) and L_∞ (1026 mm FL). Age-constant estimates of M based on the methods reported in Then et al. (2015) yielded M=0.088 with equation 4 and M=0.091 with equation 5. These 2 estimates are remarkably similar given that they are based on 2 fundamentally different estimators. The M estimates from both age-varying estimators indicate a type-3 survival curve, which is common among finfish species, for North Atlantic wreckfish (Fig. 7). The Charnov et al. (2013) method yielded M at age 0=0.398, and with an expected rapid decrease in M values to age 15 years and a leveling off at around M=0.120. The Gislason et al. (2010) method (eq. 6) yielded a lower value of M at age 0 (M=0.231), than that with the Charnov et al. (2013) method (eq. 7), but with a similar rapid decline up to age 15 years and reaching an asymptotic M value of around 0.060.

For evaluation of age-varying estimators against the age-constant M estimators, we compared the proportion of recruits surviving from age at full recruitment to the fishery to maximum age as estimated from each

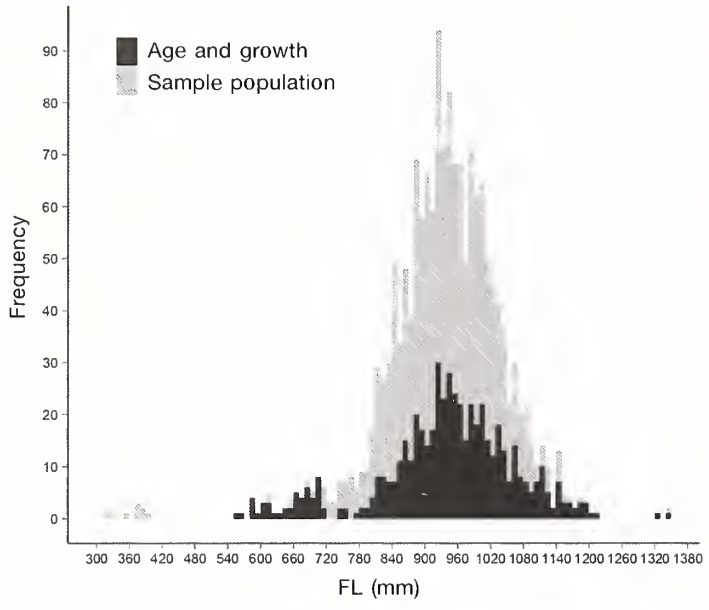

Figure 4

Length frequency (in 10-mm bins) of fork lengths (FLs) from the samples of wreckfish (*Polyprion americanus*) collected in the North Atlantic in 1991 and used in age and growth analysis (n=563; black), the data of which are overlaid on the total sample population from which these samples were randomly selected. Note that the specimens that had sizes <700 mm FL or >1100 mm FL were not randomly selected.

of the 4 methods. We defined age at full recruitment to the fishery as the age calculated for the most common (900 mm FL and 12 years old) length in the fishery-dependent samples based on our calculated VBGM. This approach resulted in 2.5%, 2.1%, 1%, and 0% recruits surviving to maximum age with Equations 4, 5, 6, and 7, respectively.

Discussion

Age validation, here referring to confirmation of absolute age and periodicity of growth increment formation, is a crucial step for stock assessment of any fish species. Without validated age data, greater uncertainty in estimates of age-related life history parameters (e.g., growth and natural mortality) and age compositions would persist, resulting in an increase in uncertainty in stock assessment models. Particularly daunting is the task of validating the ages of long-lived fishes because few techniques are applicable to these species and most attempts have unclear results (Tracey and Horn, 1999; Harris et al., 2004). For the techniques available, Campana (2001) suggests that validation through bomb radiocarbon levels has high scientific merit and therefore is preferable to most other techniques, and only modest sample sizes (20–30 individuals) are needed.

Annual increment formation in the otoliths of wreckfish was validated by the radiocarbon dating method used in our study for wreckfish from the North Atlantic, and by the comparison with the haddock standard. As expected, with the exception of one outlier believed to have resulted from contamination, we detected no measurable radiocarbon in the otolith cores that were formed before 1958. One caveat for the use of a bomb radiocarbon technique for age validation is that it allows for validation of a maximum age only to the year of bomb radiocarbon onset (1958). Because all specimens of North Atlantic wreckfish used in this study were collected in 1991, we were able to validate a maximum age of up to 33 years with this technique. Collection and validation of age of otoliths in later years should eliminate the need for this caveat in the future. Still, the results of this study are useful today. The bomb radiocarbon technique validated the structure and annual formation of increments, indicating increment counts can successfully be used to age otoliths from wreckfish.

A distinct phase shift of approximately 5–6 years was apparent when comparing the chronology of radiocarbon levels in wreckfish with the standard chronology of haddock.

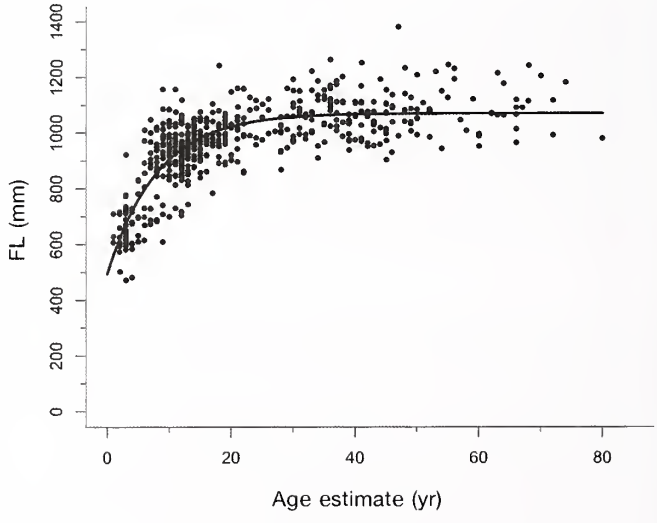

Figure 5

Observed length-at-age data for wreckfish (*Polyprion americanus*) collected in the North Atlantic from 2000 through 2011 used in the growth analysis. The solid line represents estimates from the fitted von Bertalanffy growth model.

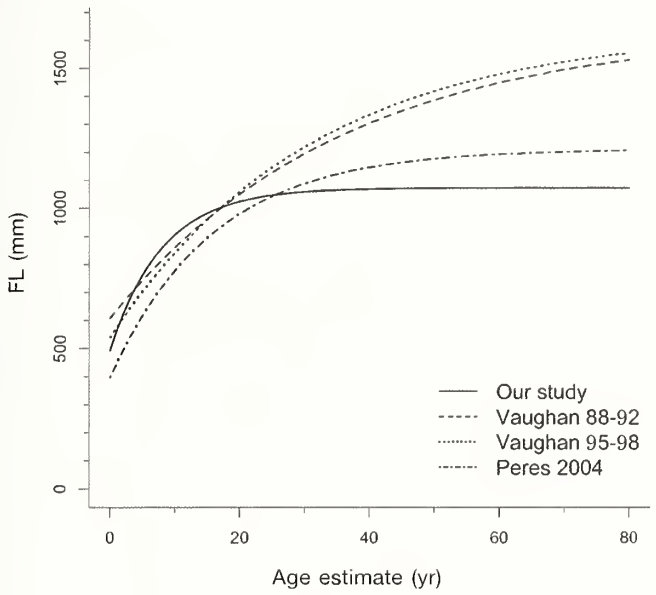

Figure 6

Comparison of growth curves from the fitted von Bertalanffy growth models for wreckfish (*Polyprion americanus*) from Peres and Haimovici (2004, dashed-and-dotted line), Vaughan for specimens caught in 1988–1992 (dashed line), Vaughan et al. (2001) for the specimens caught in 1995–1998 (dotted line), and the study described in this paper (solid line)

At face value, such a phase shift indicates a systematic underaging of wreckfish by 5–6 years, but Filer and Sedberry (2008) observed a similar phase shift in an age validation study performed on barrelfish (*Hyperoglyphe perciformis*) captured from the Charleston Bump. The authors hypothesized that the phase shift observed in barrelfish resulted from differences in oceanographic conditions experienced by barrelfish, compared with those experienced by haddock in the standard chronology for that species, variances caused by localized upwelling events or regional differences in onset of increases in ^{14}C in surface waters. Because the only known spawning location for adult wreckfish in the North Atlantic is the Charleston Bump, juvenile wreckfish may also have been exposed to lower levels of radiocarbon in a given year compared with the levels to which known-age haddock captured off the eastern coast of Canada were exposed.

Researchers also have also documented a similar phase shift in bomb radiocarbon levels in the Pacific Ocean. A radiocarbon validation study performed on canary rockfish (*Sebastes pinniger*) revealed that differences in oceanographic conditions caused by upwelling caused a phase shift of 5–6 years between the radiocarbon chronologies of canary rockfish and that of a reference chronology developed from Pacific halibut (*Hippoglossus stenolepis*) (Piner et al., 2004).

Two additional sources of aging error that could explain the observed phase shift and apparent underaging in aging studies are 1) the misidentification of the first annulus and 2) the annulus overlay at older ages due to otolith section thickness. Misidentification of the first annulus could be directly related to our reliance on the aging protocol developed for the population of wreckfish in the South Atlantic by Peres and Haimovici (2004). On the basis of the daily increment counts in their study, Peres and Haimovici proposed that there were 1–3 false rings before the first annual increment. Inclusion of the false rings as annuli in our age estimates would have potentially shifted the curve to a later date, leading to a better phase agreement with the standard curve. Interestingly, such systematic underaging of wreckfish due to incorrect first annuli identification would shift the resulting growth curve along the x-axis and would provide a more realistic estimate of the t_0 parameter. Researchers have not performed

Table 2

Parameters from the von Bertalannfy growth model (VBGM), with associated standard errors (SE), from our study in which the converted total lengths (TLs) [see *Methods and methods* section] and from 2 previous studies on wreckfish (*Polyprion americanus*) in Atlantic ocean waters. An asterisk (*) indicates that Vaughan et al. 2001 experienced problems with convergence when trying to freely estimate VBGM parameters with data collected in 1988–1992. To alleviate this issue, they fixed L_∞ to 1638 mm TL, constraining the values that the other VBGM parameters can take because of correlation among parameters.

Source	Population	Period	Sex	n	L_∞	SE	k	SE	t_0	SE	t_{max}
Our Study	North	2000–2011	Combined	554	1071	6.80	0.124	0.007	−4.96	0.553	80
Vaughan et al., 2001	North	1988–1992	Combined	738	1638*		0.028	0.001	−16.56	0.590	39
		1995–1998	Combined	117	1638	121.92	0.032	0.006	−12.48	1.760	30
Peres and Haimovici, 2004	South	1986–1997	Combined	337	1210		0.063		−6.30		76

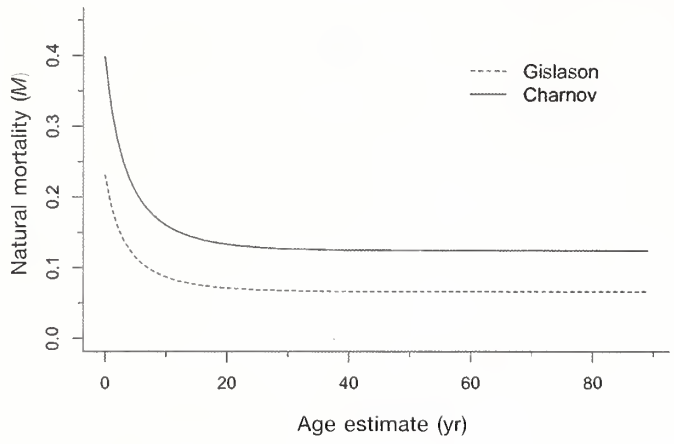

Figure 7

Estimates of age-varying natural mortality (M) for wreckfish (*Polyprion americanus*) caught in the North Atlantic from 2000 through 2011, based on the Gislason et al. (dashed line) and the Charnov et al. (solid line) methods.

daily increment analysis on North Atlantic wreckfish to validate the first annulus; therefore, no conclusion can be made as to which method is correct.

Peres and Haimovici (2004) also suggested annulus overlay could be a source of aging error in their study, with the implication being that it would cause underaging of wreckfish in a population. To investigate this possibility, Peres and Haimovici (2004) experimented with different thicknesses of otolith sections, suggesting that much thinner sections (0.11–0.15 mm for ages greater than 40 years compared with 0.2–0.25 mm for small fish [TL <75 cm]) were needed to clearly discern banding patterns in older wreckfish. Further research is warranted to determine whether the phase shift is due to regional differences in ^{14}C concentrations, to systematic underaging of specimens that results from incorrect first annulus identification, to annulus overlay, or to other reasons.

Irrespective of the observed phase shift, we validated annual increment formation, and, having found no evidence of overaging in our bomb radiocarbon study and having identified several individuals aged over 75 years in our relatively small sample, we are confident that wreckfish are living in excess of 75 years. The maximum age observed, 80 years, is approximately twice the previously reported maximum age of 39 years (Vaughan et al., 2001). Our revised maximum age estimate is consistent with findings for the congeneric species Hapuku (63 years; Francis et al., 1999) and the South Atlantic stock of wreckfish (76 years; Peres and Haimovici, 2004). The finding that wreckfish live twice as long as previously reported by Vaughan et al. (2001) can be attributed to a difference in aging technique. We aged wreckfish using transverse otolith sections that were 0.25–0.30 mm wide, and the prior study used sections that were 0.35–0.50 mm wide (Potts[2]).

The surface of an otolith from a wreckfish is far from uniform; there are many raised bumps along the surface, and edges are often serrated. Because of the narrow width between outer increments along these irregularities, the same band may be seen along different planes when the otolith is sectioned at thicker widths. Inclusion of the same band at different planes can potentially cause a "smear," that masks other nearby growth increments, resulting in the bands being grouped together and leading to under-estimates of ages. A similar argument was put forward to justify the use of thinner sections as reported in Peres and Haimovici (2004).

The k value obtained in our study (k=0.124/year, sexes combined) is approximately 4 times the value previously reported for wreckfish in the North Atlantic (k=0.032/year and k=0.028/year for sexes combined for the periods 1995–1998 and 1988–1992; Vaughan et al., 2001) and double that for the South Atlantic stock (k=0.063/year, sexes combined; Peres and Haimovici, 2004).

All t_0 values reported for wreckfish are negative, and the value obtained in our study (t_0=−4.96 years) is similar to the values reported for the population in the South Atlantic (t_0=−6.30 years; Peres and Haimovici, 2004) but very different from the t_0 values (t_0=−12.48 years and t_0=−16.56 years for the periods 1995–1998 and 1988–1992) previously reported for North Atlantic wreckfish (Vaughan et al., 2001). The difference in t_0 values is most likely due to the lack of smaller, younger fish in the samples used in the Vaughan et al. (2001) study. It is expected that if samples of younger (0–3 years old) fish are available and included in an analysis, the resulting estimates of VBGM parameters would shift t_0 values closer to zero. As noted previously, if the phase shift observed in the bomb radiocarbon analysis is the result of systematic underaging of wreckfish by 5–6 years because of issues with first annulus identification, any such correction should result in a shift of t_0 toward zero.

The L_∞ values obtained in our study (L_∞=1071 mm TL, sexes combined) were lower than those of the population in the South Atlantic (L_∞=1210 mm TL, sexes combined; Peres and Haimovici, 2004) and the stock in the North Atlantic (L_∞=1638 mm TL; Vaughan et al., 2001). Note that the largest specimen (1340 mm TL) in our samples was nearly 300 mm TL smaller than the L_∞ value reported by Vaughan et al. (2001), and 95% of all the specimens in our study were less than 1200 mm TL. The difference in reported L_∞ values between our study and the study of the South Atlantic stock by Peres and Haimovici (2004) could simply be

[2] Potts, J. 2014. Personal commun. NOAA Southeast Fisheries Science Center, Beaufort, NC 28516.

due to a disparity in growth between the 2 stocks. The difference in estimates between the Vaughan et al. (2001) and our study may have resulted from the lack of larger fish (>1100 mm TL) in our sample; however, the length frequency of the subsample used in age and growth analysis in our study mirrored the length frequency of our total sample population. It is more likely that the difference in L_∞ values between the aforementioned study and ours was caused by incorrect age assignments, which in turn would impact the VBGM parameters. Either way, this difference in L_∞ values has implications for estimating related life history parameters and highlights the importance of validation efforts, as well as the importance of the inclusion of sufficient samples from the oldest age groups when developing a VBGM.

Our samples contained only 3 specimens that were less than 500 mm FL, the proposed size at settlement for wreckfish from both the North and South Atlantic (Sedberry et al., 1998; Peres and Haimovici, 2004). The smallest specimen was 452 mm FL and was estimated to be 3 years old. The lack of smaller and younger fish (only 14 specimens <2 years old) within the sample is consistent with the notion that juvenile North Atlantic wreckfish settle at a size around 500 mm TL and at an age of 1–2 years. If juveniles are present at the same locations as adults, gear selectivity is unlikely to have excluded them from our sampling because juvenile wreckfish have relatively large mouths and would be susceptible to hook-and-line capture.

Natural mortality is a fundamental life history parameter used in stock assessments. Without a realistic estimate of M, fishing-induced mortality cannot be estimated from the age or size composition of commercial catches, and the effects of fishing mortality on future yields cannot be predicted. Methods used to estimate M treat it either as a constant value (Pauly, 1980; Hoenig, 1983; Alagajara, 1984; Polovina and Ralston, 1987; Hewitt and Hoenig, 2005; Then et al., 2015) or as an age- or size-varying parameter (Lorenzen, 1996; Gislason et al., 2010; Charnov et al., 2013), but the latter is the generally preferred method for estimating M.

Although treating M as a constant value has been a historically common practice, today researchers generally accept that M is highest during larval stages and decreases as a fish ages, finally arriving at some steady state (Gislason et al., 2010). Assuming M varies with age, managers can consider the effects of size composition when examining alternate management strategies. Data from our study indicated that age-based estimates of M reached an asymptote by approximately age 15. The value of the asymptote varied according to the aging method used, ranging from 0.07 for Gislason et al. (2010) to 0.12 for Charnov et al. (2013), respectively. Most fish captured along the Charleston Bump are greater than 900 mm FL (Sedberry et al., 1999), corresponding to an age of around 10–15 years from the VBGM. If managers were to select a point estimate of M, because of the absence of younger age classes, it is likely that the point estimate of M used to determine the allowable biological catch would fall between the asymptotic values of M from the age-varying methods. This value would represent the M experienced by the fished portion of the stock.

When selecting the appropriate method for estimation of M, researchers are faced with a daunting selection of estimation techniques, most of which involve the use of estimates of one or multiple parameters from the VBGM, t_{max}, or weight-at-age data. Proper selection of a technique will first depend on the information available and then on the confidence in the accuracy of the parameter estimate being used (e.g., whether a researcher is more confident in the accuracy of the VBGM parameters or of t_{max}). However, Then et al. (2015) asserts that t_{max} is the best proxy for estimating M when a value is available. Because this study validated age estimates of wreckfish captured in the North Atlantic and because the M estimate based on VBGM parameters (M=0.091) was close to the M estimate that was based on t_{max} (M=0.088), 0.09 is an appropriate value to use for M in stock assessments of wreckfish.

The new information presented here on the life history of wreckfish in the North Atlantic represents the North Atlantic stock more accurately because it is based on recent samples collected during 2000–2011, because new aging criteria and resulting estimates have been validated with bomb radiocarbon analysis, and because the new age estimates are similar to estimates for other *Polyprion* species. Several aspects of the life history of wreckfish in the North Atlantic are still in need of study. The validation of the maximum age of 80 years reported here cannot be validated by radiocarbon analysis until the year 2038. However, we have validated the aging criteria used to determine ages of wreckfish through bomb radiocarbon analysis. In addition, the structure and formation of the first annual increment needs to be elucidated and investigated because it may potentially affect age estimates by up to 3 years. Samples from the eastern Atlantic are needed to compare potential differences in life history parameters within the North Atlantic population and to investigate connectivity between populations. Finally, the determination of size and age at maturity and sex-specific differences in age and growth is essential for future stock assessments and requires samples from whole, rather than gutted, fish.

Acknowledgments

We thank J. Potts (NOAA Southeastern Fisheries Science Center in Beaufort, North Carolina) for the donation of otoliths used in this study. We also thank the commercial fishermen who collected the samples used in this study. G. Sedberry is thanked for sharing his knowledge on wreckfish and his assistance with the preparation of this manuscript. This research was supported by NOAA grants NA11NMF4540174 (MARMAP) and NA11NMF4350043 (SEAMAP-SA) and by the South Carolina Department of Natural Resources.

Literature cited

Alagaraja, K.
1984. Simple methods for estimation of parameters for assessing exploited fish stocks. Indian J. Fish. 31:177–208.

Ball, A. O., G. R. Sedberry, M. S. Zatcoff, R. W. Chapman, and J. L. Carlin.
2000. Population structure of the wreckfish *Polyprion americanus* determined with microsatellite genetic markers. Mar. Biol. 137:1077–1090.

Baker, M. S., Jr., and C. A. Wilson.
2001. Use of bomb radiocarbon to validate otolith section ages of red snapper, *Lutjanus campechanus*, from the northern Gulf of Mexico. Limnol. Oceanogr. 46:1819–1824.

Begg, G. A., and M. J. Sellin.
1998. Age and growth of school mackerel (*Scomberomorus queenslandicus*) and spotted mackerel (*S. munroi*) in Queensland east-coast waters with implications for stock structure. Mar. Freshw. Res. 49:109–120.

Campana, S. E.
1997. Use of radiocarbon from nuclear fallout as a dated marker in the otoliths of haddock, *Melanogrammus aeglefinus*. Mar. Ecol. Prog. Ser. 150:49–56.
2001. Accuracy, precision and quality control in age determination, including a review of the use and abuse of age validation methods. J. Fish Biol. 59:197–242.

Charnov, E. L., T. F. Turner, and K. O. Winemiller.
2001. Reproductive constraints and the evolution of life histories with indeterminate growth. Proc. Natl. Acad. Sci. 98:9460–9464.

Charnov, E. L., H. Gislason, and J. G. Pope.
2013. Evolutionary assembly rules for fish life histories. Fish Fish. 14:213–224.

Clark, M.
2001. Are deepwater fisheries sustainable?—the example of orange roughy (*Hoplostethus atlanticus*) in New Zealand. Fish. Res. 51:123–135.

Clarke, M. W., C. J. Kelly, P. L. Connolly, and J. P. Molloy.
2003. A life history approach to the assessment and management of deepwater fisheries in the Northeast Atlantic. J. Northwest Atl. Fish. Sci. 31: 401–411.

Collins, M. R., C. W. Waltz, W. R. Roumillat, and D. L. Stubbs.
1987. Contribution to the life history and reproductive biology of gag, *Mycteroperca microlepis* (Serranidae), in the South Atlantic Bight. Fish. Bull. 85:648–653.

Coulson, P. G., S. A. Hesp, N. G. Hall, and I. C. Potter.
2009. The western blue groper (*Achoerodus gouldii*), a protogynous hermaphroditic labrid with exceptional longevity, late maturity, slow growth, and both late maturation and sex change. Fish. Bull. 107:57–75.

Filer, K. R., and G. R. Sedberry.
2008. Age, growth and reproduction of the barrelfish *Hyperoglyphe perciformis* (Mitchill) in the western North Atlantic. J. Fish Biol. 72:861–882.

Fenton, G. E., Short, S. A., and Ritz, D. A.
1991. Age determination of orange roughy, *Hoplostethus atlanticus* (Pisces: Trachichthyidae) using ^{210}Pb:^{226}Ra disequilibria. Mar. Biol. 109:197–202.

Francis, M. P., K. P. Mulligan, N. M. Davies, and M. P. Beentjes.
1999. Age and growth estimates for New Zealand hapuku, *Polyprion oxygeneios*. Fish. Bull. 97:227–242.

Friess, C., and G. R. Sedberry.
2011. Age, growth, and spawning season of red bream (*Beryx decadactylus*) off the southeastern United States. Fish. Bull. 109:20–33.

Gislason, H., N. Daan, J. C. Rice, and J. G. Pope.
2010. Size, growth, temperature and the natural mortality of marine fish. Fish Fish. 11:149–158.

Harris, P. J., D. M. Wyanski, and P. T. Mikell.
2004. Age, growth, and reproductive biology of blueline tilefish along the southeastern coast of the United States, 1982–1999. Trans. Am. Fish. Soc. 133:1190–1204.

Hewitt, D. A., and J. M. Hoenig.
2005. Comparison of two approaches for estimating natural mortality based on longevity. Fish. Bull. 103:433–437.

Hoenig, J. M.
1983. Empirical use of longevity data to estimate mortality rates. Fish. Bull. 81:898–903.

Lorenzen, K.
1996. The relationship between body weight and natural mortality in juvenile and adult fish: a comparison of natural ecosystems and aquaculture. J. Fish Biol. 49:627–647.

Pauly, D.
1980. On the interrelationships between natural mortality, growth parameters, and mean environmental temperature in 175 fish stocks. J. Cons. Int. Explor. Mer 39:175–192.

Peres, M. B., and M. Haimovici.
2004. Age and growth of southwestern Atlantic wreckfish *Polyprion americanus*. Fish. Res. 66:157–169.

Piner, K. R. and S. G. Wischniowski.
2004. Pacific halibut chronology of bomb radiocarbon in otoliths from 1944 to 1981 and a validation of ageing methods. J. Fish Biol. 64:1060–1071.

Polovina, J. J., and S. Ralston (eds.).
1987. Tropical snappers and groupers: biology and fisheries management, 659 p. Westview Press, Boulder, CO.

R Core Team.
2012. R: a language and environment for statistical computing. R Foundation for Statistical Computing, Vienna, Austria. [Available at website, accessed December 2013.]

Roberts, C. M.
2002. Deep impact: the rising toll of fishing in the deep sea. Sci. Soc. 17: 242–245.

Sedberry, G. R., J. L. Carlin, and G. M. Menezles.
1998. Movements of a pelagic-phase wreckfish, *Polyprion americanus* (Schneider, 1801), as indicated by tag and recapture. Arquipel. Cienc. Biol. Mar. 16A:69–72.

Sedberry, G. R., C. A. P. Andrade, J. L. Carlin, R. W. Chapman, B. E. Luckhurst, and C.S. Manooch III, G. Menezes, B. Thomsen, and G. F. Ulrich.
1999. Wreckfish *Polyprion americanus* in the North Atlantic fisheries, biology, and management of a widely distributed and long-lived fish. Am. Fish. Soc. Symp. 23:27–50.

Then, A. Y., J. M. Hoenig, N. G. Hall, and D. A. Hewitt.
2015. Evaluating the predictive performance of empirical estimators of natural mortality rate using information on over 200 fish species. ICES J. Mar. Sci. 72:82–92.

Tracey, D. M. and P. L. Horn.
1999. Background and review of ageing orange roughy (*Hoplostethus atlanticus*, Trachichthyidae) from New Zealand and elsewhere. N.Z. J. Mar. Freshw. Res. 33:67–86.

Vaughan, D. S., C. S. Manooch III, and J. C. Potts.
2001. Assessment of the wreckfish fishery on the Blake Plateau. Am. Fish. Soc. Symp. 25:105–120.

von Bertalanffy, L.
1938. A quantitative theory of the organic growth (inquiries on growth laws. II). Hum. Biol. 10:181–213.

NOAA
National Marine
Fisheries Service

Fishery Bulletin
established 1881

Spencer F. Baird
First U.S. Commissioner
of Fisheries and founder
of *Fishery Bulletin*

Age at maturity, skipped spawning, and fecundity of female sablefish (*Anoplopoma fimbria*) during the spawning season

Cara J. Rodgveller (contact author)
James W. Stark
Katy B. Echave
Peter-John F. Hulson

Email address for contact author: cara.rodgveller@noaa.gov

Alaska Biological Laboratories
Alaska Fisheries Science Center
National Marine Fisheries Service, NOAA
17109 Point Lena Loop Road
Juneau, Alaska 99801

Abstract—Accurate maturity-at-age data are necessary for estimating spawning stock biomass and setting reference points for fishing. This study is the first on age at maturity of female sablefish (*Anoplopoma fimbria*) sampled in Alaska during their winter spawning period, when maturity is most easily assessed. Skipped spawning, the situation where fish that have spawned in the past do not spawn during the current season, was documented in female sablefish for the first time. Determination of age at maturity was heavily influenced by whether these fish that would skip spawning were classified as mature or immature; age at 50% maturity was 6.8 years when fish that would skip spawning were classified as mature, and 9.9 years when classified as immature. Skipped spawning was more common on the continental shelf, and rates of skipped spawning increased with age through age 15. Estimates of age at maturity were similar for samples collected in winter and summer, when fish that would skip spawning sampled during winter were classified as mature. When fish that would skip spawning were considered immature in the sablefish population model for Alaska, estimates of spawning biomass decreased. Relative fecundity did not change with size and age, verifying the assumption made in the Alaska sablefish stock assessment that relative reproductive output is linearly related to female spawning biomass.

Manuscript submitted 25 November 2014.
Manuscript accepted 20 November 2015.
Fish. Bull. 115:89–102 (2016).
Online publication date: 8 December 2015.
doi: 10.7755FB.114.1.8

Maturity-at-age data are used in stock assessments to estimate reproductive output of fish populations. Commonly, these data are collected without the aid of histological analysis and often during surveys that do not correspond with the time of the reproductive cycle when maturity can be gauged with the greatest accuracy, the time just before spawning (Hunter et al., 1992). These discrepancies can result in the misclassification of maturity and in inaccuracies in estimations of age at maturity. Misclassifying maturity can result in over- or underestimation of spawning stock biomass (SSB), which is used as a proxy for egg production in population models. An inaccurate estimation of SSB can affect management decisions. In some cases, egg production is not linearly related to SSB, a situation that occurs when relative fecundity changes with age or size (e.g., Hislop, 1988). If relative fecundity is not constant, incorporating the assumption that SSB is linearly related to fecundity in population models will lead to bias in estimates of productivity.

Although it is generally assumed that marine fish in northern latitudes reproduce on an annual cycle, it is not always the case. For example, it has been documented that a portion of mature Atlantic cod (*Gadus morhua*) skips spawning annually; therefore, the reproductive cycle for some individuals is longer than 1 year (Marshall et al., 2000). In the North Pacific Ocean, the Pacific halibut (*Hippoglossus stenolepis*) has been thought to also skip spawning on the basis of their movements during the spawning season (Loher and Seitz, 2008). Skipped spawning, which occurs when mature fish that have spawned in prior seasons do not spawn in the current season, is likely to be a more common phenomenon than previously thought (Rideout and Tomkiewicz, 2011), having been documented in at least 30 freshwater and marine fishes (Secor, 2008; Skjæraasen et al., 2012).

Sablefish (*Anoplopoma fimbria*) are part of a commercially important resource in the North Pacific Ocean; the fishery in Alaska is val-

ued at more than $100 million annually (Fissel et al.[1]). In Alaska, the sablefish population is assessed annually with a split-sex, age-structured population model (Hanselman et al.[2]). Age at maturity is an integral component for estimating female SSB, which is used to set target biological reference points for this stock. The current female age-at-maturity model is based on data collected during surveys conducted in the summers of 1978–1983 (Sasaki, 1985). Because these data were collected more than 30 years ago, it is important to re-assess the age at maturity of female sablefish. In addition to potentially being outdated, those age-at-maturity data are from summer samples for which maturity was evaluated macroscopically and was not confirmed with histological examination. These maturity data were also categorized by fish length, the values of which were later converted to ages for stock assessments, introducing further error through the use of an age–length key.

The sablefish is a batch spawner with group synchronous oocyte development and determinate fecundity. This species spawns during the winter or early spring in Alaska. Before this period, immature fish can be unambiguously distinguished from fish that will spawn, and total fecundity can be calculated. During the summer, gonads may be resting and may not show obvious signs that sablefish will spawn in the coming winter; therefore, fish that will skip spawning are difficult to distinguish from fish that will spawn if they are sampled during the summer. If maturity is consistently misclassified when summer samples are used, then estimates of maturity at age can be biased. Skipped spawning has not been documented in sablefish, but skipped spawning rates that have been observed in other species have ranged from 9% to 86% (Secor, 2008).

Since 1996, maturity classifications and age data have been collected during the annual summer longline surveys conducted by the NOAA Alaska Fisheries Science Center (AFSC) in Alaska to sample the slope of the Gulf of Alaska, the eastern Bering Sea, and the Aleutian Islands from the end of May through the end of August. Approximately 1000 females are assessed for maturity each year, and about 600 of them are aged. These data have not been incorporated into estimates of age at maturity for stock assessment, but they continue to be collected annually. Until our work occurred, there had been no studies of sablefish maturity in winter to compare with the estimates of age at maturity in summer, and there are no estimates of fecundity for sablefish in Alaska.

There were multiple objectives for this study. The first objective was to estimate the age at maturity for prespawning female sablefish caught near the epicenter of their distribution in Alaska and to determine whether females reproduce annually. The second objective was to compare estimates of age at maturity based on histological data from samples collected in winter with estimates of age at maturity based on macroscopic examination of samples collected in summer. The third objective was to determine whether SSB is proportional to fecundity, as is assumed in the population models for sablefish.

Materials and methods

Winter sampling

The study area was located off Kodiak Island in the Gulf of Alaska between latitudes 59°03′ and 56°30′N and longitudes 148°26′ and 154°35′E. A commercial trawl vessel, the FV *Gold Rush*, was chartered to conduct 10 days of fishing beginning 12 December 2011, a period that was estimated to be within the prespawning period for sablefish. To locate specimens for the full range of ages and lengths of mature and immature females, trawling operations were planned for sampling over a wide range of depths and topography, including the continental slope (depths of 500–700 m) and the shelf (depths shallower than 300 m), which included bays, gullies, and troughs. Locations were chosen on the basis of catches from commercial fisheries and AFSC bottom trawl surveys. Because of inclement weather, only 4 tows were conducted on the slope, whereas 37 tows were completed on the shelf.

Maturity samples were collected on the basis of a length-stratified sampling design in which up to 7 sablefish were sampled for each centimeter of total length. Each specimen was weighed with the stomach evacuated, and the sagittal otoliths were collected for aging. Both ovaries were excised and weighed. Ovaries were preserved in 10% formalin. Personnel of the AFSC Age and Growth Program aged otoliths by using standard validated methods (Fargo and Chilton, 1987; Kimura and Anderl, 2005; Kimura et al., 2007).

Maturity classification during winter

We prepared histological samples from the posterior region of the ovaries for all fish sampled. In addition, for a subsample of specimens representing a range of ovary sizes, the consistency of oocyte development within the ovaries was assessed by using sections from the medial and anterior areas of one ovary and from the posterior section of both ovaries. In another subsample of fish, posterior sections were taken from both ovaries.

[1] Fissel, B. M. Dalton, R. Felthoven, B. Garber-Yonts, A. Haynie, A. Himes-Cornell, S. Kasperski, J. Lee, D. Lew, L. Pfeiffer, J. Sepez, and C. Seung. 2012. Stock assessment and fishery evaluation report for the groundfish fisheries of the Gulf of Alaska and Bering Sea/Aleutian Islands area: economic status of the groundfish fisheries off Alaska, 2011, 299. Alaska Fish. Sci. Cent., Natl. Mar. Fish. Serv., NOAA, Seattle, WA. [Available at website, accessed July 2014.]

[2] Hanselman D. H., C. R. Lunsford, and C. J. Rodgveller. 2013. Assessment of the sablefish stock in Alaska. *In* Stock assessment and fishery evaluation report for the groundfish resources of the Gulf of Alaska, p. 267–376. North Pacific Fishery Management Council, Anchorage, AK. [Available at website, accessed July 2014.]

Table 1

Microscopic (histological) and macroscopic (visual) descriptions of oocyte stage and ovarian maturity of female sablefish (*Anoplopoma fimbria*) sampled before spawning in the central Gulf of Alaska during December 2011. For the histological classification of ovarian maturity, the most advanced stage of oocytes present is described followed by the maturity stage of the ovary. The stages that were observed are marked with an X.

Structures defining maturity	Oocyte stage	Maturity	Observed
Microscopic classification of ovarian maturity			
Oocytes with multiple nucleoli or perinucleolar; thin ovarian wall.	Primary growth	Immature	X
Oocytes with multiple nucleoli or perinucleolar; thick ovary wall; thick stroma; blood vessels present.	Primary growth	Mature; skipped spawning	X
Yolk accumulated within eosinophylic spheres (vitellogenesis).	Secondary growth	Mature	X
Yolk spheres have coalesced and yolk has fused.	Oocyte maturation	Mature	X
Ovulatory follicles remain in the ovary after ovulation.	Postovulatory follicle	Mature	
Macroscopic classification of ovarian maturity			
Ovaries thin and tubular; no oocytes visible.		Immature	X
Ovaries tubular in shape, contain transparent oocytes, which appear indistinct through ovary wall.		Immature	
Ova opaque, white, and clearly discernible through the distended, transparent ovary wall.		Mature	X
Ovaries engorged with free-flowing, translucent eggs.		Mature; spawning	X
Ovaries large, flaccid, and may be bloodshot.		Spent	
Ovary small, flaccid; oocytes not discernible.		Mature; skipped spawning	X

Ovarian tissues were embedded in paraffin, sectioned at 5–6 µm, stained with hematoxylin, and counterstained with eosin.

Histological slides were examined microscopically by 2 readers, and maturity was classified according to the most advanced ooctye stage or structure contained in the ovary, as well as other features (Table 1) (e.g., Hunter et al., 1992; Stark, 2007). Ovaries with primary growth oocytes as the most advanced stage were classified as immature. However, if ovaries had 1) primary growth oocytes accompanied by a thick stroma and structural reorganization (loose structure of oocytes with tissue surrounding oocytes), 2) blood vessels within the lamellae, and 3) a thick tunica (ovarian wall), the ovaries were classified as resting. Because sampling was conducted immediately before spawning, fish with resting ovaries were classified as fish that would skip spawning in the current spawning season. The presence of thick tunica and stroma before the spawning period has been used as criteria for identifying skipped spawning in multiple fish species, including winter flounder (*Pseudopleuronectes americanus* [Burton and Idler, 1984]) and Atlantic cod (e.g., Burton et al., 1997; Rideout et al., 2000, 2005; Rideout and Tomkiewicz, 2011). Mature females that had vitellogenic oocytes, hydrated oocytes, or postovulatory follicles were characterized as females that were expected to spawn in the current spawning season. Ovarian wall widths were measured on images taken from the slides used for histological examination. Five measurements were taken and averaged for each fish.

Macroscopic determination of maturity during summer

Macroscopic determination of maturity has been completed and accompanying otoliths have been collected for aging annually since 1996 during AFSC summer longline surveys, which are conducted from the end of May through the end of August. Sampling stations are spaced systematically 35–55 km apart along the continental slope of the Gulf of Alaska, the eastern Bering Sea, and the Aleutian Islands (Sasaki, 1985). At each station in the Gulf of Alaska, 7200 hooks are set. For this study, we examined only samples collected in the central Gulf of Alaska (17 stations) for comparison with samples collected during the winter survey. The fish were collected by using a random, systematic method so that samples were taken from all depth strata (100–200-m intervals from depths of 200–1000 m).

During the summer, fish are classified as immature, or juvenile, if ovaries are string-like or are slightly enlarged and are clear or pink and contain no visible oo-

cytes. They are considered mature if ovaries are large, are turning white but still may have a pinkish hue, and veins are developing. For ovaries classified as mature, small oocytes are sometimes discernible and are firmly attached to the tissue. Fish are spawning if eggs are loose or extruding, and they are considered to be resting, or spent, if ovaries are flaccid; spent or resting ovaries may also have a dark coloration. Interpretation of these various stages involves some subjectivity, but technicians are trained to standardize their interpretation of juvenile and mature ovaries.

Estimation of age at maturity

Age at maturity of female sablefish, for both the histologically analyzed winter samples and the visually analyzed summer samples, was modeled with a logistic function. The 2-parameter logistic function is given by the following equation:

$$\hat{p}_a = 1/(1+e^{-\delta(a-a_{50\%})}), \quad (1)$$

where $\hat{p}_a$ = the estimate of the proportion of mature fish at age;
δ = the parameter that describes the slope (the speed at which maturity approaches 100%); and
$a_{50\%}$ = the parameter that describes the age at which 50% of the fish are mature.

The observed proportion at age was calculated as

$$p_a = \frac{m_a}{n_a}, \quad (2)$$

where m_a = the number of mature fish observed at age a; and
n_a = the total number of fish at age a.

We used the binomial likelihood to fit the observed proportion of mature fish at age with the logistic model given in equation 1 in AD Model Builder.[3] vers. 11.2 (Fournier et al., 2012), with an additional penalty that accounted for maturity at age 0 being 0%.

Age at maturity was estimated for the winter samples in 2 ways: 1) fish that would skip spawning were classified as mature, and 2) they were classified as immature. In actuality, fish that would skip spawning are not immature but have spawned in the past. In the determination of maturity during all previous collections of sablefish in Alaska, fish that would skip spawning were either not distinguished from immature fish or could have been considered mature. For comparison with these data sets, we ran maturity-at-age models with the winter data in which sablefish that would skip spawning were classified as either immature or mature.

Age at maturity was analyzed for all samples pooled and stratified by area, shelf (depths less than 300 m), and slope (depths of 500–700 m), to identify possible differences between these habitats. To examine the relationship between age and skipped spawning the proportion of fish that would skip spawning, by age, was examined for the shelf, where fish that would skip spawning were much more common; ages for which there was only one sample were excluded from this analysis.

Biomass and reference points for target fishing

Several logistic maturity models were used within the age-structured population model currently used for sablefish in Alaska for determining SSB (Hanselman et al.[2]): these included the logistic model fit to the age-at-maturity data from the trawl survey conducted in the winter of 2011, the summer longline survey conducted in 2011, the mean fit to all data from annual summer longline surveys, and the maturity curve currently used in stock assessment.

A time series of female SSB was estimated when each maturity curve was input into the sablefish population model. In short, SSB is calculated in the assessment model with the age structure of the population and the age-at-maturity curve (see Hanselman et al.[2]). In addition, $F_{40\%}$, the fishing rate that reduces SSB per recruit (lifetime egg production) to 40% of the unfished level, was estimated, for the most current year in the time series, when each of the 4 maturity curves was used to determine SSB in the sablefish population model.

Fecundity

Ovaries were chosen for estimation of fecundity if they had advanced vitellogenic oocytes and if no postovulatory follicles were identified in histological cross sections; postovulatory follicles would indicate that partial spawning had occurred. In ovaries with these features an advanced (mature) cohort of oocytes was clearly separable from the early developing (immature) cohort on the basis of oocyte size and appearance, as described for sablefish by Mason et al. (1983) and Hunter et al. (1989). This clear separation indicates that sablefish have determinate fecundity, in which there is only one cohort of maturing oocytes within a spawning season. Fecundity was measured with the gravimetric method (Murua et al., 2003), whereby a subsample of mature oocytes is weighed and the number of oocytes is counted. The number of eggs per gram in the subsample is multiplied by the ovary weight to obtain a total fecundity. Samples were taken from the anterior, middle, and posterior sections of both ovaries, and the 6 measurements were averaged to estimate overall fecundity.

As ovaries develop, oocytes enlarge and the number of oocytes per gram of sample weight decreases. Such a decrease will not affect estimates of fecundity unless the decrease is caused by a loss of oocytes through batch spawning or atresia. To confirm that spawning had not commenced, a linear regression of oocytes per gram of subsample weight and fecundity was computed

[3] Mention of trade names or commercial companies is for identification purposes only and does not imply endorsement by the National Marine Fisheries Service, NOAA.

and histological slides were examined for postovulatory follicles. Determinations of any oocyte loss due to atresia were done by examination of histological slides. The number of oocytes per gram was also compared for 2 categories of mature fish: younger (age <12 years) and older (age ≥12 years) fish. Age 12 is approximately the age at which female sablefish were 100% mature in most maturity curves in our study. Differing values of the number of eggs per gram of sample weight would indicate a larger egg size for one age group. Additionally, the relationship between relative fecundity (the number of mature oocytes per gram of ovary-free fish weight) and age was examined for indications that relative reproductive output changes with increasing age.

Gonad weight in relation to body weight (gonadosomatic index [GSI], gonad weight/body weight×10) of fish that would skip spawning, as well as spawning and immature fish was determined to see if it could be used to predict spawning status during the winter.

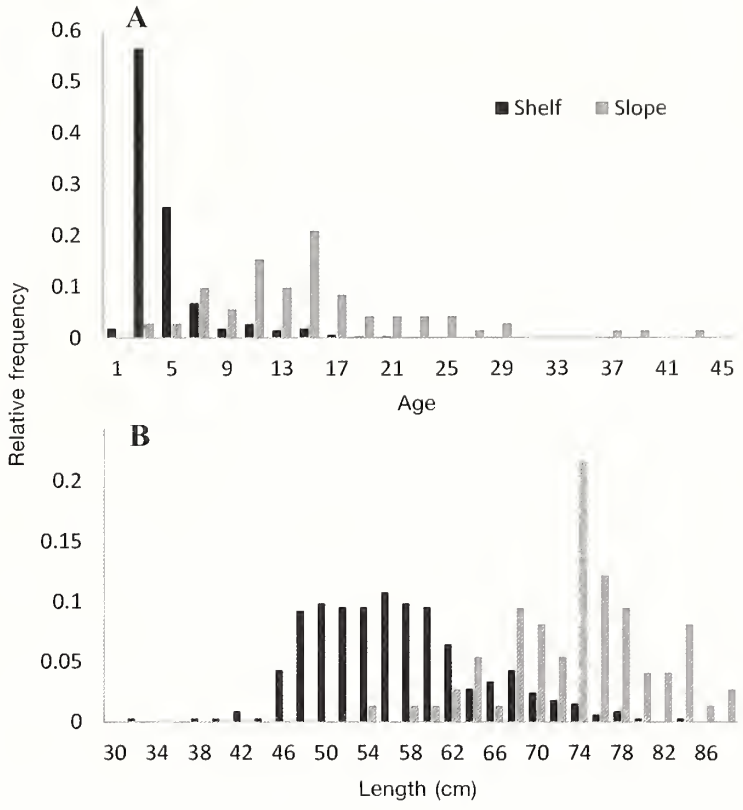

Figure 1

The frequency (in numbers) of female sablefish (*Anoplopoma fimbria*) sampled in December 2011 on the continental shelf or slope in the central Gulf of Alaska, by (**A**) age and (**B**) length.

Results

Distribution of fish on shelf and slope

Because of weather, sampling in the winter of 2011 was restricted primarily to the shelf; there were 37 tows on the shelf and 4 tows on the slope. In total, 393 female sablefish were sampled: 320 on the shelf and 73 on the slope. The majority of fish from the shelf were smaller and younger than those sampled on the slope (Fig. 1). The average total length of fish was 628 mm on the shelf and 747 mm on the slope. Of the samples from the shelf, 90% (290 of 320) were age 1–7; 15% (11 of 73) of the samples taken on the slope were age 2–7, and no age-1 fish were collected on the slope.

Maturity classification for fish sampled during the winter

Ovarian development was uniform throughout both ovaries for individual fish. Oocyte stages were consistent within the 33 specimens that were assessed at 3 regions in both ovaries. Development of both ovaries was the same in the 188 specimens for which samples were taken from the posterior end of both ovaries. Immature gonads contained only primary growth oocytes and macroscopically looked thin and tubular and had a pinkish hue. Gonads were easily determined to be mature on the basis of the presence of mature, advanced vitellogenic oocytes (Table 1). Without the aid of histological examination, it could be seen that these ovaries were engorged with white, opaque oocytes (Table 1). The cortical alveoli stage was absent from all ovaries.

The second category of mature fish was composed of fish that would skip spawning. These fish had a much thicker tunica than immature fish and sometimes contained atretic primary growth oocytes that had mean wall width of 35 μm (95% confidence intervals [CI] 30–41) for immature fish and of 318 μm (95% CI 267–370) for fish that would skip spawning (Fig. 2). They also had thick stroma and blood vessels in the lamellae between oocytes, whereas immature ovaries had tightly packed oocytes with little tissue in between. These characteristics indicated that sablefish exhibit the resting type of skipped spawning, in which vitellogenic oocytes are not produced. Macroscopically, fish that would skip spawning had small ovaries, more similar in size to an immature ovary than to an ovary with yolked oocytes, but they were more flaccid than immature ovaries and had a red coloration. Without adequate experience, or the aid of histological examination, fish that would skip spawning could be mistaken easily for immature fish.

Of 110 mature fish, 23 fish (21%) were fish that would skip spawning (here, the number of mature fish

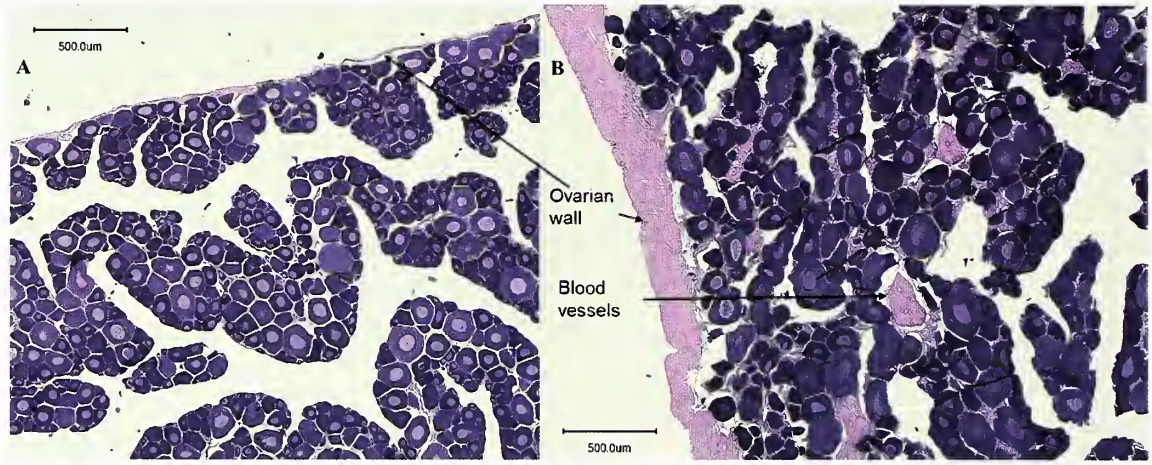

Figure 2

Histological preparations of thin sections of ovaries from sablefish (*Anoplopoma fimbria*) sampled in the central Gulf of Alaska in December 2011. (**A**) An ovarian section from an immature fish that has a thin ovarian wall and thin lamellae without blood vessels. (**B**) An ovarian section from a fish that will skip spawning and has a thicker ovarian wall, thicker lamellae that surround the oocytes, and many blood vessels. In both specimens, there are no maturing, vitellogenic oocytes.

was the sum of the numbers of those that would skip spawning and fish that would spawn in the current season). The great majority of those that would skip spawning (20 out of 23, 87%) were caught on the shelf, specifically in troughs at stations adjacent to the slope. Most of the fish on the slope were mature (fish that would either spawn or skip spawning, 90%), but only 4.5% of mature fish were fish that would skip spawning (3 of 63). Only 14% of the fish on the shelf were mature and 43% of these mature fish (19 out of 44) were fish that would skip spawning. Skipped spawning was observed in fish ranging in age from 4 to 17 years, although sample sizes for fish (both mature and immature) >17 years of age were often limited to 1 or 2 fish. There was a significant, positive correlation between age and the proportion of mature fish that would skip spawning on the shelf, where the great majority of those that would skip spawning were found (Fig. 3). For that analysis, only fish that were age 4 and older were included, because that age was the first age at which skipped spawning was observed; in addition, only those ages that had a sample size of at least 2 fish were included (ages 4–15) (Fig. 3).

Age at maturity

The age at maturity of sablefish on the shelf when fish that would skip spawning were classified as mature was dramatically different from the age at maturity when fish that would skip spawning were classified as immature (Fig. 4A). The 95% CI of each maturity curve did not encompass the other curve. Classifying fish that would skip spawning as mature increased the proportion of fish mature at age. On the slope, age at maturity was also higher when fish that would skip spawning were classified as mature; however, there was not a significant difference (Fig. 4B). The large CIs for slope data can be at least partially attributed to smaller sample sizes.

As with maturity data collected on the shelf, the age at maturity of the pooled samples was significantly different when fish that would skip spawning were classified as mature as opposed to immature (Fig. 4C, solid lines). The $a_{50\%}$ was 6.8 years when fish that would skip spawning were classified as mature, compared with 9.9 years when they were classified as immature (Fig. 4C, solid lines). When fish that would skip spawning were classified as immature, ages at maturity on the slope and shelf were different. Pooled age at maturity was intermediate between the slope and shelf (Fig. 4C, gray lines). When fish that would skip spawning were classified as mature, age at maturity on the shelf and slope matched closely (Fig. 4C, black lines). The similarity between the 2 age-at-maturity curves indicates that fish in both habitats are mature at the same age but that the majority of fish that would skip spawning reside on the shelf, at least during winter. When fish that would skip spawning were classified as either mature or immature, the pooled data were closer in value to the shelf data because there were more samples on the shelf.

The logistic model fits to the age-at-maturity data from AFSC annual summer longline surveys were variable; $a_{50\%}$ ranged from 5.5 to 8.6 years and the slope parameters ranged from 0.6 to 1.3 (Fig. 5A). In the winter survey, the proportion of mature fish at age was

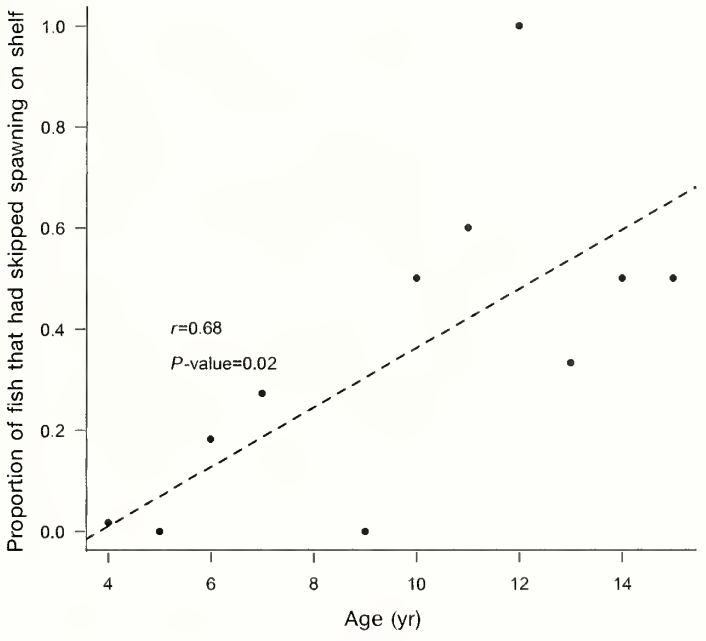

Figure 3

Proportion of mature female sablefish (*Anoplopoma fimbria*) by age that would skip spawning on the continental shelf in the central Gulf of Alaska in December 2011. Immature fish are not included. The great majority of fish that would skip spawning were found on the shelf. The correlation coefficient (r) with its associated P-value is also provided.

more similar to the proportion in the annual summer longline surveys, when fish that would skip spawning were classified as mature, than when they were classified as immature (Fig. 5A). When fish that would skip spawning were classified as mature (Fig. 5A, black line), the annual estimates of maturity from the summer longline surveys were similar to the estimates from the winter survey at moderate ages (Fig. 5A). At younger ages, the annual estimates of the proportion of mature fish from summer surveys were higher than the estimates from the winter survey; conversely, at older ages, the proportion of mature fish was lower in estimates from the summer survey. When fish that would skip spawning were classified as immature in the winter survey (Fig. 5A, gray line), the estimated proportions of mature fish at each age from the summer surveys were discernibly higher in all years (Fig. 5A).

The logistic curve fitted to samples taken during the summer of 2011, the year in which the winter survey occurred, was intermediate between the curves from the winter where fish that would skip spawning were classified as mature and the curve where fish that would skip spawning were classified as immature, and the fit was dissimilar to both, especially at moderate ages (Fig. 5B, Table 2). The $a_{50\%}$ was 6.8 years in the winter when fish that would skip spawning were classified as mature, 8.0 years for samples collected during the summer, and 9.9 years in the winter when fish that would skip spawning were classified as immature. Unlike the majority of curves based on data from the annual summer longline surveys, estimates of the proportion of mature fish in the summer of 2011 were very similar to those from the winter at young ages (Fig. 5B). The difference in the curves based on data from the winter and summer surveys conducted in 2011 can be attributed more to a difference in $a_{50\%}$ than to a difference in slope.

The estimates of maturity at age currently used in the stock assessment for sablefish in Alaska, determined from samples taken during the summer in the early 1980s, were higher than the estimates from the winter survey at younger ages (6 years), when fish that would skip spawning were classified as mature (Fig. 5C), but were similar at older ages. The pooled maturity at age for fish captured during the summer longline surveys (from 1996 to 2012) was also higher at younger ages, but it was lower at older ages (Fig. 5C). This pattern can be attributed primarily to differing slopes (Table 2). This trend is the same one that was apparent in the majority of curves fitted to data from the annual summer longline surveys (Fig. 5A). The age-at-maturity values currently used in the stock assessment of sablefish in Alaska and the mean age at maturity from the annual summer longline surveys were much higher than the values from the winter survey, when fish that would skip spawning were classified as immature (Fig. 5C).

Biomass and target-fishing reference points

The estimates of SSB were similar when the Alaska sablefish population model was run with the maturity curve fitted to data from the winter survey conducted in 2011 (when fish that would skip spawning were classified as mature), the mean age at maturity across all summer longline surveys, or the maturity curve currently used in stock assessment (base model) (Fig. 5). Estimates of SSB were lower when maturity data were used from the summer longline survey conducted in 2011, and lowest when data were used from the winter survey conducted in 2011 and fish that would skip spawning were classified as immature (Fig. 6). Compared with the base model, the maturity curves based on data from winter and summer 2011 caused larger dips in SSB in years when model projections included large recruitment. The dips in SSB occurred because these maturity curves had lower estimates for the proportion of mature fish at young ages, and such low proportions translate to fewer mature fish when there are more young fish

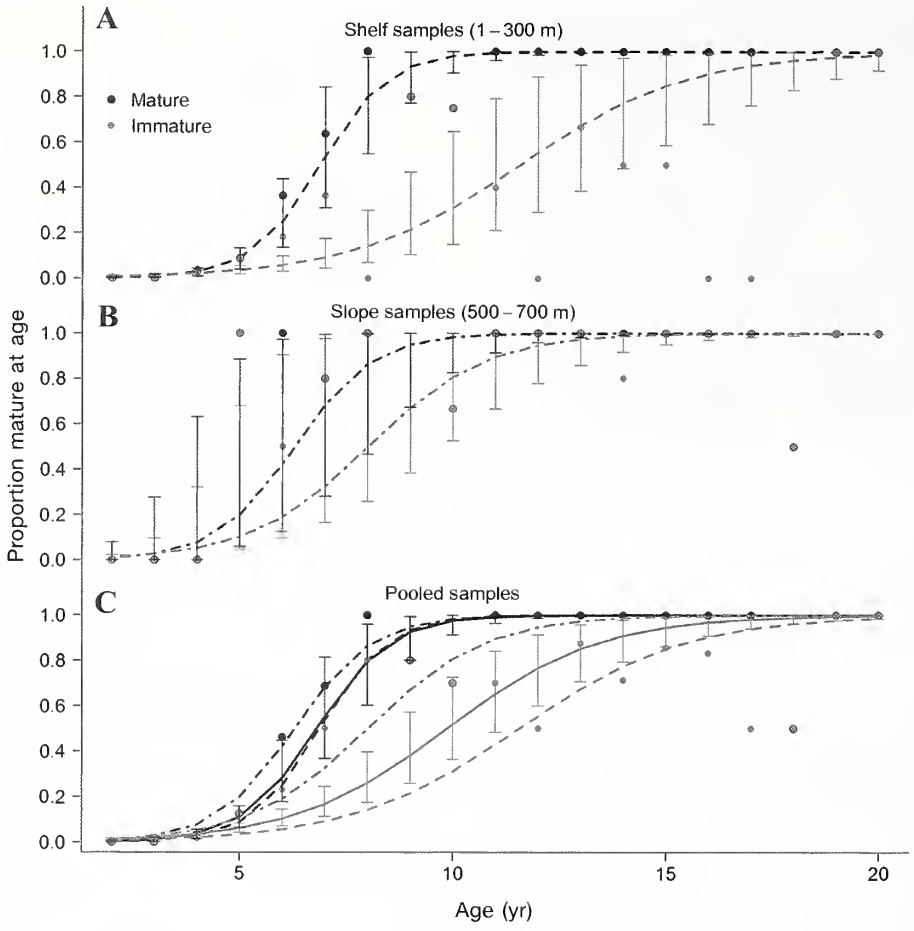

Figure 4

Observed and estimated maturity at age of female sablefish (*Anoplopoma fimbria*) collected in the winter of December 2011 on the (**A**) continental shelf, (**B**) slope, or (**C**) both shelf and slope (pooled). Fish that would skip spawning were classified as either mature (black points and lines) or immature (gray points and lines). Larger, gray points indicate that data did not differ at that age because there were no fish that were going to skip spawning. Logistic regression models and 95% confidence intervals at each age are presented. In panel C, solid lines indicate the age at maturity for the pooled samples. The maturity curves (dashed lines) for the shelf and slope, from panels A and B respectively, are also included in panel C for a comparison with pooled data. The *x*-axis was truncated at age 20 because the proportion mature at ages older than 20 all remained at 100% and had increasingly small confidence intervals.

in the population. The $F_{40\%}$ in the most recent year (2013) followed the same pattern: the value from the base model, the mean of summer longline surveys, and value from the winter survey (when SS were classified as mature) were similar: 9.40%, 9.45%, and 9.30%, respectively. The data from the summer longline survey conducted in 2011 provided a lower estimate (8.45%), and the estimate from the winter survey (when fish that would skip spawning were classified as immature) was the lowest (7.45%). A lower $F_{40\%}$ translates to more conservative management and lower allowable catches.

Fecundity

Fecundity was calculated for 47 sablefish. Total fecundity, measured as the total number of oocytes per fish that will be spawned in the current season, ranged from 214,577 to 900,700. There was no evidence of batch spawning (postovulatory follicles) or atresia in any ovaries containing maturing, vitellogenic oocytes. The mean number of oocytes per gram of sample weight was significantly higher for younger fish (ages <12), with a mean of 10,667 (standard error [SE] 467) than for older fish (ages ≥12), with a mean of 8804 (SE

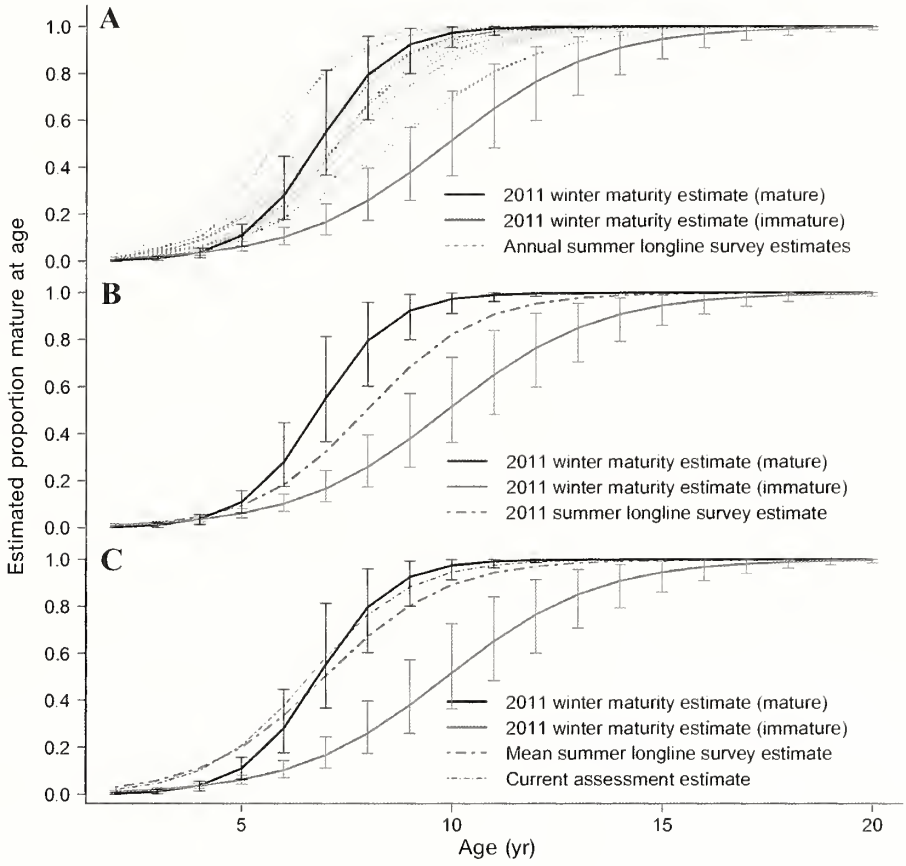

Figure 5

Logistic regression model fitted to the proportion of female sablefish (*Anoplopoma fimbria*) mature at age based on data from a survey conducted in winter (December 2011) (all graphs), (**A**) on data from annual summer longline surveys conducted by the NOAA Alaska Fisheries Science Center in 1996–2012, (**B**) on the maturity-at-age data currently used in the Alaska sablefish stock assessment, and (**C**) on the mean maturity at age data collected from annual summer longline surveys (mean of annual estimates in panel A). Graph B provides a comparison of data collected in surveys conducted in summer with data collected in winter 2011. Fish that would skip spawning were classified as either mature or immature and were identified only in the winter.

231) (t-test assuming unequal variance: P=0.001), indicating that, on average, younger fish have smaller maturing oocytes. The range in number of eggs per gram of sample weight was greater for younger fish than for older fish.

The relationship between relative fecundity and age was not significant. Very little of the variation in fecundity was explained by age (coefficient of determination [r^2]=0.02), and the regression was not significant (slope: −0.49, P=0.37; intercept=123). Relative fecundity ranged from 66 to 205 per gram.

The GSI of fish that would spawn (mean=7.361, 95% lower confidence interval [LCI]=6.908, 95% upper confidence interval [UCI]=7.814) was much higher than the GSI of fish that would skip spawning (mean=1.064, 95% LCI=0.936, 95% UCI=1.191) and of immature fish (mean=0.486, 95% LCI=0.471, 95% UCI=0.502). Fish that would skip spawning had a higher GSI than immature fish (there was no overlap of the 95% CIs), although there was some overlap in the raw data (skipped spawning range=0.486–1.659; immature range=0.145–1.110)

Discussion

We found that the logistic models that were fitted to the pooled age-at-maturity data collected during summer longline surveys and to the data currently used in the stock assessment, also collected during the summer, were similar to the maturity curve from the winter data, when fish that would skip spawning were

Table 2

Slope and age at 50% maturity ($a_{50\%}$) determined from logistic models of age at maturity for female sablefish (*Anoplopoma fimbria*) sampled before spawning during winter (in December 2011) in the central Gulf of Alaska, during summer (May–August), 1996–2012, in the central Gulf of Alaska, and during the summer, 1978–1983, in the Gulf of Alaska. For the winter surveys, fish that would skip spawning were classified as either mature (m) or immature (i). Fish that would skip spawning were not looked for in the summer.

Survey	Year	Slope	a_{50}
Winter (m)	2011	1.14	6.77
Winter (i)	2011	0.56	9.88
Summer	2011	0.76	7.97
Current assessment	1978–1983	0.84	6.60
Mean (summer longline survey)	1996–2012	0.70	6.98
Range (summer longline survey range)	1996–2012	0.60–1.30	5.5–8.6

classified as mature. Additionally, the $a_{50\%}$ parameters of these logistic models (ranging from 6.60 to 6.98 years) were very similar to recent estimates of age at maturity from the U.S. West Coast that were based on histological findings (6.86 years) (Head et al., 2014). It is unknown if any fish that would skip spawning were sampled in those studies. In our study, the small differences in the maturity curves at young ages caused differences in estimates of female SSB when there were larger than average recruitment classes (see Hanselman et al. [2] for a time series of recruitment). A lower SSB translated to lower fishing rates ($F_{40\%}$). Compared with data that are currently used in the assessment, the data from the surveys conducted in winter 2011 provided a slightly lower $F_{40\%}$ when fish that would skip spawning were classified as mature (0.18%) and an $F_{40\%}$ that was 1.95% lower when these fish were classified as immature. A similar situation has been reported for Atlantic cod, where an overestimation of egg production, by 8–41%, resulted from not accounting for fish that had skipped spawning (Rideout and Rose, 2006). For both species this reduction in SSB should result in a lower allowable biological catch.

For all maturity curves in this study, we used the standard model (i.e., a logistic function with asymptote at 100%). The standard model was chosen because it illustrates how differences in age at maturity would impact sablefish management if current methods were used. Although we found that skipped spawning increases with age, our data do not necessarily negate the use of the standard logistic model. The standard model still could be applicable because the increase in skipped spawning occurred at younger ages (4–15), the logistic curves reached 100% around age 12 (close to age 15), and fish commonly reach ages >50. There are many potential methods for incorporating the loss in reproductive output due to skipped spawning depending on how skipped spawning is related to age, the longevity of the species of interest, and the annual or spatial variability in skipped spawning (e.g., Secor, 2008; Brooks, 2013). As more data on the consistency of skipped spawning in the sablefish population in Alaska become available, a complete evaluation of alternative methods for incorporating skipped spawning into the assessment is warranted.

The most direct comparison of estimates of age at maturity for summer and winter was between the samples collected in the winter and summer of 2011. The data from summer 2011 provided estimates of the proportion of mature fish at age that were similar to the values based on data from the winter survey for fish at young ages (≤5 years) and that were intermediate between the 2 winter curves for fish at ages 5–13 years. Use of the maturity curve based on data from summer 2011, therefore, produced estimates of SSB, and $F_{40\%}$ that were also intermediate. It is possible that during the summer some fish that would skip spawning during the upcoming winter were classified as mature and some as immature, and that is why the resulting summer curve was intermediate. It is also possible that fewer fish that would skip spawning were encountered during the summer surveys. The winter survey covered areas on the shelf that were not covered by the summer longline survey in 2011, and the shelf was the area where the majority of these fish were found in the winter. More winter sampling is needed for comparison of winter data with summer data to determine whether the difference we saw in data for 2011 is consistent over time.

It is important to note that we pooled samples from the shelf and slope to produce an overall maturity curve. To test for any bias due to disproportionate sampling in relation to the distribution of the population, we weighted our calculations according to the abundance of fish in each area; abundance values were calculated with data from AFSC bottom trawl surveys conducted in summer. There was little difference between the values from these calculations and the unweighted results, indicating that our results are reflective of the population in Alaska as a whole.

Movement and habitat use during the spawning season have been reported to indicate whether a fish is spawning or has skipped spawning for Pacific halibut (Loher and Seitz, 2008) and Atlantic cod (Hüssy et al., 2009; Jónsdóttir et al., 2014). Sablefish are highly migratory throughout their lives; in Alaska, 11% of tagged fish have been recovered at locations more than 2000 km from their release sites (Echave et al., 2013). However, preliminary data from tagging sablefish during the winter survey in 2011 indicate that sablefish do

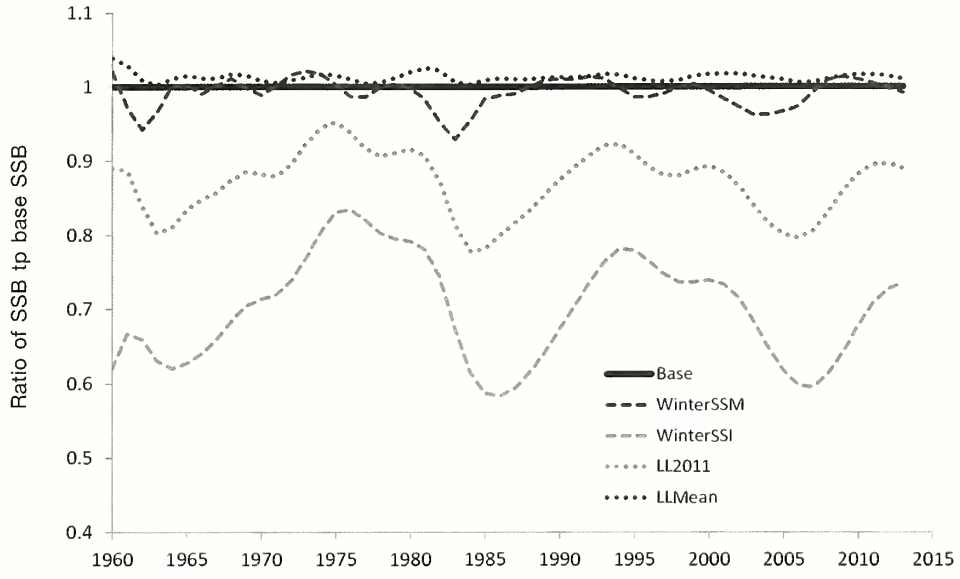

Figure 6

Ratio of the estimates of spawning stock biomass (SSB) when different female maturity curves were incorporated into the population model for sablefish (*Anoplopoma fimbria*) in Alaska in relation to the SSB when maturity data currently used in the stock assessment of sablefish (base SSB) are used. The maturity curves used in the model included data collected in winter 2011 when fish that would skip spawning were classified as mature (WinterSSM), in winter 2011 when fish that would skip spawning were classified as immature (WinterSSI), in 2011 during the annual summer longline survey conducted by the NOAA Alaska Fisheries Science Center (AFSC) (LL2011), and the mean of data collected during AFSC annual summer longline surveys, 1996–2012.

not move large distances during the spawning season. During the winter survey, we deployed popoff satellite tags on 4 fish >850 mm in fork length. We assumed that the tagged fish were female because, in summer longline surveys, only 0.5% of fish >850 mm in fork length have been male. Tags were preprogrammed to pop off fish within the current spawning season (35–52 days after release), and the geolocation of a tag was recorded when it was released from a fish. The 2 fish that were released where they were caught on the shelf remained within 1 km of their tagging location, and the 2 fish that were captured on the slope but released 75 km away on the shelf moved to locations in the vicinity of their capture site (within 0.5 km or 9 km).

As with Pacific halibut and Atlantic cod, habitat use by sablefish during the spawning season may be related to spawning. Data on sablefish movement in the winter is greatly lacking because there are no surveys or directed fisheries in the winter. The use of popoff satellite tags enables research on movement to occur during this period. Future research on habitat use and movement related to spawning of sablefish is badly needed both for identifying spawning areas and for tracking the movement of fish that skipped spawning and those that spawned.

Rates of skipped spawning are highly variable among species; a range from 9% to 86% has been reported in 21 freshwater and marine species (reviewed in Secor, 2008). Rates are higher for species that have to make large-scale, energetically costly migrations because fish that skip spawning can forgo these migrations. Skipped spawning rates are also hypothesized to be higher for long-lived species because they have the ability to skip spawning to increase their survival and growth and, thereby, to maximize their lifetime reproductive output (Rideout et al., 2005). For example, sturgeons (Acipenseridae), Pacific halibut, and Atlantic cod are long-lived fish that make large-scale spawning migrations and have skipped spawning rates of 10–86% (Loher and Seitz, 2008; Skjæraasen et al., 2012; Kuhajda, 2014). Sablefish move long distances during their lives, but it is unknown whether their movements are related to spawning. However, they are long-lived and have a maximum age similar to that of other species that skip spawning.

Skipped spawning is related to energy reserves (i.e., relative liver weight) and body condition (the ratio of body weight to length) for Atlantic cod, and rates of skipped spawning can vary by year (Skjæraasen et al., 2009; Skjæraasen et al., 2012). Both of these factors

indicate that skipped spawning rates may be related to annual environmental conditions and that skipped spawning should be monitored in the future before any conclusions are made on rates in the Alaska population of sablefish. Measurements of relative liver size during the summer may be a good indicator of whether a sablefish will spawn in the coming winter; relative liver size could prove to be a good alternative to histological analysis during the summer. We intend to explore the relationship between energy reserves, spawning, and egg production in the future by sampling both during summer longline surveys and during the winter prespawning period.

Maturity status determined during the summer may be reasonably close to that determined from observations made in the winter, but maturity values based on summer longline surveys are not as accurate. The variability we observed in the estimates from annual summer longline surveys may be attributed to sample size, subjectivity of maturity classification, or fluctuations in the age at maturity or skipped spawning. Inaccuracy in estimates from summer longline surveys could also be the result of survey timing; some fish macroscopically classified as immature during summer surveys may become visibly mature later in the fall and winter, closer to spawning. Another factor that may have caused inaccuracy in estimates is that examination for skipped spawning was not part of the sampling protocol on summer sampling cruises.

It is unknown when fish that would skip spawning stop progressing in development and become distinguishable from spawning fish. For example, in Atlantic cod, fish that would skip spawning could be distinguished histologically at approximately 3 months before spawning but not before (Skjæraasen et al., 2009). If sablefish have a similar development time, this period for distinguishing fish that would skip spawning would fall around October or November, a time that is several months after the end of the annual summer longline surveys. In the future, it will be important to determine the months when immature, skipped spawning, and prespawning sablefish can be differentiated from one another—in order to accurately classify maturity during portions of summer longline surveys, which extend from May through August. Because they exhibited the resting type of skipped spawning and never developed maturing oocytes, fish that will skip spawning can be identified by the absence of vitellogenic oocytes and a thick ovarian wall. Sablefish that will spawn may also have greater energy reserves before spawning; therefore, measurements of body condition and relative liver weight may be useful for predicting spawning (as seen in Atlantic cod, Skjæraasen et al., 2009; Skjæraasen et al., 2012).

The GSI of fish that would skip spawning and immature fish were significantly different for sablefish in this study. The observation of such a difference may not be useful in other species; for example, GSI could not be used to separate skipped spawning and immature Atlantic cod (Skjæraasen et al., 2012). However, this measurement holds great promise for separating immature from skipped spawning sablefish. Although both of these maturity categories showed only early developing, immature oocytes, the additional tissue, such as stroma, blood vessels, and ovarian wall, that we found in the ovaries of fish that would skip spawning, is likely to contribute to the difference observed in GSI values. More data is needed on the GSI of fish that skip spawning to improve our confidence in the use of GSI as a tool for determining maturity.

Comparing the maturity data from the annual summer longline surveys conducted in the Gulf of Alaska, the Aleutian Islands, and the eastern Bering Sea would be beneficial because each fixed station is sampled on the same date each year. Differences in estimates of age at maturity for sablefish from these areas may be a function of the phase of the reproductive cycle when fish were collected. For example, the Bering Sea is sampled in early June, whereas the western Gulf of Alaska is sampled in late August. Ovaries sampled in late August will be more developed and are likely to result in different estimates of age at maturity. Because of the bias that may be introduced as a result of sampling date, winter sampling in multiple areas also is needed to determine whether there is truly geographic variability in maturity at age and skipped spawning. Differences in the age and length at maturity have been documented in sablefish off the coast of the United States, south of Canada (Head et al., 2014); therefore, it will be important to consider geographic differences farther north in Alaska as well.

Our estimates of fecundity were similar to those for sablefish off California (Hunter et al., 1989), but they were higher than estimates from a study off of British Columbia, Canada (Mason et al., 1983). We compared the fecundity of females that were 700 mm in total length in our study with fecundity determined from other studies because this length is approximately the average female size in the longline fishery for sablefish in Alaska (Hanselman et al. [2]). The average fecundity for females 700 mm in total length was 412,000 eggs—a level that was very similar to an estimate from California of 416,000 eggs (Hunter et al., 1989) but more than double the estimate of 182,000 eggs from the British Columbia study (Mason et al., 1983). A microscopic examination of ovarian tissue samples for evidence of postovulatory follicles was not undertaken in the Canadian study; therefore, batch spawning may have occurred but was undetected. If batch spawning occurred, it would decrease the estimated total fecundity and would explain why other studies found higher estimates. Batch spawning was documented for sablefish off central California (Hunter et al., 1989) and likely also occurs in other geographic areas.

We found no significant relationship between relative fecundity and age. This verifies the assumption made in the Alaska sablefish population model that relative reproductive output is linearly related to female spawning biomass and does not change with age. There were few fish older than 25 years (3 fish out of

47) (sablefish maximum age is reported to be 94 years [Kimura et al. 1998]); data from older fish are needed to further test this model assumption.

Although the relative reproductive output did not increase with age, mature oocyte size did. Mature oocyte size could have increased with age because older females have more energy reserves for reproduction than have younger females. These energy reserves could be contributed to development of oocytes, and more energy put to that end would result in larger oocytes. If larger eggs in sablefish increase larval fitness, older females (≥12 years, the age at which almost 100% of fish are mature) may contribute more to the population than do younger females. For example, an increase in energy reserves and survival of larval black rockfish (*Sebastes melanops*) has been observed for offspring from older, larger females (Berkley et al., 2004). Alternatively, older females may initiate oocyte development earlier than younger sablefish and, therefore, have larger oocytes. Earlier development may also indicate an earlier spawning date for older females, as has been seen in other marine fish species (Stark, 2007; Wright and Trippel, 2009; Rodgveller et al., 2012). Mason's (1984) study of sablefish fecundity indirectly supports the hypothesis that older females spawn earlier than younger females. A decrease in relative fecundity with length could have been caused by an earlier spawning time of larger females. If larger females initiated maturation earlier than smaller females and had spawned at least 1 batch of eggs, the result would be a decrease in relative fecundity with length. Mason may have missed evidence of batch spawning in larger fish because there was no microscopic examination for classification of ovaries in that study.

Acknowledgments

We thank Captain B. Ashley and the crew of the chartered FV *Gold Rush*. We also thank our coworkers at NOAA's AFSC: S. Kotwicki; C. Conrath for logistics; D. Anderl for aging otoliths; G. Fleischer and P. Rigby for assistance with the vessel charter; and P. Rigby, J. Heifetz, and D. Hanselman for helpful reviews.

Literature cited

Berkeley, S. A., C. Chapman, and S. M. Sogard.
2004. Maternal age as a determinant of larval growth and survival in a marine fish, *Sebastes melanops*. Ecology 85:1258–1264.

Brooks, E. N.
2013. Effects of variable reproductive potential on reference points for fisheries management. Fish. Res. 138:152–158.

Burton, M. P. and D. R. Idler.
1984. The reproductive cycle in winter flounder, *Pseudopleuronectes americanus* (Walbaum). Can. J. Zool. 62:2563–2567.

Burton, M. P. M., R. M. Penney, and S. Biddiscombe.
1997. Time course of gametogenesis in Northwest Atlantic cod (*Gadus morhua*). Can. J. Fish. Aquat. Sci. 54(suppl. 1):122–131.

Echave, K., D. H. Hanselman, and N. E. Maloney.
2013. Report to industry on the Alaska sablefish tag program, 1972–2012. NOAA Tech. Memo. NMFS F/NWC-254, 47 p.

Fargo, J., and D. E. Chilton.
1987. Age validation for rock sole in Hecate Strait, British Columbia. Trans. Am. Fish. Soc. 116:776–778.

Fournier, D. A., H. J. Skaug, J. Ancheta, J. Ianelli, A. Magnusson, M. N. Maunder, A. Nielsen, and J. Sibert.
2012. AD Model Builder: using automatic differentiation for statistical inference of highly parameterized complex nonlinear models. bOptimiz. Methods Softw. 27:233–249.

Head, M. A., A. A. Keller, and M. Bradburn.
2014. Maturity and growth of sablefish, *Anoplopoma fimbria*, along the U.S. West Coast. Fish.Res. 159:56–67.

Hislop, J. R. G.
1988. The influence of maternal length and age on the size and weight of the eggs and the relative frequency of the haddock, *Melanogrammus aeglefinus*, in British waters. J. Fish Biol. 32:923–930.

Hunter, J. R., B. J. Macewicz, and C. A. Kimbrell.
1989. Fecundity and other aspects of the reproduction of sablefish, *Anoplopoma fimbria*, in central California waters. CalCOFI Rep. 30:61–72. [Available at website, accessed July 2014.]

Hunter, J. R., B. J. Macewicz, N. C.-H. Lo, and C. A. Kimbrell.
1992. Fecundity, spawning, and maturity of female Dover sole *Microstomus pacificus*, with an evaluation of assumptions and precision. Fish. Bull. 90:101–128.

Hüssy, K., B. Nielsen, H. Mosegaard, and L. W. Clausen.
2009. Using data storage tags to link otolith macro-structure in Baltic cod *Gadus morhua* with environmental conditions. Mar. Ecol. Prog. Ser. 378:161–170.

Jónsdóttir, I. G., V. Thorsteinsson, Ó. K. Pálsson, G. G. Tómasson, and C. Pampoulie.
2014. Evidence of spawning skippers in Atlantic cod from data storage tags. Fish. Res. 156:23–25.

Kimura, D. K., and D. M. Anderl.
2005. Quality control of age data at the Alaska Fisheries Science Center. Mar. Freshw. Res. 56:783–789.

Kimura, D. K., D. M. Anderi, and B. J. Goetz.
2007. Seasonal marginal growth on otoliths of seven Alaska groundfish species support the existence of annual patterns. Alaska Fish. Res. Bull. 12:243–251. [Available at website, accessed April 2015.]

Kimura, D. K., A. M. Shimada, and F. R. Shaw.
1998. Stock structure and movement of tagged sablefish, *Anoplopoma fimbria*, in offshore northeast Pacific waters and the effects of El Niño–Southern Oscillation on migration and growth. Fish. Bull. 96:462–481.

Kuhajda, B. R.
2014. Acipenseridae: Sturgeons. *In* Freshwater fishes of North America. Vol. 1: Petromyzontidae to Catastomidea (M. L. Warren Jr., and B. M. Burr, eds.), p 160–206. John Hopkins Univ. Press, Baltimore, MD.

Loher, T., and A. C. Seitz.
2008. Characterization of active spawning season and depth for eastern Pacific halibut (*Hippoglossus stenolepis*) and evidence of probable skipped spawning. J. Northwest Atl. Fish. Sci. 41:23–36.

Marshall, C. T., N. A. Yaragina, B. Ådlandsvik, and A. V. Dolgov.
2000. Reconstructing the stock-recruitment relationship for Northeast Arctic cod using bioenrgetic index of reproductive potential. Can. J. Fish. Aquat. Sci. 57:2433–2442.

Mason, J. C.
1984. On the fecundity of the sablefish (*Anoplopoma fimbria*) in Canadian waters. Can. Tech. Rep. Fish. Aquat. Sci. 1290, 17 p. [Available at website.]

Mason, J. C., R. J. Beamish, and G. A. McFarlane.
1983. Sexual maturity, fecundity, spawning, and early life history of sablefish (*Anoplopoma fimbria*) off the Pacific Coast of Canada. Can. J. Fish. Aquat. Sci. 40:2126–2134.

Murua, H., G. Kraus, F. Saborido-Rey, P. R. Witthames, A. Thorsen, and S. Junquera.
2003. Procedures to estimate fecundity of marine fish species in relation to their reproductive strategy. J. Northwest Atl. Fish. Sci. 33:33–54.

Rideout, R. M., M. P. M. Burton, and G. A. Rose.
2000. Observations on mass atresia and skipped spawning in northern Atlantic cod, from Smith Sound, Newfoundland. J. Fish Biol. 57:1429–1440.

Rideout, R. M., and G. A. Rose.
2006. Suppression of reproduction in Atlantic cod *Gadus morhua*. Mar. Ecol. Prog. Ser. 320:267–277.

Rideout, R. M., G. A. Rose, and M. P. M. Burton.
2005. Skipped spawning in female iteroparous fishes. Fish Fish. 6:50–72.

Rideout, R. M., and J. Tomkiewicz.
2011. Skipped spawning in fishes: More common than you think. Mar. Coast. Fish. 3:176–189.

Rodgveller, C. J., C. R. Lunsford, and J. T. Fujioka.
2012. Effects of maternal age and size on embryonic energy reserves, developmental timing, and fecundity in quillback rockfish (*Sebastes maliger*). Fish. Bull. 110:36–45.

Sasaki, T.
1985. Studies on the sablefish resources in the North Pacific Ocean. Bull. Far Seas Fish. Res. Lab. 22, 108 p.

Secor, D. H.
2008. Influence of skipped spawning and misspecified reproductive schedules of biological reference points in sustainable fisheries. Trans. Am. Fish. Soc. 137:782–789.

Skjæraasen, J. E., J. Kennedy, A. Thorsen, M. Fonn, B. N. Strand, I. Mayer, and O. S. Kjesbu.
2009. Mechanisms regulating oocyte recruitment and skipped spawning in Northeast Arctic cod (*Gadus morhua*). Can. J. Fish. Aquat. Sci. 66:1582–1596.

Skjæraasen, J. E., R. D. M., Nash, K. Korsbrekke, M. Fonn, T. Nilsen, J. Kennedy, K. H. Nedreaas, A. Thorson, P. R. Witthames, A. J. Geffen, H. Høie, and O. S. Kjesbu.
2012. Frequent skipped spawning in the world's largest cod population. Proc. Natl. Acad. Sci. 109:8995–8999.

Stark, J. W.
2007. Geographic and seasonal variations in maturation and growth of female Pacific cod (*Gadus macrocephalus*) in the Gulf of Alaska and Bering Sea. Fish. Bull. 105:396–407.

Wright, P. J, and E. A. Trippel.
2009. Fishery-induced demographic changes in the timing of spawning: consequences for the reproductive success. Fish Fish. 10:283–304.

NOAA
National Marine
Fisheries Service

Fishery Bulletin
established 1881

Spencer F. Baird
First U.S. Commissioner
of Fisheries and founder
of *Fishery Bulletin*

A passive acoustic survey of fish sound production at Riley's Hump within Tortugas South Ecological Reserve: implications regarding spawning and habitat use

James V. Locascio[1] (contact author)
Michael L. Burton[2]

Email address: locascio@mote.org

[1] Mote Marine Laboratory
1600 Ken Thompson Parkway
Sarasota, Florida 34236

[2] Beaufort Laboratory
Southeast Fisheries Science Center
National Marine Fisheries Service, NOAA
101 Pivers Island Road
Beaufort, North Carolina 28516-9722

Abstract—Passive acoustic recorders were used to monitor sound production indicative of the use of spawning habitat by groupers (Serranidae) at Riley's Hump, which is located in the Tortugas South Ecological Reserve (TSER), part of the Florida Keys National Marine Sanctuary. Sound production by black grouper (*Mycteroperca bonaci*), red grouper (*Epinephelus morio*), and red hind (*E. guttatus*) was recorded year-round and at all times of day but occurred more often in the evening during the winter–spring spawning period than during other times of the day and year. This pattern for these species is consistent with results of previous studies that documented the association of sound production with reproductive behavior at spawning sites. Distinct diel and seasonal patterns of sound production by the longspine squirrelfish (*Holocentrus rufus*) and bicolor damselfish (*Stegastes partitus*) also were recorded. Riley's Hump is a documented spawning site for mutton snapper (*Lutjanus analis*), and recordings of black grouper, red grouper, and red hind indicate that it is used for reproductive purposes by these species as well. These results showed the importance of the TSER and the need for continued research to understand its role in the recovery and sustainability of managed fish populations.

Manuscript submitted 7 May 2015.
Manuscript accepted 23 November 2015.
Fish. Bull. 114:103–116 (2016).
Online publication date: 10 December 2015.
doi: 10.7755FB.114.1.9

Because most large groupers support large commercial and recreational fisheries, there is an increasing focus on the conservation and management of their stocks and habitats. Fundamental to management decisions about these species is information on trends in population abundance and distribution, life history, and habitat use. Data that are used to understand these topics typically are generated from long-term time series based on visual surveys by divers, active acoustic surveys, mark and recapture studies, or subsampling of commercial catches. Recognition and protection of critical habitat, both essential for the sustainability of groupers and other reef fishes, have been realized through the establishment of marine protected areas and reserves (Roberts et al., 2005). An important consideration when selecting a location for a marine reserve is whether the area is used as a spawning aggregation site (Koenig et al., 2000). In many cases, fish spawning aggregation sites were first discovered by commercial fisherman and later established as marine reserves when their conservation value was understood. Such sites become prime locations for implementing long-term field studies to evaluate the efficacy of reserves for population recovery and to learn more about the behavior and dynamics of spawning aggregations (Burton et al., 2005).

Groupers, as the name implies, form seasonal spawning aggregations at traditional sites. The structure and size of these aggregations vary by species and may directly influence their vulnerability to overfishing. For example, Nassau grouper (*Epinephelus striatus*) and red hind (*E. guttatus*) form few, large aggregations (Whaylen et al., 2004; Kadison et al., 2009), a characteristic that increases their risk to recruitment overfishing. Because of this vulnerability, it has been important to consider spawning locations of red hind in the establishment of marine protected areas and seasonal closures in the U.S. Caribbean (Nemeth, 2012). Evidence from Belize indicates that black grouper (*Mycteroperca bonaci*) form numerous medium-size aggregations (<200 individuals) at various locations

among offshore atolls (Paz and Sedberry, 2008). In contrast, red grouper (*E. morio*) do not form large aggregations but instead appear to use more discretely formed spawning sites, where individual male territories are indicated by shallow pits excavated in the sediment (Coleman and Koenig, 2010; Nelson et al., 2011).

At many traditional aggregation sites, a variety of species may co-occur and form seasonal reproductively active communities; hence these sites are of value for conservation and research purposes (Heyman et al., 2001). The establishment of marine reserves at such locations provides an effective approach for the management of stocks in multispecies fisheries (Huntsman et al., 1999; Ault et al., 2008a).

In addition to the more traditional methods, passive acoustics represents a relatively new and underused approach to survey fish populations at spawning sites. Sound production is common among many fishes and is associated most often with courtship and spawning behaviors (Mok and Gilmore, 1983). Because sounds are species-specific, once the source has become positively identified, the information can be referenced to all future recordings to identify the presence of a given species at a monitoring site. Time series from the acoustic monitoring of fish sound production, therefore, can be used as a proxy to document the timing and location of reproductive behavior (Locascio and Mann, 2008). Recording technologies now allow multiyear deployments during which short periods of data (e.g., tens of seconds) may be recorded every few minutes. The trend in recording technologies becoming more sophisticated and less costly to acquire and deploy will continue and result in the collection of larger, synoptic acoustic data sets at more locations.

Groupers are among the most economically important fishes currently being studied with passive acoustics, and accomplishments from such monitoring are still few but increasing. Thus far, the sounds of Atlantic goliath grouper (*E. itajara*), red hind, red grouper, yellowfin grouper (*M. venenosa*), Nassau grouper, and black grouper have been positively identified and correlated with known spawning seasons (Mann et al., 2009; Mann et al., 2010; Nelson et al., 2011; Schärer et al., 2012, 2013). Other grouper species are also likely to produce sound, and these sounds await discovery. Only one study has attempted to quantify population size of a grouper species (red hind) with the use of passive acoustics in combination with visual surveys made by divers (Rowell et al., 2012).

Riley's Hump was a historically productive commercial fishing ground, particularly for mutton snapper (*Lutjanus analis*) (Burton et al., 2005). Anecdotal input from fishermen and the recommendations of a 25-member working group of commercial and recreational fishermen, divers, conservationists, scientists, concerned citizens, and representatives from government agencies led to the creation of the Tortugas South Ecological Reserve (TSER), a research-only marine reserve, in 2001 to protect the overexploited population of mutton snapper. Mutton snapper use Riley's Hump as a spawning aggregation site in the late spring and early summer months (NOAA[1]; Domeier, 2004; Burton et al., 2005). Since the inception of the TSER and the protection of the aggregation of mutton snapper at Riley's Hump, increased numbers of mutton snapper have been seen in visual surveys at Riley's Hump, at downstream locations along the Florida Keys reef tract (Ault et al., 2013), and in recreational headboat fishery landings (Brennan[2]). Many grouper species also inhabit Riley's Hump, but their use of the site for reproductive purposes has not been documented. The primary purpose of this study was to conduct an acoustic survey of Riley's Hump to document grouper sound production, which is generally used as a proxy for reproductive behavior.

Materials and methods

Riley's Hump, a geologic feature of approximately 10 km^2, marks the western extent of the south Florida reef tract and lies entirely within the TSER (Fig. 1, A and B). The limestone composition at Riley's Hump is typical of the sedimentary geology of the Gulf of Mexico, and its surface ranges from sandy bare areas to rugose hard bottom and low-relief outcroppings. Depths range from approximately 30 m on the hump to approximately 60 m immediately adjacent to it (Mallinson et al., 2003). Relief is highest along the edges, especially from the northeast to southern edges in a clockwise direction. The steepest vertical drop-off is located along the south–southwestern edge, which also has been observed to have the highest fish densities (Burton et al., 2005). The benthic community is composed of hard and soft corals, gorgonians, and a variety of sponges (Weaver et al., 2006).

Acoustic digital spectrum recorders (Loggerhead Instruments[3], Sarasota, FL) were deployed at 7 locations on Riley's Hump during multiple periods from 2010 through 2012 (Table 1; Fig. 1). These locations included 3 previously established study sites (12, 12A, and 15), where visual surveys of fishes were conducted during prior years, along with 4 new sites established for this study, including 3 sites on Riley's Hump (RH1, RH2, and RH3) and a deepwater site off the southwestern edge of Riley's Hump (RHDW) at a depth of approximately 60 m. Digital spectrum recorders were programmed to record 10 s of sound every 10 min at a

[1] NOAA. 2000. Draft supplemental environmental impact statement/draft supplemental management plan for the Tortugas Ecological Reserve, 250 p. Mar. Sanctuaries Div., Off. Ocean Coast. Resour. Manage., Natl. Ocean Serv., NOAA, Silver Spring, MD. [Available at website.]

[2] Brennan, K. J. 2013. Personal commun. Beaufort Laboratory, Southeast Fisheries Science Center, National Marine Fisheries Service, NOAA, Beaufort, NC 28516-9722.

[3] Mention of trade names or commercial companies is for identification purposes only and does not imply endorsement by the National Marine Fisheries Service, NOAA.

15,094 Hz sample rate; they were moored to steel rebar anchored in the limestone substrate. All recorders were deployed and recovered by scuba divers, except for the deployment of the deepwater recorder (RHDW), which was dropped in a weighted housing unit from the swim platform of the MV *Spree* and recovered by scuba divers. Visual surveys were conducted along transects of 50 m by divers to document the presence of grouper species at acoustic monitoring sites (12, 12A, 15, RH1) during April 2010 and January and February 2011. All field operations were conducted from the MV *Spree*.

Each 10-s acoustic file was analyzed in MATLAB, vers. R2009B (The Mathworks Inc., Natick, MA) with a fast Fourier transform to generate a power spectrum from which the band sound pressure level (SPL) in 100-Hz-wide bins was calculated. Patterns in fish sound production on daily and seasonal scales were examined in plots of power spectra and, for grouper species, by direct counts of calls in a subsample of 10,000 files randomly selected from the entire database of acoustic recordings. The number of calls counted for each grouper species in the subsample was normalized as a ratio of the number of calls to number of files reviewed for each month at each site. Spectrograms of acoustic recordings were reviewed with Adobe Audition, vers. 2.0 (Adobe Systems Inc., San Jose, CA) to identify species present in the recordings or previously undescribed calls. Daily sound patterns were estimated by binning the number of calls for each species (sites combined) into three 8-h periods (0000–0800, 0800–1600, and 1600–0000, all local time) and comparing them by means of tests for analysis of variance. Acoustic time-series data were examined for peaks associated with lunar phases.

Custom underwater audio and video (A/V) systems were used to verify sources of fish sound production and to understand the behavioral context associated with that sound production. The recording system included a low-light, 0.001-lux, black-and-white flat lens board camera and 2 HTI 96-MIN hydrophones (sensitivity −164 dB reference pressure [re]: 1V/µPa) (High Tech Inc., Long Beach, MS) that recorded to a ChaseCam deck (Chase Vision, LLC, Cleveland, TN). Each A/V system was deployed in a clear, waterproof housing unit and placed on the seafloor overnight at select sites where long-term acoustic recorders were deployed. The A/V system recorded continuously to compact flash memory cards for approximately 20 h. A Sony HDR-XR100 video camera (Sony Corp., Tokyo) fitted with an HTI 96-MIN hydrophone was used during visual surveys conducted by divers to record fish sound production and associated behavior. Audio and video data were reviewed with Corel Video Studio software, vers. X6 (Corel Corp., Ottawa, Ontario) and with Adobe Audition software to identify species-specific acoustic signals and associated behavioral context.

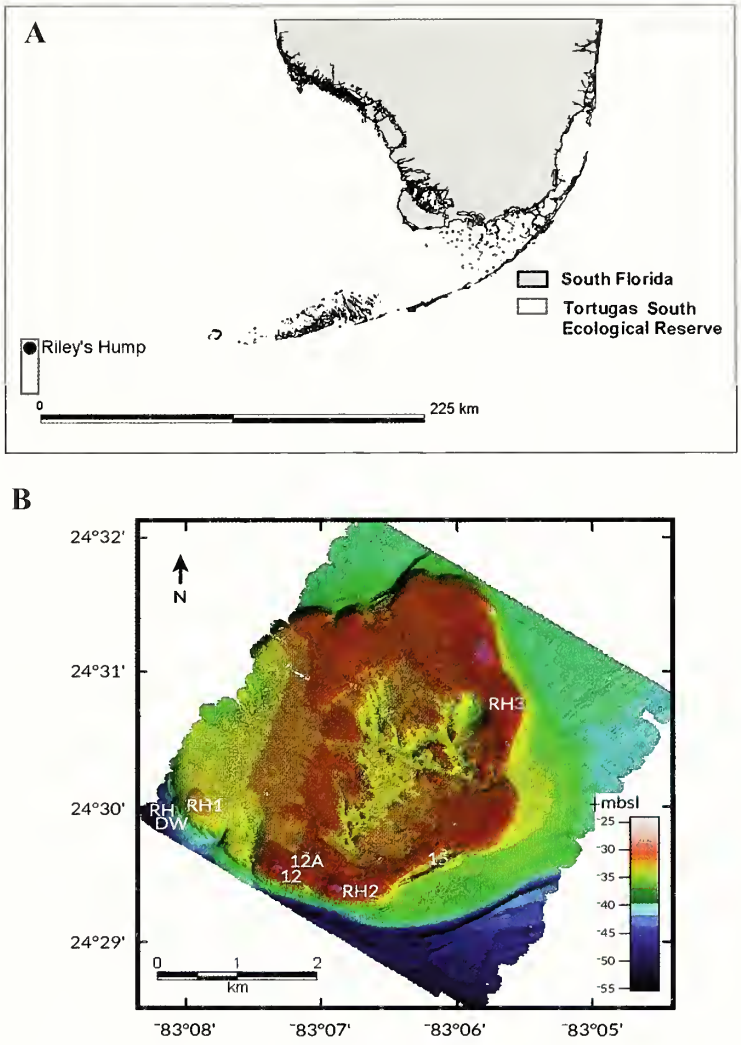

Figure 1

(**A**) Location of Riley's Hump within the Tortugas South Ecological Reserve and in relation to mainland Florida, and (**B**) locations of acoustic monitoring sites on Riley's Hump indicated on the multibeam bathymetric image of this geologic feature. The scale of the image represents meters below sea level (mbsl). The deepwater site (RHDW) that would be on the left side of the image is located a bit farther west than what is indicated in this figure. The depth of this site was approximately 60 m; depths at all other acoustic montioring sites located on Riley's Hump were approximately 30 m. Bathymetric image is taken from figure 7 of Mallinson et al., 2003.

Table 1

Record of deployment locations, periods, and number of records used to monitor sound production by groupers and other fish species at Riley's Hump (RH), Tortugas South Ecological Reserve, Florida Keys National Marine Sanctuary. All recorders were programmed to record 10 s of sound every 10 min at a sample rate of 15,094 Hz. At the deepwater site (RHDW), located off the southwestern edge of Riley's Hump, the recorder was deployed at a depth of 60 m.

Site	Deployment Period	Days	Records
12	29 April–28 June 2010	60	8640
12	18 January–14 July 2011	177	25,488
12A	29 April 2010–16 July 2011	443	63,792
15	29 April 2010–9 December 2011	589	84,816
RH1	18 January 2011–17 June 2012	516	74,304
RH2	18 January 2011–17 June 2012	516	74,304
RH3	18 January 2011–21 June 2012	516	74,304
RHDW	17 July 2011–13 June 2012	332	47,808

Results

Patterns in fish sound production recorded at all study sites were classified into 3 frequency ranges: <200 Hz, 300–400 Hz, and 500–800 Hz. Identifiable sounds produced in the lowest frequency range (<200 Hz) were associated mainly with 3 grouper species: red grouper, red hind, and black grouper. Positive identification of these species in the recordings was based on previous descriptions of their sounds (Mann et al., 2010; Nelson et al., 2011; Schärer et al., 2013) and on additional evidence from this study of sound production by black grouper documented with the A/V systems. Sound production by each of these species was greatest during the evening period (1600–0000) but was not significantly different from any of the 3 time periods (black grouper: F=3.1, P=0.05; red grouper: F=1.4, P=0.24; and red hind: F=4.5, P=0.64) (Fig. 2). Diel variability in SPLs during the winter–spring period ranged from about 5 to 10 dB SPL (re: 1 µPa) above daily background levels in the frequency range used by groupers (<200 Hz) at all sites during 2011 and 2012 except RHDW. This

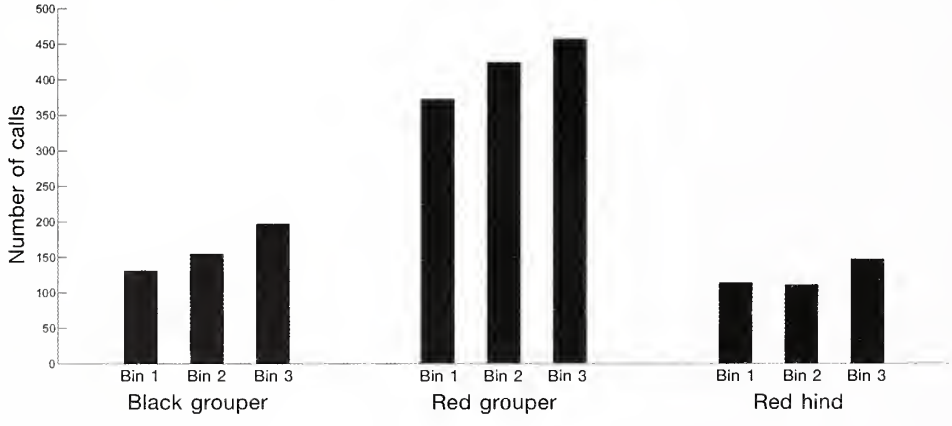

Figure 2

Diel pattern of sound production by black grouper (*Mycteroperca bonaci*), red grouper (*Epinephelus morio*), and red hind (*Epinephelus guttatus*) at Riley's Hump, Tortugas South Ecological Reserve, Florida Keys, in 2012. Data are distributed in 3 bins of 8 h each (bin 1=0000–0800; bin 2=0800–1600; bin 3=1600–0000) and are the sum total of calls identified in analysis of 10,000 files randomly selected from the entire database of acoustic recordings. The number of calls is greatest during the evening period for these species, but significant differences do not exist between time periods for any species based on the methods used in this study.

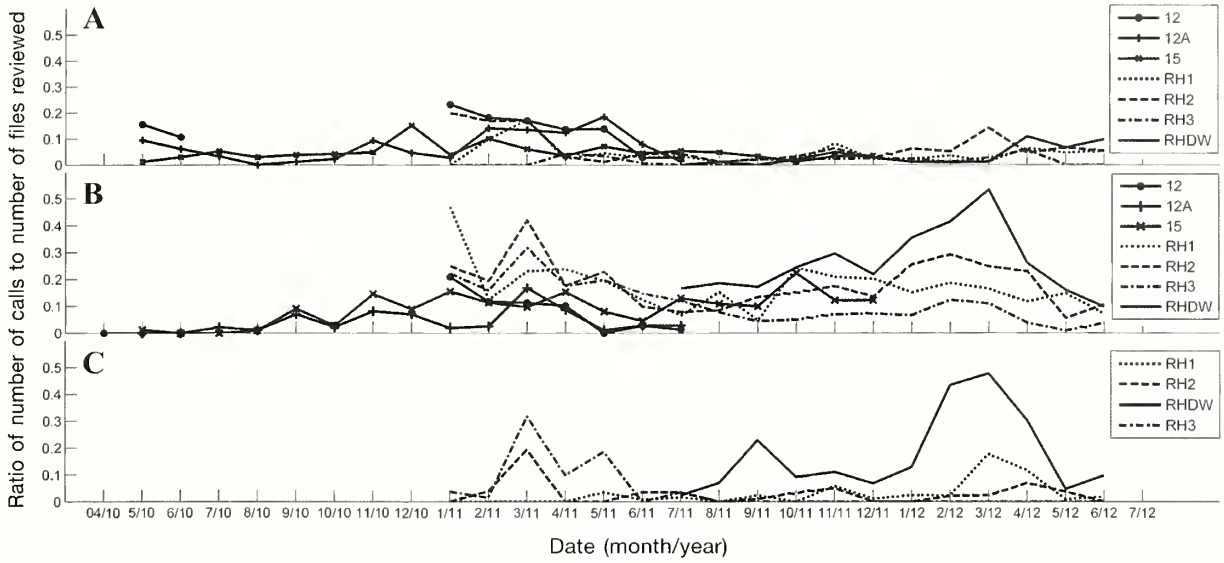

Figure 3

Time series of the ratio of the number of calls of 3 grouper species, (**A**) black grouper (*Mycteroperca bonaci*), (**B**) red grouper (*Epinephelus morio*), and (**C**) red hind (*Epinephelus guttatus*), recorded at Riley's Hump, Tortugas South Ecological Reserve, Florida Keys, 2010–2012 to the number of files reviewed in a subsample of 10,000 randomly selected audio files. For each species, call volume increased during the winter–spring reproductive season. The 2012 season had a greater call volume and appears more protracted than the 2011 season for red grouper and red hind; the higher numbers of calls in 2012 may represent the presence of more fish species at these sites in 2012 than in 2011. Red grouper and red hind both demonstrated a preference for the deepwater site (RHDW) in 2012 and for sites RH2 and RH3 in 2011, respectively. Black grouper were recorded at all sites yet did not produce particularly high numbers of calls at a specific site, although, overall, most sound production by this species was recorded at site RH2 during both years.

resulted in relatively poor signal-to-noise ratios which prevented identification of a clear diel pattern in the power spectra results associated with groupers. Recordings of red hind at the RHDW site were the only exception to this and diel patterns in the power spectra associated with this species were clearly discernible from background levels.

Sound production by each grouper species occurred year-round, but levels were highest from January through May and typically peaked in March for each species during 2011 and 2012 (Fig. 3). Black grouper were recorded at all sites; the highest standardized number of calls was recorded at site 12A in 2011 and at site RH2 in 2012. A modestly higher number of black grouper calls were recorded in 2011. Red grouper were recorded at all sites; the highest number of calls by this species was recorded at site RH2 in 2011 and at site RHDW in 2012. Red hind were recorded only at sites RH1, RH2, and RH3 and at site RHDW; the highest number of calls by this species was recorded at site RH3 in 2011 and at site RHDW in 2012. The seasonal pattern of calls by black grouper indicates a more even distribution over the winter–spring period than that of the seasonal pattern of sound production by red grouper and red hind, which peaked more sharply in March and April of each year. Sound pressure levels recorded at site RHDW reached amplitudes that were 15 dB SPL (re: 1 µPa) greater than daytime background levels and were positively associated with the last quarter moon phase. All 3 grouper species were recorded at site RHDW, but sound production was dominated at this site by the red hind (Figs. 3 and 4).

Red and black groupers and red hind were the dominant grouper species recorded at Riley's Hump, but other low-frequency, pulsed and modulated tonal calls were occasionally discovered during review of audio files. Three instances of calls by yellowfin grouper were positively identified in recordings made at site 12A during November 2010 by comparison with documented characteristic sound production of yellowfin grouper (Schärer et al., 2012). Several instances of a call type that resembled that of the Nassau grouper were also noted in recordings made during winter–early spring at site RHDW. Both the yellowfin grouper and Nassau grouper were observed in visual surveys conducted by divers at Riley's Hump during this study. More detailed studies of sound production of Nassau grouper are in progress, and the results will be useful for quantifying the presence of this species in the recordings made at Riley's Hump.

Additional information on sound production by black grouper was documented in this study. Two

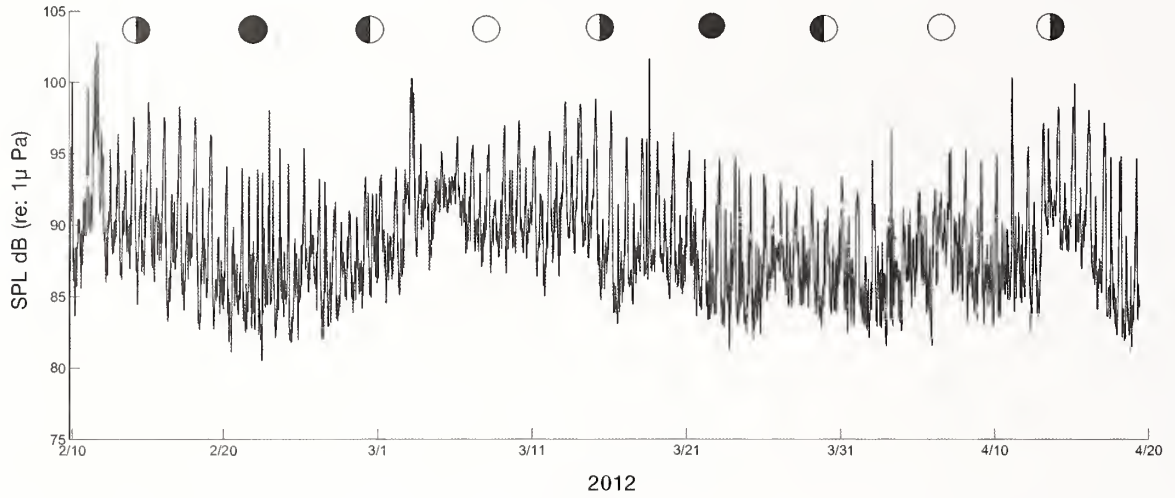

Figure 4

An example of seasonal periodicity of sound pressure levels (SPLs) in the time series of acoustic data for the frequency range <200 Hz recorded at the deepwater site (RHDW) at a depth of 60 m at Riley's Hump, Tortugas South Ecological Reserve, Florida Keys, 2010–2012. Red grouper (Epinephelus morio), black grouper (Mycteroperca bonaci), and red hind (Epinephelus guttatus) all were recorded at this site, but the red hind was the dominant sound producer during the period shown. Sound production occurred during all lunar phases, but peaks were coincident with the last quarter moon phase. Lunar symbols represent moon phases as follows: new moon, ●; first quarter moon, ◐; full moon, ○; and last quarter moon, ◑.

variations of the call of black grouper were identified. One variation, BGV1, was composed of a relatively long, frequency-modulated tonal portion only. The other variation, BGV2, was composed of an initial, shorter-duration frequency-modulated tone followed by several individual pulses and concluded with a longer frequency-modulated tonal portion characteristic of the BGV1 (Fig. 5, A–D). The long, frequency-modulated tonal portion common to both variations (n=20) had a mean duration of 5.2 s (standard deviation [SD] 1.2) and was modulated between 60–120 Hz at a mean rate of 170 ms (SD 0.03. The highest received root-mean-square (RMS) SPL for the long, frequency-modulated portion of the call was estimated at 149.9 dB RMS SPL (re: 1 µPa). The highest received RMS SPL for the introductory portion of the call only and the overall combined portions of the call were 143.3 and 144.3 dB SPL (re: 1 µPa), respectively.

This call type was identified 76 times in the audio track of the recordings made with the remote A/V systems. Black grouper appeared in the video from the A/V systems during 18 of the 76 times either call variation was identified and 10 additional times within 25 s of the call being made. No other grouper species were recorded on video at or near the time during which either variation of this call was produced. Other grouper species were verified at these sites by divers during visual surveys, including the Nassau grouper, yellowmouth grouper (*M. interstitialis*), scamp (*M. phenax*), yellowfin grouper, rock hind (*E. adscensionis*), and coney (*Cephalopholis fulva*).

In most cases, only a single black grouper appeared in the video when a call of either variation (BGV1 or BGV2) was made and only once was interaction between 2 fish recorded (site 12A). On this occasion, one fish with a blotched pattern approached another more monochromic fish from below and behind and briefly made contact as it passed under the rear portion of the other's body. The 2 fish then swam slowly away in opposite directions and out of the video frame (Fig. 6, A–D). The blotch-patterned fish swam toward the camera and out of the frame, and within 10 s a relatively high amplitude (149.9 dB SPL) BGV1 call was recorded. This behavior could indicate possible courtship, but it could also represent a territorial display.

On the morning that the A/V system that made this recording was deployed (27 April 2010) divers reported seeing several black grouper at this site (12A) swimming together in a daisy chain pattern high in the water column. Apparent courtship behavior between 2 black grouper was also observed during a visual survey conducted at site RH1 on 19 January 2011. On this occasion, a large, light-colored black grouper was observed to approach a smaller black grouper from behind and swim alongside it for a few moments and then to rub and shake its body against it for about 2 s. No sound associated with this behavior was heard by divers, but it may have gone unnoticed. Similar courtship behavior of black grouper was described by Paz

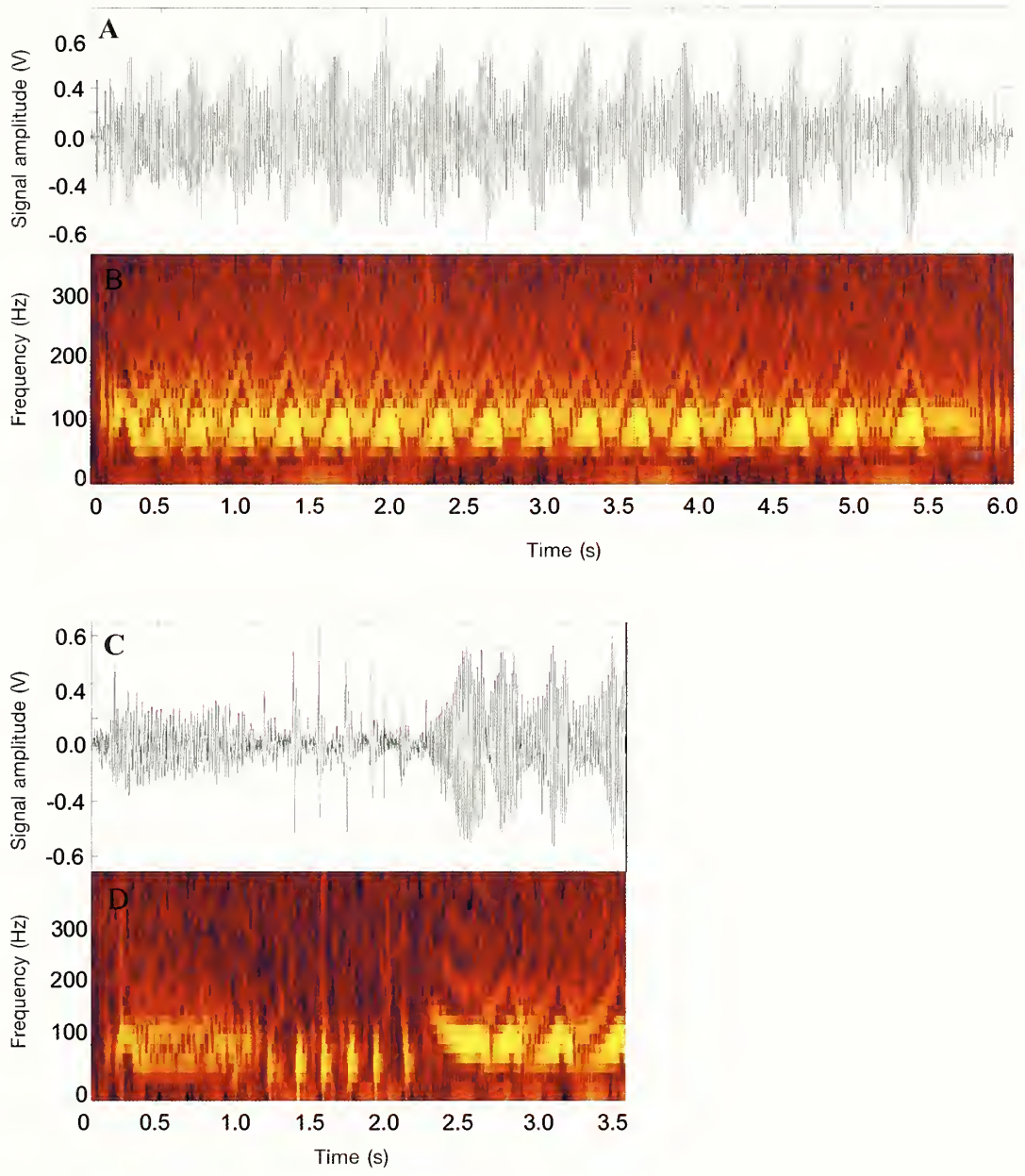

Figure 5

Examples of acoustic recordings of black grouper (*Mycteroperca bonaci*) sounds made at site 12 at Riley's Hump, Tortugas South Ecological Reserve, Florida Keys in April 2012: (**A**) in waveform and (**B**) as a spectrogram of black grouper call variation 1 (BGV1), which is frequency modulated between 60–120 Hz at a rate of about 0.2 s. Average duration of this variation was 5.2 s (SD 1.2, n=20), and highest received levels recorded were 149.9 dB SPL (re: 1 µPa). (**C**) Waveform and (**D**) spectrogram of black grouper call variation 2 (BGV2), which contains an introductory portion composed of a short frequency-modulated period followed by individual pulses and then the longer frequency-modulated portion common to BGV1. The BGV2 call was uncommon in field recordings. How the context of the 2 call variants differs is unknown. The longer frequency-modulated end portion of the BGV2 call is truncated because the programmed 10-s recording period elapsed during the call.

Figure 6

Interaction between black grouper (*Mycteroperca bonaci*) was captured only once in video recordings made at Riley's Hump, Tortugas South Ecological Reserve, Florida Keys, and that interaction is shown in these video stills from videos taken at site 12A on 27 April 2010: (**A**) and (**B**) a blotch-patterned black grouper (right side of figure) approaches a second black grouper from below. (**C**) The approaching fish passes directly beneath the rear portion of the second fish and briefly makes contact, but no additional interaction occurs. (**D**) The 2 fish swim away from each other in opposite directions and a BGV1 call is produced a few seconds later. This interaction may have been courtship or territorial associated behavior. When the audio and video system was deployed at this site, divers reported seeing several black grouper midway in the water column swimming together in a generally circular pattern, similar to behavior observed in a spawning aggregation documented in Belize.

and Sedberry (2008) at spawning aggregation sites of black grouper in Belize, where these authors also noted that the blotched-color phase was seen during the morning of the day that spawning occurred.

Sound production in the frequency range of 300–400 Hz was dominated by the longspine squirrelfish (*Holocentrus rufus*). This finding was validated by an analysis of recordings made with the handheld Sony video camera fitted with a hydrophone and also by comparison with descriptions made by Winn et al. (1964). This species produced a pulsatile call with received SPLs of 6.0–8.0 dB (re: 1 µPa) above daytime background levels. The diel pattern was crepuscular with slightly higher SPLs reached during the evening than during the morning. Patterns in the SPLs and timing of this call type began in early spring and continued through late summer and early fall. These patterns were similar among sites and between years, and they were not associated with a lunar period (Fig. 7).

Sound production in the frequency range of 500–800 Hz was also dominated by a pulsatile call, typical of the family Pomacentridae and attributed to the bicolor damselfish (*Stegastes partitus*). Some energy associated with this call extended above and below the range of 500–800 Hz but was minimal by comparison. Sound production in this range was considered to be from a different source than that of the signal produced in the range of 300–400 Hz by the longspine squirrelfish because plots of each signal indicated they were out of phase with each other (i.e., not temporally synchronized). Sound production and behavior by this species were also recorded by the remotely deployed A/V sys-

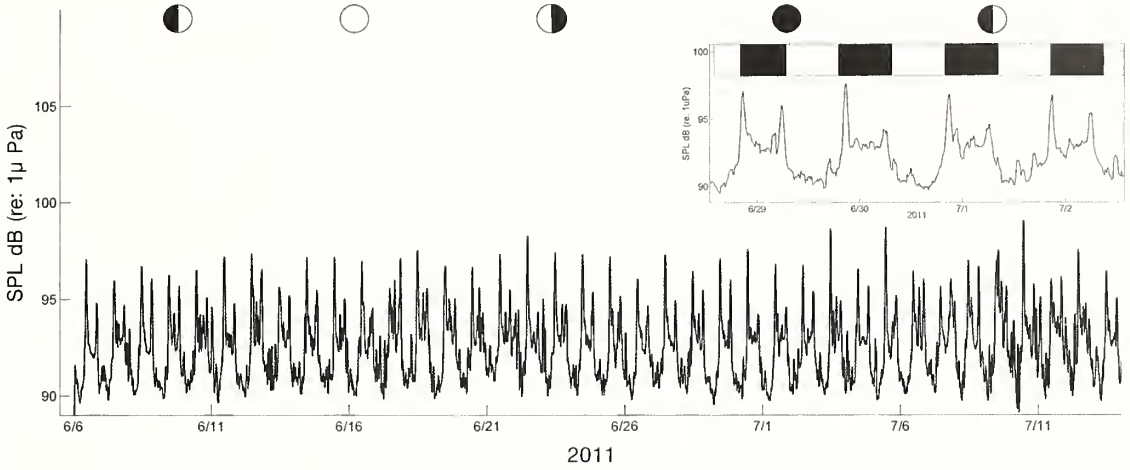

Figure 7

An example of sound production by longspine squirrelfish (*Holocentrus rufus*), measured in sound pressure levels (SPLs), from the time series of acoustic data recorded in the frequency range of 300–400 Hz at site RH1 at Riley's Hump, Tortugas South Ecological Reserve, Florida Keys, in 2011. The seasonal period of sound production in this frequency range occurred from early spring through late summer and early fall, beyond the limits of the x-axis. Illustrated more closely in the inset figure, with bars that indicate periods of day and night, diel periodicity of sound production by this species is defined by a crepuscular pattern. No lunar periodicity is evident. Lunar symbols are defined as follows: new moon, ●; first quarter, ◐; full moon, ○; and last quarter moon, ◑.

tems. This call type occurred at all sites between late March and mid-July and had an associated lunar period that began on or within 2 days of the full moon and continued to about the first quarter moon of the following lunar cycle, a period of approximately 18–20 days. Nightly maximum SPLs associated with this call were about 25 dB above daytime background levels during peak season, and they increased rapidly just after the full moon and decreased rapidly near the new moon (Fig. 8). The relatively high signal-to-noise ratio indicates that the source was close to the hydrophone.

Discussion

In this study, the common occurrence of sound production by red grouper, black grouper, red hind, longspine squirrelfish, and bicolor damselfish was documented at Riley's Hump along, as well as the rare occurrence of sound production by yellowfin grouper and possible sound production by Nassau grouper. Several other relatively uncommon call types were recorded and noted during review of audio files and may be identified to source in future research. Temporal patterns in sound production by red grouper and red hind were similar to the patterns observed in analysis of previous recordings made at sites in the Gulf of Mexico and Puerto Rico, patterns in which sound production was positively correlated with spawning season (Mann et al., 2010; Nelson et al., 2011). The last quarter lunar phase associated with maximum vocalizations of red hind in this study was consistent with the lunar period in sound production of red hind reported from the western coast of Puerto Rico (Rowell, et al,. 2012). The temporal association of a lunar phase with aggregations of red hind has been shown previously to vary between sites. The significance of this finding is not well understood, but it may be associated with patterns in local currents (Nemeth, 2012). Patterns in lunar periodicities associated with sound production by black grouper require more detailed analysis of time-series data and are the subject of a future study.

In these prior studies, observations of grouper behavior associated with sound production did not include actual spawning; rather, they included courtship interactions and territorial behavior during which the presumed male was the sound producer. In our study, apparent courtship or territoriality between 2 black grouper was recorded on video, and one observation of similar behavior was made during a visual survey conducted on 19 January 2011 at site RH1. Because spawning is rarely observed, the exact timing and context of sound production in relation to gamete release is not well understood for grouper species, but sound production does generally correlate well with the reproductive period on a seasonal basis (Locascio and Mann, 2011a).

In this study, more calls of red grouper and red hind were recorded over a longer seasonal period in 2012 than in 2011. The more protracted period of sound pro-

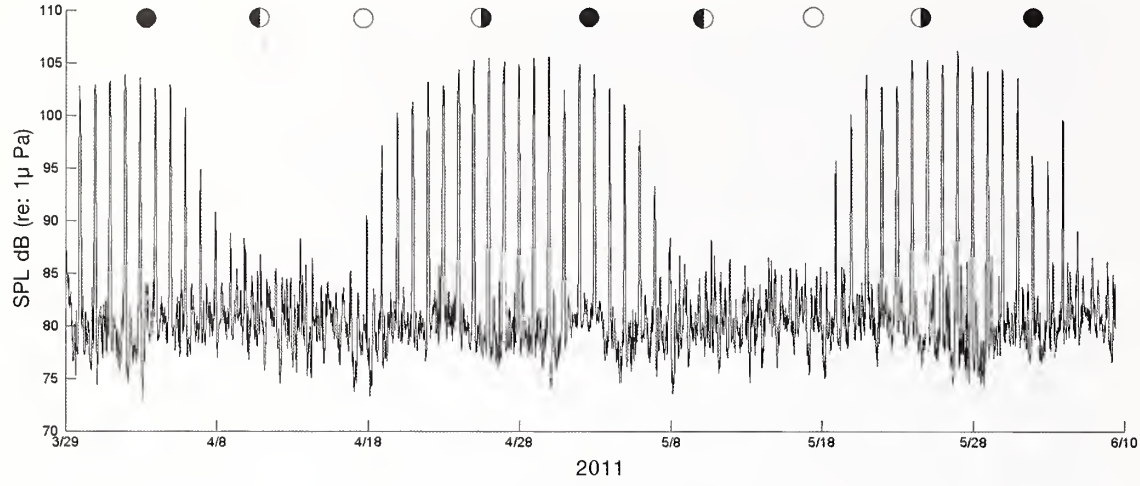

Figure 8

An example of sound production attributed to the bicolor damselfish (*Stegastes partitus*) from the time series of acoustic data recorded in the frequency range of 500–800 Hz at site RH2 at Riley's Hump, Tortugas South Ecological Reserve, Florida Keys, in 2011. The seasonal period of sound production in this frequency range occurred from early spring through mid-summer. Sound pressure levels (SPLs) increased and decreased gradually over a period of about 18 days, beginning near the new moon. Lunar symbols are defined as follows: new moon, ●; first quarter, ◐; full moon, ○; and last quarter moon, ◑.

duction in 2012 by these species could indicate that a longer spawning season occurred during that year and possibly also that a greater number of fishes were present. During 2012, both species demonstrated a preference for site RHDW, which was not monitored in 2011 in our study. This site is located near the base of the steepest vertical relief of Riley's Hump, a habitat feature of aggregation sites associated with relatively high densities of fishes (Kobara et al., 2013).

The spawning season of the red grouper occurs approximately from March through July in the Gulf of Mexico and peaks between March and June, although there is some variability with latitude. This timing is consistent with peak levels of sound production recorded in this study. This species is not considered currently to be overfished or experiencing overfishing (Lowerre-Barbieri et al.[4]).

The spawning season of the black grouper is reported to occur from December through March in the Gulf of Mexico, although Crabtree and Bullock (1998), on the basis of gonad condition, suggested that spawning may occur year-round. The results of our study show that sound production of black grouper occurs year-round, but at levels higher from December through May than during other periods. The black grouper is not considered presently to be overfished or experiencing overfishing (SEDAR[5]).

Red hind in the U.S. Caribbean form spawning aggregations associated with various lunar phases from December through March (Mann et al., 2010; Nemeth, 2012). In our study at Riley's Hump, seasonal and lunar periods in sound production by red hind were similar to the periods observed in studies conducted in the U.S. Virgin Islands, although the timing of peak levels occurred 1–2 months later in the year at Riley's Hump. Results of a stock assessment conducted during 2013–2014 (SEDAR[6]) indicate that the red hind is not overfished or experiencing overfishing in the U.S. Caribbean, but this notion was not strongly conclusive on the basis of available data.

Although most sound production by each grouper species reported here occurred during the winter and spring, calls also were recorded at other times of the year. It is difficult to conclude an alternative meaning for this finding without concurrent observations of behavior, but one possibility may be that limited spawning occurs during other times of the year. The black grouper, for example, has been reported to remain in sexually mature condition year-round (Crabtree and

[4] Lowerre-Barbieri, S., L. Crabtree, T. S.Switzer, and R.H. McMichael Jr. 2014. Maturity, sexual transition, and spawning seasonality in the protogynous red grouper on the West Florida Shelf. Southeast Data Assessment and Review SEDAR42-DW-07, 21 p. [Available at website.]

[5] SEDAR (Southeast Data Assessment and Review). 2010. SEDAR 19 stock assessment report Gulf of Mexico and South Atlantic black grouper, 656 p. SEDAR, North Charleston, SC. [Available at website.]

[6] SEDAR (Southeast Data Assessment and Review). 2014. SEDAR 35 stock assessment report U.S. Caribbean red hind, 350 p. SEDAR, North Charleston, SC. [Available at website.]

Bullock, 1998). Another possible explanation is that sound production is associated with other forms of behavior besides courtship and spawning. For example, red grouper excavate and maintain pits in the sediment that are used by other species, and red grouper are believed to have strong site fidelity to these engineered features (Coleman and Koenig, 2010; Wall et. al, 2011). Given these circumstances, sound production may be used in other social contexts, such as territorial or agonistic interactions.

The calls recorded in our study that were attributed to black grouper are consistent with the stereotypical characteristics of calls by groupers (low frequency, modulated, and long duration) and agree with descriptions of sound production of black grouper from recordings made in Puerto Rico (Schärer, et al., 2013). Although apparent courtship or territorial behavior was followed closely by a BGV2 call in only one video segment, the black grouper was the only grouper species appearing in the video recorded at or near the time that a call of either variation was produced, strongly indicating that this species was the source. Additionally, for black grouper, the relatively high received RMS SPLs of the call variations indicate that the source was close to the hydrophone, and, in these cases, black grouper appeared in the video within a few seconds of these call types. A source level (i.e., decibels of SPL at 1 m from source) can be roughly estimated with a spreading loss model (Urick, 1983) and a received SPL of a call. In our study, a spherical model that estimates a 6-dB loss per distance doubling was used with the highest received SPL of 149.9 dB RMS SPL (re: 1 µPa), which was recorded when black grouper appeared to be only a few meters from the A/V system. Adding 6 dB to the highest received level is equivalent to 1 distance doubling, placing the source 2 m away from the A/V system and resulting in an estimated source level of 155.9 dB RMS SPL (re: 1 µPa). Adding 12 dB to the highest received level would be equivalent to 2 distance doublings and would place the source 4 m away from the A/V system with an estimated source level of 161.9 dB RMS SPL (re: 1 µPa), and so on. For reference, estimates of source levels produced by black drum (*Pogonias cromis*) are 165 dB RMS SPL (re: 1 µPa) (Locascio and Mann, 2011b). Extrapolated estimates of source levels for black grouper that were calculated with the spherical spreading loss model seem reasonable in the context of source levels reported for black drum.

Calls of black grouper contain a frequency-modulated feature, a mechanism associated with sound production that speeds up and slows down over the duration of a call, but the structure of calls of black grouper are unique from the calls of red grouper, yellowfin grouper, and red hind in that they do not feature a long frequency down-sweep. The BGV2 call was differentiated from the BGV1 call by a series of initial pulses. This difference also exists between call types of the red grouper (Nelson et al., 2011), but the significance of those differences is not understood for either species. Sounds of most grouper species documented thus far, with the exception of the call of the Atlantic goliath grouper, give evidence of a complex structure relative to the more common pulsatile structure of many fish calls. The mechanisms associated with the sound production of groupers have been reported only in general terms as bilateral muscles that work in conjunction with the swim bladder (Hazlett and Winn, 1962). A more detailed analysis of the mechanisms and processes responsible for sound production of groupers and the associated behavioral context is warranted given the unusual modulated tones.

Estimates of acoustic communication ranges for fish require data on source levels and hearing thresholds, along with site-specific information on loss of signal transmission and on background levels. Locascio and Mann (2011b) estimated that the acoustic communication range of black drum was 33–108 m on the basis of direct measurements of each of these parameters and found that the range for this species was limited by background levels rather than by hearing thresholds. Data for the complete suite of these parameters do not exist for any grouper species; however, based on the highest received levels of 142.0 dB SPL (re: 1µPa) reported by Nelson et al. (2011) for red grouper and of 149.9 dB SPL (re: 1µPa) recorded in our study for black grouper, a reasonable estimate of communication ranges of groupers in a noisy reef habitat would be on the order of tens of meters.

Spawning sites of black grouper are not well known in the United States. Only 2 probable spawning sites have been documented in the literature, one in the Florida Keys Marine Sanctuary (Eklund et al., 2000) and the other at Mona Island, Puerto Rico (Schärer et al., 2013). In addition to demonstrating that Riley's Hump is also a likely spawning site for black grouper, the information generated in this study can be used to help document other spawning aggregation sites and provide opportunities to learn more about the role of sound production by this species.

The source of sounds produced in the range of 300–400 Hz was verified as longspine squirrelfish by comparing descriptions of the call of this species made by Winn et al. (1964) and that made in our study with a handheld A/V system. Recordings were made as longspine squirrelfish emitted sounds just before retreating into their den after they were approached by a diver. This agonistic behavior is associated with sound production by this species. This behavioral context, together with this species' strong site fidelity to dens (Ménard, et. al, 2008) and its nocturnal behavior, may explain the crepuscular pattern observed in sound production by this species in our study. Other less commonly observed holocentrid species that occupy Riley's Hump s include the longjaw squirrelfish (*Neoniphon marianus*) and blackbar soldierfish (*Myripristis jacobus*). Sound production by these species has not yet been documented in the field, but on the basis of their taxonomy it is likely that these species do produce sounds.

Acoustic signals generated in the range of 500–800

Hz were attributed to the bicolor damselfish on the basis of analysis of A/V recordings and comparison with descriptions of the acoustic signature and associated behavior of this species by Myrberg (1972). Sound production, termed *chirping*, is used in conjunction with short vertical ascents and dives, termed *dipping*, by males to attract females to nest sites. Lunar patterns in sound production were very similar to those patterns described for spawning by this species. Schmale (1981) reported that most spawning by bicolor damselfish occurred between the full moon and just after the first quarter moon—timing that corresponds to the onset and sustained period of sound production by bicolor damselfish that was recorded in our study. Sound production was sustained at high levels beyond the first quarter moon to about the time of the new moon and then decreased sharply. Hatching occurs for this species near the time of the new moon (Schmale, 1981); therefore, the prolonged period of sound production that extended past the time of spawning is likely associated with nest guarding. The bicolor damselfish is among the most abundant pomacentrids reported in visual surveys made by divers at Riley's Hump as part of our study. Other common pomacentrids at the study sites included the blue chromis (*Chromis cyanea*) and purple reeffish (*C. scotti*), neither of which have been documented as sound producers, but it is a possibility that they produce sounds given the common use of sound by this family.

The seasonal and lunar timing of the sounds produced at 500–800 Hz do overlap somewhat with the period of reproductive aggregation of mutton snapper at Riley's Hump in May–July. However, on many occasions when videos of large schools of mutton snapper were recorded by remote A/V systems, as well as video of courtship and spawning behavior (senior author, unpubl. data), the call type of this species was not recorded coincidentally, and there is yet no published evidence of sound production by snappers.

The potential of Riley's Hump as a source of mutton snapper larvae for the Florida Keys and southeastern Florida was demonstrated by Domeier (2004). Its upstream location in the Florida Reef Tract positions Riley's Hump as the starting point of a larval pathway that could populate downstream juvenile habitats throughout the Florida Keys and southeastern Florida. In addition to being a documented spawning aggregation site for mutton snapper, Riley's Hump is a location where divers have observed courtship behavior of permit (*Trachinatus falcatus*), and it has been recorded with the use of A/V systems. The general geomorphology of Riley's Hump is consistent with features of multispecies spawning aggregation sites described by Heyman and Kobara (2010). The results of this study provide additional documentation of the importance of Riley's Hump as a multispecies spawning site and a possible source of larval recruits for populations of red hind, red grouper, and black grouper.

Ault et al. (2008b) reported spawning potential ratios of 0.8% and 17.7% for black grouper and red grouper in the Florida Keys, respectively. These values are far below the federally defined benchmark of 30% for sustainability of these species, especially for the black grouper. Although a managed species, the red hind is not currently targeted commercially in the southeastern United States but is targeted in the U.S. Caribbean; this species was the focus of a stock assessment recently held by Southeast Data Assessment and Review (SEDAR[6]). Estimates of spawning potential ratios for this species are unavailable.

Results from this study indicate that at least 3 economically important grouper species use Riley's Hump as a reproductive habitat, further indicating its importance as part of a marine reserve and the need for continued research to understand its significance on the recovery of fish populations in the southeastern United States. Sonic tagging of groupers at Riley's Hump during the spawning season could provide useful information on whether they are resident or transient and on their geographic range, especially in regard to the reserve boundaries and level of connectivity that may exist among regional populations. For example, estimated mean home ranges of black grouper and red grouper in the Dry Tortugas were 1.44–7.72 km^2; a range of areas slightly smaller than that of Riley's Hump and considerably smaller than the total area (206 km^2) of the TSER (Farmer and Ault, 2011).

Remote monitoring of fish behavior with passive acoustics was especially effective for assessment of the use of spawning habitat in the deep water adjacent to the highest vertical relief associated with Riley's Hump. Little is known about fish use of this deepwater habitat because most research has been conducted on the hump at depths <37 m. Black grouper, red grouper, and red hind all used site RHDW, and it was the preferred site of red grouper and red hind during the 2012 spawning season. Divers also reported that they saw a school of 50–100 cubera snapper (*Lutjanus cyanopterus*) during the dive to recover the acoustic recorder at site RHDW in July 2012.

In addition to providing the first evidence of the use of Riley's Hump by groupers for reproductive purposes, we provide evidence of the value of the use of passive acoustics for exploring long-term monitoring of habitat use by important sound-producing fish. Such efforts will continue to be useful for fishery biologists and ecologists but will require the skilled management of large data sets and additional work for the documentation of sound production by other species.

Acknowledgments

This research was funded by a grant from the NOAA Coral Reef Conservation Program, project number 20205-2010. Expert field assistance was provided by members of the NOAA Southeast Fisheries Science Center laboratories in Beaufort, North Carolina, and Miami, Florida; the National Ocean Service's Center for Coastal Fisheries and Habitat Research in Beau-

fort, North Carolina; the Florida Fish and Wildlife Conservation Commission's Overseas Research Laboratory in Marathon, Florida; and the Reef Environmental Education Foundation of Key Largo, Florida. All field operations were conducted from the MV *Spree*.

Literature cited

Ault, J. S., S. G. Smith, J. A. Bohnsack, J. Luo, N. Zurcher, D. B. McClellan, T. A. Ziegler, D. E. Hallac, M. Patterson, M. W. Feeley, B. I. Ruttenberg, J. Hunt, D. Kimball, and B. Causey.
2013. Assessing coral reef fish population and community changes in response to marine reserves in the Dry Tortugas, Florida, USA. Fish. Res. 144:28–37.

Ault, J. S., S. G. Smith, J. Luo, M. E. Monaco, and R. S. Appeldoorn.
2008a. Length-based assessment of sustainability benchmarks for coral reef fishes in Puerto Rico. Environ. Conser. 35:221–231.

Ault, J. S., S .G. Smith, and J. T. Tilmant.
2008b. Are the coral reef finfish fisheries of south Florida sustainable? *In* Proc. 11th Int. Coral Reef Symp.; Ft. Lauderdale, FL, 7–11 July 2008 (B. M. Riegl and R. E. Dodge, eds.), p. 989–993. Natl. Coral Reef Inst., Nova Southeastern Univ., Dania Beach, FL. [Available at website.]

Burton, M. L., K. J. Brennan, R. C. Munoz, and R. O. Parker Jr.
2005. Preliminary evidence of increased spawning aggregations of mutton snapper (*Lutjanus analis*) at Riley's Hump two years after establishment of the Tortugas South Ecological Reserve. Fish. Bull. 103:404–410.

Coleman, F. C., and C. C. Koenig.
2010. The effects of fishing, climate change, and other anthropogenic disturbances on red grouper and other reef fishes in the Gulf of Mexico. Integr. Comp. Biol. 50:201–212.

Crabtree, R. E., and L. H. Bullock.
1998. Age, growth, and reproduction of black grouper, *Mycteroperca bonaci*, in Florida waters. Fish. Bull. 96:735–753.

Domeier, M. L.
2004. A potential larval recruitment pathway originating from a Florida marine protected area. Fish. Oceanogr. 13:287–294.

Eklund, A.-M., D. B. McClellan, and D. E. Harper.
2000. Black grouper aggregations in relation to protected areas within the Florida Keys National Marine Sanctuary. Bull. Mar. Sci. 66:721–728.

Farmer, N. A., and J. S. Ault.
2011. Grouper and snapper movements and habitat use in Dry Tortugas, Florida. Mar. Ecol. Prog. Ser. 433:169–184.

Hazlett B., and H. E. Winn.
1962. Sound producing mechanism of the Nassau grouper, *Epinephalus striatus*. Copeia 1962:447–449.

Heyman, W. D., R. T. Graham, B. Kjerfve, and R. E. Johannes.
2001. Whale sharks *Rhincodon typus* aggregate to feed on fish spawn in Belize. Mar. Ecol. Prog. Ser. 215: 275–282.

Huntsman, G. R., J. Potts, R. W. Mays, and D. Vaughan.
1999. Groupers (Serranidae, Epinephelinae): endangered apex predators of reef communities. Am. Fish. Soc. Symp. 23:217–231.

Kadison, E., R. S. Nemeth, and J. E. Blondeau.
2009. Assessment of an unprotected red hind (*Epinephelus guttatus*) spawning aggregation on Saba Bank in the Netherlands Antilles. Bull. Mar. Sci. 85:101–118.

Kobara, S., and W. D. Heyman.
2010. Sea bottom geomorphology of multi-species spawning aggregation sites in Belize. Mar. Ecol. Prog. Ser. 405:243–254.

Kobara, S., W. D. Heyman, S. J. Pittman, and R. S. Nemeth.
2013. Biogeography of transient reef-fish spawning aggregations in the Caribbean: a synthesis for future research and management. *In* Oceanography and marine biology: an annual review, vol. 51 (R. N. Hughes, D. J. Hughes, and I. P. Smith, eds.), p. 281–326. CRC Press, Boca Raton, FL.

Koenig, C. C., F. C. Coleman, C. B. Grimes, G. R. Fitzhugh, K. M. Scanlon, C. T. Gledhill, and M. Grace.
2000. Protection of fish spawning habitat for the conservation of warm-temperate reef-fish fisheries of shelf-edge reefs of Florida. Bull. Mar. Sci. 66:593–616.

Locascio, J. V. and D. A. Mann.
2008. Diel periodicity of fish sound production In Charlotte Harbor, Florida. Trans. Am. Fish. Soc. 137:606–615.
2011a. Diel and seasonal timing of sound production by black drum (*Pogonias cromis*). Fish. Bull. 109:327–338.
2011b. Localization and source level estimates of black drum (*Pogonias cromis*) calls. J. Acoust. Soc. Am. 130:1868–1879.

Mallinson, D., A. Hine., P. Hallock, S. Locker, E. Shinn, D. Naar, B. Donahue, and D. Weaver.
2003. Development of small carbonate banks on the south Florida platform margin: response to sea level and climate change. Mar. Geol. 199:45–63.

Mann, D. A., J. V. Locascio, F. C. Coleman, and C. C. Koenig.
2009. Goliath grouper *Epinephelus itajara* sound production and movement patterns on aggregation sites. Endang. Species Res. 7:229–236.

Mann, D., J. Locascio, M. Schärer, M. Nemeth, and R. Appeldoorn.
2010. Sound production by red hind *Epinephelus guttatus* in spatially segregated spawning aggregations. Aquat. Biol. 10:149–154.

Ménard, A., K. Turgeon, and D. L. Kramer.
2008. Selection of diurnal refuges by the nocturnal squirrelfish, *Holocentrus rufus*. Environ. Biol. Fish. 82:59–70.

Mok, H. K., and R. G. Gilmore Jr.
1983. Analysis of sound production in estuarine aggregations of *Pogonias cromis*, *Bairdiella chrysoura*, and *Cynoscion nebulosus* (Sciaenidae). Bull. Inst. Zool. Acad. Sin. 22:157–186.

Myrberg, A. A.
1972. Social dominance and territoriality in bicolor damselfish (*Eupomacentrus partitus* (Poey) (Pisces: Pomacentridae). Behaviour 41:207–230.

Nelson, M. D, C. C. Koenig, F. C. Coleman, and D. A. Mann.
2011. Sound production of red grouper *Epinephelus morio* on the West Florida Shelf. Aquat. Biol. 12:97–108.

Nemeth, R. S.
2012. Species case studies: red hind—*Epinephelus guttatus*. *In* Reef fish spawning aggregations: biology, research and management (Y. Sadovy de Mticheson and P. L. Colin, eds.), p.412–417. Springer, New York.

Paz, G., and G. R. Sedberry.
2008. Identifying black grouper (*Mycteroperca bonaci*) spawning aggregations off Belize: conservation and management. Proc. Gulf Caribb. Fish. Inst. 60:577–584.

Roberts, C. M., J. P. Hawkins, and F. R. Gell.
2005. The role of marine reserves in achieving sustainable fisheries. Philos. Trans. R. Soc. Lond., B 360:123–132.

Rowell, T. J., M. T. Schärer, R. S. Appeldoorn, M. I. Nemeth, D. A. Mann, and J. A. Rivera.
2012. Sound production as an indicator of red hind density at a spawning aggregation. Mar. Ecol. Prog. Ser. 462:241–250.

Schärer, M. T., M. I. Nemeth, D. Mann, J. Locascio, R. S. Appeldoorn, and T. J. Rowell.
2012. Sound production and reproductive behavior of Yellowfin grouper, *Mycteroperca venenosa* (Serranidae) at a spawning aggregation. Copeia 2012:136–145.

Schärer, M. T., M. I. Nemeth, T. J. Rowell, and R. S. Appeldoorn.
2013. Sounds associated with the reproductive behavior of the black grouper (*Mycteroperca bonaci*). Mar. Biol. 161:141–147.

Schmale, M. C.
1981. Sexual selection and reproductive success in males of the bicolor damselfish, *Eupomacentrus partitus* (Pisces: Pomacentridae). Anim. Behav. 29:1172–1184.

Urick, R. J.
1983. Propagation of sound in the sea: transmission loss, I. *In* Principals of underwater sound, 3rd ed. (D. Heiberg and J. Davis, eds.), p. 99–146. McGraw-Hill Inc., New York.

Wall, C. C., B. T. Donahue, D. F. Naar, and D. A. Mann.
2011. Spatial and temporal variability of red grouper holes within Steamboat Lumps Marine Reserve, Gulf of Mexico. Mar. Ecol. Prog. Ser. 431:243–254.

Weaver, D. C., D. F. Naar, and B. T. Donahue.
2006. Deepwater reef fishes and multibeam bathymetry of the Tortugas South Ecological Reserve, Florida Keys National Marine Sanctuary, Florida. *In* Emerging technologies for reef fisheries research and management (J. C. Taylor, ed.), p. 48–68. NOAA Professional Paper NMFS 5.

Winn, H. E., J. A. Marshall, and B. Hazlett.
1964. Behavior, diel activities, and stimuli that elicit sound production and reactions to sounds in the longspine squirrelfish. Copeia. 1964:413–425.

Whaylen, L, C. V. Pattengill-Semmens, B. X. Semmens, P.G. Bush, and M.R. Boardman.
2004. Observations of a Nassau grouper, *Epinephelus striatus*, spawning aggregation site in Little Cayman, Cayman Islands, including multi-species spawning information. Environ. Biol. Fish. 70:305–313.

NOAA
National Marine
Fisheries Service

Fishery Bulletin
established 1881

Spencer F. Baird
First U.S. Commissioner
of Fisheries and founder
of *Fishery Bulletin*

Unreported catch and tourist demand on local fisheries of small island states: the case of The Bahamas, 1950–2010

Nicola S. Smith[1]
Dirk Zeller[2]

Email address for contact author: nicolas@sfu.ca

[1] Earth to Ocean Research Group
Department of Biological Sciences
Simon Fraser University
8888 University Drive
Burnaby, British Columbia, Canada V5A 1S6

[2] Sea Around Us
Global Fisheries Cluster
University of British Columbia
2202 Main Mall
Vancouver, British Columbia, Canada V6T 1Z4

Abstract—Tourism is vital to the economy of small island states like The Bahamas and is closely linked to fisheries. Fish is a protein source for tourists and residents, and both groups expect to catch and eat local fish. To adequately manage these dual demands, we need to know total removals of fish, as well as patterns of demand by tourists and residents in the past and present. Using a reconstruction approach, we performed a comprehensive accounting of fisheries catches in The Bahamas from commercial and noncommercial sectors for 1950–2010 and estimated the demand from tourism over the same period. Our results distinctly contrast with national data supplied to the Food and Agriculture Organization of the United Nations (FAO), which presents only commercial landings. Reconstructed total catches (i.e., reported catches and estimates of unreported catches) were 2.6 times the landings presented by the FAO for The Bahamas. This discrepancy was primarily due to unreported catches from the recreational and subsistence fisheries in the FAO data. We found that recreational fishing accounted for 55% of reconstructed total catches. Furthermore, 75% of reconstructed total catches were attributable to tourist demand on fisheries. Incomplete accounting for catches attributed to the tourist industry, therefore, makes it difficult to track potentially unsustainable pressures on fisheries resources.

Manuscript submitted 19 January 2015.
Manuscript accepted 3 December 2015.
Fish. Bull. 114:117–131 (2016).
Online publication date: 29 December 2015.
doi: 10.7755FB.114.1.10

Tourism is one of the largest and fastest growing industries globally (UNWTO, 2014a), and is vital to many small island developing states in which it can account for more than one-quarter of gross domestic product (GDP) (UNWTO, 2014b). In addition to its influence on island economies, tourism can have large effects on the extraction of natural resources like fisheries, particularly in the Caribbean, where visitors can greatly outnumber resident populations (Table 1, Fig. 1). Tourism, through recreational fishing and the consumption of local seafood by tourists, increases the demand on local fisheries.

Consider the case of the Commonwealth of The Bahamas, a nation of small islands, for which tourism is the primary industry, which accounted for 51% of GDP in 2003 (Sacks[1]). Located in the northern Caribbean east of Florida and northeast of Cuba, between 20–27°N and 72–79°W, The Bahamas form an archipelago of more than 3000 low-lying islands and cays. They comprise a total land area of just under 14,000 km,[2] and the area of its exclusive economic zone (EEZ) is more than 629,000 km^2 (Fig. 2). Tourism did not become a year-round industry in The Bahamas until the 1950s, when the advent of air-conditioning in local hotels made the hotter months of the year bearable for visitors (Cleare, 2007). Since then, the total number of visitors per year has grown substantially; by 2010, visitors swelled to more than 5.3 million per year (The Bahamas Ministry of Tourism[2]) and outnumbered the resident population of more than 350,000 (The Bahamas Department of Statistics[3]) by an order of magnitude (Table 1, Fig. 1).

[1] Sacks, A. 2006. The Bahamas total tourism economic impact: preliminary results, 8 p. Report prepared for Ministry of Tourism, The Bahamas. Global Insight Inc, Waltham, MA.

[2] The Bahamas Ministry of Tourism. 2011. December 2010 preliminary revised foreign arrivals by first port of entry. [Spreadsheet available at website.]

[3] The Bahamas Department of Statistics. 2010. Percentage distribution of population by island:2000 and 2010 Censuses, 1 p. [Available at website.]

Table 1

Number of tourists compared with residents in 2010 for the Caribbean countries and territories where the top 10 greatest number of stopover visitors were reported that year.

Country	Stopover visitors (10^3) [1]	Cruise visitors (10^3) [1]	Total visitors (10^3)	Resident population (10^3) [1]	Stopover visitors as % of resident population	Mean length of stay for stopover visitors (nights) [1]
Aruba	824	569	1394	108	763	7.8
Bahamas	1370	3810	5180	347	395	6.8
Barbados	532	665	1197	275	194	9.8
Cuba	2532	unavailable	unavailable	11,242	23	10.9
Dominican Republic	4125	353	4477	9974	41	9.2
Jamaica	1922	910	2831	2702	71	9.0
Martinique	476	75	551	400	119	13.3
Puerto Rico	1369	1191	2560	3979	34	2.6
St. Maarten	443	1513	1956	37	1198	unavailable
U.S. Virgin Islands	691	1859	2550	110	628	unavailable

[1] Source: Caribbean Tourism Organization.

The combined demand for local fishes in The Bahamas by a burgeoning tourist industry and a growing resident population raises an important question: can domestic fisheries keep up with the current patterns of fishing and seafood consumption of both groups in the long term? To address this question, comprehensive statistics on total removals from commercial and noncommercial fishing sectors and on patterns of local demand on fisheries by tourists and residents are fundamental, as are assessments of the status of stocks of the main target species. The government of The Bahamas, however, currently lacks the financial resources and technical expertise needed to adequately assess fish stocks (CFU[4]), and it does not track the local demand on fisheries by either residents or tourists. Similarly, although some national statistics exist for commercial landings, catch from other important noncommercial sectors, like recreational fishing, are ignored.

Fisheries in The Bahamas, like most tropical nearshore fisheries of the Caribbean, western Pacific, and Southeast Asia, are data poor in that they lack conventional, "scientific" data (e.g., on stock age structure, natural and fishing mortality, catch per unit of effort over time) or lack rigorous analyses of reliable data (Johannes, 1998; Bentley and Stokes, 2009). In such instances, a variety of alternative approaches to traditional stock assessment have been used to develop reference points for management—methods that include sequential trends analysis (e.g., depletion-corrected average catch [DCAC], MacCall, 2009; cumulative sum [CUSUM], Manly and Mackenzie, 2000), vulnerability analysis (e.g., productivity-susceptibility analysis of vulnerability [PSA], Field et al., 2010), and extrapolation (e.g., Robin Hood approach, Smith et al., 2009).

These methods for analysis of data-poor fisheries often overlap, are complementary, or are nested within other methods. Moreover, these methods differ in their requirements for the quality and quantity of data and, therefore, involve varying degrees of uncertainty and require precautionary buffers (Honey et al., 2010). For example, a variety of techniques are used in sequential trends analysis to detect trends and infer changes in fish populations or stocks from available time-series data, whereas extrapolation methods, such as the Robin Hood approach, are used when virtually no conventional, scientific data are available. For the latter analyses, the local knowledge of fishermen and other resource users are used, as well as the information inferred from assumptions based on data-rich fisheries (Honey et al., 2010).

In this study, we used the recent, globally established catch reconstruction approach of Zeller et al. (2007, 2015) for data-limited fisheries, a method that also has been used successfully in nontropical areas (e.g., Zeller et al., 2011a, 2011b), to retroactively estimate a time series of commercial and noncommercial marine fisheries catches for The Bahamas during 1950–2010. We chose the year 1950 as our starting point because it is the first year for which data were available in the global landings database of the FAO. Another objective of this study was to estimate local demand on fisheries by the tourist industry over the same period. As described previously, tourism is the primary industry in The Bahamas and is closely linked to fisheries. To better understand historical trends in fisheries catches (and predict future trends), we must view these patterns in light of changes in tourist demand on local fisheries.

[4] CFU (CARICOM Fisheries Unit). 2001. Report of the multidisciplinary survey of the fisheries of the Bahamas, 43 p. CFU, Belize City, Belize. [Available at website.]

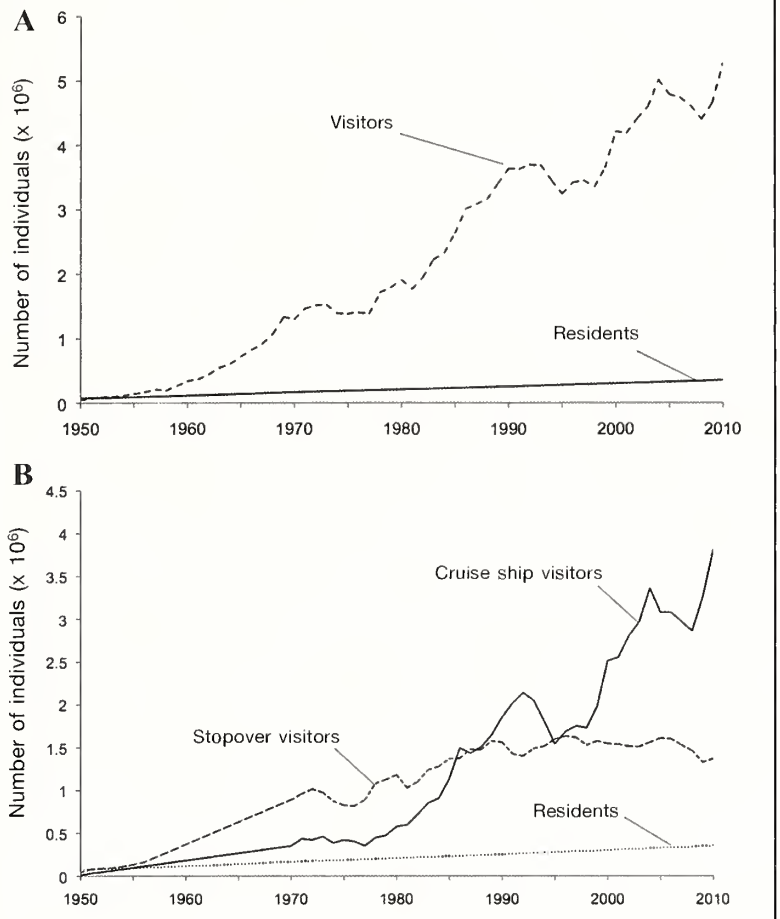

Figure 1

For The Bahamas during 1950–2010, (**A**) number of residents compared with total number of visitors and (**B**) number of residents compared with total number of stopover visitors, who stay at least one night, and total number of cruise ship visitors, who partake in shore visits.

Materials and methods

Reconstruction of marine fisheries catches

Reconstruction of fisheries catches is an approach to retroactively estimate catches when reliable time-series data are lacking (Zeller et al., 2007, 2015). In some instances, this approach has involved interpolations, cautious extrapolation, and assumptions based on local expert opinion in lieu of quantitative data. The use of interpolations, extrapolation, and assumptions has resulted in potentially higher uncertainty in some of the data provided here (see also Zeller et al., 2011a, 2015), but this approach is justifiable because of the unacceptable alternative, namely that catches for missing sectors, taxa, or time periods would be interpreted as zero catches—an outcome that has serious consequences for effective management and conservation (Pauly, 1998).

The catch reconstruction approach used here consists of 7 general steps (Zeller et al., 2007, 2015):

1. Identification of existing time-series data on catches to validate the quality of data transfer from national (e.g., annual reports from the Bahamas Department of Marine Resources, previously named the Department of Fisheries) to international (e.g., FAO reported landings data by FAO area, taxon, and year) levels.
2. Identification of sectors, time periods, taxa, etc. not covered by step 1 through literature searches and local expert consultations.
3. Search for available information sources to serve as alternatives to missing catch data identified in step 2, through comprehensive literature searches and local expert consultations. In this step, we look for any source of information, including case studies, health studies, household surveys, technical reports, data sets, and expert opinion.
4. Development of data *anchor points* in time for missing segments based on data and information sources discovered in step 3, and expansion of them to countrywide catch estimates for each sector or taxa by using clearly stated and conservative assumptions.
5. Application of interpolation for time periods between data anchor points for each fishing sector or taxa, either linearly or on the basis of assumptions for commercial sectors, and application of interpolation, typically through per capita catch rates for noncommercial sectors, taking into account major political, socioeconomic, and environmental impacts.
6. Estimation of final time series of total catch by combining reported catches (identified in step 1) and interpolated, country-expanded, missing data segments (produced in step 5). The final data series shows catch by fisheries sector, taxon, and year. We define fisheries sectors using country- or regional-specific definitions: large-scale commercial, *artisanal* (small-scale commercial), *subsistence* (small-scale noncommercial), and *recreational* (small-scale noncommercial)
7. Expression of the level of uncertainty in the data and information sources and in the assumptions made during reconstruction, by fishing sectors and time periods of the reconstruction. This final step is based on "scoring" criteria inspired by the Intergovernmental Panel on Climate Change (Mastrandrea et al., 2010; Table 2). Because the senior author of

Table 2

Score used for evaluating the quality of the time series of reconstructed catches, with their range of uncertainty (Intergovernmental Panel on Climate Change [IPCC] criteria from Figure 1 of Mastrandrea et al. [2010]).

Score		Range of uncertainty – %	Range of uncertainty + %	Corresponding IPCC criteria
4	Very high	10	20	High agreement between multiple sources for the same data and robust evidence of data accuracy
3	High	20	30	High agreement between multiple sources for the same data and medium evidence of data accuracy, or medium agreement between multiple sources for the same data and robust evidence of data accuracy
2	Low	30	50	High agreement between multiple sources for the same data and limited evidence of data accuracy, or medium agreement between multiple sources for the same data and medium evidence of data accuracy, or low agreement between multiple sources for the same data and robust evidence of data accuracy
1	Very low	50	90	Low agreement between multiple sources for the same data and low evidence of data accuracy

the study described here was most familiar with the data and information sources used, she reviewed the underlying data and assumptions of the reconstruction, by fishing sectors and by 3 time periods, and assigned relative uncertainty scores, by sector and time period. Scores were then catch-weighted by sector to derive average upper and lower ranges of uncertainty for each of 3 time periods (Table 3): early (1950–1969), mid (1970–1989) and late (1990–2010). Note that scoring does not reflect the method of reconstruction but actually the relative "trustworthiness" of the data and information sources per sector and time period.

Details on these steps in general and as they were applied specifically to The Bahamas are provided in Zeller et al. (2015) and Smith and Zeller[5], respectively. Here, we summarize the major information and data sources, approaches, and assumptions involved in estimating catches from 3 sectors: 1) commercial fisheries, which is further subdivided into the artisanal fishery and the large-scale fishery for Caribbean spiny lobster (*Panulirus argus*); 2) subsistence fishery; and 3) recreational fishery. We also estimated the demand on fisheries from the tourist industry for the period 1950–2010. It is of key importance for readers to understand that we aim to address and improve the accuracy of catch data, and not the precision of the estimates, as we attempt to address an inherent negative bias in reported data (i.e., the result of the absence of data, and hence effective substitution with a zero, for catches taken by sectors, such as recreational fisheries, that are not part of the current data monitoring system; see also Covey, 2000).

Commercial fishery

The Bahamas provide national data on only commercial (i.e., both artisanal and large-scale Caribbean spiny lobster) landings to FAO (Braynen[6]). We compared available national statistics (based on data from annual reports published by colonial and national governments of The Bahamas[HMSO[7], BDF[8]]) with

[5] Smith, N. S., and D. Zeller. 2013. Bahamas catch reconstruction: fisheries trends in a tourism-driven economy (1950–2010), 28 p. Fisheries Centre Working Paper #2013-08. Univ. British Columbia, Vancouver, Canada. [Available at website.]

[6] Braynen, M. 2011. Personal commun. The Bahamas Department of Marine Resources, Nassau, The Bahamas 3028.

[7] HMSO (Her Majesty's Stationery Office). 1952. Report for The Bahama Islands, 1950–1951, 42 p. Colonial Annual Reports. Colonial Office, HMSO, London.
HMSO (Her Majesty's Stationery Office). 1955. Report for The Bahama Islands, 1952–1953, 48 p. Colonial Annual Reports. Colonial Office, HMSO, London.
HMSO (Her Majesty's Stationery Office). 1957. Report for The Bahama Islands, 1954–1955, 50 p. Colonial Annual Reports. Colonial Office, HMSO, London.
HMSO (Her Majesty's Stationery Office). 1959. Report for The Bahama Islands, 1956–1957, 64 p. Colonial Annual Reports. Colonial Office, HMSO, London.
HMSO (Her Majesty's Stationery Office). 1961. Report for The Bahama Islands, 1958–1959, 70 p. Colonial Annual Reports. Colonial Office, HMSO, London.
HMSO (Her Majesty's Stationery Office). 1963. Report for The Bahama Islands, 1960–1961, 75 p. Colonial Annual Reports. Colonial Office, HMSO, London

[8] BDF (Bahamas Department of Fisheries). 1990. Annual Report 1990, 85 p. BDF, Nassau, The Bahamas.
BDF (Bahamas Department of Fisheries). 1991. Annual Report 1991, 130 p. BDF, Nassau, The Bahamas.
BDF (Bahamas Department of Fisheries). 1992. Annual Report 1992, 85 p. BDF, Nassau, The Bahamas.
BDF (Bahamas Department of Fisheries). 1993. Annual Report 1993, 116 p. BDF, Nassau, The Bahamas.
BDF (Bahamas Department of Fisheries). 1996. Annual Report 1996, 35 p. BDF, Nassau, The Bahamas.

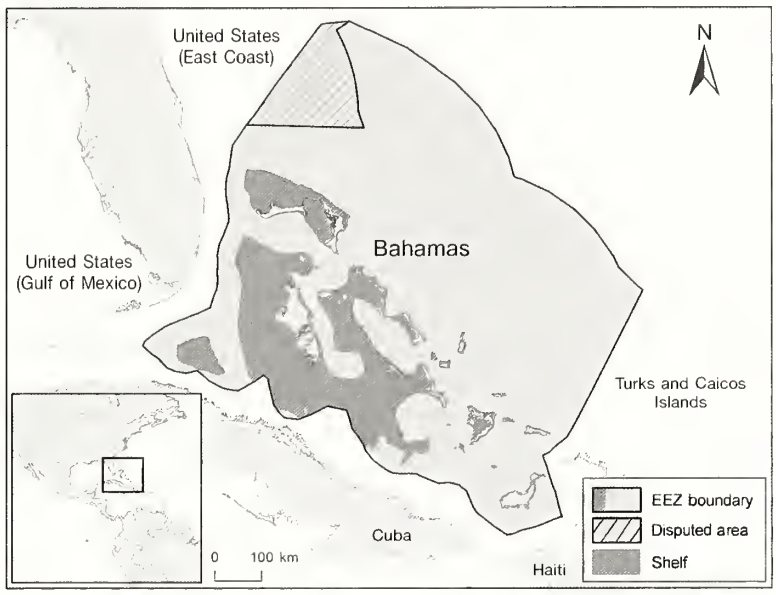

Figure 2

Map of the Commonwealth of The Bahamas showing the exclusive economic zone (EEZ), which has an area of more than 629,000 km^2, and shelf areas (to a depth of 200 m) that cover more than 108,000 km^2.

FAO data that we accessed through the FAO application FishStatJ (Capture Production data set, available at website), and we concluded that there was a good transfer of data from the national to the international level for the postcolonial period (i.e., ~1970–2010). We, therefore, used FAO data as the basis for further calculations for 1970–2010. National commercial landings from 1970 to 2010, however, were systematically underreported because they were based on the sampling of a subset of landing sites (i.e., sites where commercial fishing boats "land" or dock) and there was no attempt to expand the data set to include sites that were not sampled (Braynen[6]). Given that the total number of landing sites in The Bahamas is unknown, we relied on local expert opinion from staff of The Bahamas Department of Marine Resources regarding the fraction of commercial catch for each taxon that was likely not to be reported. We then retroactively adjusted FAO data from 1970 to 2010 to account for countrywide, unreported commercial landings (Braynen[6]; Table 4).

We concluded that FAO data on capture tonnage are underestimates of the actual tonnage of commercial catches during the colonial period because FAO data did not closely match national (colonial) statistics for the period 1950–1969. Colonial statistics for these years consisted almost entirely of domestic catches that were exported. For example, FAO reports a total catch of 600 metric tons (t) in 1950, but a Colonial Annual Report for The Bahamas states that more than twice that amount (i.e., 1381 t) was exported as Caribbean spiny lobster alone in that year (HMSO, report 1950–1952[7]). To address the problem of underreported commercial catches, we calculated the average per capita commercial catch rate for the years 1970–1975 (on the basis of our expanded, countrywide commercial catch estimates) and applied this catch rate to the human population census data for 1950–1969. Our method resulted in an estimate of total commercial catch for the colonial period that was 11% higher than the level reported in the FAO data. We acknowledge that per capita commercial catch rates likely were greater in 1970–1975 than in 1950–1969; however, our estimates for earlier time periods are still conservative because our assessment of total commercial catches in 1950 (i.e., 1221 t) was less than the level reported for exports of Caribbean spiny lobster alone.

To determine the taxonomic composition of the commercial catches for 1950–2010, we combined FAO data with statistics from the annual reports published by the national government and with expert opinion of staff from the Department of Marine Resources (for details, see Smith and Zeller[5]).

Subsistence fishery

We are unaware of any written reports that quantify the extent of subsistence fishing in The Bahamas. Therefore, we relied on 2 sources to estimate catch from this sector: 1) resident population data and 2) expert opinion of staff of the Department of Marine Resources (Table 4).

Using the groupings and definitions used in The Bahamas, we divided the islands of The Bahamas into 1) the more developed islands of New Providence and Grand Bahama and 2) the remaining, less developed islands, which are referred to collectively as the "Family

Table 3

Fisheries sectors and associated ranges of uncertainty for reconstruction of catches in The Bahamas for 3 time periods. We divided catch into 3 sectors: 1) commercial fisheries, which was further subdivided into the artisanal fishery and the large-scale fishery for Caribbean spiny lobster (*Panulirus argus*), 2) the recreational fishery, defined as small-scale noncommercial fishing that is primarily for recreation and in which catch is not sold or bartered and, 3) subsistence fishery, defined as small-scale noncommercial fishing in which catch does not enter the formal market but is taken home and consumed by fishermen and their families or is locally bartered.

Sector	Years	Score	Uncertainty range	
			–%	+%
Artisanal	1950–1969	3	20	30
Artisanal	1970–1989	4	10	20
Artisanal	1990–2010	4	10	20
Large-scale Caribbean spiny lobster	1950–1969	2	30	50
Large-scale Caribbean spiny lobster	1970–1989	4	10	20
Large-scale Caribbean spiny lobster	1990–2010	4	10	20
Recreational	1950–1969	1	50	90
Recreational	1970–1989	2	30	50
Recreational	1990–2010	3	20	30
Subsistence	1950–1969	1	50	90
Subsistence	1970–1989	1	50	90
Subsistence	1990–2010	1	50	90

Islands." Few economic opportunities existed for most Bahamians during 1950–1969, particularly in the less developed Family Islands. On the basis of local expert opinion, we assumed that, for the period 1950–1969, 40% of the residents of the Family Islands ate per week the equivalent in weight of 2 plate-size snappers (i.e., ~32.55 kg·person^{-1}·year^{-1}) obtained from subsistence fishing and that 10% of residents of the more developed islands of New Providence and Grand Bahama ate per week the equivalent in weight of 1 plate-size snapper (i.e., ~16.29 kg·person^{-1}·year^{-1}) obtained through subsistence fishing (Braynen[6]).

Following the beginning of the political rule of the black majority in 1967 and of independence from Britain in 1973, economic opportunities increased considerably for most Bahamians; hence, their reliance on subsistence fisheries was expected to have decreased. On the basis of local expert opinion, we assumed that throughout the 1970s the number of people dependent on subsistence fisheries steadily decreased so that, by 1980–2010, only 20% of residents of the Family Islands had a subsistence catch rate of 32.55 kg·person^{-1}·year^{-1} and 5% of the residents of New Providence and Grand Bahama had a subsistence catch rate of 16.29 kg·person^{-1}·year^{-1} (Braynen[6]).

We are unaware of any published subsistence catch rates for other Caribbean countries that are based on empirical data. However, our estimates are comparable to fresh seafood consumption rates determined from household surveys for Anguilla (26.2 kg·person^{-1}·year^{-1}) (Jones[9]) and for the Turks and Caicos Islands, where 97% of households ate fish at least once per week, 79% ate queen conch (*Strombus gigas*) more than once per week, and 46% of households consumed Caribbean spiny lobster more than once per week (Maitland, 2006).

To determine the taxonomic composition of subsistence catches throughout the time series, we assumed the same species composition and relative species proportions as those of the commercial shallow-water fisheries. However, we excluded deepwater finfishes, sharks, crabs, and sea cucumbers from subsistence composition (Smith and Zeller[5]).

Recreational fishery

We divided recreational catches into 2 categories: 1) fish that were caught during major tournaments and 2) fish that were caught for recreation outside of tournaments (Table 4).

The United States Recreational Billfish Survey (RBS) program recorded total billfish catches (in numbers) and effort data from major fishing tournaments in several parts of the Atlantic, including in The Bahamas during 1972–2007. Data from the RBS also include the fate of fish that were caught (i.e., retained, released, or tagged and released [Diaz et al., 2007]). We used data directly from the RBS program to determine the quantity of blue marlin (*Makaira nigricans*), white marlin (*Kajikia albida*), and sailfish (*Istiophorus platypterus*) that were retained during tournaments during 1972–

[9] Jones, T. P. 1985. The fishing industry of Anguilla 1985, 38 p. A report prepared for the Anguillan government and Commonwealth Secretariat, Anguilla.

Table 4

Data sources, assumptions, and parameters used for reconstruction of catches in The Bahamas for the period 1950–2010. The FAO data used for this study came from the Capture Production data set accessed through the FAO application FishStatJ.

Sector	Year	Sources	Comments	Parameter
Commercial	1950–1969	Assumption and resident population census data	Used mean per capita commercial catch rate for years 1970–1975 based on our expanded, countrywide commercial catch estimates	Per capita catch rate of 153.3 kg·person^{-1}·year^{-1}
Commercial	1970–2010	FAO data and expert opinion from staff of The Bahamas Dep. Mar. Res.	Retroactively raised FAO data by major taxa each year to account for countrywide, unreported commercial landings	*Haemulon* spp.=1.1 times FAO data Jacks (Carangidae)=1.15 times FAO data Nassau grouper (*Epinephelus striatus*)=1.1 times FAO data Other groupers (Epinephelidae)=1.1 times FAO data Misc. marine fishes=1.15 times FAO data Queen conch (*Strombus gigas*)=1.15 times FAO data Sharks=1.05 times FAO data Snappers (Lutjanidae)=1.15 times FAO data Caribbean spiny lobster (*Panulirus argus*)=1.05 times FAO data Florida stone crab (*Menippe mercenaria*)=1.03 times FAO data
Subsistence	1950–1969	Expert opinion of staff from Dep. Mar. Res. and resident population census data	Assumed a heavy reliance on subsistence fisheries because few economic opportunities existed for most Bahamians during colonial period	Per capita subsistence catch rate of 32.55 kg·person^{-1}·year^{-1} for 40% of residents of the Family Islands Per capita subsistence catch rate of 16.29 kg·person^{-1}·year^{-1} for 10% of residents of the more developed islands of New Providence and Grand Bahama
Subsistence	1970–1979	Assumption	Linearly interpolated total annual catch by residents of the Family Islands and of New Providence and Grand Bahamas between 1969 and 1980.	Total annual subsistence catch declined by 27 t/year for the Family Islands and by 7 t/year for New Providence and Grand Bahama
Subsistence	1980–2010	Expert opinion from staff of the Dep. Mar. Res. and resident population census data	Assumed reliance on subsistence fisheries decreased after the beginning of black majority political rule in 1967 and independence from Britain in 1973. Assumed that the per capita subsistence catch rate was the same as the rate in 1950–1969 but that the percentage of people dependent on subsistence fisheries decreased by 50% for residents of the Family Islands and of New Providence and Grand Bahama.	Per capita subsistence catch rate of 32.55 kg·person^{-1}year^{-1} for 20% of residents of the Family Islands Per capita subsistence catch rate of 16.29 kg·person^{-1}·year^{-1} for 5% of residents of more developed islands of New Providence and Grand Bahama
Recreational (billfish catch from major tournaments)	1950	Assumption based on data from the U.S. Recreational Billfish Survey (RBS) program	There were fewer tournaments in 1950 than in 1972, which is the first year of RBS data for The Bahamas. Assumed that total catches in 1950 were half that of 1972.	Total catch was 3.65 t/year

Table continued

Table 4 (continued)

Sector	Year	Sources	Comments	Parameter
Recreational (billfish catch from major tournaments)	1951–1971	Assumption	Linearly interpolated total tournament catches for 1951–1971.	Total catch increased at rate of 0.17 t/year
Recreational (billfish catch from major tournaments)	1972–2006	Data from the RBS program	Used data directly from the RBS program	Contact the NOAA Southeast Fisheries Science Center for details
Recreational (billfish catch from major tournaments)	2007–2010	Assumption based on data from the RBS program	Organizers stopped reporting catches to the RBS program after 2007, and incomplete reporting likely occurred in 2007. Used mean annual catch for the years 2000–2006 for remainder of time series	Total catch of 6.08 t/year
Recreational (catch outside of tournaments—tourists)	1950–1985	Assumption based on visitor arrival data, 1980 visitor activities survey report and 1986 recreational fishing regulations for visitors to The Bahamas	Prior to 1986, there were no maximum catch limits for recreational fishing. Assumed that visitors retained twice as much as the maximum per capita catch limits stipulated in the 1986 legislation	Per capita recreational catch rate of 136 $kg \cdot person^{-1} \cdot visit^{-1}$
Recreational (catch outside of tournaments—tourists)	1986–2006	Visitor arrival data, 1980 visitor activities survey report, and recreational fishing regulations for visitors to The Bahamas	Catch rate represents 80% of the per capita allowable catch limit. Assumed that visitors adhered to the catch limits	Per capita recreational catch rate of 54 $kg \cdot person^{-1} \cdot visit^{-1}$
Recreational (catch outside of tournaments—tourists)	2007–2010	Assumption based on visitor arrival data, 1980 visitor activities survey report, and 1986 recreational fishing regulations for visitors to The Bahamas	Recreational fishing legislation revised with the aim of reducing total annual catch by 50%. Catch rate represents 50% of the per capita allowable catch limit based on 1986 legislation. Assumed that visitors adhered to the catch limits	Per capita recreational catch rate of 34 $kg \cdot person^{-1} \cdot visit^{-1}$
Recreational (catch outside of tournaments—residents)	1950–1969	Expert opinion from staff of the Dep. Mar. Res., resident population census data, and 1986 recreational fishing regulations for visitors	Assumed that 0.5% of residents of the Family Islands fished for recreation 6 times a year and 1% of residents of New Providence and Grand Bahama fished for recreation 4 times a year. For each trip, we assumed that residents caught 50% of the 1986 maximum per capita catch limits for visitors (i.e., 34 $kg \cdot fisherman^{-1} \cdot trip^{-1}$).	Recreational catch rate of 204 $kg \cdot fisherman^{-1} \cdot year^{-1}$ for residents of the Family Islands and 136 $kg \cdot fisherman^{-1} \cdot year^{-1}$ for residents of New Providence and Grand Bahama
Recreational (catch outside of tournaments—residents)	1970–2010	Expert opinion from staff of the Dep. Mar. Res., resident population census data, and recreational fishing regulations for visitors	Assumed that recreational fishing increased with increasing economic opportunities, particularly for residents of New Providence and Grand Bahama. Assumed that both the percentage of residents that fished for recreation and the frequency of recreational fishing doubled for residents of New Providence and Grand Bahama. Hence, 2% of residents of New Providence and Grand Bahama fished for recreation 8 times a year. Assumed that the percentage of residents of the Family Islands that fished for recreation did not change during 1950–1969 (i.e., 0.5%) but that the frequency with which they fished doubled to 12 times a year. For each trip, we assumed that residents of the Family Islands and of New Providence and Grand Bahama caught 50% of the 1986 maximum per capita catch limits for visitors (i.e., 34 $kg \cdot fisherman^{-1} \cdot trip^{-1}$).	Recreational catch rate of 408 $kg \cdot fisherman^{-1} year^{-1}$ for 0.5% of residents of the Family Islands and 272 $kg \cdot fisherman^{-1} \cdot year^{-1}$ for 2% of residents of New Providence and Grand Bahama

2006 (Table 4). Before 1972, data for The Bahamas were not collected during the RBS program, and there were also fewer tournaments and, therefore, presumably, lower total tournament catches (Cleare, 2007). Hence, we assumed that billfish catches in 1950 were half those in 1972, and we linearly interpolated catches for 1951–1971 (Table 4). In 2007, the quality of the tournament catch data that was reported to the RBS program was likely to have deteriorated; after 2007 organizers stopped reporting catches for The Bahamas to the RBS program altogether (Venizelos[10]). We, therefore, calculated mean annual tournament catch for the years 2000–2006 and held this value constant for the remainder of the time series, although this calculation could have resulted in an underestimate (Table 4).

It is important to note that other pelagic species, such as dolphinfish (*Coryphaena hippurus*), wahoo (*Acanthocybium solandri*), and tunas, are also caught during tournaments. We did not, however, have access to any data or information on the quantities of non-billfish species that were retained during tournaments. Therefore, our estimate of total retained catch during tournaments is limited to billfish species and is highly conservative.

To estimate catches outside of tournaments, we separated data into 2 categories: 1) fish caught by visitors and 2) fish caught by residents.

We relied on 3 information sources to reconstruct visitor catches: 1) visitor arrival data; 2) the Ministry of Tourism visitor activities survey report; and 3) recreational fishing regulations for visitors to The Bahamas (Table 4). We estimated recreational catch of visitors by combining data on the number of visitors per year with the proportion of visitors that indicated that they fished during their stay (values were based on the Ministry of Tourism 1980 visitor activity survey report, as presented in Thompson [1989]), along with per capita maximum allowable catch for demersal and pelagic species, as stipulated in the Fisheries Resources (Jurisdiction and Conservation) Regulations of 1986 [available at website]. We estimated a per capita recreational catch rate of 54 kg·person^{-1}·visit^{-1} during 1986–2006. This catch rate was determined with the assumption that the proportion of visitors that fished during their stay remained constant during 1986–2006 (i.e., 6.2%, 5.3%, and 20.0% of stopover visitors to New Providence, Grand Bahama, and the Family Islands, respectively), and this rate represents 80% of the per capita allowable catch for key taxa. This catch rate is conservative given that the number of visitors who have fished in The Bahamas during their stay has increased in recent times and given that catches by visitors to The Bahamas were often thought to exceed maximum catch limits (Cox et al., 2005).

Before 1986, there were no maximum catch limits for recreational fishing in The Bahamas. Moreover, during this period many visitors exploited this lack of regulation by actually fishing commercially (Thompson, 1989). We, therefore, assumed (on the basis of the number of stopover visitors per year and the visitor activity survey report) that, during 1950–1985, visitors who fished in The Bahamas during their stay caught and retained twice as much as the maximum per capita catch limits stipulated for key taxa in the 1986 legislation (i.e., ~136 kg·person^{-1}·visit^{-1}). In 2007, the government of The Bahamas revised the maximum catch limits for key taxa with the aim of reducing total catch. The government assumed that this revision would result in a 50% reduction in catches from the catch rate observed in 1986 (Braynen[6]). In the absence of better data, we accepted this assumption and applied a recreational per capita catch rate of 34 kg·person^{-1}·visit^{-1}, estimating that visitors caught 50% of the 1986 catch limits for key taxa (Table 4).

Much less is known about the regular recreational fishing habits of residents. Unlike the existence of legislation for visitors, there is currently no legislation that limits the quantity of fish that may be caught by residents for recreational purposes. Therefore, we relied on 3 sources to estimate catch for this component: 1) resident population data; 2) expert opinion of staff from the Department of Marine Resources; and 3) The Bahamas recreational fishing regulations for visitors (Table 4). We assumed that, during 1950–1969, 0.5% of residents of the Family Islands fished for recreation 6 times a year and 1% of residents of New Providence and Grand Bahama fished recreationally 4 times a year (Braynen[6]). For each trip, it was assumed that residents caught 50% of the 1986 maximum per capita catch limits for key taxa for visitors (i.e., 34 kg·person^{-1}·trip^{-1}). This assumption amounts to an annual recreational catch rate of 204 kg·fisherman^{-1}·year^{-1} and 136 kg·fisherman^{-1}·year^{-1} for Family Islanders and residents of New Providence and Grand Bahama, respectively.

With increasing economic opportunities in the 1970s, recreational fishing is also likely to have increased, particularly on New Providence and Grand Bahama. According to expert opinion from staff of the Department of Marine Resources (Braynen[6]), during 1970–2010, 2% of residents of New Providence and Grand Bahama fished for recreation 8 times a year. By comparison, although the proportion of residents fishing recreationally in the Family Islands did not change, the frequency with which they fished increased. Hence, it was assumed that during 1970–2010, 0.5% of Family Islanders fished for recreation once a month. A catch rate of 34 kg·person^{-1}·trip^{-1} translates to annual catches of 272 kg·fisherman^{-1}·year^{-1} for residents of New Providence and Grand Bahama and to a rate of 408 kg·fisherman^{-1}·year^{-1} for residents of the Family Islands.

To determine the taxonomic composition for recreational catches from tournaments, we relied on information from the RBS program; for catches outside of tournaments, we relied on 3 sources: 1) recreational fishing regulations; 2) Thompson (1989); and 3) demersal catch composition from commercial fisheries (for details, see Smith and Zeller[5]).

[10]Venizelos, A. 2012. Personal commun. Southeast Fish. Sci. Cent., Natl. Mar. Fish. Serv., NOAA, Miami, FL 33149.

Use of expert opinion in reconstruction of fisheries catch data

An expert is someone who possesses knowledge about a given topic through training, research, practicing of skills, or personal experience (Burgman et al., 2011). Elicitation of expert opinion has been used for a variety of environmental issues, including conservation (e.g., Murray et al., 2009), invasive species management (e.g., Kuhnert, 2011), climate change impacts (e.g., Morgan et al., 2001), and models of managed systems, such as logged forests (e.g., Crome et al., 1996) and data-limited fisheries (e.g., Griffiths et al., 2007). Many of the parameters in our reconstruction are derived from the opinion of a single expert (i.e., M. Braynen, Director of the Department of Marine Resources) because of limited empirical data (Table 4). Nevertheless, we followed the 5 general steps described by Martin et al. (2012) to elicit expert knowledge:

1. Decide how information will be used;
2. Determine what to elicit;
3. Design the process for eliciting information;
4. Execute the process for eliciting information; and
5. Translate the information for use in a model.

We elicited expert information both directly and indirectly for use in our catch reconstruction. Direct elicitation of information involved posing questions that would provide quantitative responses that could be used directly in the reconstruction. For example, we asked: What percentage of commercial catch of Caribbean spiny lobster do you think is unreported?

In contrast, indirect elicitation of information involved posing questions that resulted in responses that were subsequently converted to quantitative values for use in our reconstruction. For example, to come up with the estimate for the subsistence catch rate of 32.55 $kg \cdot person^{-1} \cdot year^{-1}$ for 40% of residents of the Family Islands during 1950–1969, we asked 2 questions: 1) what percentage of residents of the Family Islands do you think relied on subsistence fishing for at least part of their dietary requirements from 1950 through 1969? and 2) Given your answer to question 1, if we estimated the amount of seafood obtained through subsistence fishing from 1950 through 1969 in terms of the number of plate-sized snappers consumed per person per week, how many plate-size snappers per person per week do you think were obtained by subsistence fishing in the Family Islands?

In all instances, information was elicited through one-on-one interviews with the expert either in person or over the telephone. It should be noted, however, that we did not directly elicit an estimate of uncertainty around a model parameter from the expert. Instead, we relied on the more general approach to estimating uncertainty involved in catch reconstructions—an approach that was inspired by criteria used by the Intergovernmental Panel on Climate Change, as previously described (Mastrandrea et al., 2010; Table 2).

As with any research method, there are limitations to expert advice. Most notable is the range of subjective and psychological biases that experts, and indeed all humans, are prone to (see overview in Supporting Information of Martin et al., 2012). Given the above, we agree with the statement of Martin et al. (2012) that: "Expert knowledge should be regarded only as a snapshot of the expert's judgments in time, and expert assumptions and reasoning should be documented in such a way that they can be updated as new empirical knowledge accrues."

Tourist demand for local fishes

We separated tourist demand for local fishes into 2 categories: 1) demand by stopover visitors and 2) demand by visitors who arrived on cruise ships. For our study, we define stopover visitors as tourists that spend at least one night in The Bahamas (Cleare, 2007). Most stopover visitors arrive by air, but some of them arrive by other means (e.g., private yacht). Stopover visitors fish recreationally and consume local fishes in restaurants in The Bahamas. In contrast, tourists that arrive by cruise ship, as defined in our study, typically spend only a few hours ashore in The Bahamas and increase demand for local fishes only through seafood consumption during shore visits.

To estimate stopover visitor demand for local fishes through seafood consumption in hotel restaurants, we designed and successfully administered a local seafood consumption survey with 11 major hotels on 5 different island groups. Our study sample represented 37% of all hotel rooms in The Bahamas in 2010. Hotels in our survey ranged in size from 19 to 2932 rooms. In all instances, the purchasing manager or head chef of a hotel restaurant completed the survey, which included requests for information on the type, quantity, origin (i.e., The Bahamas versus imported), and dollar value of fishes supplied to the restaurant on a yearly basis (Smith and Zeller[5]).

In our survey, there was a suspiciously large quantity of seafood that was purported to be of local origin. We, therefore, assumed that 10% of all so-called local seafood was actually imported and we adjusted consumption accordingly. Visitors to The Bahamas consume both local and imported (e.g., salmon) seafood in hotel restaurants. Our study focused only on local seafood consumption. Overall seafood consumption (i.e., both local and imported products) by visitors to The Bahamas is therefore much greater than our estimates provided here.

Then we combined tourist data (e.g., hotel occupancy rates, number of visitor nights per year) with results from our survey to estimate a consumption rate *per stopover visitor* for consumption of local seafood. Although staff at hotels provided data for a period that ranged from 2 through 18 years, most hotels provided data for only the last 2 years of our time series (i.e., 2009–2010). We are unaware of any previous estimates of local seafood consumption rates in hotels in The

Bahamas. Hence, we maintained the average consumption rate per stopover visitor for the years 2009–2010 based on our survey results (i.e., 0.49 kg·visitor^{-1}·night^{-1} and 1.08 kg·visitor^{-1}·night^{-1} for visitors to New Providence and Grand Bahama and to the Family Islands, respectively) for the remainder of the time series (i.e., 1950–2008), although this extrapolation may have resulted in a slight overestimate of local seafood consumption rates in the earliest parts of the time series (e.g., the 1950s).

Stopover visitors, by fishing recreationally, also increase local demand on fisheries resources (see the previous *Recreational fishery* section). However, because our tournament data did not distinguish between resident and tourist individuals that fish, we assumed that 98% of all tournament catch was taken by stopover visitors. The assumption that most tournament catch was taken by tourists is based on the fact that most sport fishing tournaments in The Bahamas are geared toward tourists (Thompson, 1989; Cleare, 2007) and on the notion that only a small percentage of the Bahamian resident population fishes for recreation (see the previous *Recreational fishery* section).

We are unaware of any estimates of local seafood consumption by visitors who arrive on cruise ships during their shore visits in The Bahamas. To be conservative, we assumed that, during 1950–2010, 10% of all visitors from cruise ships consumed local seafood equivalent to 1 plate-size snapper during their visit (i.e., 0.31 kg·visitor^{-1}·trip^{-1}).

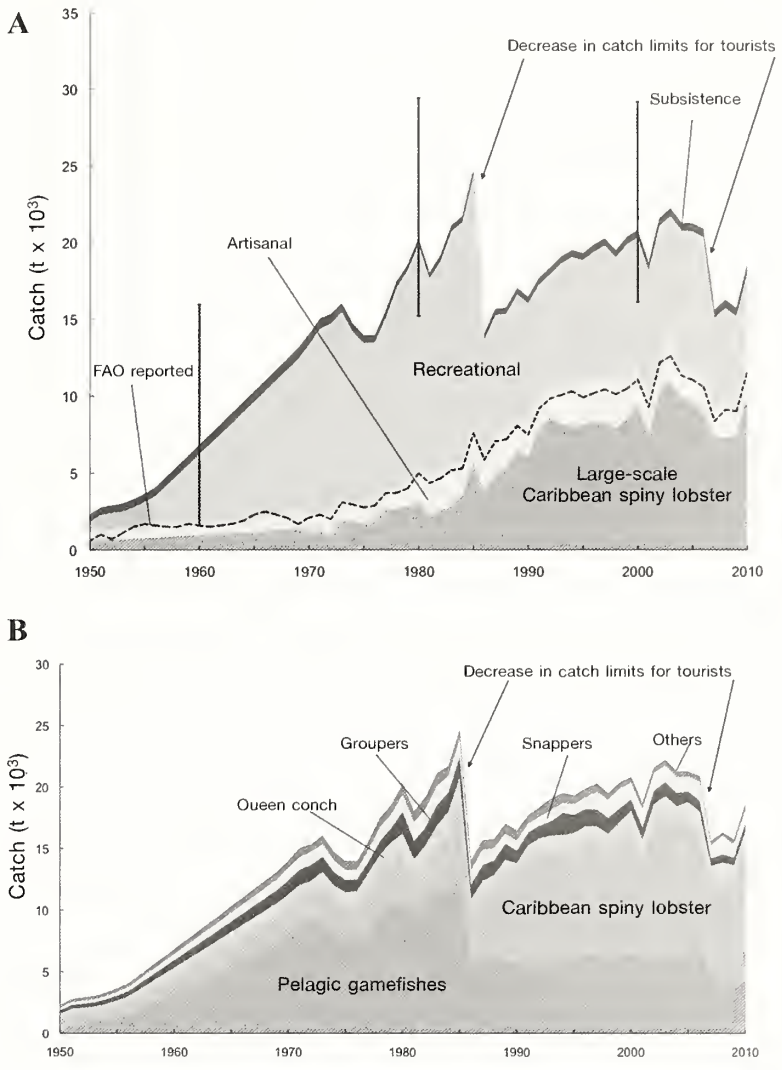

Figure 3

Reconstructed catch in metric tons (t) for The Bahamas during 1950–2010 by (**A**) fisheries sector, where bars indicate ranges of uncertainty for 1960 (for the period 1950–1969), 1980 (for the period 1970–1989), and 2000 (for the period 1990–2010), and by (**B**) major taxa. In graph A, the dashed line represents official landings data reported to FAO, and the commercial sector is subdivided into the artisanal fishery and the large-scale fishery for Caribbean spiny lobster (*Panulirus argus*). For a list of species within each taxon shown in graph B, see Smith and Zeller.[5] In both graphs, arrows indicate the period when changes were made in catch limit regulations for tourists engaged in recreational fishing.

Results

Reconstructed total catch

Reconstructed total catch from 1950 through 2010 was 884,500 t, a level that is 2.6 times the 336,190 t reported by FAO for The Bahamas. Catches increased from around 2300 t/year in 1950 to a peak of 24,700 t/year in 1985 and a second, smaller peak of 22,200 t/year occurred in 2003, before declining to 18,600 t/year by 2010 (Fig. 3A). Notably, recreational fishing accounted for more than half of the reconstructed total catch over the full time period (i.e., 55% or 490,100 t), followed by the large-scale, commercial Caribbean spiny lobster (29%), artisanal (12%), and subsistence (4%) fisheries (Fig. 3A). In contrast, for the most recent decade (i.e., 2000–2010), recreational catch mainly declined but still accounted for more than one-third (i.e., 39%) of the reconstructed total catch; in the same period, a generally increasing trend was observed for the large-scale, commercial fishery for Caribbean spiny lobster (Fig. 3A).

Reconstructed total catch comprised nearly 40 taxonomic groups (for details, see Smith and Zeller[5]; sum-

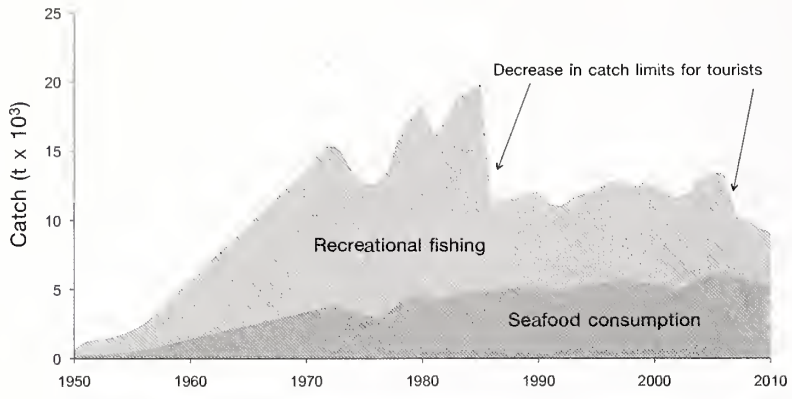

Figure 4

Demand for local fishes, measured as catch in metric tons (t), driven by tourism by both stopover visitors and visitors who arrived by cruise ship in The Bahamas during 1950–2010. Arrows indicate periods when changes were made to regulations of catch limits for tourists engaged in recreational fishing.

marized in Fig. 3B). Pelagic gamefishes accounted for the greatest proportion of catch during 1950–2010 (41%), followed closely by Caribbean spiny lobster (35%), and queen conch, groupers, and snappers each accounted for less than 10% of total catch (Fig. 3B). Over the last decade (i.e., 2000–2010), however, catch of Caribbean spiny lobster (51%) has surpassed catch of pelagic gamefishes (29%).

Commercial fishery

Reconstructed total catch during 1950–2010 by the artisanal fishery totaled 103,800 t, increasing from 560 t/year in 1950 to a peak of 3060 t/year in 1994 before declining to just under 2180 t/year by 2010 (Fig. 3A). In contrast, catch of the large-scale fishery for Caribbean spiny lobster during 1950–2010 totaled 257,400 t, accounting for 71% of reconstructed total commercial catch (i.e., catch from both the artisanal fishery and the large-scale fishery for Caribbean spiny lobster). Large-scale commercial catch of Caribbean spiny lobster increased from just under 660 t/year in 1950 to a peak of nearly 10,900 t/year in 2003, before declining slightly to 10,200 t/year in 2010 (Fig. 3A).

Subsistence fishery

Reconstructed subsistence catch totaled nearly 33,100 t during 1950–2010, increasing from 500 t/year in 1950 to a peak of around 740 t/year in the late 1960s, before declining to 590 t/year in 2010 (Fig. 3A). The majority of catch (69%) was taken by residents of the Family Islands, despite the size of the population of residents there being 75% smaller than that of the resident population on the more developed islands of New Providence and Grand Bahama.

Recreational fishery

Reconstructed recreational catch for the period 1950–2010 was 490,100 t; of this catch, less than 1% (around 420 t) was attributed to major tournaments. Catch increased from 600 t/year in 1950 to a peak of around 16,100 t/year in 1985, before declining rapidly to 7300 t/year in 1986 after the introduction of maximum catch limits for key taxa for visitors who fish recreationally. A second, but smaller peak occurred in 2006 at 9000 t/year before again declining sharply to just under 5700 t/year in 2010 because of revisions made in 2007 to the recreational fishing regulations for visitors (Fig. 3A).

Tourist demand for local fishes

Tourist demand for local fishes (through recreational fishing and from hotel restaurants) from 1950 through 2010 totaled 661,800 t, accounting for 75% of reconstructed total catches in the entire country (Fig. 4). The total number of visitors to The Bahamas each year is in the millions, and visitors have outnumbered the resident population by an order of magnitude for nearly half a century (Fig. 1). It is, therefore, not surprising that tourism has such a sizeable effect on fisheries removals in The Bahamas. Demand increased from 660 t/year in 1950 to a peak of more than 19,800 t/year in 1985 before declining to 9100 t/year in 2010 (Fig. 4). Almost two-thirds of this demand (435,900 t) was driven by recreational fishing by stopover visitors, and the remainder was a result of seafood consumption by stopover visitors (34%) and by visitors from cruise ships (0.3%) (Fig. 4). Although there were 13% more visitors from cruise ships than stopover visitors during 1950–2010, it is not surprising that less than 1% of demand was attributed to visitors who arrived by cruise ship, given that only a small fraction of them consumed local seafood and that none fished recreationally during their stay.

Discussion

Reconstructed total catches were 2.6 times the landings reported by the FAO for The Bahamas. The magnitude of the discrepancy between our reconstructed estimate and officially reported statistics is comparable to results from reconstruction studies of the fisheries of other small island nations, findings that ranged from a 1.2-fold difference in the case of the Azores (1950–2010; Pham et al., 2013) to an average 2.5-fold difference for 25 Pacific island countries and territories (Zeller et al., 2015).

In our study, the source of discrepancy for The Bahamas was twofold. First, only commercial landings

are accounted for in official statistics, a practice that is common in many countries as a result of the historic focus on commercial landings for economic development purposes (Ward, 2004). The lack of reporting on noncommercial sectors is justified currently by real or perceived costs and difficulties associated with quantifying spatially dispersed fisheries (Zeller et al., 2007, 2015). Even official, commercial landings statistics for The Bahamas are deficient and known to be underreported by up to 15% per year for some taxa (Table 4). The second and more important cause of discrepancy is that catches by the recreational and subsistence fisheries are substantial and missing entirely in national statistics, accounting for roughly 55% and 4% of reconstructed total catch during 1950–2010, respectively (Fig. 3A). These unreported, noncommercial sectors, therefore, represent major sources of impact on species and stocks of marine resources that would never be accounted for if one considers only official data.

Another major discrepancy between our reconstructed estimate and official data is the year in which fisheries catches peaked. According to our reconstruction, total catches peaked in the mid-1980s, not in 2003 as indicated by FAO national data (Fig. 3A). The peak in reconstructed catches was driven by recreational fishing in which, before 1986, no maximum allowable catch legislation existed for tourists. The primary reason for this legislation was that, before 1986, tourists were thought to be removing large quantities of fish from the waters of The Bahamas by essentially engaging in commercial fishing "under the guise of sport fishing" (Thompson, 1989). Our reconstruction indicates that a second peak in fisheries catches did in fact occur in 2003, but at more than 22,200 t/year as opposed to 12,610 t/year (Fig. 3A). This second peak was driven by increased catches in the large-scale commercial fishery for Caribbean spiny lobster, where the annual catch totaled nearly 11,000 t in 2003. The fact that the general trend in the reconstruction for The Bahamas differs somewhat from the trend that was based on officially reported statistics is common among reconstruction studies. For example, the synthesis of reconstructions for 25 Pacific island countries and territories showed that there was a distinct and significant difference in the time-series trends between reported and reconstructed catches (Zeller et al., 2015).

The fact that, in 1986 and again in 2007, the government of The Bahamas introduced maximum recreational catch limits for key taxa for tourists indicates that even in the absence of quantitative catch statistics, there was (and remains) a local perception that catches from this sector are substantial and in need of regulation (Braynen[6]). Indeed, the magnitude of estimated recreational catches from 1950 through 2010 is astounding (55% of total reconstructed catch), equating to 1.4 times the commercial catch over the same period. Although recreational catches can exceed commercial landings for some marine fish populations (e.g., see Schroeder and Love, 2002; Coleman et al., 2004), it is rare for recreational catches to dominate reconstructed estimates, as they do for The Bahamas. In comparison, recreational catches accounted for only 3% and 25% of total removals in reconstruction studies of marine fisheries in the Baltic Sea (1950–2007; Zeller et al., 2011b) and the Azores (1950–2010; Pham et al., 2013), respectively. Yet, despite their significance, recreational catches remain unaccounted for in The Bahamas, as in most other parts of the world, but Freire et al. (in press) is using the reconstruction process to estimate catches from marine recreational fisheries for 126 countries and territories.

Our findings debunk the notion, at least for The Bahamas, that catches from recreational fisheries are generally relatively small and, therefore, negligible when compared with the catches from other major sectors. McClenachan (2013) makes a similar point for the Florida Keys, where recreational fishing, driven primarily by the tourist industry, has contributed to the decline of vulnerable nearshore fishes. Indeed, our findings take on added importance as evidence accumulates regarding the role of recreational fishing in the exploitation of fish populations that require conservation (Coleman et al., 2004; Cooke and Cowx, 2004; Shiffman et al., 2014).

The magnitude of the impact of tourism on fisheries removals is a concern. A major issue is the open access nature of recreational fishing, for which managers regulate per capita maximum allowable catch (at least in principle) but have no control over the number of visitors that fish recreationally (Coleman et al., 2004). Because, as we have noted previously, total visitors now outnumber resident populations in many small island states and territories in the wider Caribbean, including those in The Bahamas (Table 1), trends in tourist demand for local fish (through recreational fishing and seafood consumption in local hotels) are similar across the Caribbean. Incomplete or missing reports of fisheries removals by the tourist industry can lead to inadequate fisheries management, creating a situation in which continued population growth and rising fisheries demands by residents and tourists could place unsustainable pressures on fisheries resources.

Numerous studies of the reconstruction of catch time series have revealed that official landings data for most countries are incomplete (e.g., Zeller et al., 2006, 2007; Wielgus et al., 2010; Zeller at al., 2011a, 2011b; Le Manach et al., 2012; Belhabib et al., 2014; Zeller et al., 2015). The results of this study clearly illustrate that The Bahamas can be added to the growing list of countries with inadequate reporting and highlight the rare situation that recreational fishing (primarily driven by the tourist industry) dominates reconstructed total catches. This rare situation is worrisome because of its obvious implications for effective conservation and resource management, particularly in light of the dual fisheries demands by a burgeoning tourist industry and a growing resident population.

Acknowledgments

We thank The Bahamas Department of Marine Resources, particularly M. Braynen for data, for expert opinion, and helpful discussions. We also thank The Bahamas Ministry of Tourism, particularly G. Delancy, for data. Data provided by A. Venizelos from the NOAA Southeast Fisheries Science Center are also greatly appreciated. DZ acknowledges the support of the Sea Around Us, funded by The Pew Charitable Trusts and The Paul G. Allen Family Foundation.

Literature cited

Belhabib, D., V. Koutob, A. Sall, V. W. Y. Lam, and D. Pauly.
2014. Fisheries catch misreporting and its implications: the case of Senegal. Fish. Res. 151:1–11.

Bentley, N., and K. Stokes.
2009. Contrasting paradigms for fisheries management decision making: how well do they serve data-poor fisheries? Mar. Coast. Fish. 1:391–401.

Burgman, M., A. Carr, L. Godden, R. Gregory, M. McBride, L. Flander, and L. Maguire.
2011. Redefining expertise and improving ecological judgment. Conserv. Lett. 4:81–87.

Cleare, A. B.
2007. History of tourism in The Bahamas: a global perspective, 633 p. Xlibris, Bloomington, IN.

Coleman, F. C., W. F. Figueira, J. S. Ueland, and L. B. Crowder.
2004. The impact of United States recreational fisheries on marine fish populations. Science 305:1958–1960.

Cooke, S. J., and I. G. Cowx.
2004. The role of recreational fishing in global fish crises. BioScience 54:857–859.

Covey, C.
2000. Beware the elegance of the number zero. Clim. Chang. 44:409–411.

Cox, L., J. L. Hammerton, and N. Wilchcombe (eds.).
2005. GEO Bahamas 2005: The Bahamas state of the environment report, 62 p. United Nations Environment Program, Global Environment Outlook. Bahamas Environment, Science, and Technology (BEST) Commission, Nassau, Bahamas. [Available at website.]

Crome, F. H. J., M. R. Thomas, and L. A. Moore.
1996. A novel Bayesian approach to assessing impacts of rain forest logging. Ecol. Appl. 6:1104–1123.

Diaz, G. A., M. Ortiz, and E. D. Prince.
2007. Updated white marlin (*Tetrapturus albidus*) and blue marlin (*Makaira nigricans*) catch rates from the U.S. recreational tournament fishery in the northwest Atlantic, U.S. Gulf of Mexico, Bahamas and U.S. Caribbean 1973–2005. Collect. Vol. Sci. Pap. ICAAT 60:1678–1695.

Field, J., J. Cope, and M. Key.
2010. A descriptive example of applying vulnerability evaluation criteria to California nearshore species. *In* Managing data-poor fisheries: case studies, models and solutions; Berkeley, CA, 1–4 December 2008 (R. M. Starr, C. S. Culver, C. Pomeroy, S. McMillan, T. Barnes, and D. Aseltine-Neilson, eds.), p. 235–246. [Available in CD-ROM from California Sea Grant, 9500 Gilman Dr., #0232, La Jolla, CA 92093-0232.]

Freire, K., D. Belhabib, B. Doherty, K. Kleisner, V. Lam, J. Mendonca, P. Moro, F. Motta, M. L. D. Palomares, D. Pauly, N. Smith, A. McCrea Strub, L. Teh, D. Zeller, and K. Zylich.
In press. Estimating global catches from marine recreational fisheries. FAO Tech. Rep. FAO, Rome.

Griffiths, S. P., P. M. Kuhnert, W. N. Venables, and S. J. M. Blaber.
2007. Estimating abundance of pelagic fishes using gillnet catch data in data-limited fisheries: a Bayesian approach. Can. J. Fish. Aquat. Sci. 64:1019–1033.

Honey, K. T., J. H. Moxley, and R. M. Fujita.
2010. From rags to fishes: data-poor methods for fishery managers. *In* Managing data-poor fisheries: case studies, models and solutions; Berkeley, CA, 1–4 December 2008 (R. M. Starr, C. S. Culver, C. Pomeroy, S. McMillan, T. Barnes, and D. Aseltine-Neilson, eds.), p.159–184. [Available as CD-ROM from California Sea Grant, 9500 Gilman Dr., #0232, La Jolla, CA 92093-0232.]

Johannes, R. E.
1998. The case for data-less marine resource management: examples from tropical nearshore finfisheries. Trends Ecol. Evol. 13:243–246.

Kuhnert, P. M.
2011. Four case studies in using expert opinion to inform priors. Environmetrics 22:662–674.

Le Manach, F., C. Gough, A. Harris, F. Humber, S. Harper, and D. Zeller.
2012. Unreported fishing, hungry people and political turmoil: the recipe for a food security crisis in Madagascar? Mar. Policy 36:218–225.

MacCall, A. D.
2009. Depletion-corrected average catch: a simple formula for estimating sustainable yields in data-poor situations. ICES J. Mar. Sci. 66:2267–2271.

Maitland, T. E.
2006. Dietary habits, diversity and the indigenous diet of the Turks and Caicos Islands: implications for island-specific nutrition intervention. West Indian Med. J. 55:1–13.

Manly, B. F. J., and D. Mackenzie.
2000. A cumulative sum type of method for environmental monitoring. Environmetrics 11:151–166.

Martin, T. G., M. A. Burgman, F. Fidler, P. M. Kuhnert, S. Low-Choy, M. McBride, and K. Mengersen.
2012. Eliciting expert knowledge in conservation science. Conserv. Biol. 26:29–38.

Mastrandrea, M. D., C. B. Field, T. F. Stocker, O. Edenhofer, K. L. Ebi, D. J. Frame, H. Held, E. Kriegler, K. J. Mach, P. R. Matschoss, G.-K. Plattner, G. W. Yohe, and F. W. Zwiers.
2010. Guidance note for lead authors of the IPCC fifth assessment report on consistent treatment of uncertainties, 4 p. Intergovernmental Panel on Climate Change (IPCC), Geneva, Switzerland. [Available at website.]

McClenachan, L.
2013. Recreation and the "Right to Fish" movement: anglers and ecological degradation in the Florida Keys. Environ. Hist. 18:76–87.

Morgan, M. G., L. F. Pitelka, and E. Shevliakova.
2001. Elicitation of expert judgments of climate change impacts on forest ecosystems. Clim. Chang. 49:279–307.

Murray, J. V., A. W. Goldizen, R. A. O'Leary, C. A. McAlpine, H. P. Possingham, and S. L. Choy.
2009. How useful is expert opinion for predicting the distribution of a species within and beyond the region of

expertise? A case study using brush-tailed rock wallabies *Petrogale penicillata*. J. Appl. Ecol. 46:842–851.

Pauly, D.
1998. Rationale for reconstructing catch time series. Bull. EC Fish. Coop. 11(2):4–7.

Pham, C. K., A. Canha, H. Diogo, J. G. Pereira, R. Prieto, and T. Morato.
2013. Total marine fishery catch for the Azores (1950–2010). ICES J. Mar. Sci. 70:564–577.

Schroeder, D. M., and M. S. Love.
2002. Recreational fishing and marine fish populations in California. CalCOFI Rep. 43:182–190.

Shiffman, D. S., A. J. Gallagher, J. Wester, C. C. Macdonald, A. D. Thaler, S. J. Cooke, and N. Hammerschlag.
2014. Trophy fishing for species threatened with extinction: a way forward building on a history of conservation. Mar. Policy 50:318–322.

Smith, D., A. Punt, N. Dowling, A. Smith, G. Tuck, and I. Knuckey.
2009. Reconciling approaches to the assessment and management of data–poor species and fisheries with Australia's harvest strategy policy. Mar. Coast. Fish. 1:244–254.

Thompson, R. W.
1989. Marine recreational fishing in the Bahamas—a case study. Proc. Gulf Caribb. Fish. Inst. 39:75–85.

UNWTO (World Trade Organization).
2014a. UNTWO tourism highlights: 2014 edition, 14 p. World Tourism Organization, Madrid, Spain. [Available Article.]
2014b. Tourism in small island developing states (SIDS): building a more sustainable future for the people of islands, 5 p. World Tourism Organization. [Available at website.]

Ward, M.
2004. Quantifying the world: UN ideas and statistics, 352 p. Indiana Univ. Press, Bloomington, IL.

Wielgus, J., D. Zeller, D. Caicedo-Herrera, and U. R. Sumaila.
2010. Estimation of fisheries removals and primary economic impact of the small-scale and industrial marine fisheries in Colombia. Mar. Policy 34:506–513.

Zeller, D., S. Booth, P. Craig, and D. Pauly.
2006. Reconstruction of coral reef fisheries catches in American Samoa, 1950–2002. Coral Reefs 25:144–152.

Zeller, D., S. Booth, G. Davis, and D. Pauly.
2007. Re-estimation of small-scale fishery catches for U.S. flag-associated island areas in the western Pacific: the last 50 years. Fish. Bull. 105:266–277.

Zeller, D., S. Booth, E. Pakhomov, W. Swartz, and D. Pauly.
2011a. Arctic fisheries catches in Russia, USA, and Canada: baselines for neglected ecosystems. Polar Biol. 34:955–973.

Zeller, D., P. Rossing, S. Harper, L. Persson, S. Booth, and D. Pauly.
2011b. The Baltic Sea: estimates of total fisheries removals 1950–2007. Fish. Res. 108:356–363.

Zeller, D., S. Harper, K. Zylich, and D. Pauly
2015. Synthesis of underreported small-scale fisheries catch in Pacific island waters. Coral Reefs 34:25–39.

Fishery Bulletin

Guidelines for authors

Contributions published in *Fishery Bulletin* describe original research in marine fishery science, fishery engineering and economics, as well as the areas of marine environmental and ecological sciences (including modeling). Preference will be given to manuscripts that examine processes and underlying patterns. Descriptive reports, surveys, and observational papers may occasionally be published but should appeal to an audience outside the locale in which the study was conducted.

Although all contributions are subject to peer review, responsibility for the contents of papers rests upon the authors and not on the editor or publisher. *Submission of an article implies that the article is original and is not being considered for publication elsewhere.*

Plagiarism and double publication are considered serious breaches of publication ethics. To verify the originality of the research in papers and to identify possible previous publication, manuscripts may be screened with plagiarism-detection software.

Manuscripts must be written in English; authors whose native language is not English are strongly advised to have their manuscripts checked by English-speaking colleagues before submission.

Once a paper has been accepted for publication, online publication takes approximately 3 weeks.

Types of manuscripts accepted by the journal

Articles

Articles generally range from 20 to 30 double-spaced typed pages (12-point font) and describe an original contribution to fisheries science, engineering, or economics. Tables and figures are not included in this page count, but the number of figures should not exceed one figure for every four pages of text. Articles contain the following divisions: **abstract, introduction, methods, results, and discussion.**

Short communications

Short communications are generally less than 20 double spaced typed pages (12-point font) and, like articles, describe an original contribution to fisheries science. They follow the same format as that for articles: **abstract, introduction, results and discussion, but the results and discussion sections may be combined.** Short communications are distinguished from full articles in that they report a noteworthy new observation or discovery—such as the first report of a new species, a unique finding, condition, or event that expands our knowledge of fisheries science, engineering or economics—and do not require a lengthy discussion.

Companion articles

Companion articles are presented together and published together as a scientific contribution. Both articles address a closely related topic and may be articles that result from a workshop or conference. They must be submitted to the journal at the same time.

Review articles

Review articles generally range from 40 to 60 double-spaced typed pages (12-point font) and address a timely topic that is relevant to all aspects of fisheries science. They should be forward thinking and address novel views or interpretations of information that encourage new avenues of research. They can be reviews based on the outcome from thematic workshops, or contributions by groups of authors who want to focus on a particular topic, or a contribution by an individual who chooses to review a research theme of broad interest to the fisheries science community. **A review article will include an abstract, but the format of the article *per se* will be up to the authors.** Please contact the Scientific Editor to discuss your ideas regarding a review article before embarking on such a project.

Preparation of manuscript

Title page should include authors' full names, mailing addresses, and the senior author's e-mail address.

Abstract should be limited to 200 words (one-half typed page), state the main scope of the research, and emphasize the authors conclusions and relevant findings. Do not review the methods of the study or list the contents of the paper. Because abstracts are circulated by abstracting agencies, it is important that they represent the research clearly and concisely.

General text must be typed in 12-point Times New Roman font throughout. A brief introduction should convey the broad significance of the paper; the remainder of the paper should be divided into the following sections: Materials and methods, Results, Discussion, and Acknowledgments. Headings within each section must be short, reflect a logical sequence, and follow the rules of subdivision (i.e., there can be no subdivision without at least two subheadings). The entire text should be intelligible to interdisciplinary readers; therefore, all acronyms, abbreviations, and technical terms should be written out in full the first time they are mentioned. Abbreviations should be used sparingly because they are not carried over to indexing databases and slow readability for those readers outside a discipline. They should never be used for the main subject (species, method) of a paper.

For general style, follow the U.S. *Government Printing Office Style Manual* (2008) [available at website] and *Scientific Style and Format: the CSE Manual for Authors, Editors, and Publishers* (2014, 8th ed.) published by the Council of Science Editors. For scientific nomenclature, use the current edition of the American Fisheries Society's *Common and Scientific Names of Fishes from the United States, Canada, and Mexico* and its companion volumes (*Decapod Crustaceans, Mollusks, Cnidaria and Ctenophora*, and *World Fishes Important to North Americans*). For species not found in the above mentioned AFS publications and for more recent changes in nomenclature, use the Integrated Taxonomic Information System (ITIS) (available at website), or, secondarily, the California Academy of Sciences *Catalog* of *Fishes* (available at website) for species names not included in ITIS. Common (vernacular) names of species should be lowercase. Citations must be given of taxonomic references used for the identification of specimens. For example, "Fishes were identified according to Collette and Klein-MacPhee (2002); sponges were identified according to Stone et al. (2011)."

Dates should be written as follows: 11 November 2000. Measurements should be expressed in metric units, e.g., 58 metric tons (t); if other units of measurement are used, please make this fact explicit to the reader. Use numerals, not words, to express whole and decimal numbers in the general text, tables, and figure captions (except at the beginning of a sentence). For example: We considered 3 hypotheses. We collected 7 samples in this location. Use American spelling. Refrain from using the shorthand slash (/), an ambiguous symbol, in the general text.

Word usage and grammar that may be useful are the following:

- *Aging* For our journal the word *aging* is used to mean both age determination and the aging process (senescence). The author should make clear which meaning is intended where ambiguity may arise.

- *Fish and fishes* For papers on taxonomy and biodiversity, the plural of *fish* is *fishes,* by convention. In all other instances, the plural is *fish.*
  Examples:
  The fishes of Puget Sound [biodiversity is indicated];
  The number of fish caught that season [no emphasis on biodiversity];
  The fish were caught in trawl nets [no emphasis on biodiversity].
  The same logic applies to the use of the words *crab* and *crabs, squid* and *squids,* etc.

- *Sex* For the meaning of male and female, use the word *sex*, not *gender.*

- *Participles* As adjectives, participles must modify a specific noun or pronoun and make sense with that noun or pronoun.
  Incorrect:
  Using the recruitment model, estimates of age-1 recruitment were determined. [Estimates did not use the recruitment model.]
  Correct:
  Using the recruitment model, we determined age-1 estimates of recruitment. [The participle now modifies the word *we,* i.e., those who were using the model.]
  Incorrect:
  Based on the collected data, we concluded that the mortality rate for these fish had increased. [*We* were not based on the collected data.]
  Correct:
  We concluded on the basis of the collected data that the mortality rate for these fish had increased. [Eliminate the participle and replace it with an adverbial phrase.]

Equations and mathematical symbols should be set from a standard mathematical program (MathType) and tool (Equation Editor in MS Word). LaTex is acceptable for more advanced computations. For mathematical symbols in the general text (α, χ^2, π, $\pm$, etc.), use the symbols provided by the MS Word program and italicize all variables, except those variables represented by Greek letters. Do not use photo mode when creating these symbols in the general text.

Number equations (if there are more than 1) for future reference by scientists; place the number within parentheses at the end of the first line of the equation.

Literature cited section comprises published works and those accepted for publication in peer-reviewed journals (in press). Follow the name and year system for citation format in the "Literature cited" section (that is to say, citations should be listed alphabetically by the authors' last names, and then by year if there is more than one citation with the same authorship. A list of abbreviations for citing journal names can be found at website.

Authors are responsible for the accuracy and completeness of all citations. Literature citation format: Author (last name, followed by first-name initials). Year. Title of article. Abbreviated title of the journal in which it was published. Always include number of pages. For a sequence of citations in the general text, list chronologically: (Smith, 1932: Green. 1947; Smith and Jones, 1985).

Digital object identifier (doi) code ensures that a publication has a permanent location online. Doi code should be included at the end of citations of published literature. Authors are responsible for submitting accurate doi codes. Faulty codes will be deleted at the page-proof stage.

Cite all software, special equipment, and chemical solutions used in the study within parentheses in the general text: e.g., SAS, vers. 6.03 (SAS Inst., Inc., Cary, NC).

Footnotes are used for all documents that have not been formally peer reviewed and for observations and personal communications. These types of references should be cited sparingly in manuscripts submitted to the journal.

All reference documents, administrative reports, internal reports, progress reports, project reports, contract reports, personal observations, personal communications, unpublished data, manuscripts in review, and council meeting notes are footnoted in 9 pt font and placed at the bottom of the page on which they are first cited. Footnote format is the same as that for formal literature citations. A link to the online source (e.g., [http://www/..... , accessed July 2007.]), or the mailing address of the agency or department holding the document, should be provided so that readers may obtain a copy of the document.

Tables are often overused in scientific papers; it is seldom necessary to present all the data associated with a study. Tables should not be excessive in size and must be cited in numerical order in the text. Headings should be short but ample enough to allow the table to be intelligible on its own.

All abbreviations and unusual symbols must be explained in the table legend. Other incidental comments may be footnoted with italic numeral footnote markers. Use asterisks only to indicate significance in statistical data. Do not type table legends on a separate page; place them above the table data. *Do not submit tables in photo mode.*

- Notate probability with a capital, italic *P*.
- Provide a zero before all decimal points for values less than one (e.g., 0.07).
- Round all values to 2 decimal points.
- Use a comma in numbers of five digits or more (e.g., 13,000 but 3000).

Figures must be cited in numerical order in the text. Graphics should aid in the comprehension of the text, but they should be limited to presenting patterns rather than raw data. Figures should not exceed one figure for every four pages of text and must be labeled with the number of the figure. Place labels **A, B, C,** etc. within the upper left area of graphs and photos. Avoid placing labels vertically (except for the y axis).

Figure legends should explain all symbols and abbreviations seen in the figure and should be double-spaced on a separate page at the end of the manuscript.

Line art and halftone figures should be submitted as pdf files with >800 dpi and >300 dpi, respectively. Color is allowed in figures to show morphological differences among species (for species identification), to show stain reactions, and to show gradations in temperature contours within maps. Color is discouraged in graphs, and for the few instances where color may be allowed, the use of color will be determined by the Managing Editor. Approved color figures should be submitted as TIFF ore JPG files in CMYK format.

- Capitalize the first letter of the first word in all labels within figures.
- Do not use overly large font sizes in maps and for units of measurements along axes in graphs.
- Do not use bold fonts or bold lines in figures.
- Do not place outline rules around graphs.
- Place a North arrow and label degrees latitude and longitude (e.g., 170°E) in all maps.
- Use symbols, shadings, or patterns (not clip art) in maps and graphs.

Failure to follow these guidelines and failure to correspond with editors in a timely manner will delay publication of a manuscript.

Copyright law does not apply to *Fishery Bulletin,* which falls within the public domain. However, if an author reproduces any part of an article from *Fishery Bulletin*, reference to source is considered correct form (e.g., Source: Fish. Bull. 97:105).

Submission of manuscript

Submit manuscript online at the ScholarOne website. Commerce Department authors should submit papers under a completed NOAA Form 25-700. For further details on electronic submission, please contact the Associate Editor, Kathryn Dennis, at

kathryn.dennis@noaa.gov

When requested, the text and tables should be submitted in Word format. Figures should be sent as separate PDF files (preferred), TIFF files, or JPG files. Send a copy of figures in the original software if conversion to any of these formats yields a degraded version of the figure.

Questions? If you have questions regarding these guidelines, please contact the Managing Editor, Sharyn Matriotti, at

sharyn.matriotti@noaa.gov

Questions regarding manuscripts under review should be addressed to Kathryn Dennis, Associate Editor.

Fishery Bulletin

Subscription form

Superintendent of Documents **Publications** Order Form

*5178

☐ YES, please send me the following publications:

____ Subscriptions to *Fishery Bulletin*
for $32.00 per year ($44.80 foreign)

The total cost of my order is $ _____ . Prices include regular domestic postage and handling and are subject to change.

_____
(Company or Personal Name) (Please type or print)

_____
(Additional address/attention line)

_____
(Street address)

_____
(City, State, ZIP Code)

_____
(Daytime phone including area code)

_____
(Purchase Order No.)

Charge your order. IT'S EASY!

VISA

MasterCard

Please Choose Method of Payment:

☐ Check payable to the Superintendent of Documents
☐ GPO Deposit Account ☐☐☐☐☐☐☐–☐
☐ VISA or MasterCard Account
☐☐☐☐☐☐☐☐☐☐☐☐☐☐☐☐
☐☐☐☐ (Credit card expiration date)

To fax your orders (202) 512-2104

_____
(Authorizing Signature)

Mail to: Superintendent of Documents
P.O. Box 979050, St. Louis, Missouri 63197
Tel. no. (U.S. callers): 866-512-1800
Tel. no. (International callers): 1-202-512-1800

Thank you for your order!

Also available online at
http://bookstore.gpo.gov/actions/GetPublication.do?stocknumber=703-023-00000-2
email: ContactCenter@gpo.gov